Doctoral thesis

Doctoral theses at NTNU, 2023:293

Karen Karolina Høisæter

Stability of Solvents for Gas Purification

NTNU
Norwegian University of Science and Technology
Thesis for the Degree of
Philosophiae Doctor
Faculty of Natural Sciences
Department of Chemical Engineering

NTNU
Norwegian University of
Science and Technology

Karen Karolina Høisæter

Stability of Solvents for Gas Purification

Thesis for the Degree of Philosophiae Doctor

Trondheim, September 2023

Norwegian University of Science and Technology
Faculty of Natural Sciences
Department of Chemical Engineering

NTNU
Norwegian University of
Science and Technology

NTNU
Norwegian University of Science and Technology

Thesis for the Degree of Philosophiae Doctor

Faculty of Natural Sciences
Department of Chemical Engineering

ISBN 978-82-326-7286-8 (printed ver.)
ISBN 978-82-326-7285-1 (electronic ver.)
ISSN 1503-8181 (printed ver.)
ISSN 2703-8084 (online ver.)

Doctoral theses at NTNU, 2023:293

Printed by NTNU Grafisk senter

Abstract

The main objective of this work was to increase the understanding of the chemical processes occurring as solvents used in gas purification degrade. Amine systems for CO_2 capture and glycol systems for gas dehydration were in focus. The work included a literature review, oxidative and thermal degradation studies of both amines and glycols and development of analytical methods.

In thermal degradation experiments with MEA, the concentration of CO_2 was found to increase the degradation rates, while the water and amine concentrations had no effect. Replacing water with TEG resulted in increased thermal degradation rates for MEA, AP, MMEA, and EAE. Also changing the cosolvent to organic diluents, DEG, MEG, THFA, NFM/water, and NMP resulted in increased thermal degradation of MEA.

In oxidative degradation experiments of MEA, increasing the concentration of MEA in loaded solutions resulted in increased degradation rates when the CO_2 concentration was kept constant. The same was not seen when the CO_2 concentration was increased simultaneously with the MEA concentration.

Independent analytical techniques were developed for the quantification of small glycols and small organic acids. GC-FID and quantitative ^{13}C NMR were successfully used to quantify the glycols. HPLC-UV and HSS analysis were successfully used to quantify the acids.

Thermal degradation experiments of TEG show that the added impurities, water and formic acid, reduced the thermal stability of TEG. DEG and MEG were confirmed as thermal degradation products of TEG. Gas bubbles were observed in the degraded solutions, but no other degradation components were identified.

The oxidative stability of TEG was reduced both by an increase in temperature and oxygen available. The degradation products identified and quantified were DEG, MEG, formic, acetic, glycolic, glyoxylic, and oxalic acid, formaldehyde and acetaldehyde, water, and CO_2. Identification of additional degradation compounds, tetraethylene glycol, pentaethylene glycol, and diethylene glycol monoethyl ether was achieved by a GC-MS analysis. Oxidative degradation experiments with MEG showed that the stability of MEG is considerably higher than TEG under the given conditions.

Acknowledgements

First and foremost, I would like to thank my wonderful supervisor, Prof Hanna K. Knuutila. Thank you for giving me this opportunity, for your support and guidance, and for making this work such a fun and rewarding experience.

I would also like to express my gratitude to my two co-supervisors. Dr Solrun J. Vevelstad, you possess what has always seemed to me like endless knowledge of the various amine degradation mechanisms and products. Your thoughts and input on my work have been truly invaluable. Dr Vanja Buvik, your passion and drive for what you do is truly inspiring. Having you on my team has made all challenges seem more manageable.

Doing experimental work is seldom unproblematic. A thanks to Gøril Flatberg, Michael Hammer, and Ardi Hartono for always helping out when things did not work as they should in the laboratory, and to Max Lukas Teschner for endless amounts of dilutions and analyses. A special thanks should also go to Torun M. Melø, Kåre A. Kristiansen, Julie Asmussen, and Susana V. Gonzalez for making the analytical work possible through their experience and guidance.

I would like to thank both old and new colleagues for memorable lunches, cake breaks, trips, conferences, and social gatherings. Coming to work has always been fun. A special thanks to my brilliant workout buddy, Ricardo, for always keeping me “on track”, fellow crafter, Tobi, for finally teaching me how to whistle, and to the best of office mates, Bahareh, Lucas, and Maxime. Sharing an office with such caring, helpful, and smart people has truly been a blessing. My geography knowledge is immensely improved.

Lastly, I would like to thank my family. Thanks to my parents and brother, for your support and encouragement along the way and for teaching me from an early age to be curious and to love learning. Thank you, Jørgen, for all the fun and all the love. Thank you for being patient even when I have been tired and grumpy. And thanks to my little Serina, for being all kinds of wonderful.

In this world, there are things you can do alone, and things you can only do with somebody else. It’s important to combine the two in just the right amount.

- After Dark, Murakami

Contents

List of Abbreviations

^{1}H	proton
^{13}C	carbon-13
α	$mol_{CO2}\ mol_{amine}^{-1}$
abs	absolute
AQ	acquisition
aq.	aqueous
ATR	attenuated total reflectance
BW	base wash
C	concentration
CAS	Chemical Abstracts Service reference number
CCS	carbon capture and storage
CCUS	carbon capture, utilization, and storage
CHP	combined heat and power
COSY	correlation spectroscopy
DeNOx	removal of nitrogen oxides (NOx)
DeSOx	removal of sulfur oxides (SOx)
DI	deionized
ED	electrodialysis
EDX	energy dispersive X-ray microanalysis
EI	electron impact ionization
ELPI	electrical low-pressure impactor
ESI+	positive electrospray ionization

ESP	electrostatic precipitator
FGD	flue gas desulfurization
FID	flame ionization detection (GC) or free induction decay (NMR)
FMPS	fast mobility particle sizer
FT-IR	Fourier-transform infrared spectroscopy
GC	gas chromatography
HMBC	heteronuclear multiple-bond correlation spectroscopy
HSE	health, safety, and environment
HSQC	heteronuclear single-quantum correlation spectroscopy
HSS	heat stable salts
IC	ion chromatography
ICE	ion chromatography exclusion
ICP	inductively coupled plasma
KFT	Karl Fischer titration
LC	liquid chromatography
LOD	limit of detection
LOQ	limit of quantification
m	mass
M	mol L^{-1}
MFC	mass flow controller
MS	mass spectrometry
NDIR	non-dispersive infrared
NG	natural gas
NMR	nuclear magnetic resonance
NOE	nuclear Overhauser effect

OES	optical emission spectroscopy
OPC	optical particle counter
ppb	parts per billion
ppm	parts per million
PR	particulate removal
PTR	proton-transfer reaction
RFCC	residual fluidized cracker
RH	radical hydrogenation
RT	retention time
SCR	selective catalytic reduction
SEM	scanning electron microscope
T	temperature
T_1	spin-lattice relaxation time
TA	total alkalinity
TIC	total inorganic carbon
TOC	total organic carbon
TOF	time of flight
TONO	total nitrosamine
UPLC	ultra-performance liquid chromatography
VOC	volatile organic compounds
WESP	wet electrostatic precipitator
WFGD	wet flue gas desulphurization
WTE	waste-to-energy
wt	weight
QTOF	quad time of flight

Chemical abbreviations, and CAS-numbers

AcN	acetonitrile	75-05-8
AEHEIA	*N*-(2-aminoethyl)-*N*'(2-hydroxyethl)-imidazolidione	no CAS
AMP	2-amino-2-methyl-1-propanol	124-68-5
AP	3-amino-propanol	156-87-6
BHEOX	*N,N'*-bis(2-hydroxyethyl) oxamide	1871-89-2
DEEA	2-(diethyl-amino)ethanol	100-37-8
DEG	diethylene glicol	111-46-6
DMMEA	2-dimethyl-amino-ethanol	108-01-0
DMPA	3-dimethyl-amino-1-propanol	3179-63-3
DNPH	2,4-dinitrophenylhydrazine	119-26-6
EAE	2-(ethyl-amino)ethanol	110-73-6
HEA	*N*-(2-hydroxyethyl)acetamide	142-26-7
HEEDA	2-(2-hydroxyethyl-amino)ethanol	111-41-1
HEF	*N*-(2-hydroxyethyl)-formamide	693-06-1
HEI	*N*-(2-hydroxyethyl)-imidazole	1615-14-1
HEIA	*N*-(2-hydroxyethyl)-2-imidazolidione	3699-54-5
HeGly	*N*-(2-hydroxyethyl)-glycine	5835−28-9
HEPO	4-(2-hydroxyethyl)-2-piperazinone	23936-04-1
MEA	monoethanolamine	141-43-5
MEA-urea	*N,N*'-bis(2-hydr-oxyethyl)urea	15438-70-7
MDEA	*N*-methyl diethanolamine	105-59-9
MEG	ethylene glycol	107-21-1
MMEA	2-(methyl-amino)ethanol	109-83-1
NFM	*N*-formyl morpholine	4394-85-8
NMP	*N*-methyl-2-pyrrolidone	872-50-4
OZD	2-oxazolidinone	497-25-6

PC	propylene carbonate	108-32-7
PEG	polyethylene glycol	25322-68-3
PZ	piperazine	110-85-0
Selexol	poly(ethylene glycol)dimethyl ether	24991-55-7
TEA	triethanolamine	102-71-6
TEG	triethylene glycol	112-27-6
THFA	tetrahydro-furfuryl alcohol	97-99-4
TMS	sulfolane	126-33-0
TMSP	tris(trimethylsilyl)phosphine	15573-38-3
TREG	tetraethylene glycol	112-60-7
TRIMEA	*N'*-(2-hydroxyethyl)-diethylentriamine	1965-29-3

Chapter 1

Introduction

1.1 Background

Gas purification involves removing unwanted compounds from a gas-phase. The most important technique for achieving this is through absorption with a liquid solvent.[1] In order to get the desired purification, more often than not, multiple techniques need to be employed. Examples of some components commonly removed by liquid absorption are H_2S, CO_2, water vapor, and SO_2.[2]

Absorption used for gas purification can be divided into three categories: physical absorption, reversible reactions, and irreversible reactions.[1] Physical absorption is based on the concept of solubility. If the compound is more soluble in the liquid than in the gas stream, it will be physically absorbed. In the case of reversible and irreversible reactions, the gaseous component reacts with a component in the liquid phase. It is categorized as a reversible reaction if the resulting bond is possible to break by, for example, applying heat to the system. If the bond is not readily broken, it is considered irreversible.

There are multiple reasons for the need to remove components from a gas stream. Flue gases contain species that can be harmful to health and environment if released into the atmosphere. Fuel gases, on the other hand, can contain components that damage equipment and pipelines.[3] In addition, the presence of certain compounds might result in the final product not meeting quality specifications.[4] During the absorption processes, the solvent can undergo unwanted irreversible reactions caused by the presence of oxidizing species in the gas, or elevated temperatures. This results in lowered absorption capacity, operational issues and possible damage to the absorption unit.

In this PhD thesis, the focus has been on the solvent degradation related to two different gas purification applications: CO_2 capture using amine-based solvents and gas dehydration based on glycols. These two processes will be described in further detail in the following sections.

1.1.1 Carbon Capture

CO_2 is a component in flue gases and is considered the single largest contributor to global greenhouse gas emissions.[5] The greenhouse gases trap energy from the sun, increasing the earth's temperatures.[6] This will affect the weather and climate systems of the planet, which in turn will have serious consequences for life on earth. To tackle this issue, carbon capture and storage (CCS) has the potential to be an effective tool. In the report of 2018 by the Intergovernmental Panel on Climate Change (IPCC), carbon capture and storage (CCS) or carbon capture, utilization, and storage (CCUS) were included in three out of four proposed scenarios to sufficiently reduce emissions. The four scenarios are cases where carbon emissions will be sufficiently reduced whilst the global energy requirements are still met during the shift towards full implementation of renewable energy.[7] The scenario not including CCS or CCUS is based on reducing the energy requirements, use of emission-intensive goods, and land use by the global society. It should also be mentioned that even in an ideal case, where renewable energy could cover the current energy demand, processes such as metal production, cement production, and waste-to-energy (WTE) would still be necessary, and so CCS would still be an important technology.

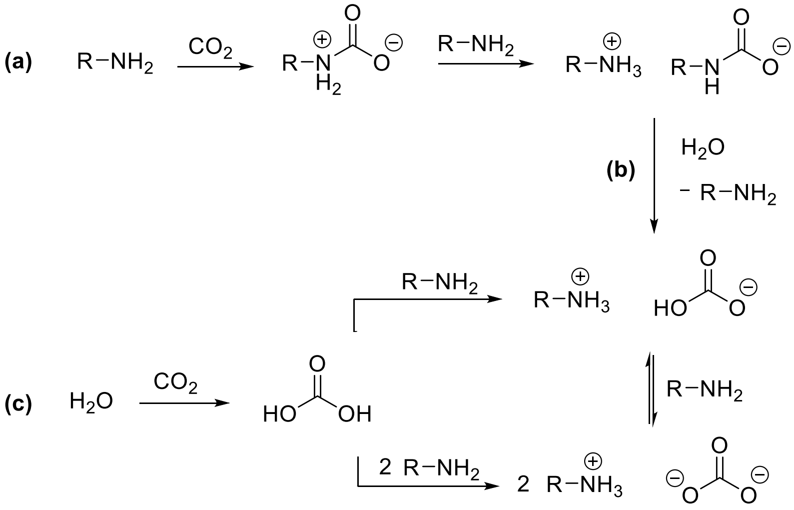

Scheme 1.1: CO_2 absorption pathways for a primary aqueous amine.[8]

Though other technologies are available, absorption with amines is by far the most mature technology to capture CO_2.[9,10] This absorption technology is based on the amines' ability to chemically bind with CO_2 through acid-base reactions. Amines are categorized as primary, secondary, or tertiary, depending on how many substituents they have. Scheme 1.1 shows an example of CO_2 absorption with an aqueous primary amine. Following route (a), both primary and secondary amines readily undergo formation to a carbamate, potentially via the formation of a short-lived zwitterion, requiring two moles of MEA per mole CO_2.[11–13] Tertiary amine cannot undergo this reaction as they do not have a proton to take part in the proton transfer from zwitterion to carbamate. The carbamate formation is also less favored for some sterically hinder primary and secondary amines, e.g. 2-amino-2-methyl-1-propanol (AMP). These, and the tertiary amines, can undergo reactions with CO_2 to form bicarbonate and carbonate salts via the formation of carbonic acid as presented in route (c). Bicarbonate and carbonate can also be formed through hydrolysis of the carbamate, following route (b).[14,15]

These reactions are exothermic and can be reversed by applying heat to the amine solution. An overview of this process is presented in Figure 1.1. The gas enters an absorber column at the bottom and travels up countercurrent to the amine solvent. The cleaned flue gas leaves the absorber via a water wash. In the water wash, the flue gas is treated to catch possible amine compounds following the gas. The rich amine solution is pumped via a lean/rich heat exchanger and enters the top of the desorber. In the desorber, the amine is regenerated by adding heat, reversing the absorption reactions and releasing the chemically bound CO_2. The heat is supplied by the reboiler at the bottom of the desorber. Here, part of the water in the aqueous amine solution is evaporated, providing stripping steam for the regeneration column. A part of the water vapor and the freed CO_2 leave the column at the top, and the water vapor is recovered in a condenser, while the CO_2 leaves the system. The lean amine solution then leaves the reboiler and is cooled down in the rich/lean heat exchanger. After an additional cooler, it reenters the absorber column.

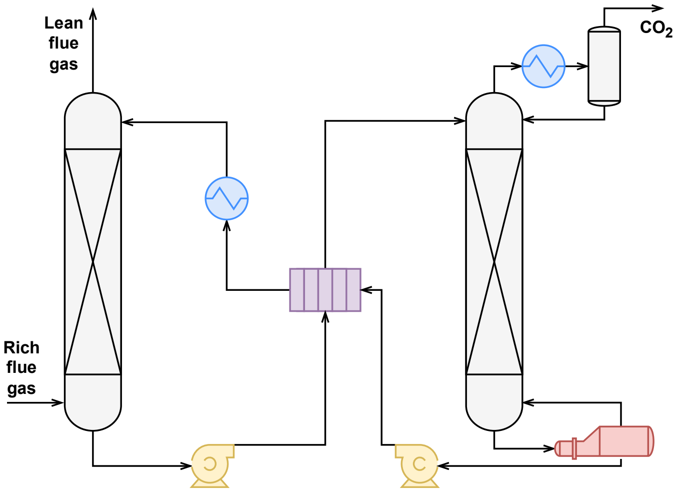

Figure 1.1: Simplified overview of the amine scrubbing process.

During this process, the amines are prone to undergo irreversible degradation reactions. This can occur as the solvent comes into contact with oxidizing species in the gas or when it is heated to high temperatures during the regeneration step.[16,17] The degradation of the solvent causes operational problems such as corrosion, foaming, and solvent losses.[18]

Typical amine solvents consist of a single amine, or a mixture of amines, in water. Monoethanol amine (MEA) is one of the most studied amines, and 30wt% aqueous MEA has long been considered the benchmark solvent for CCS.[19] An aqueous mixture of piperazine (PZ) and 2-amino-2-methyl-1-propanol (AMP) has, however, later been called the new benchmark solvent.[20] In recent years, water-lean amine systems have been proposed as a possible new solvent for chemical absorption.

Water-lean solvents, also known as hybrid or mixed solvents, are solvents with the common denominator of reduced water content. The idea behind reducing the water content is that the absence of water will reduce energy consumption during solvent regeneration.[21,22] The collective term of water-lean solvents covers a broad variety of solvents. The reduction in water can be achieved simply by increasing the concentration of the amine or by exchanging the water with another cosolvent. Solvent systems of both kinds have been developed[23–32], and some have been tested at pilot scale.[33–36]

1.1.2 Gas Dehydration

Natural gas is usually saturated with water when it is extracted from the reservoirs and/or water is added during the sweetening process.[37] This water can cause problems in processing and transportation. The most severe problem is the possible formation of hydrates.[38–39] Hydrates are crystalline structures consisting of cages of water encapsulating smaller molecules, e.g. methane. The formation of hydrates can result in plugging of the equipment and the pipelines. Corrosion can also occur as the water condenses, especially if the gas contains acid components such as CO_2 and H_2S.[40,41] In addition, water in the gas increases the volume and decreases the heating value of the gas.[3] Due to this, gas transportation companies usually have specific requirements for the content of water in natural gas. To meet the water content specifications, the natural gas must be dehydrated.

There are several ways of removing water from natural gas. Commercially available methods include adsorption, absorption, condensation, and membrane separation.[42] The most common of these is absorption with glycols, where the water in the gas stream is absorbed into a liquid glycol stream. Glycols are a class of solvents with a wide variety of uses. Structurally, they are aliphatic diols and are a good choice as solvents for dehydration due to their hygroscopic properties, i.e. their affinity towards water.[43] Four glycols are commonly available for dehydration: ethylene glycol (MEG), diethylene glycol (DEG), triethylene glycol (TEG), and tetraethylene glycol (TREG). Their overall strengths in this application are that they have a high absorption efficiency, can be easily regenerated, are in themselves non-corrosive, have a minimal capacity to absorb hydrocarbons and have a low cost.[3] The most commonly used glycol is TEG. This is because it has lower solvent losses and is more stable than the others during the generation, meaning a higher purity of the lean glycol can be achieved with TEG.

Overall, the process is very similar to the amine scrubbing process, with an absorber and a stripper column as the main components. An overview of a glycol dehydration unit is presented in Figure 1.2. The wet gas enters the bottom of the absorber and flows upwards, countercurrent to lean glycol. The glycol enters the column at the top, and as it flows down, it absorbs water from the gas. At the bottom of the absorber, the water-containing rich glycol is transported to a flash tank. In the flash tank, most of the volatile components, such as methane, absorbed into the rich glycol are flashed out. After this, the rich glycol is passed through carbon filters and a lean/rich glycol heat exchanger, before entering the regenerator. The water is removed from the glycol in the regenerator by heat at pressures close to atmospheric. The lean glycol is then cooled in the lean/rich glycol heat exchanger and a glycol cooler before being reintroduced at the top of the absorption column.

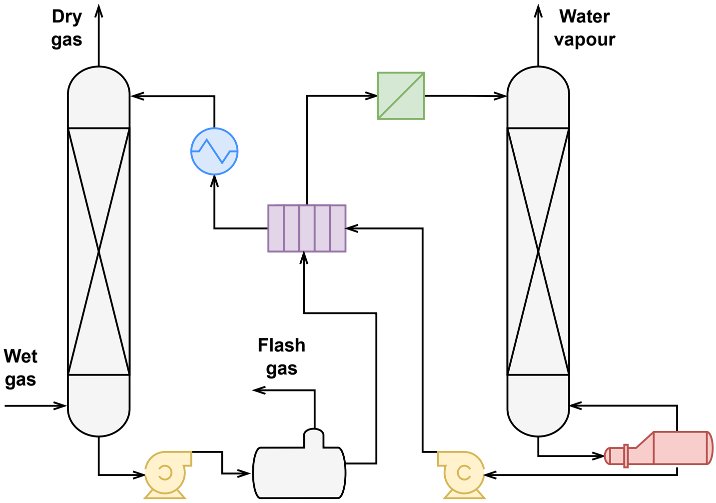

Figure 1.2: Simplified overview of the glycol dehydration process.[45]

During this process, degradation of the glycol can occur. As with the amines, this happens as the glycol comes into contact with oxidizing components in the gas and at elevated temperatures. The oxidizing species can enter the system with incoming gas and through packing glands. Heating the glycol too much can occur if the reboiler temperature is too high or by localized overheating. During operation, degradation of the glycol can cause problems such as corrosion, foaming, and loss of performance.[3,42,45,46]

1.1.3 Solvent Degradation

Solvent degradation has in many cases become synonymous with amine degradation due to the large effort of this research community to overcome this issue. However, as mentioned in the previous section, it is clear that it is also an issue for other solvent systems, such as glycols. Due to the harsh conditions the solvents are exposed to in their respective process, solvent degradation occurs. This results in operational issues and reduced efficiency of the overall process.

The cost of the dehydration is covered by the profits of selling methane. CCS, on the other hand, is not considered profitable for the industry, though there are incentives in place. Naturally, solvent degradation increases the costs for running the processes. This can cause amine-based CO_2 capture from flue gases to become less interesting for the industry from an economic perspective. Reducing costs is an important step to make the technology more viable.

There is also an environmental aspect to consider. As either amine or glycol solvents degrade and must be replaced, the problem of the large amounts of solvent waste becomes apparent. There are options for treating the degraded solvent,[47,48] but also this results in concentrated degradation residue, which must be handled. This chemical waste can be a potential strain on the environment and should be minimized.

Knowledge of what is occurring in the solvent systems is important to counteract or lessen the impact of solvent degradation. This includes knowledge of which components are being formed and by which reactions they are being formed, to which parameters are affecting the reactions. With this knowledge, techniques for monitoring, options for reclaiming, and potential degradation inhibitors can be developed.

1.2 Objectives of the Thesis

The main objective of this work was to increase the understanding of the chemical processes occurring as solvents used in amine-based CO_2 capture and in glycol-based gas dehydration degrade. There has been an emphasis on laboratory-scale experiments, which were conducted with the intent of achieving enhanced degradation rates.

Oxidative and thermal degradation of selected water-lean amine systems were studied. Through this, the aim was to study the effect of the solvent on the stability of the amine. The oxidative and thermal stability of glycols was also studied. Triethylene glycol was selected as the test solvent due to its importance in the gas dehydration process. The goal of this part was to map degradation components formed during the degradation process. Simultaneously, there was a focus on developing analytical methods for quantifying glycols and their degradation products.

1.3 Outline of the Thesis

This thesis is a collection of published or submitted papers.

Chapter 2 contains a short literature review of the current knowledge on the stability of amines and glycols.

Chapter 3 describes the experimental and analytical methods employed in this work.

Chapter 4 presents a review paper on degradation and emissions in pilot-scale CO_2 capture.

Chapter 5 presents a journal paper on how the choice of solvent affects the thermal stability of amines.

Chapter 6 presents a conference paper on effect of increased amine concentrations the oxidative degradation of MEA, in addition to a discussion of the challenges related to doing experimental studies on the stability of water-lean solvent systems.

Chapter 7 presents a manuscript about developed analytical tools for the monitoring of glycols degradation, in addition to results from a thermal degradation study of TEG.

Chapter 8 presents a manuscript on the oxidative degradation of triethylene glycol.

Chapter 9 contains a summary of the findings of this thesis and recommendations for further work.

1.4 Papers and Presentations

1.4.1 List of Journal Publication

Buvik, Vanja; **Høisæter, Karen K.**; Vevelstad, Solrun & Knuutila, Hanna K., A review of degradation and emissions in post-combustion CO_2 capture pilot plants. Int. J. Greenh. Gas Control, Vol 106, 2021, 103246.
https://doi.org/10.1016/j.ijggc.2020.103246

The second author contributed to data collection, writing parts of the first draft, revision of the manuscript before and after peer review and editing before resubmission.

Høisæter, Karen K.; Vevelstad, Solrun; Braakhuis, Lucas & Knuutila, Hanna K. The Impact of the Solvent on the Thermal Stability of Amines. Ind. Eng. Chem. Res., Vol 61, 2022, 16179–16192.
https://doi.org/10.1021/acs.iecr.2c01934

The first author carried out most of the experimental work and wrote the first draft of the manuscript.

Høisæter, Karen K.; Buvik, Vanja; Vevelstad, Solrun; & Knuutila, Hanna K. Analytical Tools for Monitoring Glycol Degradation. To be submitted.

The first author carried out the experimental work and parts of the analyses and wrote the first draft of the manuscript.

Høisæter, Karen K.; Buvik, Vanja; Gonzalez, Susana Villa; Vevelstad, Solrun; & Knuutila, Hanna K. Oxidative Degradation of Triethylene Glycol. Under revision.

The first author carried out the oxidative degradation experiments, parts of the analyses and wrote the first draft of the manuscript.

1.4.2 List of Conference Publications

Høisæter, Karen K., Nordberg, Andrea E., Buvik, Vanja, Vevelstad, Solrun J., Grimstvedt, Andreas & Knuutila, Hanna K. An Experimental Assessment on the Impact of Amine Concentration on the Oxidative Degradation of Amines. Proceedings of the 16th Greenhouse Gas Control Technologies Conference (GHGT-16) 23-24 Oct 2022. http://dx.doi.org/10.2139/ssrn.4286486

The first author supervised the second author and wrote the first draft of the manuscript.

1.4.3 List of Conference Presentations

Høisæter, Karen K. & Knuutila, Hanna K. Degradation Potential of Aqueous and Water-Lean MEA (17.-19.06.2019). Trondheim CCS Conference TCCS-10. *Oral presentation*.

Høisæter, Karen K. & Knuutila, Hanna K. Degradation Potential of Aqueous and Water-Lean MEA – part 2 (17.-20.09.2019). 5th Post Combustion Capture Conference PCCC-5, Kyoto Japan. *Oral presentation*.

Høisæter, Karen K.; Nordberg, Andrea E.; Buvik, Vanja; Vevelstad, Solrun J., Grimstvedt, Andreas, & Knuutila, Hanna K. An Experimental Assessment on the Impact of Amine Concentration on the Oxidative Degradation of Amines. 16th International Conference on Greenhouse Gas Control Technologies GHGT-16, Lyon, France. *Oral presentation*.

1.4.4 List of Publications not Part of the Thesis

Janakiram, Saravanan; Espejo, Juan L. M.; **Høisæter, Karen K.**; Lindbråthen, Arne; Ansaloni, Luca & Deng, Liyuan. Three-phase hybrid facilitated transport hollow fiber membranes for enhanced CO_2 separation. Appl. Mater. Today, Vol 21, 2020, 100801. https://doi.org/10.1016/j.apmt.2020.100801

Wanderley, Ricardo R.; **Høisæter, Karen K**. & Knuutila, Hanna K. Signs of alkylcarbonate formation in water-lean solvents: VLE-based understanding of pKa and pKs effects. Int. J. Greenh. Gas Control, Vol. 109, 2021, 103398. https://doi.org/10.1016/j.ijggc.2021.103398

Braakhuis, Lucas; **Høisæter, Karen K.** & Knuutila, Hanna K. Modeling the Formation of Degradation Compounds during Thermal Degradation of MEA. Ind. Eng. Chem. Res., Vol. 61, 2022, 2867-2881. https://doi.org/10.1021/acs.iecr.1c04496

1.5 References

(1) Kohl, A. L.; Nielsen, R. B. Introduction. *Gas Purif*. **1997**, 1–39. https://doi.org/10.1016/B978-088415220-0/50001-X.

(2) Eimer, D. Gas Treating: Absorption Theory and Practice. **2014**, 441.

(3) Mokhatab, S.; Poe, W. A.; Mak, J. Y. Natural Gas Dehydration. In *Handbook of Natural Gas Transmission and Processing*; 2015; pp 223–263. https://doi.org/10.1016/b978-0-12-801499-8.00007-9.

(4) Zevenhoven, R.; Kilpinen, P. Chapter 2 - Flue Gases and Fuel Gases. In *Control of pollutants in flue gases and fuel gases*; 2001; pp 1–12.

(5) Feron, P. H. M. M. Introduction. In *Absorption-Based Post-combustion Capture of Carbon Dioxide*; Elsevier Inc., 2016; pp 3–12. https://doi.org/10.1016/b978-0-08-100514-9.00001-9.

(6) Zevenhoven, R.; Kilpinen, P. Chapter 9 - Greenhouse Gases, Ozone-Depleting Gases. In *Control of pollutants in flue gases and fuel gases*; 2001; pp 1–12.

(7) Rogelj, J.; Shindell, D.; Jiang, K.; Fifita, S.; Forster, P.; Ginzburg, V.; Handa, C.; Kheshgi, H.; Kobayashi, S.; Kriegler, E.; Mundaca, L.; Séférian, R.; Vilariño, M. V. *Mitigation Pathways Compatible with 1.5°C in the Context of Sustainable Development*; Pallav Purohit, 2018.

(8) Braakhuis, L.; Høisæter, K. K.; Knuutila, H. K. Modeling the Formation of Degradation Compounds during Thermal Degradation of MEA. *Ind. Eng. Chem. Res.* **2022**, 61 (7), 2867–2881. https://doi.org/10.1021/acs.iecr.1c04496.

(9) Bui, M.; Adjiman, C. S.; Bardow, A.; Anthony, E. J.; Boston, A.; Brown, S.; Fennell, P. S.; Fuss, S.; Galindo, A.; Hackett, L. A.; Hallett, J. P.; Herzog, H. J.; Jackson, G.; Kemper, J.; Krevor, S.; Maitland, G. C.; Matuszewski, M.; Metcalfe, I. S.; Petit, C.; Puxty, G.; Reimer, J.; Reiner, D. M.; Rubin, E. S.; Scott, S. A.; Shah, N.; Smit, B.; Trusler, J. P. M.; Webley, P.; Wilcox, J.; Mac Dowell, N. Carbon Capture and Storage (CCS): The Way Forward. *Energy Environ. Sci.* **2018**, 11 (5), 1062–1176. https://doi.org/10.1039/c7ee02342a.

(10) Rochelle, G. T. Conventional Amine Scrubbing for CO_2 Capture. In *Absorption-Based Post-Combustion Capture of Carbon Dioxide*; Elsevier Inc., 2016; pp 35–67. https://doi.org/10.1016/B978-0-08-100514-9.00003-2.

(11) Danckwerts, P. V. The Reaction of CO_2 with Ethanolamines. *Chem. Eng. Sci.* **1979**, 34 (4), 443–446. https://doi.org/10.1016/0009-2509(79)85087-3.

(12) Johnson, S. L.; Morrison, D. L. Kinetics and Mechanism of Decarboxylation of *N*-Arylcarbamates. Evidence for Kinetically Important Zwitterionic Carbamic Acid Species of Short Lifetime. *J. Am. Chem. Soc.* **2002**, 94 (4), 1323–1334. https://doi.org/10.1021/JA00759A045.

(13) Da Silva, E. F.; Svendsen, H. F. Computational Chemistry Study of Reactions, Equilibrium and Kinetics of Chemical CO_2 Absorption. *Int. J.*

Greenh. Gas Control **2007**, 1 (2), 151–157. https://doi.org/10.1016/S1750-5836(07)00022-9.

(14) Kortunov, P. V; Siskin, M.; Baugh, L. S.; Calabro, D. C. In Situ Nuclear Magnetic Resonance Mechanistic Studies of Carbon Dioxide Reactions with Liquid Amines in Aqueous Systems: New Insights on Carbon Capture Reaction Pathways. *Energy and Fuels* **2015**, 29 (9), 5919–5939. https://doi.org/10.1021/acs.energyfuels.5b00850.

(15) Park, J. Y.; Yoon, S. J.; Lee, H. Effect of Steric Hindrance on Carbon Dioxide Absorption into New Amine Solutions: Thermodynamic and Spectroscopic Verification through Solubility and NMR Analysis. *Environ. Sci. Technol.* **2003**, 37 (8), 1670–1675. https://doi.org/10.1021/es0260519.

(16) Gouedard, C.; Picq, D.; Launay, F.; Carrette, P. L. Amine Degradation in CO_2 Capture. I. A Review. *Int. J. Greenh. Gas Control* **2012**, 10, 244–270. https://doi.org/10.1016/j.ijggc.2012.06.015.

(17) Mazari, S. A.; Si Ali, B.; Jan, B. M.; Saeed, I. M.; Nizamuddin, S. An Overview of Solvent Management and Emissions of Amine-Based CO_2 Capture Technology. *Int. J. Greenh. Gas Control* **2015**, 34, 129–140. https://doi.org/10.1016/j.ijggc.2014.12.017.

(18) Chakma, A.; Meisen, A. Methyl-Diethanolamine Degradation — Mechanism and Kinetics. *Can. J. Chem. Eng.* **1997**, 75 (5), 861–871. https://doi.org/10.1002/cjce.5450750506.

(19) Moser, P.; Wiechers, G.; Schmidt, S.; Garcia Moretz-Sohn Monteiro, J.; Charalambous, C.; Garcia, S.; Sanchez Fernandez, E. Results of the 18-Month Test with MEA at the Post-Combustion Capture Pilot Plant at Niederaussem – New Impetus to Solvent Management, Emissions and Dynamic Behaviour. *Int. J. Greenh. Gas Control* **2020**, 95, 102945. https://doi.org/10.1016/J.IJGGC.2019.102945.

(20) Feron, P. H. M.; Cousins, A.; Jiang, K.; Zhai, R.; Garcia, M. An Update of the Benchmark Post-Combustion CO_2-Capture Technology. *Fuel* **2020**, 273, 117776. https://doi.org/10.1016/J.FUEL.2020.117776.

(21) Wanderley, R. R.; Pinto, D. D. D.; Knuutila, H. K. From Hybrid Solvents to Water-Lean Solvents – A Critical and Historical Review. *Sep. Purif. Technol.* **2021**, 260, 1383–5866. https://doi.org/10.1016/j.seppur.2020.118193.

(22) Heldebrant, D. J.; Koech, P. K.; Glezakou, V.-A.; Rousseau, R.; Malhotra, D.; Cantu, D. C. Water-Lean Solvents for Post-Combustion CO Capture: Fundamentals, Uncertainties, Opportunities, and Outlook. *Chem. Rev.* **2017**, 117 (14), 9594. https://doi.org/10.1021/acs.chemrev.6b00768.

(23) Zheng, C.; Tan, J.; Wang, Y. J.; Luo, G. S. CO 2 Solubility in a Mixture Absorption System of 2-Amino-2-Methyl-1-Propanol with Glycol. *Ind. Eng. Chem. Res.* **2012**, 51 (34), 11236–11244. https://doi.org/10.1021/IE3007165.

(24) Karlsson, H. K.; Sanku, M. G.; Svensson, H. Absorption of Carbon Dioxide in Mixtures of *N*-Methyl-2-Pyrrolidone and 2-Amino-2-Methyl-1-Propanol. *Int. J. Greenh. Gas Control* **2020**, 95, 102952. https://doi.org/10.1016/j.ijggc.2019.102952.

(25) Karlsson, H. K.; Drabo, P.; Svensson, H. Precipitating Non-Aqueous Amine Systems for Absorption of Carbon Dioxide Using 2-Amino-2-Methyl-1-Propanol. *Int. J. Greenh. Gas Control* **2019**, 88, 460–468.

(26) Garcia, M.; Knuutila, H. K.; Aronu, U. E.; Gu, S. Influence of Substitution of Water by Organic Solvents in Amine Solutions on Absorption of CO_2. *Int. J. Greenh. Gas Control* **2018**, 78, 286–305. https://doi.org/10.1016/J.IJGGC.2018.07.029.

(27) Barzagli, F.; Mani, F.; Peruzzini, M. Efficient CO_2 Absorption and Low Temperature Desorption with Non-Aqueous Solvents Based on 2-Amino-2-Methyl-1-Propanol (AMP). *Int. J. Greenh. Gas Control* **2013**, 16, 217–223. https://doi.org/10.1016/J.IJGGC.2013.03.026.

(28) Wanderley, R. R.; Knuutila, H. K. Mapping Diluents for Water-Lean Solvents: A Parametric Study. *Ind. Eng. Chem. Res.* **2020**, 59 (25), 11656–11680. https://doi.org/10.1021/acs.iecr.0c00940.

(29) Skylogianni, E.; Perinu, C.; Cervantes Gameros, B. Y.; Knuutila, H. K. Carbon Dioxide Solubility in Mixtures of Methyldiethanolamine with Monoethylene Glycol, Monoethylene Glycol–Water, Water and Triethylene Glycol. *J. Chem. Thermodyn.* **2020**, 151, 106176. https://doi.org/10.1016/j.jct.2020.106176.

(30) Pakzad, P.; Mofarahi, M.; Izadpanah, A. A.; Afkhamipour, M.; Lee, C. H. An Experimental and Modeling Study of CO_2 Solubility in a 2-Amino-2-Methyl-1-Propanol (AMP) + *N*-Methyl-2-Pyrrolidone (NMP) Solution. *Chem. Eng. Sci.* **2018**, 175, 365–376. https://doi.org/10.1016/j.ces.2017.10.015.

(31) Barzagli, F.; Lai, S.; Mani, F. Novel Non-Aqueous Amine Solvents for Reversible CO_2 Capture. *Energy Procedia* **2014**, 63, 1795–1804. https://doi.org/10.1016/j.egypro.2014.11.186.

(32) Barzagli, F.; Giorgi, C.; Mani, F.; Peruzzini, M. Reversible Carbon Dioxide Capture by Aqueous and Non-Aqueous Amine-Based Absorbents: A Comparative Analysis Carried out by ^{13}C NMR Spectroscopy. *Appl. Energy* **2018**, 220, 208–219. https://doi.org/10.1016/j.apenergy.2018.03.076.

(33) RTI International. *Testing of RTI's Non-Aqueous Solvent CO_2 Capture Process at NCCC Using the SSTU*; 2018.

(34) Freeman, C. *Molecular Refinement of Transformational Solvents for CO_2 Separations*; 2019.

(35) Brown, A. "Buz"; Awtry, A.; Meuleman, E. *ION Advanced Solvent CO_2 Capture Pilot Project*; Pittsburgh, PA, and Morgantown, WV (United States), 2018. https://doi.org/10.2172/1484045.

(36) Hancu, D. *Large Pilot-Scale Carbon Dioxide (CO_2) Capture Project Using Aminosilicone Solvent*; Pittsburgh, PA, and Morgantown, WV (United States), 2017. https://doi.org/10.2172/1414342.

(37) Piemonte, V.; Maschietti, M.; Gironi, F. A Triethylene Glycol-Water System: A Study of the TEG Regeneration Processes in Natural Gas Dehydration Plants. *Energy Sources, Part A Recover. Util. Environ. Eff.* **2012**, 34 (5), 456–464. https://doi.org/10.1080/15567031003627930.

(38) Englezos, P. Reviews - Clathrate Hydrates. *Ind. Eng. Chem. Res* **1993**, 32, 1251–1274.

(39) Hammerschmidt, E. G. Formation of Gas Hydrates in Natural Gas Transmission Lines. *Ind. Eng. Chem.* **1934**, 26 (8), 851–855. https://doi.org/10.1021/ie50296a010.

(40) Chebbi, R.; Qasim, M.; Abdel Jabbar, N.; Jabbar, N. A. Optimization of Triethylene Glycol Dehydration of Natural Gas. *Energy Reports* **2019**, 5, 723–732. https://doi.org/10.1016/J.EGYR.2019.06.014.

(41) Karimi, A.; Abedinzadegan Abdi, M. Selective Dehydration of High-Pressure Natural Gas Using Supersonic Nozzles. *Chem. Eng. Process.* **2009**, 48, 560–568. https://doi.org/10.1016/j.cep.2008.09.002.

(42) John M. Campbell and Company. *Gas Conditioning and Processing*; 2004.

(43) Moss, G. P.; Smith, P. A. S.; Tavernier, D. Glossary of Class Names of Organic Compounds and Reactive Intermediates Based on Structure (IUPAC Recommendations 1995). *Pure Appl. Chem.* **1995**, 67 (8–9), 1307–1375. https://doi.org/10.1351/pac199567081307

(44) GPSA. Dehydration. In *Engineering data book*; Gas Processors Suppliers Association: Tulsa, Oklahoma, 2014.

(45) AlHarooni, K.; Pack, D.; Iglauer, S.; Gubner, R.; Ghodkay, V.; Barifcani, A. Effects of Thermally Degraded Monoethylene Glycol with Methyl Diethanolamine and Film-Forming Corrosion Inhibitor on Gas Hydrate Kinetics. *Energy & Fuels* **2017**, 31 (6), 6397–6412. https://doi.org/10.1021/acs.energyfuels.7b00733.

(46) Alef, K.; Smith, C.; Iglauer, S.; Gubner, R.; Barifcani, A. MEG on Hydrate Inhibition Performance over Multiple Regeneration Cycles. *Fuel* **2018**, 222, 638–647. https://doi.org/10.1016/j.fuel.2018.02.190.

(47) Kentish, S. E. Reclaiming of Amine-Based Absorption Liquids Used in Post-Combustion Capture. In *Absorption-Based Post-Combustion Capture of Carbon Dioxide*; Elsevier Ltd, 2016; pp 426–438. https://doi.org/10.1016/B978-0-08-100514-9.00017-2.

(48) Ju, H.; ElMoudir, W.; Aboudheir, A.; Mahinpey, N. Development of a Facile Reclaiming Process for Degraded Alkanolamine and Glycol Solvents Used for CO_2 Capture Systems. *Int. J. Greenh. Gas Control* **2018**. 74, 174-181. https://doi.org/10.1016/j.ijggc.2018.05.004.

Chapter 2

Literature review

This chapter will be divided into two parts, covering each of the two solvent classes studied in this PhD work. Each part will give an overview of what is known about the oxidative and thermal degradation of the solvents and an overview on analytical techniques used to monitor the solvent systems.

2.1 Amine Degradation

Amines are known to oxidatively and thermally degrade during the amine scrubbing process. Even though MEA is no longer considered the most commonly used amine in this process, it is by far the most thoroughly studied amine when it comes to degradation. As a laboratory test system for amine degradation, MEA works very well. It degrades more readily than many other amines, which allows experiments to be conducted within a reasonable timeframe. In addition, due to the extensive research done on the degradation of MEA, many degradation components are already identified, and multiple mechanisms have been proposed. Many of the more stable amines seem to undergo similar degradation reactions as MEA, so the knowledge gained from this system can be valuable for the overall picture of amine degradation.[1] Because of this, the mechanistic study presented here will focus on MEA.

2.1.1 Oxidative Degradation of Amines

Oxidative degradation of amines occurs as the amine comes into contact with oxidizing species in the flue gas, such as O_2, SOx, and NOx. The degradation products formed are categorized into three groups, primary degradation products, secondary degradation products, and nitrous amines. A selection of the main primary and secondary oxidative degradation products is presented in Table 2.1.

Table 2.1: Names, abbreviations, CAS numbers, and chemical structures of many of the primary and secondary oxidative degradation products of MEA.

Name	**Abbrev.**	**CAS number**	**Structure**
		Primary degradation products	
Acetaldehyde	-	75-07-0	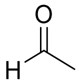
Acetic acid	-	64-19-7	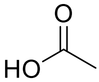
Formic acid	-	71-47-6	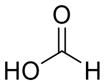
Formaldehyde	-	50-00-0	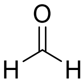
Glycolic acid	-	79-14-1	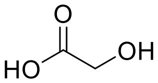
Glyoxal	-	131543-46-9	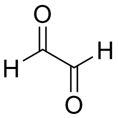
Glyoxylic acid	-	298-12-4	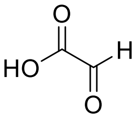
Oxalic acid	-	144-62-7	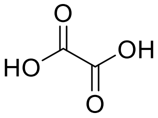
		Secondary degradation products	
N,N'-Bis(2-hydroxyethyl)-oxamide	BHEOX	1871-89-2	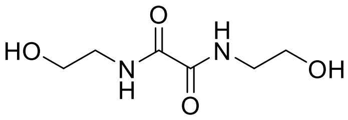
N-(2-Hydroxyethyl)-acetamide	HEA	142−26-7	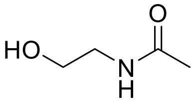

N-(2-Hydroxyethyl)-formamide	HEF	693−06-1	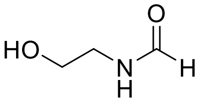
N-(2-Hydroxyethyl)-glycine	HeGly	5835-28-9	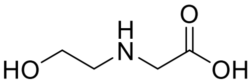
(*N*-(2-Hydroxyethyl)-2-(hydroxyethyl)-amino)acetamide	HEHEAA	144236-39-5	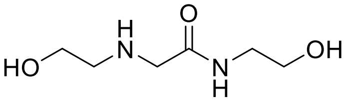
N-(2-Hydroxyethyl)-imidazole	HEI	1615−14-1	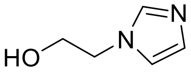
2-((2-Hydroxy-ethyl)amino)-2-oxoacetic acid	HEOX	5270-73-5	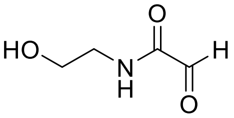
4-(2-Hydroxyethyl)-2-piperazinone	HEPO	23936-04-1	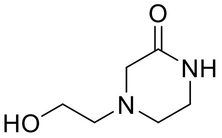
1-(2-Hydroxyethyl)-2-piperazinone	1HEPO	59702-23-7	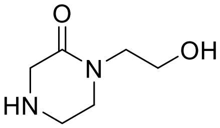
2-Hydroxy-*N*-(2-hydroxyethyl)-acetamide	HHEA	3586-25-2	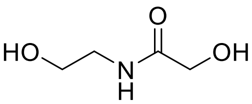

The initial oxidative degradation mechanism is believed to happen via a radical mechanism with the amine and the oxidizing species. How it is occurring is still unclear, though it is believed to happen via oxidation initiated by an electron or hydrogen abstraction.[2–4] The reaction forms oxidized fragments in the form of ammonia, organic acids, aldehydes and alkylamines. A collection of these is shown in Scheme 2.1.[5] Secondary degradation products are formed as the solvent amine reacts with the primary degradation products or with other secondary degradation products.

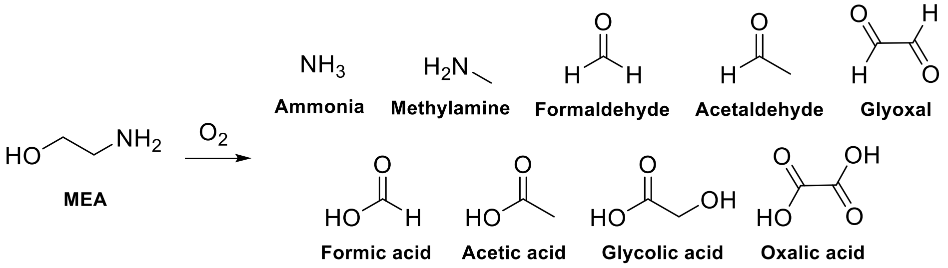

Scheme 2.1: Formation of primary oxidative degradation products of MEA.[5]

Many of the secondary degradation products are suspected to form through reactions between the solvent amine and the acidic primary degradation products. HEF, HEA, HHEA, and HEOX are such compounds. An overview of the formation of these is presented in Scheme 2.2.[5–7] As oxalic acid has two acid groups, once HEOX is formed, it can potentially react one more time to form BHEOX.[6] It should be noted that HEOX is only tentatively identified, as it has not been identified by MS or by a commercially available standard. The identification has been done based on a standard synthesized in the laboratory, confirmed by qualitative NMR analysis. The peak in the IC chromatogram of this standard overlapped with an unknown peak in oxidatively degraded MEA.[8]

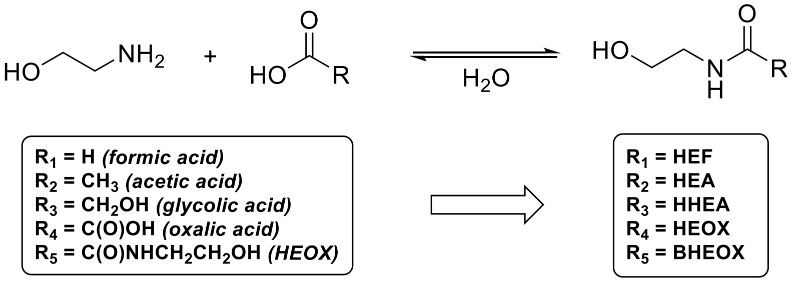

Scheme 2.2: Proposed formation of HEF, HEA, HHEA, HEOX, and BHEOX following da Silva et al.[5], Lepaumier et al.[6], and Strazisar et al.[7]

There are some oxidative degradation compounds whose formation is not as straightforward to explain. In laboratory experiments, HeGly has not been found to be a condensation product of any two other degradation products. Vevelstad et al.[9] have proposed that HeGly is formed through a reaction between MEA and glyoxylic acid, as presented in Scheme 2.3. Gouedard[10] has, on the other hand, proposed that the formation of HeGly occurs in an equilibrium reaction of HEHEAA and MEA.

This would require an initial formation of HEHEAA, which is explained by a reaction between glyoxal and two MEA molecules. The total mechanism proposed for the formation of HEHEAA and HeGly is presented in Scheme 2.4.

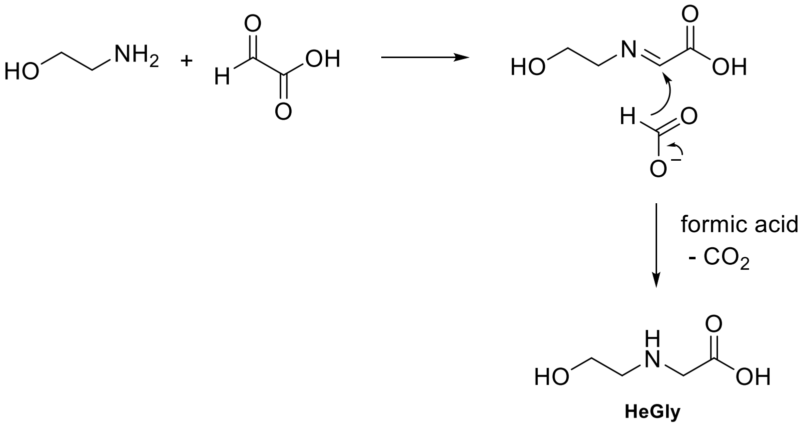

Scheme 2.3: Formation of HeGly from MEA and glycolic acid, as proposed by Vevelstad et al.[9]

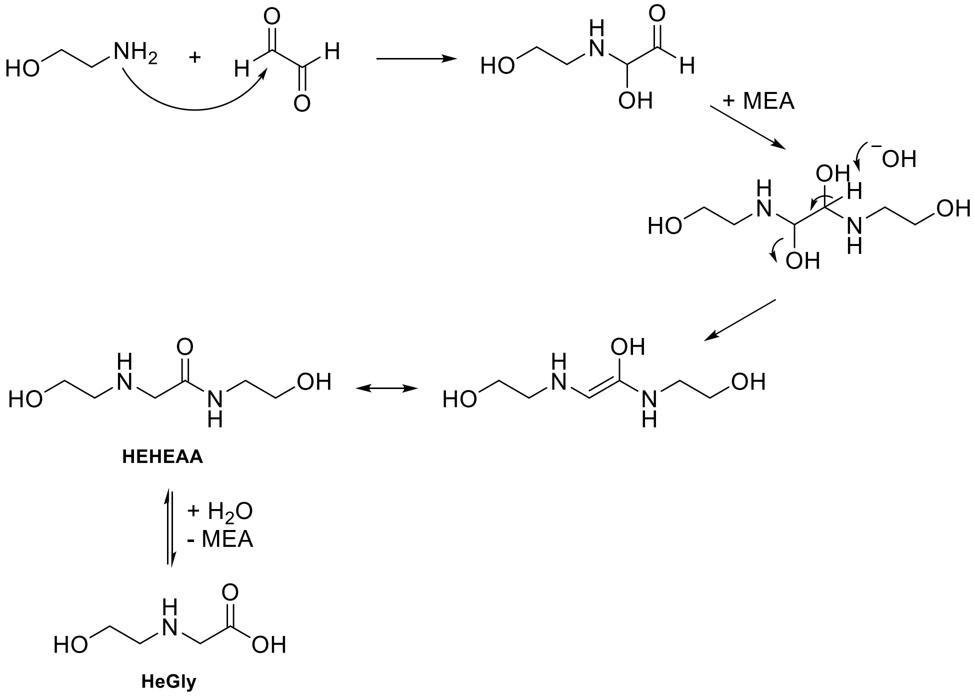

Scheme 2.4: Formation of HeGly from MEA and glyoxal via HEHEAA as proposed by Gouedard.[10]

Da Silva et al.[5] have proposed that the formation of HEHEAA happens with HeGly and MEA as reactants, similar to the last equilibrium reaction of Scheme 2.4. In this case, the reaction is expected to be a condensation reaction similar to those with the acid primary degradation compounds. Additionally, Strazisar et al.[7] have proposed that the formation of HEHEAA occurs through an iron-catalyzed radical reaction between MEA and HEA.

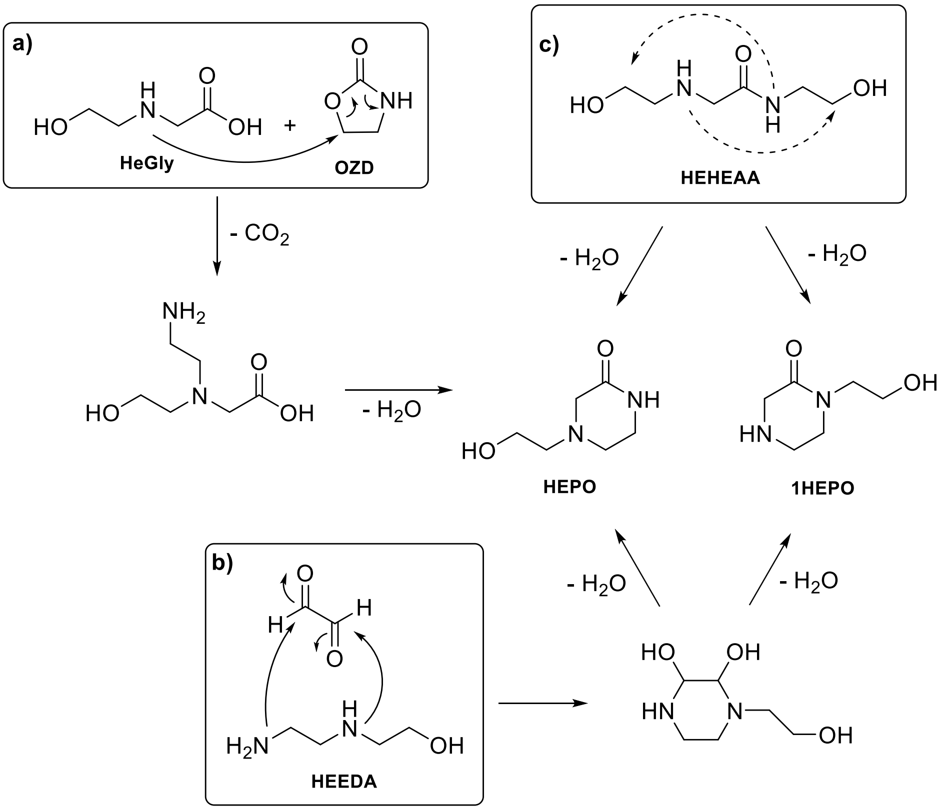

Scheme 2.5: Formation of HEPO and 1HEPO following a) and b) as described by Gouedard[10] and c) as described by Strazisar et al.[7] and da Silva et al.[5]

Multiple mechanisms have been proposed to explain the formation of HEPO and 1HEPO. An overview of these is presented in Scheme 2.5. Gouedard[10] have proposed a possible pathway for the formation of HEPO and 1HEPO, in addition to one pathway for the formation of only HEPO. In the former, HEEDA and glyoxal react and depending on where carbonyl is formed HEPO or 1HEPO is formed. In the latter, the formation of HEPO occurs as a result of HeGly attacking OZD. After the ring opening of OZD, a nucleophilic attack by the amine group on the acid group results in a new ring formation and the formation of HEPO. HEPO is generally found in higher concentrations than 1HEPO, and this additional pathway to form HEPO is explained as the possible reason for this. Strazisar et al.[7] and da Silva et al.[5] have proposed another mechanism for the formation of HEPO and 1HEPO starting from HEHEAA. This is expected to be a self-condensation, and depending on which carbon is attacked, either HEPO or 1HEPO is formed. Da Silva et al.[5] additionally report that the formation of HEPO and 1HEPO required high temperatures. They propose that this is the reason why there are such large deviations in how much HEPO is found at different plants, as strippers are operated differently at different plants.

Though HEI is an important degradation product found in pilot plants, it is still unclear how it is formed. Vevelstad et al.[9] have proposed a mechanism where MEA reacts with glyoxylic acid, via an imine, to form HEI, as presented in Scheme 2.6. The formation of HEI has been found to increase with both oxygen and temperature.

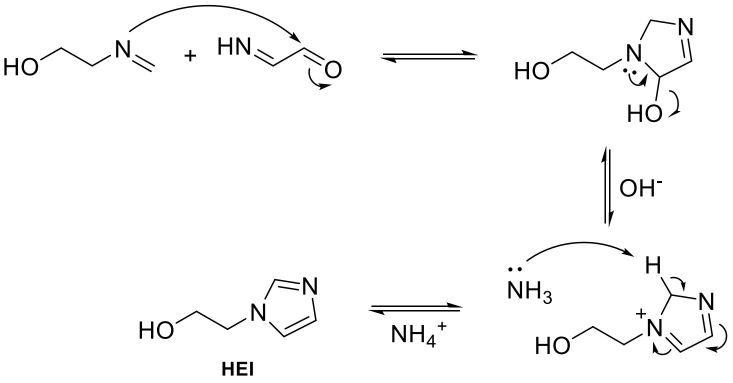

Scheme 2.6: Formation of HEI as proposed by Vevelstad et al.[11]

Which degradation compounds are the major ones found in laboratory scale experiments and pilot scale samples do not coincide. In pilot scale, HEPO and HeGly are reported to be the major degradation compounds.[5,12] In laboratory experiments, however, HEF and HEI are found with the highest concentrations.[11] This discrepancy is likely caused by the different conditions in the two cases. Laboratory scale experiments are often designed to enhance the degradation. This is done to allow more manageable durations of the experiments as well as higher concentrations of the degradation compounds. Vevelstad et al.[13] have conducted a study looking into parameters affecting the degradation pattern seen in open batch degradation experiments. They reported that experiments conducted at 75 °C and with 6% oxygen in the gas sparged into the amine solution gives results resembling degradation seen in cycled degradation rigs and pilot plants.

Other oxidative degradation compounds of MEA have been identified but are usually only found in small quantities. Nitrosamines and nitramines are also only formed in low concentrations, but due to their carcinogenic properties, it is important to accurately account for them.[14] They are expected to form through the reaction between the amines in the solvent and NOx components in the flue gas.[15,16]

2.1.2 Thermal Degradation of Amines

At elevated temperatures and with CO_2 present, the amine can undergo thermal degradation reactions. These reactions are expected to happen predominantly in the stripper and the reboiler.[6,17] The thermal degradation with CO_2, has been found to increase with higher temperatures, pressures, and CO_2 concentrations.[17–19] Thermal degradation of the amine can also occur at elevated temperatures without CO_2 present. In these cases, however, little degradation is observed up to 200 °C.[20]

The thermal degradation of MEA is considered a polymerization reaction, often referred to as the carbamate polymerization reaction. Thermal degradation products expected to form through this mechanism are presented in Table 2.2. MEA reacts with CO_2 to form MEA-carbamate. The MEA-carbamate, or possibly its corresponding acid, can then undergo an intramolecular cyclization to form OZD, as presented in Scheme 2.7.[7] This is suspected to be an intermediate product as it is only present at low concentrations. Furthermore, as a reactive intermediate, it is suspected to take part in many of the following carbamate polymerization reactions. It should be mentioned that OZD has also been found to form through oxidative reactions at lower temperatures.[11]

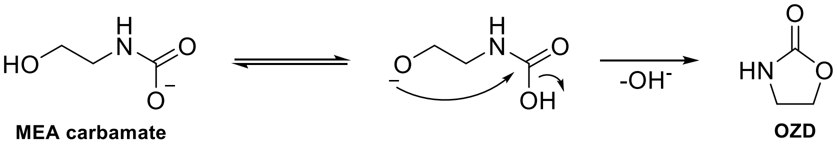

Scheme 2.7: OZD formation by MEA carbamate cyclization.[6,17,18]

Once OZD is formed, MEA will react with it to form larger polymerization products, as presented in Scheme 2.8. HEEDA and HEIA are examples of this. Polderman et al.[21] proposed that of the two, HEIA is formed first from MEA reacting with OZD. From this, HEEDA is formed by an attack of a water molecule and the expulsion of CO_2. Later, Davis[22] has shown that HEIA is readily formed when HEEDA is exposed to CO_2. HEEDA, on the other hand, does not form readily from HEIA under stripper conditions. Studying these reactions further in laboratory experiments, it has been found that HEEDA stabilizes once a certain concentration is reached. HEIA, on the other hand, accumulates over time.[6] These findings substantiate the proposition of HEEDA being an intermediate and HEIA being an end product.

Table 2.2: Names, abbreviations, CAS numbers, and chemical structures of the main thermal degradation products of MEA.

Name	**Abbrev.**	**CAS number**	**Structure**
N-(2-Aminoethyl)-*N*’(2-hydroxyethl)-imidazolidione	AEHEIA	no CAS	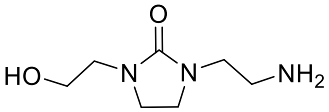
N-(2-((2-Hydroxyethyl)-amino)ethyl)-imidazolidin-2-one	HEAEIA	1154942-78-5	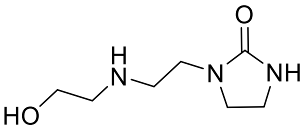
2-(2-Hydroxyethyl-amino)ethanol	HEEDA	111-41-1	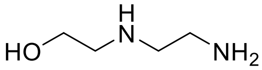
N-(2-Hydroxyethyl)-2-imidazolidione	HEIA	3699-54-5	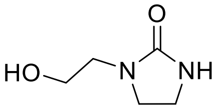
N,*N'*-Bis(2-hydroxyethyl)urea	MEA-urea	15438-70-7	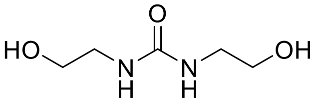
2-Oxazolidinone	OZD	497-25-6	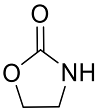
N'-(2-Hydroxyethyl)-diethylentriamine	TRIMEA	1965-29-3	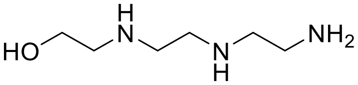

Depending on where on the OZD molecule nitrogen from MEA attacks, either HEEDA or MEA-urea can be formed. When OZD’s carbonyl is attacked, a ring cleavage occurs, and MEA-urea is formed. In this case, CO_2 is not expelled during the reaction.

Similar to the formation of HEEDA, further polymerization compounds can be formed through similar degradation mechanisms as the ones described above. As HEEDA is expected to be formed from a reaction between MEA and OZD, TRIMEA is likely formed through a reaction of HEEDA and OZD.[22] TRIMEA can then react with another OZD to then form bigger polymeric products. In addition to this, TRIMEA is also suggested to undergo a similar cyclization reaction as for the formation of HEIA by reacting with CO_2. This could result in two isomers depending on where the ring closure occurs, AEHEIA or HEAEIA.

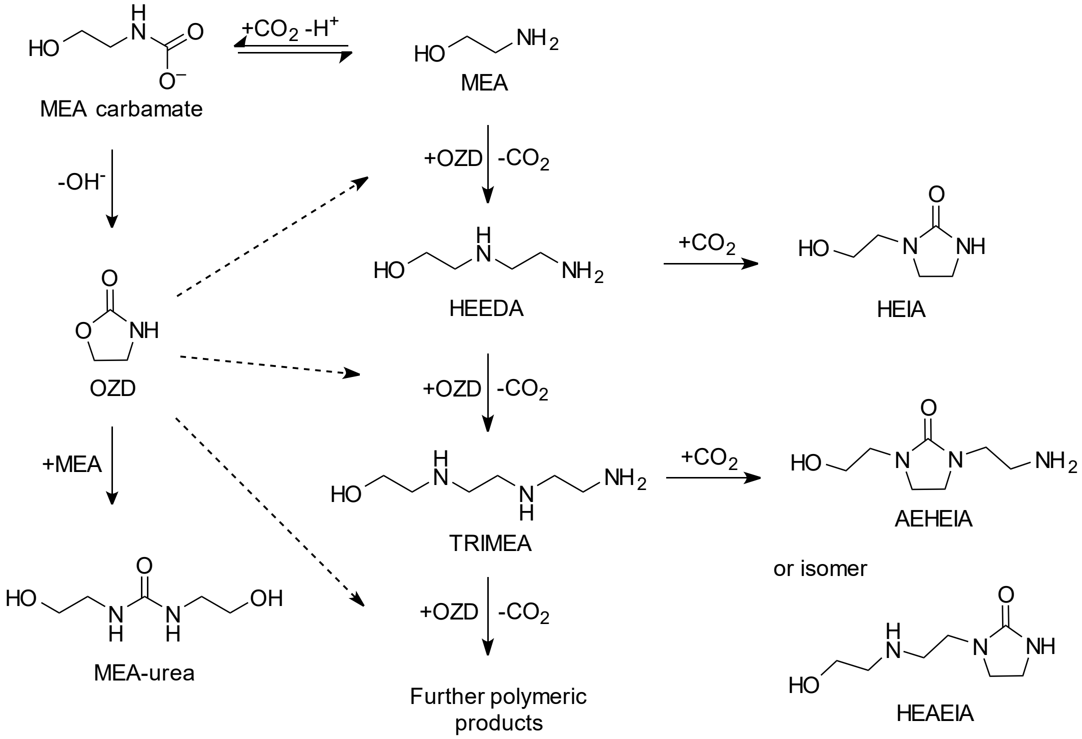

Scheme 2.8: Overview of proposed carbamate polymerization reaction of MEA at stripper conditions.[24]

These mechanisms proposed for the thermal degradation of MEA have been found to be analogous to what is seen during the thermal degradation of other amines such as AP and MMEA.[6,23] Tertiary amines, however, are much more thermally stable than the primary and secondary amines. This is because they do not form carbamate when reacting with CO_2, so naturally they cannot degrade through the carbamate polymerization reaction. For tertiary amines to thermally degrade, they are expected to first go through a dealkylation reaction. Once a secondary amine is formed, thermal degradation can occur as described above.[6]

The thermal degradation products have been found to be less dominant in pilot plants than the oxidative degradation products.[5,25] Both at laboratory and pilot scale, the same main compounds are formed. The most dominant is HEIA, followed by HEEDA and OZD.[6,17]

2.1.3 Water-Lean Solvents

The degradation described above is centered on aqueous amine systems. How it would change when changing the solvent composition is generally not known. Even the effect of the water itself has not yet been studied. For water-lean solvents, there is in general an overall problem that degradation of these systems is barely described in the literature. Of course, a problem here is also that as water-lean solvents can be so many different things, one should be careful with generalizing. All the same, as new solvent systems are being developed, degradation seems to be of very little focus.

Shoukat et al.[26,27] have compared the thermal degradation of aqueous amines to the thermal degradation of mixtures of amines, glycols, and water. In an experiment with MEA, ethylene glycol (MEG), and triethylene glycol (TEG), they found that the solutions with either of the glycols present had a much higher thermal degradation rate than that of the purely aqueous solutions. These trends were also seen in similar experiments with the much more stable methyl diethanolamine (MDEA). In experiments with various tertiary amines, however, cases where the amine was more stable in the glycol-containing solvents were observed. If this is an effect of removing the water or of the presence of the glycol solvent itself has not been further studied.

Some of the water-lean solvents tested at pilot plants claim good results in terms of stability in their reports.[28–31] Very little information is given, however, and as these are proprietary solvents no generalizations can be made.

2.1.4 Monitoring Amines

An overview of the analytical methods used in the CCUS field can be found in a review paper by Cuccia et al.[32] Additionally, Perinu at al.[33] have published a review on NMR spectroscopy applied to amine-CO_2-H_2O systems. A literature review on degradation and emissions in post-combustion CO_2 capture pilot plants can be found in Chapter 4. Included in this review is an overview and discussion of the monitoring techniques applied at pilot scale.

2.2 Glycol Degradation

Like amines, glycols have also been found to undergo oxidative and thermal degradation reactions.[34] Overall, there is very little data available on the degradation of the glycols. This is especially noticeable for TEG. Even though it is the glycol most used for gas dehydration, there are barely any publications describing degradation, and none covering the analytical method used to monitor the glycol system. In the following sections, the literature available on the oxidative and thermal degradation of the glycols will be presented. In both cases, literature on other glycols than TEG will be included, as their similar structure makes it possible that chemical reactions occurring are transferable to the TEG system. Lastly, a short overview of the analytical methods described in the literature is presented. The glycols included are presented in Table 2.3.

Table 2.3: Names, abbreviations, CAS numbers, and chemical structures of the glycols included in the literature review.

Name	Abbrev.	CAS numbers	Structure
Triethylene glycol	TEG	112-27-6	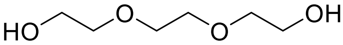
Diethylene glycol	DEG	111-46-6	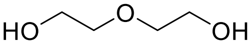
Monoethylene glycol	MEG	107-21-1	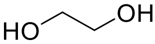
Tetraethylene glycol	TREG	112-60-7	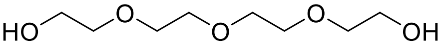
Polyethylene glycol	PEG	25322-68-3	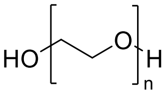

2.2.1 Oxidative Degradation of Glycols

The oxidative degradation of the glycols occurs when the glycols are in contact with oxidizing species, typically oxygen. As this issue is enhanced at elevated temperatures, it is often referred to as thermal-oxidative degradation. The chemical structure of the glycols makes them susceptible to attack by oxygen. The two alcohol groups, typical for all glycols, can potentially be oxidized to first aldehydes and then further to carboxylic acids. For the glycols with longer chains, such as DEG and TEG, the ether bonds are very reactive under oxidating conditions.[35]

As stated earlier, there is not much published on the degradation of TEG. Mokhatab et al.[36] report that the oxidative degradation of TEG results in the formation of organic acids. Forster[37] presents a radical degradation scheme and suggests multiple possible degradation products. It is proposed that the initial oxidation of the TEG occurs on a carbon atom adjacent to the oxygen of the ether. This results in cleavage of the TEG chain, forming smaller molecules. These consist of carboxylic acids (e.g. formic and acetic acid), smaller glycols (e.g. MEG and DEG), and aldehydes. Additionally, the formation of glycol ethers and glycol esters is proposed. Metal ions further accelerate these reactions. There is no data provided to support this.

Data on the oxidative degradation of DEG is also lacking. It has been studied by Lloyd et al.[38] at temperatures up to 95 °C. At low temperatures, they report autoxidation of DEG resulting in the formation of formic acid, formaldehyde, diethylene glycol formate, water, MEG, and 1,3-dioxolane. The structure of some of these is presented in Figure 2.1. In addition, glycol peroxides are suspected of having formed. No CO_2 was detected in their gas phase. At higher temperatures, the formation of total aldehyde and total acid concentrations increased. The existence of MEG and formaldehyde in the system can likely be the cause of formation of 1,3-dioxolanes, which is an acid-catalyzed reaction used industrially.[39,40]

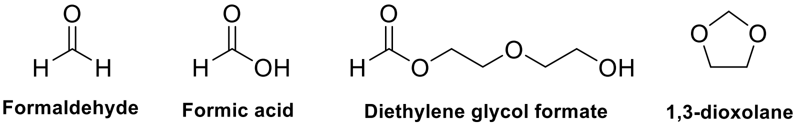

Figure 2.1: Structure of some reported oxidative degradation products of DEG.[38]

MEG is the glycol whose degradation has been most studied. This is due to it being used in heat transfer fluids in solar energy collection systems, where it also has been found to degrade. The literature mainly reports that MEG forms small organic acids as it oxidatively degrades.[41–45] These include formic, acetic, glycolic, glyoxylic, and oxalic acid, shown in Figure 2.2. In this case, simple oxidation of the alcohol groups to form the aldehydes or carboxylic acids is proposed. Formic and glycolic acid are both reported as the main acidic degradation product, though which one is dominant varies.[41,43,44]

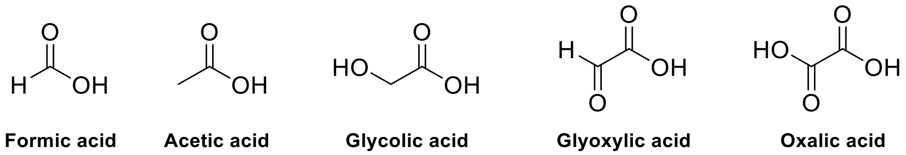

Figure 2.2: Small organic acids formed during the oxidation of MEG.

Brown et al.[46] report the formation of CO_2 during the oxidative degradation of aqueous MEG solutions. This formation occurred at temperatures down to 100 °C, which was the lowest temperature of the experimental study and increased with increasing temperatures. They propose that the formation of CO_2 could occur through a decarboxylation reaction from oxalic acid. Psarrou et al.[44] propose that water is formed as a byproduct of the formation of formic and glycolic acid from MEG. There is however no data to confirm this. The effect of aluminum and copper on the formation of the degradation products of MEG has been studied.[41,46,47] Copper has been found to drastically increase the formation rates of these. Aluminum has a similar effect but to a lesser degree. Increased temperature has also been found to increase the degradation rate of MEG.[46,47]

There are also some studies done on the degradation of glycols with longer carbon chains. The degradation of propylene glycol has for example been studied in connection with the study of MEG.[41,47] The oxidative degradation of propylene glycol resulted in the formation of acids corresponding to those of MEG.

Studies on longer chained glycols are also interesting for understanding possible outcomes of the degradation of TEG. Oxidative degradation of TREG has been reported to result in radical reactions forming hydroperoxides of the ethers in a study by Glastrup et al.[48] This study also reports that the presence of iron or copper decreases the degradation rates, while the presence of nickel accelerates it. In addition, an increase in the temperature was found to increase the degradation rate of TREG. In an additional study by Glastrup,[49] the oxidation of TREG resulted in a bond breakage and the formation of a shortened glycol molecule and formic acid. The formic acid was found to react with TREG, forming first the mono TREG formate and as the reaction went on the di TREG formate was found. An overview of these reactions is presented in Scheme 2.9 and Scheme 2.10.

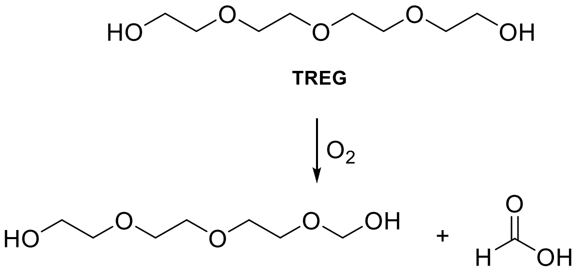

Scheme 2.9: Oxidation of TREG resulting in the formation of a shortened glycol and formic acid.[49]

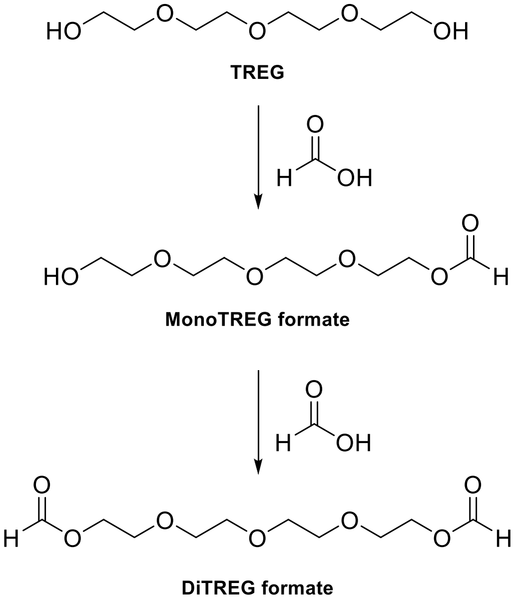

Scheme 2.10: Formation of mono- and di TREG formate through reaction between TREG and formic acid.[49]

A study by Goglev and Neiman[50] on the oxidative degradation of polyethylene glycol (PEG) has also shown this, in addition to the formation of water, CO_2, formaldehyde, acetaldehyde, methyl formate, and ethyl formate. They also present results from isotope marking of the oxygen gas. The formed CO_2 and formaldehyde are found to have oxygen mainly from the labelled gas, while the water contains approximately equal parts labelled and unlabeled. In a study by Han et al.[51] on the oxidative degradation of PEG, peroxides were also proposed to form as a precursor to bond breakage of the esters and the formation of aldehydes. The proposed scheme is presented in Scheme 2.11.

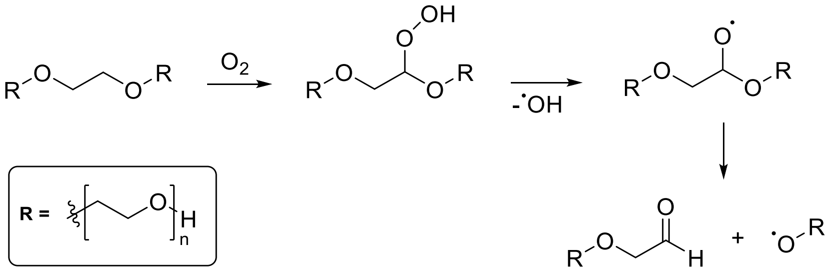

Scheme 2.11: Peroxide formation on a PEG chain, resulting in chain breakage and formation of an aldehyde and a radical fragment.[51]

2.2.2 Thermal Degradation of Glycols

Thermal degradation, also called cracking and pyrolysis, of the glycol are the mechanisms taking place when high temperatures are applied to the glycol without oxygen being present. In the literature, it is reported that TEG starts to thermally degrade at temperatures exceeding 204-206 °C.[34,52,53] As with oxidative degradation, the literature on the thermal degradation of TEG is lacking. Mokhatab et al.[36] report that the thermal degradation of TEG produces acidic degradation products. Forster[37] describes that the thermal degradation of TEG occurs through the formation of radical fragments. These decompose to form smaller fragments, such as small glycols (e.g., DEG and MEG), methanol, ethanol, small aldehydes, and ethers. A corresponding fragmentation has been seen during the thermal degradation of PEG.[54] Madorsicy et al.[54] also describe further breakdown of the PEG chain caused by intramolecular radical reactions forming ethylene oxide, as shown in Scheme 2.12.

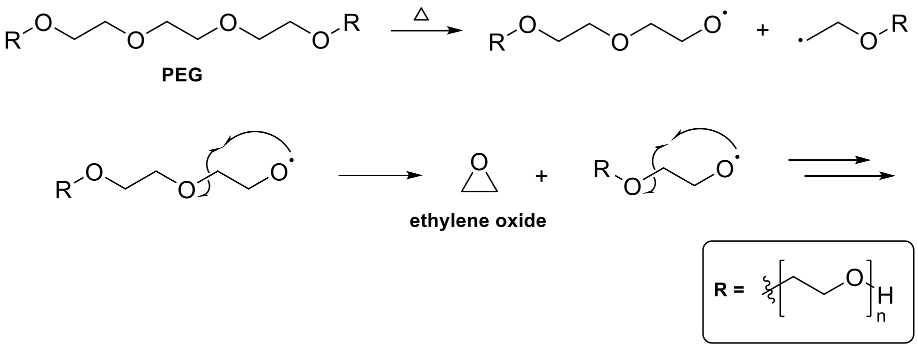

Scheme 2.12: Radical fragmentation of PEG, followed by a chain fragmentation reaction forming ethylene oxide.[54]

Thermal degradation of MEG has been reported to produce acetaldehyde and water, and ethylene oxide and water, through dehydration reactions.[55] The formation of acetaldehyde is supported by MEG's ability to rearrange to convert into acetaldehyde in a concerted migration of a hydride with water loss, as presented in Scheme 2.13.[56] In a study by Vidal et al.[39], MEG was found to polymerize above the boiling point of MEG (197 °C) in a dehydration reaction to form DEG. This opens for the formation of larger glycol chains.

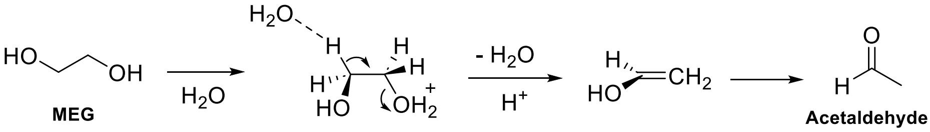

Scheme 2.13: Rearrangement mechanism from MEG to acetaldehyde.[56]

2.2.3 Monitoring Glycols

Just as there is little data published on the degradation of TEG, there are subsequently few publications on analytical techniques for monitoring its degradation. In degradation studies of the various glycols, no analytical technique is published for the quantification of TEG, DEG, or MEG themselves. A method for the quantification of TREG by GC-MS analysis has been published by Glastrup and Padfield[48] and Glastrup[49]. Additionally, techniques for quantification of MEG are described in literature from other fields.[57–60]

Analysis of the small organic acids is published mainly in connection with the oxidative degradation of MEG happening when it is used in heat-transfer fluids in solar collector systems. In this case, multiple techniques have been used. Ion chromatography (IC)[43] and ion chromatography exclusion (ICE)[41] have been used and the methods have been described. In addition, FT-IR and X-ray have been used to study copper(II)salts formed between copper ions and acid products.[42] Another method suggested for quantifying the acids is pH measurements.[46,47] When later compared to results from the quantification of the acids by IC, it was found pH results do not represent the number of acid degradation products found in the degraded solutions.[41] Analysis of O_2 and CO_2 in the gas phase by mass spectroscopy (MS) has been reported, but no information on the instrument or the methodology has been given.[46]

2.3 References

(1) Vevelstad, S. J.; Buvik, V.; Knuutila, H. K.; Grimstvedt, A.; Falck Da Silva, E. Important Aspects Regarding the Chemical Stability of Aqueous Amine Solvents for CO_2 Capture. *Ind. Eng. Chem. Res.* **2022**, 61, 15737-15753. https://doi.org/10.1021/acs.iecr.2c02344.

(2) Rooney, P.; Dupart, M.; Bacon, T. Oxygen’s Role in Alkanolamine Degradation. *Hydrog. Process. (International ed.)* **1998**, 77, 109–113.

(3) Bedell, S. A.; Worley, C. M.; Darst, K.; Simmons, K. Thermal and Oxidative Disproportionation in Amine Degradation-O_2 Stoichiometry and Mechanistic Implications. *Int. J. Greenh. Gas Control* **2011**, 5, 401–404. https://doi.org/10.1016/j.ijggc.2010.03.005.

(4) Rosenblatt, D. H.; Hull, L. A.; Davis, G. T.; Weglein, R. C.; Williams, H. K. R. Oxidations of Amines. III. Duality of Mechanism in the Reaction of Amines with Chlorine Dioxide. *J. Am. Chem. Soc.* **1967**, 89 (5), 1163–1170. https://doi.org/10.1021/ja00981a023.

(5) Da Silva, E. F.; Lepaumier, H.; Grimstvedt, A.; Vevelstad, S. J.; Einbu, A.; Vernstad, K.; Svendsen, H. F.; Zahlsen, K. Understanding 2-Ethanolamine Degradation in Postcombustion CO_2 Capture. *Ind. Eng. Chem. Res.* **2012**, 51, 13329–13338. https://doi.org/10.1021/ie300718a.

(6) Lepaumier, H.; Picq, D.; Carrette, P. L. New Amines for CO_2 Capture. I. Mechanisms of Amine Degradation in the Presence of CO_2. *Ind. Eng. Chem. Res.* **2009**, 48 (20), 9061–9067. https://doi.org/10.1021/ie900472x.

(7) Strazisar, B. R.; Anderson, R. R.; White, C. M. Degradation Pathways for Monoethanolamine in a CO_2 Capture Facility. *Energy and Fuels* **2003**, 17 (4), 1034–1039. https://doi.org/10.1021/ef020272i.

(8) Vevelstad, S. J.; Svendsen, H. F. Challenges Related to Analysis of Anions in Degraded Samples from Pilot and Lab Experiments. *Energy Procedia* **2016**, 86, 181–196. https://doi.org/10.1016/J.EGYPRO.2016.01.019.

(9) Vevelstad, S. J.; Grimstvedt, A.; Knuutila, H.; Falck Da Silva, E.; Svendsen, H. F. Influence of Experimental Setup on Amine Degradation. Int. J. Greenh. Gas Control 2014, 28, 156–167. https://doi.org/10.1016/j.ijggc.2014.06.028.

(10) Gouedard, C. Novel Degradation Products of Ethanolamine (MEA) in CO_2 Capture Conditions: Identification, Mechanisms Proposal and Transposition to Other Amines, 2014.

(11) Vevelstad, S. J.; Grimstvedt, A.; Elnan, J.; da Silva, E. F.; Svendsen, H. F. Oxidative Degradation of 2-Ethanolamine: The Effect of Oxygen Concentration and Temperature on Product Formation. *Int. J. Greenh. Gas Control* **2013**, 18, 88–100. https://doi.org/10.1016/j.ijggc.2013.06.008.

(12) Hjelmaas, S.; Storheim, E.; Flø, N. E.; Thorjussen, E. S.; Morken, A. K.; Faramarzi, L.; De Cazenove, T.; Hamborg, E. S. Results from MEA Amine Plant Corrosion Processes at the CO_2 Technology Centre Mongstad. *Energy Procedia* **2017**, 114, 1166–1178. https://doi.org/10.1016/J.EGYPRO.2017.03.1280.

(13) Vevelstad, S. J.; Grimstvedt, A.; Haugen, G.; Wiig, M.; Vernstad, K. Evaluation of Results from SDR Campaigns and Pilot Data. In *TCCS-11 - Trondheim Conference on CO_2 Capture, Transport and Storage*; Røkke, N. A., Knuutila, H. K., Eds.; Trondheim, **2021**; pp 35–39.

(14) Wagner, E. D.; Osiol, J.; Mitch, W. A.; Plewa, M. J. Comparative in Vitro Toxicity of Nitrosamines and Nitramines Associated with Amine-Based Carbon Capture and Storage. *Environ. Sci. Technol.* **2014**, 48, 8203-8211. https://doi.org/10.1021/es5018009.

(15) Fine, N. A. Nitrosamine Management in Aqueous Amines for Post-Combustion Carbon Capture, 2015. https://doi.org/10.15781/T2MG7GF93.

(16) Dai, N.; Mitch, W. A. Controlling Nitrosamines, Nitramines, and Amines in Amine-Based CO_2 Capture Systems with Continuous Ultraviolet and Ozone Treatment of Washwater. *Environ. Sci. Technol.* **2015**, 49 (14), 8878–8886. https://doi.org/10.1021/acs.est.5b01365.

(17) Davis, J.; Rochelle, G. Thermal Degradation of Monoethanolamine at Stripper Conditions. In *Energy Procedia*; **2009**; Vol. 1, pp 327–333. https://doi.org/10.1016/j.egypro.2009.01.045.

(18) Gouedard, C.; Picq, D.; Launay, F.; Carrette, P. L. Amine Degradation in CO_2 Capture. I. A Review. *Int. J. Greenh. Gas Control* **2012**, 10, 244–270. https://doi.org/10.1016/j.ijggc.2012.06.015.

(19) Freeman, S. A.; Rochelle, G. T. Thermal Degradation of Aqueous Piperazine for CO_2 Capture. 1. Effect of Process Conditions and Comparison of Thermal

Stability of CO_2 Capture Amines. *Ind. Eng. Chem. Res.* **2012**, 51 (22), 7719–7725. https://doi.org/10.1021/ie201916x.

(20) Lepaumier, H.; Picq, D.; Carrette, P. L. Degradation Study of New Solvents for CO_2 Capture in Post-Combustion. *Energy Procedia* **2009**, 1 (1), 893–900. https://doi.org/https://doi.org/10.1016/j.egypro.2009.01.119.

(21) Polderman, L. D.; Dillon, C. P.; Steele, A. B. Why Monoethanolamine Solution Breaks down in Gas-Treating Service. *Oil Gas J.* **1955**, 53 (No. 2), 180–183.

(22) Davis, J. D. Thermal Degradation of Aqueous Amines Used for Carbon Dioxide Capture, 2009.

(23) Eide-Haugmo, I. Environmental Impacts and Aspects of Absorbents Used for CO_2 Capture, 2011.

(24) Braakhuis, L.; Høisæter, K. K.; Knuutila, H. K. Modeling the Formation of Degradation Compounds during Thermal Degradation of MEA. *Ind. Eng. Chem. Res.* **2022**, 61 (7), 2867–2881. https://doi.org/10.1021/acs.iecr.1c04496.

(25) Lepaumier, H.; Da Silva, E. F.; Einbu, A.; Grimstvedt, A.; Knudsen, J. N.; Zahlsen, K.; Svendsen, H. F. Comparison of MEA Degradation in Pilot-Scale with Lab-Scale Experiments. In *Energy Procedia*; Elsevier Ltd, 2011; Vol. 4, pp 1652–1659. https://doi.org/10.1016/j.egypro.2011.02.037.

(26) Shoukat, U.; Fytianos, G.; Knuutila, H. K. Thermal Stability and Corrosion Studies of Amines for Combined Acid Gas Removal and Hydrate Control for Subsea Gas Treatment Systems. In *Techno-Ocean 2016: Return to the Oceans*; 2017; pp 176–180. https://doi.org/10.1109/Techno-Ocean.2016.7890641.

(27) Shoukat, U.; Baumeister, E.; Pinto, D. D. D.; Knuutila, H. K. Thermal Stability and Corrosion of Tertiary Amines in Aqueous Amine and Amine-Glycol-Water Solutions for Combined Acid Gas and Water Removal. *J. Nat. Gas Sci. Eng.* **2019**, 62, 26–37. https://doi.org/10.1016/j.jngse.2018.11.025.

(28) RTI International. *Testing of RTI's Non-Aqueous Solvent CO_2 Capture Process at NCCC Using the SSTU*; 2018.

(29) Freeman, C. *Molecular Refinement of Transformational Solvents for CO_2 Separations*; 2019.

(30) Brown, A. “Buz”; Awtry, A.; Meuleman, E. *ION Advanced Solvent CO_2 Capture Pilot Project*; Pittsburgh, PA, and Morgantown, WV (United States), 2018. https://doi.org/10.2172/1484045.

(31) Hancu, D. Large *Pilot-Scale Carbon Dioxide (CO_2) Capture Project Using Aminosilicone Solvent*; Pittsburgh, PA, and Morgantown, WV (United States), 2017. https://doi.org/10.2172/1414342.

(32) Cuccia, L.; Dugay, J.; Bontemps, D.; Louis-Louisy, M.; Vial, J. Analytical Methods for the Monitoring of Post-Combustion CO_2 Capture Process Using Amine Solvents: A Review. *Int. J. Greenh. Gas Control* **2018**, 72, 138–151. https://doi.org/10.1016/j.ijggc.2018.03.014.

(33) Perinu, C.; Arstad, B.; Jens, K. J. NMR Spectroscopy Applied to Amine-CO_2-H_2O Systems Relevant for Post-Combustion CO_2 Capture: A Review. *Int. J. Greenh. Gas Control,* **2014**, 20, 230–243. https://doi.org/10.1016/j.ijggc.2013.10.029.

(34) John M. Campbell and Company. *Gas Conditioning and Processing*; 2004.

(35) Denisov, E. T. The Oxidation of Alcohols, Ketones, Ethers, Esters and Acids in Solution. *Compr. Chem. Kinet.* **1980**, 16 (C), 125–203. https://doi.org/10.1016/S0069-8040(08)70038-4.

(36) Mokhatab, S.; Poe, W. A.; Mak, J. Y. Natural Gas Dehydration. In *Handbook of Natural Gas Transmission and Processing*; **2015**; pp 223–263. https://doi.org/10.1016/b978-0-12-801499-8.00007-9.

(37) Forster, R. Extending Glycol Life in Natural Gas Dehydration Systems. In *International Gas Research Conference;* San Diego, **1998**; pp 113–125.

(38) Lloyd, W. G. The Low Temperature Autoxidation of Diethylene Glycol. *J. Am. Chem. Soc.* **1956**, 78 (1), 72–75. https://doi.org/10.1021/ja01582a022.

(39) Vidal, P. F.; Garnier, G.; Bouchard, J.; Overend, R. P.; Chornet, E. The Behavior of Ethylene Glycol during the Thermal Solvolysis of Cellulose. *Can. J. Chem. Eng.* **1992**, 70 (2), 301–305. https://doi.org/10.1002/cjce.5450700213.

(40) Weissermel, K.; Arpe, H.-J. Industrial Organic Chemistry, Third.; 1997.

(41) Rossiter, W. J.; Brown, P. W.; Godette, M. The Determination of Acidic Degradation Products in Aqueous Ethylene Glycol and Propylene Glycol

Solutions Using Ion Chromatography. **Sol. Energy Mater. 1983**, 9 (3), 267–279. https://doi.org/10.1016/0165-1633(83)90049-7.

(42) Brown, P. W.; Galuk, K. G.; Rossiter, W. J. Characterization of Potential Thermal Degradation Products from the Reactions of Aqueous Ethylene Glycol and Propylene Glycol Solutions with Copper Metal. *Sol. Energy Mater.* **1987**, 16 (4), 309–313. https://doi.org/10.1016/0165-1633(87)90079-7.

(43) Madera, M.; Höflinger, W.; Kadnar, R. Ion Chromatographic Identification and Quantification of Glycol Degradation Products. *J. Chromatogr. A* **2003**, 997 (1), 279–284. https://doi.org/10.1016/S0021-9673(03)00060-8.

(44) Psarrou, M. N.; Jøsang, L. O.; Sandengen, K.; Østvold, T. Carbon Dioxide Solubility and Monoethylene Glycol (MEG) Degradation at MEG Reclaiming/Regeneration Conditions. *J. Chem. Eng. Data* **2011**, 56 (12), 4720–4724. https://doi.org/10.1021/je200709h.

(45) Alef, K.; Iglauer, S.; Barifcani, A. Degradation and Hydrate Phase Equilibria Measurement Methods of Monoethylene Glycol. *MethodsX* **2019**, 6, 6–14. https://doi.org/10.1016/j.mex.2018.12.004.

(46) Brown, P. W.; Rossiter, W. J.; Galuk, K. G. A Mass Spectrometric Investigation of the Thermal Oxidative Reactivity of Ethylene Glycol. *Sol. Energy Mater.* **1986**, 13 (3), 197–202. https://doi.org/10.1016/0165-1633(86)90018-3.

(47) Clifton, J. R.; Rossiter, W. J.; Brown, P. W. Degraded Aqueous Glycol Solutions: PH Values and the Effects of Common Ions on Suppressing PH Decreases. *Sol. Energy Mater.* **1985**, 12 (1), 77–86. https://doi.org/10.1016/0165-1633(85)90026-7.

(48) Glastrup, J.; Padfield, T. The Thermal Degradation of Tetraethylene Glycol, a Model Molecule for Polyethylene Glycol. *ICOM Comm. Conserv. 10th Trienn. Meet. Washington, DC, 22-27 August 1993 Prepr*. **1993**, 251–256.

(49) Glastrup, J. Degradation of Polyethylene Glycol. A Study of the Reaction Mechanism in a Model Molecule: Tetraethylene Glycol. *Polym. Degrad. Stab.* **1996**, 52 (3), 217–222.

(50) Goglev, R. S.; Neiman, M. B. Thermal-Oxidative Degradation of the Simpler Polyalkyleneoxides. *Polym. Sci. U.S.S.R.* **1967**, 9 (10), 2351–2364. https://doi.org/10.1016/0032-3950(67)90237-7.

(51) Han, S.; Kim, C.; Kwon, D. Thermal/Oxidative Degradation and Stabilization of Polyethylene Glycol. *Polymer (Guildf).* **1997**, 38 (2), 317. https://doi.org/10.1016/S0032-3861(97)88175-X.

(52) Piemonte, V.; Maschietti, M.; Gironi, F. A Triethylene Glycol-Water System: A Study of the TEG Regeneration Processes in Natural Gas Dehydration Plants. Energy Sources, Part A Recover. *Util. Environ. Eff.* **2012**, 34 (5), 456–464. https://doi.org/10.1080/15567031003627930.

(53) Gandhidasan, P. Parametric Analysis of Natural Gas Dehydration by a Triethylene Glycol Solution. *Energy Sources* **2003**, 25 (3), 189–201. https://doi.org/10.1080/00908310390142235.

(54) Madorsicy, S. L.; Straus, S. Thermal Degradation of Polyethylene Oxide and Polypropylene Oxide. *J. Polym. Sci.* **1959**, 36 (130), 183–194. https://doi.org/10.1002/POL.1959.1203613015.

(55) Rudenko, A. I.; Gershuni, A. N.; Kalabina, L. V. Some Characteristics of Ethylene Glycol as a Heat-Transfer Agent for Closed Two-Phase Systems. *J. Eng. Phys. Thermophys.* **1997**, 70 (5), 799–804. https://doi.org/10.1007/BF02657642.

(56) Smith, W. B. Ethylene Glycol to Acetaldehyde-Dehydration or a Concerted Mechanism. *Tetrahedron* **2002**, 58 (11), 2091–2094. https://doi.org/10.1016/S0040-4020(02)00103-5.

(57) Giesen, Y.; Friedrich, C.; Breuer, D.; Fauss, J.; Hebisch, R.; Brock, T. H.; Hartwig, A. Glycols - Method for the Determination of Diethylene Glycol, Ethylene Glycol and Propylene Glycol in Workplace Air Using Gas Chromatography [Air Monitoring Methods, 2018]. MAK-Collection Occup. *Heal. Saf.* **2018**, 1584–1599. https://doi.org/10.1002/3527600418.AM10721E1918.

(58) Fu, Y.; Hao, Z.; Parker, B.; Knapp, M. A Greener Way to Screen Toothpaste for Diethylene Glycol. *Am. J. Anal. Chem.* **2011**, 02 (08), 938–943. https://doi.org/10.4236/ajac.2011.28109.

(59) Caldeira, L. R.; Madureira, F. D.; Maia, T. D. F.; Muller, C. V.; Fernandes, C. Simultaneous Quantification of Ethylene Glycol and Diethylene Glycol in Beer by Gas Chromatography Coupled to Mass Spectrometry. *Food Chem.* **2021**, 346, 128871. https://doi.org/10.1016/j.foodchem.2020.128871.

(60) Wurita, A.; Suzuki, O.; Hasegawa, K.; Gonmori, K.; Minakata, K.; Yamagishi, I.; Nozawa, H.; Watanabe, K. Sensitive Determination of Ethylene Glycol, Propylene Glycol and Diethylene Glycol in Human Whole Blood by Isotope Dilution Gas Chromatography-Mass Spectrometry, and the Presence of Appreciable Amounts of the Glycols in Blood of Healthy Subjects. *Forensic Toxicol.* **2013**, 31 (2), 272–280. https://doi.org/10.1007/s11419-013-0188-3.

Chapter 3

Materials and Methods

This chapter contains in-depth descriptions and details on experimental setups and analytical techniques employed in this PhD work.

3.1 Thermal Degradation Experiment

The thermal degradation experiments were performed by a similar approach as Eide-Haugmo et al.[1] The solvents to be tested were placed in 316 stainless steel cylinders, closed with Swagelok® end caps. The cylinders were 10 cm long, had an outer diameter of 1.3 cm and a thickness of 0.1 cm. All experiments were performed with two parallels. Thus, to acquire five data points over a time series, excluding day 0, ten cylinders were filled with the same solution.

For the experiments run directly in the cylinders, 8 mL of the solutions were added. Some of the experiments were also conducted with glass vials inserted in the cylinders to avoid contact between the solvent and the metal walls of the cylinder. In these cases, 4 mL of the solutions were added. The cylinders were closely sealed and placed in an oven at the desired temperature. During sampling, two cylinders were removed, cooled down to room temperature, weighed, and opened. The cylinders were weighed before and after the experiment to detect possible leakages. If leakages were detected, these cylinders were not included, and the reported results were only based on one sample. Once a cylinder was opened for sampling, it was not returned for further degradation.

The sampling frequency was varied depending on the solvent. For easily degradable solvents, such as primary and secondary amines, samples were taken each week. For more stable compounds, such as tertiary amines and glycols, sampling was conducted every second week to allow more degradation to occur.

The temperature for the thermal degradation of the amines was set to 135 °C. This temperature was chosen as it has been reported in other, similar studies.[1-7] In this way, the results could be compared with the data from these publications. The temperature chosen for the thermal degradation experiments with triethylene glycol (TEG) was initially tested at 205 °C but was adjusted to 220 °C to enhance the degradation rates. Conducting the experiments at temperatures above this could have been beneficial to obtain clearer results. 220 °C was, however, the highest setting available on the ovens in use.

During thermal degradation experiments where more volatile solvents were studied, the cylinders were placed within a custom-made metal casing, as shown in Figure 3.1. This was a precaution to safeguard against possible pressure buildup in the cylinders. After being removed from the oven, the case and the cylinders were not opened before they had reached room temperature. Usually, they were opened the next day.

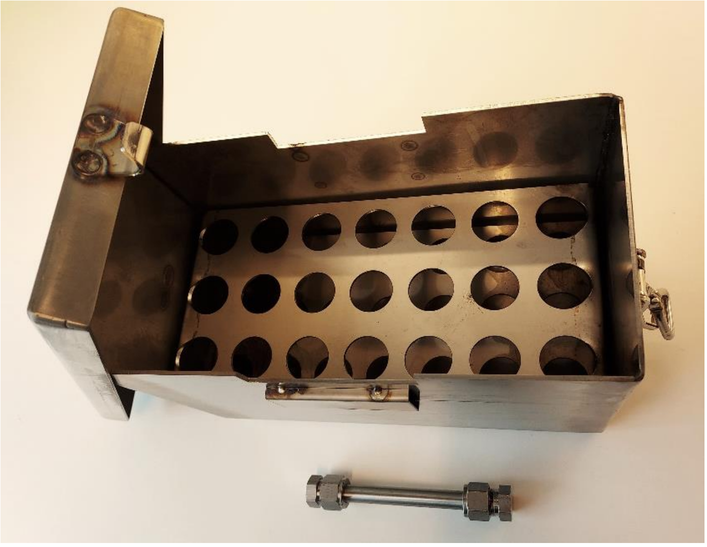

Figure 3.1: Custom-made metal casing for metal cylinders during thermal degradation experiments.

The cylinders were cleaned before reuse. This involved initially rinsing them multiple times with hot water. Then, they were rinsed with acetone until no discoloration of the acetone was visible and put in an acid bath (0.1 M, H_2SO_4) overnight. The next day, they were left in a water bath for a couple of hours and finally rinsed with deionized (DI) water and left to air dry. A visual inspection of the inside of the cylinder was done to decide if the cylinders were to be reused.

3.2 Oxidative Degradation Setup

The setup used for the oxidative degradation experiments in this work consisted of two identical custom-made semi-open setups. A similar approach to studying oxidative degradation has been conducted in other works.[8] The schematics are presented in Figure 3.2. Glass reactors had a volume of 1.5 L and were filled with 1-1.2 L liquid at the beginning of the experiments. To allow for conducting experiments with high temperatures (up to 150 °C), the reactors were placed in electrical heating mantles from ITA with integrated magnetic stirring. A Pyrex® glass sparger (grade 1) and a condenser were connected to each reactor. The condensers were cooled to 5 °C by a water bath. None of the components within the reactor were metallic, ensuring that the solvent was only in contact with metals if it was added to the solutions.

Three Alicat mass flow controllers (MFC) were used to regulate the pressure of the three available gasses, oxygen, nitrogen, and carbon dioxide. After the gasses had been mixed, two MFCs allowed equal gas flows into the two reactors via an empty gas wash bottle and the sparger. The empty gas wash bottle was added to safeguard the MFC from backflow from the reactors. A bleed valve after the inlets of the three pure gases allowed excess gas to be released. The gas in the system was recycled with a pump (400 L/h) to enhance the contact between the gas and the solvents. Continuous addition of new gas ensured a relatively constant composition of the gas. A small fraction of the gas was bled out. This gas flow was passed through different absorption media, depending on what experiment was being conducted. During the oxidative degradation of amines, acid washes (1M, H_2SO_4) were connected to the outlet. For the oxidative degradation experiments of glycols, 2,4-dinitrophenylhydrazine (DNPH) cartridges, acid washes (1M, H_2SO_4), and/or base washes (30wt%, monoethanol amine (MEA) *aq.*) were utilized.

Each experiment was conducted by adding the solutions to the reactors and turning on stirring, heating and gas flow immediately. These were left on continuously throughout the experiment. For the experiments with amine solutions, the solutions were initially loaded with CO_2 before the experiment started. Sampling was conducted three times a week, by extracting 2-4 mL from the reaction solutions. All samples were accurately weighed to keep track of the mass balance.

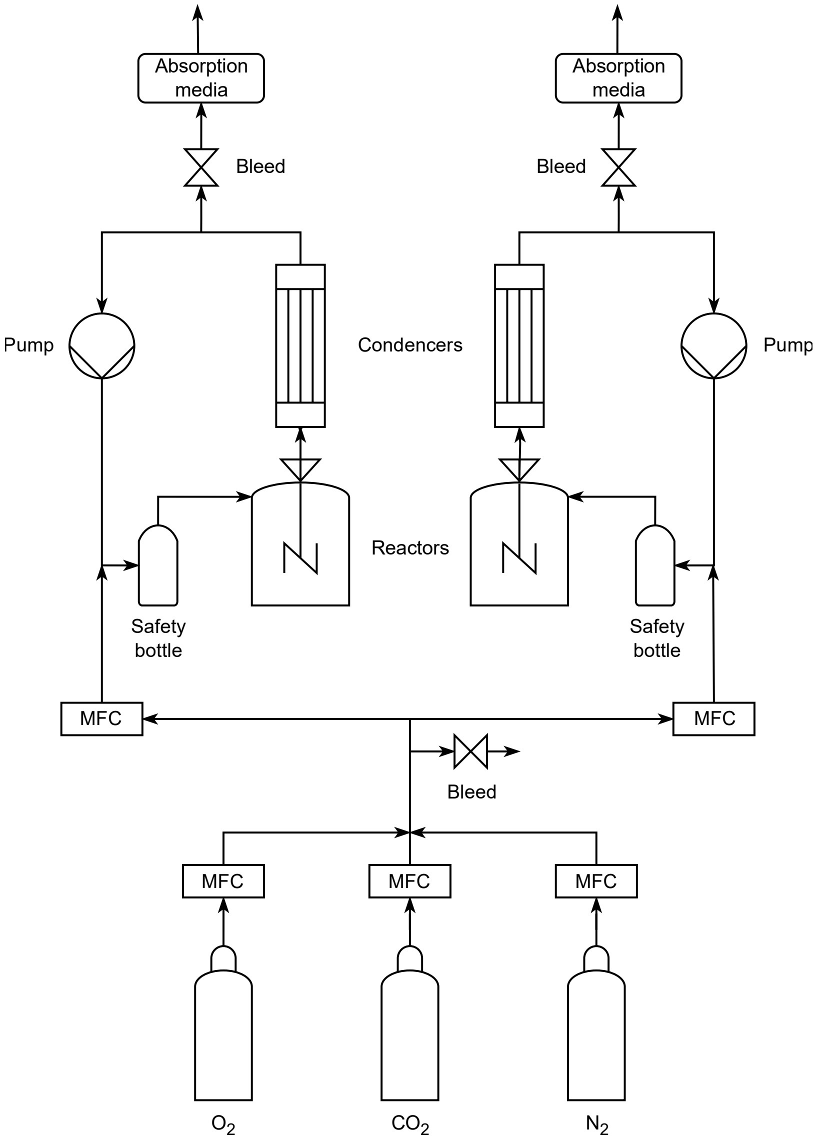

Figure 3.2: Schematic overview of the oxidative degradation setup.

The reactors and all glass pieces and tubing connected to the reactors were cleaned with hot water, acetone, and DI water between each run. When amines had been studied, discolored glass pieces were also cleaned with sulfuric acid (1M, H_2SO_4) before rinsing with DI water. When running experiments without water, the setup was dried before a new experiment was started. This was done by closing the empty system, turning on the N_2 flow and the pumps, and leaving it for 24-48 hours.

3.3 Titration

In this work, titration was used to quantify alkalinity, heat-stable salts (HSS), and water. The methodology for each is presented in the following sections.

3.3.1 Total Alkalinity

The total alkalinity (TA) of the samples was measured to quantify the amine concentration. This was done following a method described by Ma'mun et al.[26] This measurement does not give a quantitative value of a specific amine, but an overall count of the alkaline compounds in the solution. For analyzed samples from the amine degradation experiments, this would include alkaline degradation compounds in the degraded solutions as well as the solvent amine.

To measure TA, 0.2 mL of the sample was added to 50 mL DI water and accurately weighed. This solution was then titrated with sulfuric acid (1M, H_2SO_4) on a Metrohm 702 SM Titrino automatic titrator. This was done until the endpoint at about pH 4-5 was reached. Equation 3.1 is used to calculate the concentration of alkaline species in the sample. Analyzing solutions with known concentrations gave a maximum deviation of ±2%. All samples were analyzed with two parallels, and the results reported are the average of the two. If the relative standard deviation (RSD) between the two parallels exceeded 2%, the measurement was redone.

$$c_{\mathrm{amine}} = \frac{2 \cdot c_{H_2SO_4} \cdot V_{H_2SO_4}}{m_{\mathrm{sample}}} \tag{0.1}$$

3.3.2 Heat-Stable Salt

Heat stable salts (HSS) is a collective term used for the amine salts formed between protonated amines and small organic acids formed through the degradation of the amine. As the name implies, HSS are stable at elevated temperatures and are not expected to dissociate in the stripper. This temperature stability is utilized in this method, as non-heat stable salts, such as carbamates, carbonate, and bicarbonate salts, can be stripped off at elevated temperatures. This leaves the HSS, which are treated with a cation-exchanger before titration to determine concentration. The method performed was based on a method described by Reynolds et al.[10] and a method developed by SINTEF Industry. Though not necessarily considered HSS, the acidic degradation products formed through the degradation of glycols can also be measured following this method.

Before the samples could be analyzed, the ion exchange resin used during the procedure had to be activated. The resin, Dowex 50W-X8 cation exchange resin (CAS: 69011-20-7), was activated by stirring two parts resin with one-part hydrochloric acid (10%, HCl) for 10 minutes. The resin was then allowed to settle before the acidic supernatant was decanted. The resin was then rinsed until the pH of the supernatant reached the pH of DI water. This was achieved by multiple repetitions of adding DI water, stirring, allowing the resin to settle, and decanting the supernatant.

When the resin has been activated, the HSS analysis could be conducted. Initially, 2 g of the sample was added to 40 mL of activated resin in 40 mL DI water in a beaker. The sample mass was accurately weighed. The beaker was then covered with a watch glass or parafilm and heated to 70 °C while stirred continuously. After one hour, the beaker was removed from the heat, the solution cooled down, and the resin was allowed to settle. To avoid resin particles in the liquid when separating the supernatant and the resin, the supernatant was decanted through a frit and into a new beaker. The resin was then rinsed multiple times until the pH of the supernatant over the resin reached the pH of the DI water. The rinsing was performed by adding 40 mL of DI water at a time to the resin, stirring for a couple of minutes, and pouring through the frit after the resin had settled. All supernatants were collected in the same beaker. The combined supernatants were then titrated with sodium hydroxide (NaOH) on a Metrohm 702 SM Titrino automatic titrator. For the degraded amine samples 0.05 M NaOH was used for the titration. For the degraded glycol samples, however, the titrant concentration was adjusted to 0.5 M for the samples where the TEG had degraded more than 50%. The endpoint for the titration was pH 5-6. The concentration of HSS was calculated using Equation 3.2. All samples were analyzed with two parallels, and the results reported are the average of the two. Blank samples were analyzed regularly. If the RSD between two parallels exceeded 5%, the analysis was redone.

$$c_{\mathrm{HSS}} = \frac{V_{\mathrm{NaOH}} \cdot c_{\mathrm{NaOH}}}{m_{\mathrm{sample}}} \tag{0.2}$$

After use, the resin had to be reactivated. This was done by covering the resin with 10% HCl, covering the beaker and heating the solution to 70 °C while stirring continuously. After one hour, the resin was left to cool and settle. The acid was then decanted off, and the resin was rinsed multiple times with DI water until the pH reached the pH of the DI water. The resin should not be allowed to dry out between use.

Validation of the method for amine samples has previously been performed by Vanja Buvik.[11] This was done by measuring the HSS concentration of mixtures of MEA (30wt%, *aq*.) and known concentrations of formic, acetic, oxalic and/or glycolic acid. The accuracy of these analyses was ±7% or ±0.007 mol/kg. To validate the method for glycol solutions, HSS concentration was measured in mixtures of both MEG and TEG with the same acids. The lowest accuracy was found to be ±8% corresponding to ±0.18 mol/kg.

3.3.3 Karl Fischer Titration

Karl Fischer titration (KFT) is a technique for determining water concentration.[12] The principle behind this method is an oxidation of sulfur with iodine. It is either considered volumetric or coulometric, depending on what the source of iodine is. For volumetric KFT, the iodine is added mechanically. In this reaction, water and iodine are consumed in a 1:1 ratio.

$$2\,H_2O + SO_2 + I_2 \rightarrow H_2SO_4 + 2\,HI$$

Adding iodine to the solution, its concentration is measured to assert the amount needed to react with all the water present. When I_2 is in access, a quantitative value of water can be established. For coulometric KFT, the iodine is generated from KI with an electrode.

The KFT results presented in this work were performed by SINTEF Industry. It was performed volumetrically on a Mettler Toledo V20. The solvent used was Methanol Dry (Hydranal®) and the titrant was Composite 5 (Hydranal®). All end samples of the experiments and pure TEG and MEG were analyzed with KFT. All samples were analyzed with two parallels. The RSD between the two parallels for degraded samples was 4%. For the measurements of undegraded TEG and samples with very little degradation, the water concentrations were close to the limit of quantification (LOQ). This resulted in RSD between the two parallels as high as 10%. In absolute values, however, this amounts to ±0.004 mol/kg.

3.4 Total Organic Carbon Analyzer

Total Organic Carbon (TOC) analyzer is an analytical instrument which can quantify different groups of carbon. It has different modes available, so that TOC, total inorganic carbon (TIC), and total carbon (TC) can be analyzed. During the TIC analysis, the sample is sparged with phosphoric acid (H_3PO_4). This converts all inorganic carbon in the sample to CO_2, which can be quantified by a non-dispersive infrared (NDIR) detector. In the TC analysis, the sample is combusted at 680 °C in air over a platinum (Pt) catalyst. This converts all carbon in the sample to CO_2, which can be quantified by the NDIR detector. The TOC concentration can be found by subtracting the amount of TIC from the amount of TC.

The analyses were performed on a Shimadzu TOC-L_{CPH} analyzer equipped with an auto sample injector (ASI). The injection volume was 50 µL. The TOC analysis was calibrated with a TC calibration standard (1000 mg/L) acquired from Sigma-Aldrich and the TIC analysis was calibrated with sodium bicarbonate ($NaHCO_3$, CAS: 144-55-8). Amine samples with < 50wt% water was diluted 1:100 MilliPore water and more concentrated amin samples and glycol samples were diluted 1:10000 with MilliPore water. The calibration range was 0-500 ppm. This was done over three calibration curves, 0-25 ppm, 25-150 ppm, and 150-500 ppm, which all had $R^2 > 0.9995$. The method was set up so that each sample run had three injections, and the reported value was the average of these. If the coefficient of variation (CV) exceeded 1% or the RSD exceeded 2%, new injections were performed. Calibrations were performed regularly and known standards were run periodically.

3.5 Chromatography

Chromatography is a technique for separating compounds based on their properties. Compounds in the sample are moved with a mobile phase through a stationary phase. The compounds are slowed down at different rates in the stationary phase, resulting in the separation. The separated components can be detected by coupling the chromatograph with a suitable detection method. In this work, flame ionization detection, mass spectroscopy, and ultraviolet detection have been utilized. The following section will present the details of the different chromatographic methods.

3.5.1 Gas Chromatography

In gas chromatography (GC), the mobile phase is a gas. The separation of the analytes is based on the components' affinity to the stationary phase as well as their volatility. A prerequisite to analyzing a component with GC is that they are sufficiently volatile and stable at elevated temperatures. GC coupled with flame ionization detector (FID) was used to detect and quantify glycols, and GC coupled with a mass spectrometer (MS) was used to scan degraded glycol samples to identify unknown degradation compounds.

3.5.1.1 Gas Chromatography coupled with Flame Ionization Detection

Glycols were quantified with a GC coupled with an FID. FID is a common technique used with GC, where the analytes are combusted in a hydrogen flame and the ions they form are detected.

The GC-FID measurements in this work were performed on an Agilent 7890A equipped with a DB-WAX Ultra Inert fused silica column (length 30 m, inner diameter 0.25mm, film thickness 0.25 µm) was used and the injection volume was 10 µL with a 1:20 split ratio. The following temperature gradient was used to elute the three glycols: hold at 100 °C for 1 min, increase to 250 °C in increments of 10 °C/min and hold at 250 °C for 4 min. The carrier gas was helium, and methanol was used to dilute samples to contain <1000 ppm glycol.

Before the analysis of real samples, validation tests were performed with known amounts of MEG, DEG, and TEG. In addition, solutions with known concentrations of the three glycols were spiked with compounds possibly present in degraded glycol solutions. These included water and formic, acetic, glycolic, glyoxylic, and oxalic acid. None of these influenced the quantification of the glycols. Acetic acid was visible in the FID spectrum but eluted earlier than any of the glycol peaks. Mixed standards with known concentrations were run periodically, to ensure valid results. The accuracy of the method was 3%, and the precision was 1%.

The calibration curves for all three glycols were linear with $R^2 > 0.999$. The limit of detection (LOD) was defined as three times the signal-to-noise ratio (3·S/N) and the limit of quantification (LOQ) was defined as 10·S/N. The retention times (RT), LOD, LOQ, and range of the linear calibration curves are presented in Table 3.1.

Table 3.1: RT, LOD, LOQ, and linear calibration range for MEG, DEG and TEG analyzed with GC-FID.

Chemical	***RT [s]***	***LOD [ppm]***	***LOQ [ppm]***	***Linear calibration range [ppm]***
MEG	5.47	1.5	4.5	5-1000
DEG	8.93	2.0	5.1	5-1000
TEG	12.20	34	47	50-1000

3.5.1.2 Gas Chromatography coupled with Mass Spectrometry

Degraded glycol samples were scanned with GC-MS to identify unknown degradation products in the solutions. The full scan electron impact ionization (EI) mass spectra gave possible hits of chemical structures when compared with available MS Library spectra (NIST MS library). Standards were acquired to positively identify peaks. Standards for some compounds that could potentially have formed as biproducts to the formation of other degradation compounds were also tested.

The samples from the experiment were diluted with methanol to 700 ppm. When running coelutions with standards, the solutions were diluted so the degraded samples had concentrations of 250 ppm and the standards had concentrations of 70 ppm. The GC analysis of the samples was performed with an Agilent 7890A gas chromatograph with an injector ALS 7683B autosampler coupled to an Agilent 5975 single quadrupole mass spectrometer. Chromatographic separation was performed on a DB Wax-UI GC Column (30 m x 0.25 mm inner diameter x 0.25 µm film thickness), keeping the carrier gas flow (helium) at 1 mL/min, and the transfer line and the injection port temperatures at 250 °C. The injection volume was 1 µL in splitless mode and the solvent delay was set to 5 min.

One short and one extended temperature method was performed. The short method’s temperature program was as follows: starting at 100 °C for 1 min, followed by a temperature increase at a rate of 10 °C/min to 250 °C and held for 4 min. The overall analysis time for one sample with the selected temperature program was 20 min. The extended method’s temperature program was as follows: starting at 100 °C for 1 min, followed by a temperature increase at a rate of 10 °C/min to 250 °C and held for 1 min, then temperature increase by 1°C/min to 260 °C, and held for 5 min. The overall analysis time for one sample with the extended temperature program was 35 min.

The mass detector was operated in full scan mode (from 30 m/z to 550 m/z) using electron impact ionization (EI) set at 70 eV. The source temperature was set to 230 °C and the quadrupole to 150 °C.

3.5.2 Liquid Chromatography

In liquid chromatography (LC), the mobile phase is a liquid. The separation of the analytes is in this case dependent on the analytes’ affinity towards the stationary phase versus the mobile phase. High-performance liquid chromatography (HPLC) coupled with ultraviolet (UV) and refractive index (RI) detection was used to quantify small organic acids in the degraded solution, an ultra-performance (UPLC)-MS scan was conducted to identify unknown degradation compounds in degraded glycol solutions, and HPLC-MS was used to quantify amines and degradation compounds in amine degradation experiments, and aldehydes, acids, and amines in the absorption media from glycol degradation experiments.

3.5.2.1 High-Performance Liquid Chromatography coupled with Ultraviolet and Refractive Index Detector

Small organic acids were analyzed using HPLC-UV/RI. During the setup of the method, both RI and UV detection was tested. UV was found to be a good choice for the small organic acids as all of the acids were UV active.

The method was performed on a PL1170-6830 (Agilent HiPlex H) column. Sulfuric acid (0.05 mol/L, H_2SO_4) was used as an isocratic eluent with a flow of 0.5 mL/min. The column temperature was 40 °C and the injection volume was 10 µL. The method lasted for 20 minutes to allow all acids and potential contaminants that could be stuck in the column to elute. The acid peaks were all baseline separated in a standard solution of all acids.

Table 3.2: RT, LOD, LOQ, lower calibration range, and higher calibration range for oxalic acid, glyoxylic acid, glycolic acid, formic acid, and acetic acid analyzed with HPLC-UV.

Chemical	*RT [s]*	*LOD [ppm]*	*LOQ [ppm]*	*Lower calibration range [ppm]*	*Higher calibration range [ppm]*
Oxalic acid	9.50	0.67	0.84	2.5-50	50-400
Glyoxylic acid	10.84	1.9	3.7	10-50	50-400
Glycolic acid	13.45	2.0	4.5	10-50	50-400
Formic acid	15.09	12	13	50-1000	1000-8000
Acetic acid	16.45	5.3	8.3	10-50	50-400

Real samples were diluted in MilliPore water to approximately 50000 ppm of the sample and filtered through 0.2 µm syringe filters before analysis. Two calibration curves were used, one for the lower concentration range and one for the higher concentration range. Table 3.2 gives RT, LOD, LOQ, lower calibration range, and higher calibration range for the five acids. The R^2 was >0.999 in all cases. The accuracy for the quantification of formic acid and acetic acid was 2%, glycolic acid was 4%, glyoxylic acid was 8%, and oxalic acid it was 10%. The precision for all acids was 2%.

3.5.2.2 Liquid Chromatography coupled with Mass Spectrometry

Degraded glycol samples were scanned with UPLC-MS to identify unknown degradation products in the solutions. The results from the scan were processed with Progenesis DFS studio software where a library with mol files of possible molecules of interest was created. The peaks that were tested were based on this library, as well as the online Chemspider library.

The LC-MS scan was performed using an ACQUITY UPLC I Class® system connected to a Synapt G2-S Mass spectrometry detector (Waters Corporation, Milford, USA) with positive electrospray ionization sources (ESI+). 200 ng/mL of leucine enkephalin was used as a Lockmass at a flow rate of 10 µL/min to allow correction of exact mass measurements. An Acquity UPLC HSS T3 (2.1 mm × 100 mm, 1.7 µm) chromatographic column was used for reverse-phase separation. Instrumental blanks were run before and after every sample to check for carryover or cross-contamination. A mix of water:methanol (95:5) with 2 mM ammonium acetate (A) and methanol with 2 mM ammonium acetate (B) was used as mobile phase. The injection volume was 1 µL and the flow rate was 0.3 mL/min.

The chromatographic gradient used was: initial conditions 100% A; 0.00-1.00 min, 100-80% A; 1.00–6.00 min, 80-55% A; 6.00–13 min, 55-20% A; 13.00–14.00 min, 20-5% A; 14.00–17.00 min, 5% A; 17.00–18.00 min, 5-100% A; 18.00–22.00 min, 100% A. The column temperature was maintained at 35 °C.

The capillary voltage was set at + 2.50 kV (ESI+), the desolvation flow was fixed at 800 L/h with a desolvation temperature set at 350 °C and the cone voltage set at 20 V. Source Temperature was set to 120 °C. The full scan spectra were acquired within a range of 50 to 1500 m/z. The UPLC-QTOF-MS data was acquired using Masslynx V4.1 and processed with Progenesis QI V2.3 (Waters, Milford, USA).

3.5.2.3 Liquid Chromatography coupled with Mass Spectrometry (External)

Analysis of aldehydes, acids, and nitrogen-containing components was performed by SINTEF Industry. All analyses were performed on an Agilent Technologies 1290 Infinity with an Agilent Technologies 6495 Triple Quad MS.

Formaldehyde and acetaldehyde were captured in DNPH cartridges and acid washes (1M, H_2SO_4) at the outlet of the oxidative degradation setup. The quantification of these was performed on an Ascentis® Express C8, 2.7 Micron HPLC column (53843-U). The ionization technique was electrospray ionization (EI). LOQ for both analytes was 10 ng/mL, and the uncertainty of the method was ±3%. Before analysis, the samples were diluted and derivatized with DNPH.

Formic, glycolic, and acetic acid were captured in base washes (30wt% MEA, *aq.*) at the outlet of the oxidative degradation setup. These were analyzed using a Waters Acquity UPLC HSS T3 column (100Å, 1.8µm, 2.1 x 150 mm) and EI. LOQ was 100 ng/mL, 10 ng/mL, and 50 ng/mL for formic, glycolic, and acetic acid, respectively. The uncertainty of the method was ±3% for formic and acetic acid and ±5% for glycolic acid. Sample preparation consisted of dilution and derivatization with 3-nitrophenylhydrazine (CAS: 100-16-3).

The concentration of MEA in the base washes was analyzed on an Ascentis® Express Phenyl-Hexyl, 2.7 µm HPLC column and EI. LOQ was 1 ng/mL, and the uncertainty was ±3%.

Lastly, the various amine-containing species in the base washed (30wt% MEA, *aq.*) were analyzed on a Discovery® HS F5 HPLC column and with EI. Samples were diluted before analysis, and the uncertainties were ±5%.

3.6 Nuclear Magnetic Resonance Spectroscopy

Nuclear magnetic resonance (NMR) spectroscopy is a technique mainly used to determine the structures of molecules. To be able to study a nucleus with NMR, it must have a quantum number greater than zero. The result of this is that only some nuclei can be studied by NMR, the most common ones being proton (^1H) and carbon-13 (^{13}C).

3.6.1 Qualitative Nuclear Magnetic Resonance Spectroscopy

Qualitative NMR spectroscopy experiments were performed at 26.8 °C on a Bruker 600 MHz Avance III HD equipped with a 5 mm cryogenic CP-TCI z-gradient probe. The lock solvent was deuterated water (D_2O), and the internal reference standard was tri(trimethylsilyl)phosphine (TMSP). These were added to coaxial inserts placed inside the NMR tubes. The coaxial insert was filled with D_2O and TMSP (2wt%), while the outer NMR tube was filled with the solution to be analyzed. For shift assignments, ^1H, ^{13}C, correlation spectroscopy (COSY), heteronuclear single-quantum correlation spectroscopy (HSQC), and heteronuclear multiple-bond correlation spectroscopy (HMBC) NMR spectra were obtained. The spectra were analyzed in the software Bruker TopSpin 4.0.7.

3.6.2 Quantitative Nuclear Magnetic Resonance Spectroscopy

Quantitative analysis can be conducted both on the ^{1}H NMR and ^{13}C NMR. There can be various reasons for choosing one over the other, but a big difference is the experiment time. In addition, the ^{13}C experiment is less sensitive than the ^{1}H experiment. This is because the ^{13}C isotope only has a natural abundance of 1.11%.[13] In comparison, the natural abundance of ^{1}H is 99.98%. In this work, quantitative ^{13}C NMR analyses were conducted. Even with longer experiment times and lower sensitivity, there is often less overlapping of the different peaks in the ^{13}C spectra. Most of the solutions studied in this work were degraded solutions, meaning solutions composed of a mixture of unidentified compounds. Less overlapping of the peaks was therefore emphasized.

When conducting quantitative NMR experiments, the parameters must be chosen with care to obtain peak area corresponding to the real quantities in the samples. The first parameter to consider is the recycle delay. This is the time between the end of the data acquisition of one free induction decay (FID) to the start of the next excitation and should be at least 5 times the length of the longest spin-lattice relaxation time (T_1) of the carbons in the sample. The T_1 was measured through an inversion-recovery sequence.[13] The longest T_1 was found to be ~20 s, and the recovery delay time was therefore set to 120 s for all quantitative ^{13}C experiments ($6 \cdot T_1$). In addition, to avoid the recorded FID being cut prematurely, the acquisition (AQ) time might have to be adjusted. In this work, the AQ was increased to 3 s to avoid cutting off the FID.

The number of scans (also called transients) should be considered. The amount should be high enough to avoid a high S/N ratio. At the same time, a high number of scans results in an increase in the already long analysis time for ^{13}C. Ways to reduce the number of scans needed are running the analysis on a strong magnet or having the samples in high concentrations in the NMR tube. In this work, the samples were added to the NMR tube undiluted (with added internal reference standard). The lock solvent, D_2O, and the zero reference, TMSP (2wt%), were added to a coaxial insert which was then placed within the NMR tube with the sample. This allowed the number of scans to be decreased to 256.

The internal reference standard for the quantification was acetonitrile (AcN, anhydrous 99.8%). The carbon shifts of AcN (3.7 and 121 ppm) are not in the region of the glycols or their degradation compounds, and so peak overlapping with the standard is avoided. As AcN is a small molecule, it is expected to have a long T_1.[13]

As the T_1 used to set the recycle delay time was based on the long T_1 of AcN, this also assured that all the large degradation compounds would have fully recovered before the next scan was started. In addition, AcN is expected to be inert in the current systems. When preparing the samples for analysis, AcN (10 µL) was added to the solution with a Hamilton syringe model 802 as described by Perinu et al.[14] The weights of the sample and the internal reference standard were accurately registered. A disadvantage of AcN as a reference standard is that it has high volatility. Due to this, the preparation and weighing of the samples were done in closed vials with septum and with syringes.

As for the qualitative NMR, the quantitative NMR was performed at 26.8 °C on a Bruker 600 MHz Avance III HD equipped with a 5 mm cryogenic CP-TCI z-gradient probe. The NMR spectra were acquired with an inverse gate decoupling acquisition sequence with a pulse width of 9.58 µs (90° pulse angle). The decoupling sequence was done to minimize the nuclear Overhauser effect (NOE). The spectra were analyzed in the software Bruker TopSpin 4.0.7.

Validation tests were performed with mixtures of TEG, DEG, and MEG, with known concentrations. The three glycols were also spiked with components expected to be in the degraded solutions, such as formic and acetic acid. None of these influenced the quantification of the glycols noticeably. The accuracy was 2% for TEG, and 5% for DEG and MEG. The precision was 1% for TEG and 0.5% for DEG and MEG.

3.7 Inductively Coupled Plasma Mass Spectrometry

Inductively coupled plasma mass spectrometry (ICP-MS) is a technique for quantifying various atoms. The ICP atomizes the molecules of the sample, and the resulting atoms are detected with MS. This is a common technique for quantifying metals and trace elements.

The experiments were performed externally at the Department of Chemistry, NTNU. A high-resolution inductively coupled plasma ELEMENT 2 (HR-ICP-MS) instrument from Thermo Electronics was used. The analysis is verified against certified reference standards with an RSD < 5%. All samples were diluted 1:100 in MilliPore water (18.2 mΩ) and digested with 2 drops of concentrated nitric acid (HNO_3, 69.6wt%).

3.8 References

(1) Eide-Haugmo, I.; Lepaumier, H.; Einbu, A.; Vernstad, K.; Da Silva, E. F.; Svendsen, H. F. Chemical Stability and Biodegradability of New Solvents for CO_2 Capture. *Energy Procedia* **2011**, 4, 1631–1636. https://doi.org/10.1016/j.egypro.2011.02.034.

(2) Davis, J.; Rochelle, G. Thermal Degradation of Monoethanolamine at Stripper Conditions. In *Energy Procedia*; 2009; Vol. 1, pp 327–333. https://doi.org/10.1016/j.egypro.2009.01.045.

(3) Da Silva, E. F.; Lepaumier, H.; Grimstvedt, A.; Vevelstad, S. J.; Einbu, A.; Vernstad, K.; Svendsen, H. F.; Zahlsen, K. Understanding 2-Ethanolamine Degradation in Postcombustion CO_2 Capture. *Ind. Eng. Chem. Res.* **2012**, 51, 13329–13338. https://doi.org/10.1021/ie300718a.

(4) Shoukat, U.; Baumeister, E.; Pinto, D. D. D.; Knuutila, H. K. Thermal Stability and Corrosion of Tertiary Amines in Aqueous Amine and Amine-Glycol-Water Solutions for Combined Acid Gas and Water Removal. *J. Nat. Gas Sci. Eng.* **2019**, 62, 26–37. https://doi.org/10.1016/j.jngse.2018.11.025.

(5) Lepaumier, H.; Grimstvedt, A.; Vernstad, K.; Zahlsen, K.; Svendsen, H. F. Degradation of MMEA at Absorber and Stripper Conditions. *Chem. Eng. Sci.* **2011**, 66 (15), 3491–3498. https://doi.org/10.1016/j.ces.2011.04.007.

(6) Lepaumier, H.; Da Silva, E. F.; Einbu, A.; Grimstvedt, A.; Knudsen, J. N.; Zahlsen, K.; Svendsen, H. F. Comparison of MEA Degradation in Pilot-Scale with Lab-Scale Experiments. In *Energy Procedia*; Elsevier Ltd, 2011; Vol. 4, pp 1652–1659. https://doi.org/10.1016/j.egypro.2011.02.037.

(7) Fytianos, G.; Grimstvedt, A.; Knuutila, H.; Svendsen, H. F. Effect of MEA's Degradation Products on Corrosion at CO_2 Capture Plants. In *Energy Procedia;* Elsevier Ltd, 2014; Vol. 63, pp 1869–1875. https://doi.org/10.1016/j.egypro.2014.11.195.

(8) Buvik, V.; Vevelstad, S. J.; Brakstad, O. G.; Knuutila, H. K. Stability of Structurally Varied Aqueous Amines for CO_2 Capture. *Ind. Eng. Chem. Res* **2021**, 60, 5638. https://doi.org/10.1021/acs.iecr.1c00502.

(9) Ma'mun, S.; Jakobsen, J. P.; Svendsen, H. F.; Juliussen, O. Experimental and Modeling Study of the Solubility of Carbon Dioxide in Aqueous 30 Mass% 2-

((2-Aminoethyl)Amino)Ethanol Solution. *Ind. Eng. Chem. Res.* **2006**, 44, 8, 2505–2512. https://doi.org/10.1021/ie0505209.

(10) Reynolds, A. J.; Verheyen, T. V.; Adeloju, S. B.; Chaffee, A. L.; Meuleman, E. Evaluation of Methods for Monitoring MEA Degradation during Pilot Scale Post-Combustion Capture of CO_2. *Int. J. Greenh. Gas Control* **2015**, 39, 407–419. https://doi.org/10.1016/j.ijggc.2015.06.001.

(11) Buvik, V. Stability of Amines for CO_2 Capture, 2021.

(12) Fischer, K. Analytisch-Technische Untersuchungen Neues Verfahren. *Angevndte Chemie* **1935**, 48 (26), 394–396. https://doi.org/10.1002/ange.19350482605.

(13) Shoulders, B. High-Resolution NMR Techniques in Organic Chemistry. In *Tetrahedron Organic Chemistry Series Volume 19* Pergamon: Oxford. 1999. https://doi.org/10.1021/ja004717y.

(14) Perinu, C.; Bernhardsen, I. M.; Pinto, D. D. D.; Knuutila, H. K.; Jens, K. J. NMR Speciation of Aqueous MAPA, Tertiary Amines, and Their Blends in the Presence of CO_2: Influence of PKa and Reaction Mechanisms. *Ind. Eng. Chem. Res.* **2018**, *57* (5), 1337–1349. https://doi.org/10.1021/acs.iecr.7b03795.

Chapter 4

A Review of Degradation and Emissions in Post-Combustion CO_2 Capture Pilot Plants

This chapter contains a literature review of published data from pilot scale testing of amine solvent for CO_2 capture. It has been published in the International Journal of Greenhouse Gas Control in January 2021. The goal of this work was to give an overview of the various campaigns and present the learnings from these. Overall, common trends and shortcomings were identified, which can be useful for the future operation of large-scale amine-based CO_2 capture plants. In addition, recommendations for monitoring strategies and a comprehensive overview of alternatives for analytical methods are presented.

Journal publication

Buvik, Vanja; Høisæter, Karen K.; Vevelstad, Solrun & Knuutila, Hanna K., A review of degradation and emissions in post-combustion CO_2 capture pilot plants. Int. J. Greenh. Gas Control, Vol 106, 2021, 103246.

A Review of Degradation and Emissions in Post-Combustion CO_2 Capture Pilot Plants

Vanja Buvik[a], Karen K. Høisæter[a], Solrun J. Vevelstad[b], Hanna K. Knuutila[a]*

[a] Department of Chemical Engineering, NTNU, NO-7491 Trondheim, Norway

[b] SINTEF Industry, NO-7465 Trondheim, Norway

[*] Corresponding author: hanna.knuutila@ntnu.no

Abstract

Pilot plant testing of amine solvents for post-combustion CO_2 capture is an essential tool for fully understanding degradation behaviour and emission profiles under realistic process conditions. This review aims to summarise the lessons learned in different pilot campaigns, as well as to give recommendations how solvent stability and emissions can be monitored and assessed. A total of 18 different pilot plants and 29 individual campaigns were studied, of which the majority used ethanolamine and flue gas from coal-fired power plants.

The findings of the review are that solvent stability data from different pilot plants show significantly higher operation time in which the solvent is stable, when extensive flue gas pretreatment is implemented. It was also found that no single degradation compound seems to suffice for the assessment of the degradation of a solvent, even for the widely studied ethanolamine process. Monitoring of the total liquid-phase heat stable salt concentration, as well as gas phase ammonia concentration may, however, give an informative picture of the state and degradation of the solvent. There seems to be a lack of universally applied analytical methods, which makes it difficult to compare one campaign or location to another. The implementation of validated and documented analytical standards in this regard will facilitate production of reproducible, reliable and comparable data for future solvent stability assessment.

Abbreviations

Abs	absolute
AMP	2-amino-2- methyl-1-propanol
aq.	aqueous
ATR	attenuated total reflectance
CHP	combined heat and power
CCS	carbon capture and storage
DeSOx	removal of SO_X
DeNOx	removal of nitrogen oxides (NO_X)
DNPH	2,4- dinitrophenylhydrazine
ED	electrodialysis
EDX	energy dispersive X-ray microanalysis
ELPI	electrical low pressure impactor
ESP	electrostatic precipitator
FGD	flue gas desulphurisation
FMPS	fast mobility particle sizer
FT-IR	Fourier- transform infrared spectroscopy
GC	gas chromatography
HSE	Health, Safety and Environment
HSS	heat stable salts
IC	ion chromatography
ICP	inductively coupled plasma
LC	liquid chromatography
MEA	monoethanolamine
MDEA	*N*-methyl diethanolamine
MS	mass spectrometry
NDIR	non- dispersive infrared
NG	natural gas
OES	optical emission spectroscopy
OPC	optical particle counter
ppb	parts per billion
ppm	parts per million
PR	particulate removal
PTR	proton- transfer reaction
Pz	piperazine
RFCC	residual fluidised cracker
SCR	selective catalytic reduction
SEM	scanning electron microscope
TONO	total nitrosamine
VOC	volatile organic compounds
WESP	wet electrostatic precipitator
WFGD	wet flue gas desulphurisation
QTOF	quad time of flight

1 Introduction

Removal of CO_2 from gas streams has been performed industrially for almost a century to provide pure CO_2 for industrial purposes, as well as sales-quality natural gas. CO_2 capture and storage is also predicted to be vital for achieving the goals of the Paris agreement and combat anthropogenically caused global warming (Rogelj et al., 2018). In recent years, several new solvents have been developed (Feron et al., 2020) and the interest towards a safe and optimised operation of the plants has increased due to the potential use of the technology for large-scale capture of CO_2 from power plants and other industries. As a consequence of the scaling up, however, various challenges have arisen. In a large-scale plant, solvent degradation, energy consumption, and potential emissions of the solvent or degradation compounds, can have significant environmental and economic consequences. Therefore, to gain a better understanding of the large-scale operation, the process and operating conditions are first studied through a pilot campaign allowing investigation of the effect of flue gas composition, impurities, and solvent performance, including degradation, corrosion, and emissions, on the process performance and costs.

Degradation, as well as corrosion, are considerable challenges in amine-based CO_2 capture. As the degradation increases, the amount of make-up solvent that needs to be added throughout the campaigns increases. Among other, Moser et al. (2020) summarised that solvent-make-up required in 12 campaigns performed with

30wt% (*aq.*) ethanolamine (MEA) varied from 0.3 to 3.6 kg t_{CO2}^{-1}, showing a 10-fold difference. Furthermore, a feature that is often observed in pilot campaigns using MEA is that after stable operation for a certain amount of time, a sudden and rapid increase in degradation product formation and concentration of dissolved metals occurs (Dhingra et al., 2017; Rieder and Unterberger, 2013). What causes this abrupt spike in degradation rate has not yet been fully understood and prediction of when it will take place is therefore not possible. This effect has also been seen in laboratory-scale studies and it is therefore commonly assumed that dissolved iron and other metals catalyse the oxidative amine degradation in the absorption process also in pilot-scale (Bello and Idem, 2005; Chi and Rochelle, 2002; Léonard et al., 2014; Strazisar et al., 2003). Furthermore, certain degradation products also affect corrosion rates both positively and negatively, as they can act as chelators or inhibit the build-up of a protective film on the metal surface of the plant (Kohl and Nielsen, 1997; Tanthapanichakoon et al., 2006).

The identification of high concentrations of typical primary oxidative degradation products (formed in the first stages of degradation) in solvents used in pilots with real flue gas has shown that oxidative degradation indeed is a dominant degradation mechanism in the absorption process (Vega et al., 2014). Typical concentrations of oxygen in the flue gas is generally between 4 and 15% and lower in flue gases originating from coal-fired power plants than gas-fired power plants. Since the solvent has direct contact with the flue gas oxygen in the absorber and since the solubility of oxygen decreases with increasing temperature, the concentration of dissolved oxygen is the highest in the absorber and the absorber sump. Oxidative degradation is therefore assumed to primarily take place here, although the elevated temperatures in the rich solution also could increase the reactivity despite of low oxygen concentrations (Chi and Rochelle, 2002).

Thermal degradation primarily takes place during the solvent regeneration, at elevated temperatures and in the presence of CO_2 (Davis and Rochelle, 2009). Products of the thermal degradation process, as well as some of the oxidative degradation products, are often more volatile than the amines themselves and are likely to evaporate in the absorber. This increases the chance of emission to the atmosphere together with the purified flue gas, unless emission reduction technologies are in place (Rochelle, 2012).

There are well known methods to reduce degradation. Flue gas pretreatment technologies, removing impurities such as SO_X and NO_X gases, as well as particulate matter such as fly ash are implemented to some extent in most pilot campaigns. Methods such as "Bleed and Feed", removal of a part of the degraded solvent and refilling with fresh solvent throughout the process, have recently been thoroughly tested without success (Moser et al., 2020). Apart from the "Bleed and Feed", solvent reclaiming is often used to limit the amount of makeup solvent and maintaining the operation.

The purpose of this review is to summarise available data from pilot tests using amine solvents for post-combustion CO_2 capture and real flue gas or industrial gases. It covers traditional bench-mark amine 30wt% MEA as well as new amines and amine blends proposed for post-combustion CO_2 capture. The emphasis will be put on solvent stability, emissions and corrosion and how these aspects are monitored, and the three concepts are seen in light of one another. The review aims to be of help for future pilot campaigns and how these concepts can and should be monitored. Although a large number pilots and campaigns for post-combustion capture of CO_2 exist (Idem et al., 2015) and have taken place, those from which reported solvent stability or emission data are not available, are also not included here. Furthermore, most of the data given originates from journal papers and conference proceedings, but to give a complete picture and overview of the pilot plants and campaigns as possible, some of the given data has been found in conference presentations. The campaigns included have also been limited to the latest decade, to provide up-to-date information about current developments and trends.

2 Overview of pilot plants and campaigns

Table 2.1 lists the pilot plants included in this review. Most of the pilots use a slip-stream of the flue gas from power plants or industrial sources. Furthermore, the table includes only pilot plants where data for emissions or degradation has been published. A more extensive overview of pilots and demonstration plants for post-combustion CO_2 capture can be found elsewhere (Cousins et al., 2016; Idem et al., 2015).

As expected, the CO_2 capture capacity correlates with the absorber diameter, so that the pilot with the smallest absorption capacity (kg CO_2 h^{-1}) also has the smallest absorber diameter. The absorber packing heights vary from 3 meters to 24 meters. Most of the plants have at least one water wash section on the top of the absorber to limit the emissions of volatile solvent components and degradation compounds.

Table 2.2 presents an overview of the gas compositions of the pilot campaigns included in this study. It also shows the gas pretreatment performed before the amine scrubbing. Altogether 19 different flue gas sources were studied, of which 16 originated from coal-fired power plants. The concentrations of CO_2 are between 11 and 14 vol% (dry) for coal-fired power plants, whereas for gas burners, it is typically lower. Pilot campaigns performed in connection to the cement industry have to deal with CO_2 concentrations up to 18vol%. The pilot plant at Tiller in Norway, receives flue gas from a propane burner, and the gas can be diluted with air or CO_2 to simulate different industrial cases. Technology Centre Mongstad DA (TCM) has a possibility to use a slip-stream from natural gas-fired combined heat and power plant (CHP) or a slip-stream from residual fluidised cracker unit (RFCC). Similarly, the National Carbon Capture Center (NCCC) in Alabama, USA, has two available gas streams for solvent testing, one coal, and one simulated natural gas stream. Therefore, gas streams of both TCM and NCCC vary in their concentrations of H_2O, CO_2, O_2, NO_X and SO_2, depending on the choice of flue gas source. The Mobile Test Unit (MTU), built and operated by Aker Solutions, has been used at three different test locations in Norway, Scotland and the USA, two with coal-derived flue gas and one time with CHP flue gas at TCM, where degradation data is available from the first two.

In spite of this being a review focusing on pilot scale studies using real flue gas, some additional studies using synthetic flue gas have been included in the evaluation of how amine solvents degrade. These campaigns are given separately in Table 4.8, and have been included because of their extensive analytical work, giving interesting insights on solvent stability, to support trends or shed light on topics included in the discussion.

2.1 Pretreatment technologies

As mentioned in the introduction, removal of contaminants before the CO_2 capture process, limits the possibility of unwanted side reactions of the amine solvent taking place, leading to solvent degradation and deterioration of the overall process performance. The need for pretreatment varies with the type of flue gas, which contaminants it typically contains and in which concentrations they are present, it also depends on the solvent itself. As some of these contaminants are causes of respiratory problems and of environmental concern, systems for removal of these from flue gas have been in use for half a century already. As shown in Table 2.2, in most of the pilot locations at least some pretreatment is used. Here, we separate the contaminants into three categories: particulate matter (ash, soot, and catalyst fines), NO_X and SO_2/SO_X, and treatment technologies for each category will be briefly presented below (Meuleman et al., 2016).

Particulate matter is usually removed by wet or dry electrostatic precipitation (ESP). The ESP applies a negative charge to the particulate matter, facilitating their attachment to a positively charge electrode. The dry ESP then removes the particulates from the electrode by mechanical or magnetic impact whereas the wet

Table 2.1: An overview of the dimensions of the different pilot plants studied and compared in this review. (Y = yes)

Pilot plant	**CO_2 cap. rate [kg h^{-1}]**	**Water/acid wash**	**Abs. diameter [m]**	**Abs. packed height [m]**	**Reference**
Aioi Works	830	Y	0.85	15	Nakamura et al. (2013, 2014), Okuno et al. (2017)
Brindisi	2500	Y	1.5	22	Rieder et al. (2017), Mangiaracina et al. (2014), Kamijo et al. (2013), Enaasen et al. (2014)
CAER 0.1 MWth	10		0.1	3.25	Thompson et al. (2014), Frimpong et al. (2013), Cousins et al. (2016)
CAER 0.7 MWe					Thompson et al. (2017a)
Changchun	100		0.35	8	Feron et al. (2014)
Esbjerg	1000	Y	1.1	17	Knudsen et al. (2009)
Ferrybridge	4167	Y			Fitzgerald et al. (2014)
Heilbronn	300		0.6	23.9	Rieder et al. (2017), Dhingra et al. (2017), Rieder and Unterberger (2013)
Lasziska		Y	0.33	8.4	Spietz et al. (2018)
Loy Yang	20		0.21	2.7	Artanto et al. (2012), Dhingra et al. (2017), Reynolds et al. (2015a)
Maasvlakte	250	Y	0.65	8	Rieder et al. (2017), Dhingra et al. (2017), Khakharia et al. (2015)
Mikawa	420	Y		15	Saito et al. (2014, 2015
MTU	180	Y	0.4	18	da Silva et al. (2012), Morton et al. (2013), de Koeijer et al. (2011), Bade et al. (2014)
NCCC	Various	Y	0.64	6	Brown et al. (2017), Gao et al. (2019)
Niederaussem	300	Y			Moser et al. (2011a,b)
Tarong	100		0.35	7.14	Cousin et al. (2012)
TCM	5200	Y	3.5 × 2	12–24	Gorset et al. (2014), Morken et al. (2017), de Koeijer et al. (2011), Brigman et al. (2014)
Tiller	50	Y	0.2	19.5	Mejdell et al. (2011)

Table 2.2: A summary of the flue gas sources and compositions at different locations, where post-combustion CO_2 capture campaigns have been performed. SR: SO_X removal, NR: NO_X removal, PR: particle removal. Further details on pretreatment can be found in the appendix, Table S1.

Location	Flue gas source	Pretreatment	cO_2 (vol%)		cCO_2 (vol%)		cSO_X		cNO_X		Reference
			Wet	**Dry**	**Wet**	**Dry**	**ppm**	**mg m^{-3}**	**ppm**	**mg m^{-3}**	
Aioi Works (IHI), Japan	Coal or propane boiler		–	–	–	–	–	–	–	–	Nakamura et al. (2013, 2014)
Breivik, Norway	Cement		7.5	9.2	17.8	21.8	–	<130	–	180–250	Knudsen et al. (2014)
Brindisi, Italy	Coal	SR, PR, NR	–	6.3-8.2	–	11–13	–	0–20	–	24–68	Rieder et al. (2017), Mangiaracina et al. (2014)
CAER 0.1 MWth, USA	Coal	SR, PR	6	–	14.00	–	170–250	–	80–90	–	Frimpong et al. (2013), Thompson et al. (2014)
CAER 0.7 MWe, USA	Coal	SR, PR, NR	8	–	10-16	–	<5	–	<50	-	Thompson et al. (2017a)
Changchun, China	Coal	PR, SR, NR	5.8	6.4	10.80	12	–	<50	–	<160	Feron et al. (2014)
Esbjerg, Denmark	Coal	PR, SR, NR	–	5–9	12.00	–	<10	–	<65	–	Knudsen et al. (2009)
Ferrybridge, UK	Coal	PR, SR, NR	–	–	–	–	–	–	–	–	Fitzgerald et al. (2014)
Heilbronn, Germany	Coal	PR, SR, NR	–	6.4	12-14	–	–	–	–	–	Dhingra et al. (2017), Rieder et al. (2017), Mejdell et al. (2017)
Laziska, Poland	Coal	SR	–	–	13.1-13.3	–	–	<10	–	–	Spietz et al. (2018)
Longannet, Scotland	Coal		~10	–	12	–	–	–	80–170	–	da Silva et al. (2012), Graff (2010)
Loy Yang, Australia	Coal	PR, SR, NR	4–5	–	10-11	–	120–200	–	150–250	–	Reynolds et al. (2015a), Artanto et al. (2012), Dhingra et al. (2017), Bui et al. (2016)
Maasvlakte, The Netherlands	Coal	SR	–	7.4	13	–	–	–	–	–	Khakharia et al. (2015), Dhingra et al. (2017), Rieder et al. (2017)
Mikawa, Japan	Coal	PR, SR	–	–	–	12	<5	–	100	–	Saito et al. (2014, 2015)
Niederaussem, Germany	Coal	PR, SR, NR	–	5	–	14.2	–	<1	–	120–200	Moser et al. (2011a,b, 2020)
Tarong, Australia	Coal	PR, SR	6	–	10	–	200	–	150	–	Cousin et al. (2012), Cousins et al. (2016)
TCM, Norway	CPH	PR, SR	14	15	3.6	3.8	<1	–	–	3	Gorset et al. (2014), Morken et al. (2017), Shah et al. (2018)
	RFCC		3.2	3.3	15	15	5	–	–	60	
Tiller, Norway	Propane burner		<15	–	4.5-14	–	Very low		–	20	da Silva et al. (2012), Mejdell et al. (2011)
Wilsonville (NCCC), USA	Coal		–	4.5	–	14	2.5 (dry)	–	1–3 (dry)	–	Bumb et al. (2017), Morton et al. (2013), Brown et al. (2017)
	Simulated NG	PR, SR, NR	–	15.9	–	4.5					

ESP uses a water wash. It is also possible to apply a filter for the removal of particles. Pressure drops when particulates start accumulating in the filter and this limitation weighs against the otherwise high removal efficiencies (>99.95%) and simplicity of the method (Meuleman et al., 2016; Nicol, 2013).

NO_X gases are typically removed either by selective catalytic reduction (SCR) or a non-catalytic reduction (SNCR), reducing them to N_2 and water, where SCR holds the largest market share. The SCR process takes place at temperatures between 160 and 350 °C, whereas SNCR has a temperature requirement closer to 1000 °C (Meuleman et al., 2016).

SO_2/SO_X gas is not just a contaminant deriving from the combustion process itself, but is also formed when sulphur components pass through a NO_X-removal unit. It is even occasionally added to the ESP for reducing the resistivity of the fly ash. SO_2/SO_X can be removed in a wet flue gas desulphurisation (WFGD) unit, where the acidic nature of SO_X allows it to be scrubbed out by an alkaline lime stone ($CaCO_3$) solution. There are also dry or semi-dry FGD systems available, relying on dry alkaline sorbents, but the WFGD systems have approximately 84% of the market. The FGD step has the additional benefit of removing chloride from the flue gas, washing it out with the sulphur loaded lime stone (Meuleman et al., 2016; Zhu, 2010).

3 Analytical methods used in pilot campaigns

In amine-based post-combustion CO_2-capture, one of the main challenges is solvent degradation (Rochelle et al., 2001), which requires a reliable solvent monitoring strategy. The main goal of this monitoring is often to quantify the concentration of the intact starting amines. In laboratory scale experiments, knowing the change in amine concentration over time allows assessment of the stability of the solvent system. However, in pilot scale, where the amines chosen are often relatively stable, the amine concentration is also measured to ensure that the amine and water concentrations stay constant. In both cases the analytical method used has to be fast, accurate, and straightforward (Cuccia et al., 2018).

Another target for the monitoring of the solvents is to identify the degradation products of the amines. Degradation products are typically categorised into five main classes: amine derivatives, acids, aldehydes, amides, and nitrosamines. Compared to the analysis of the starting solvent components, the study of degradation compounds is a more challenging endeavour (Cuccia et al., 2018). Firstly, many of them have an unknown structure. Moreover, the high concentration of the starting amine in the solvent can make it hard to detect degradation compounds that are typically present at low levels and even at trace amounts (da Silva et al., 2012). There are multiple analytical methods to choose from when analysing these species, with different advantages and disadvantages. When choosing an analytical method, nature of the compounds, matrix and concentration ranges of the analytes must be regarded. Dissolved metal species can also be found in the solvents and these are measured to monitor corrosion. Lastly, there are many monitoring technologies for gaseous emission (Kolderup et al.). Moreover, a large number of publications studying aerosol formation mechanisms, as well as aerosol reduction technologies, have been published in the last five years using various analytical methods. The most frequently used analytical methods during pilot campaigns are described below and an overview of the methods can be found in Table 3.1.

Titration is a quick tool that can give valuable information of different aspects of a solvent. In CCS, titration is most commonly used to find total alkalinity, the CO_2-loading and amounts of heat stable salts (HSS). Total alkalinity is a measurement of the total concentration of base in a solution. It is determined by titrating a basic solution with an acid (e.g., sulphuric or hydrochloric) until the equivalence point, at which the base is neutralised, is reached. (Somridhivej and Boyd, 2016)

This method is a quick and inexpensive way of getting an estimate of amine concentration, and thus an easy way of gaining insight into the stability of the amine (Matin et al., 2012). It is, however, important to differentiate between the actual concentration of the starting amine and the total alkalinity as some degradation products are alkaline. Therefore, the result from a total alkalinity measurement incorporates the concentration of the starting amine, as well as possible alkaline degradation products that also have CO_2 binding abilities.

Titration used to find CO_2-loading or HSS concentration works in a similar way as that of the total alkalinity measurements. The difference is that bases are used instead of an acid and the solutions have to be pretreated before the titration. For CO_2-loading measurements, the CO_2 in the solution is first extracted using $BaCl_2$, before titration with NaOH (Hilliard, 2008). To get the HSS concentration, the solution is first treated with a cation exchange resin and then titrated with a base (Aronu et al., 2014; Reynolds et al., 2015a). Both of these methods are more time-consuming than the total alkalinity measurement. Nevertheless, if other, more expensive, analytical techniques are unavailable, these two methods can be a less costly alternative that provide important information.

Liquid Chromatography - Mass Spectroscopy (LC-MS) is an analytical method used to separate molecules based on their chemical and physical properties. The liquid sample passes through an LC-column, and the different species separate as a result of their varying affinity towards a stationary phase in the column. The mass spectrometer ionises the compounds, and a magnetic field separates the ions based on their mass-to-charge ratio (Lundanes et al., 2013). There are multiple additions that can be included, like an additional step for compound separation. An example of this is QTOF (quad time of flight).

LC-MS is a common choice for both quantitative and qualitative analysis of degradation compounds, as this technique can analyse most of the classes of degradation compounds (amine derivatives, acids, amides, and nitrous amines) (Chahen et al., 2016; Cuzuel et al., 2014; Vevelstad et al., 2013). In the quantitative analysis, the remaining concentration of starting amine can be determined with high accuracy using an internal standard. Known degradation compounds can also be quantified, if internal standards are available and their application can also allow for qualitative analysis to identify unknown degradation products (da Silva et al., 2012; Lepaumier et al., 2011). An approach for identifying and semi-quantifying degradation compounds using TOF-MS has been described (Thompson et al., 2017b; Thompson et al., 2017c).

There are some disadvantages to the LC-MS technique. The equipment and maintenance are very costly and require skilled operators. It is, therefore, seldom found on site, which can give rise to challenges regarding the stability of the samples. However, published data on reanalysing samples have shown a good agreement between the analysed samples right after experiments and one month later (Knuutila et al., 2014b). There is also no library with which to compare any unknown peaks (Lepaumier et al., 2011). Identification of unknown peaks in the degraded mixtures will, therefore, start with the prediction of potential degradation compounds based on chemistry, after which deuterated standards will be purchased. These can be expensive, and in some cases, they are even not commercially available (da Silva et al., 2012).

Ion Chromatography (IC) is a sub-category of liquid chromatography, and a useful method for analysing ionic species. Since many degradation products are known to have ionic properties, the IC is well-suited for amine degradation studies (Wang and Jens, 2012). Similar to normal liquid chromatography, the separation of the species occurs due to their different affinity to a stationary phase; in IC this difference is caused by the species different columbic interaction with the ion-exchanger (Lundanes et al., 2013).

There are two types of ion chromatography, namely anion-exchange and cation-exchange (Lundanes et al., 2013). Anion-exchange is commonly used to analyse for degradation products in anionic forms, such as carboxylates, nitrate, and nitrite (Kadnar and Rieder, 1995; Wang and Jens, 2012). It is also one of the most described methods for analysing the total amide content by converting the amides to their corresponding carboxylic acid through amide hydrolysis (Freeman, 2011; Sexton, 2008). The generated carboxylic acids can then be analysed with the anion-exchange, and the surplus of carboxylic acids presents the carbamate concentration. Cation-exchange, on the other hand, is commonly used to quantify solvent amines, as well as to identify and to quantify amine degradation products, like alkyl amines, in the form of heat stable salts (da Silva et al., 2012; Moser et al., 2020; Reynolds et al., 2015b; Thompson et al., 2014). Quantitative IC-analysis requires chemical standards.

IC is a relatively inexpensive analytical method. Compared to LC-MS, the equipment is cheaper and requires less maintenance. Furthermore, the implementation is also somewhat more straightforward, as dilution is the only sample preparation needed (Cuccia et al., 2018). The limitation of the IC method is that non-ionic compounds cannot be analysed. Therefore, IC is often used in combination with other analytical methods. The IC instrumentation requires both regular use and maintenance to deliver reliable results.

Gas Chromatography - Mass Spectroscopy (GC-MS) works similarly as LC-MS, but as the name implies, the analysis occurs in a gas phase. GC-MS can be used both for quantitative analyses as well as to identify some degradation products (Wang and Jens, 2012). However, only compounds that have boiling points below 300-500 °C, can be analysed. At the same time, the analytes also have to be stable at these high temperatures. This limits the number of degradation compounds that can be analysed.

On the other hand, very high-quality spectra can be achieved as the gaseous eluate allows for the solvent to be removed before entering the MS and as the analytes are easily ionisable in the gas phase. An extensive library of various pure compounds is available, and any unknown spectra can be compared to the library (Lepaumier et al., 2011). The existence of this library is one of the main advantages for this method.

Fourier Transform Infrared Spectroscopy (FT-IR) is a method that utilises molecular bonds' ability to oscillate when exposed to infrared radiation. In principle, FT-IR allows for the simultaneous analysis of up to 50 compounds with a low detection limit (∼1 ppm). FT-IR can be used both for analyses of the liquid and gas phases. However, in aqueous solvent solutions, the detection of degradation compounds is challenging, if not impossible, due to low concentrations of degradation compounds, complex chemical matrix, as well as the high concentrations of amine and water (Cuccia et al., 2018; Macbride et al., 1997).

FT-IR is mostly employed as a gas phase on-line analytical method. The method is mostly used to monitor gas effluents, e.g., NO_X, SO_X, CO, and CO_2, and to quantify amines (like Pz, MEA, MDEA and ammonia) present in the gas leaving the absorber/water wash (Bade et al., 2014; Khakharia et al., 2013; Knudsen et al., 2013; Knudsen et al., 2014; Mertens et al., 2012). FT-IR can also be used to quantify aldehydes (formaldehyde and acetaldehydes). The advantage of applying on-line FT-IR is that the only preconditioning needed is heating the gas sample to prevent condensation. However, work should be done to ensure that the heating does not induce further thermal degradation of the amine. The ability to detect aldehydes is an essential advantage for this method, as other analytical methods are often limited in this regard.

FT-IR can also be used to analyse the liquid phase. Here, FT-IR together with Attenuated Total Reflectance (ATR) is typically used to monitor the loading and solvent amine concentrations in the solvent loop. When specific degradation compounds are found in high enough concentrations, they can also be quantified and monitored. The main challenge is that degradation compounds will change the spectra, and the results will become more inaccurate overtime, requiring calibration with degraded solvent (Grimstvedt et al., 2019). In recent years, methods where FT-IR with ATR is used to analyse the speciation in the solvent has also been developed (Diab et al., 2012; Richner and Puxty, 2012).

Proton-Transfer Reaction Mass Spectroscopy (PTR-MS) is a technique used for online measurement of volatile organic compounds (VOCs) in a gas-stream. In the PTR-MS instrument, gas-phase VOCs are ionised as a proton is transferred from an ion reagent, typically H_3O^+, to the sample molecules. The ionised molecules are then mass analysed in the MS-part of the equipment (Hansel et al., 1995). For the proton transfer to take place, the analysed molecules must have higher proton affinity than water. This gives some restrictions to which compounds can be analysed. To overcome this, instruments have in later years been modified to be able to switch between H_3O^+ and for example NO^+ as reagent ions, which has increased the amount of detectable compounds (Jordan et al., 2009).

The PTR-MS can give both quantitative and qualitative measurement results. One of the main advantages of this method is that neither gas standards, nor calibration for different gases, are necessary to get a precise quantification of the different species. Another advantage is the outstanding detection sensitivity of this method. The detection limit varies for different apparatuses, but it is typically in the pptV range (Lindinger et al., 1998). A drawback in this regard is that there is a maximum measurable concentration limit. The equations that are used in the analysis are based on the assumption that the decrease of reagent ions can be neglected. With a concentration at about 10 ppmV and up, this no longer holds and the results will be incorrect. A solution is to dilute the gas with air.

Inductively Coupled Plasma Mass Spectroscopy/Optical Emission Spectroscopy (ICP-MS/-OES) are elemental analytical techniques, which enables detection of most atoms at ppm levels. This is done by atomising and ionising the molecules in the studied mixture by passing it through an inductively heated plasma, often argon (Sheppard et al., 1990). Using an ICP-MS instrument, the atomic ions that are created are then analysed with MS. The ICP-OES uses the fact that some of the atoms/ions that are created are also excited. The intensity of the radiation is proportional with the concentration of each atom, and so this technique can be used for both quantitative and qualitative analysis (Thomas, 2013).

These techniques demand sample preparation, where one usually has to add an internal standard, primarily deionised water with nitric or hydrochloric acid. The drawback is that the equipment is expensive, and the analysis has a high operation cost because it employs argon gas (Todoli and Mermet, 2011). In the field of CCS, this technique is used to monitor the amounts of trace metals in solutions. This give an indication of corrosivity of the studied solvent. It should be noted that the method has not been validated. ICP-MS can also be used for measuring the total amount of carbon in a solution, but this is not widely used in the field of CCS.

Total Organic Carbon (TOC) analyser can measure amounts of carbon in a solution. It has different modes and can also be used for analysis of the total amount of inorganic carbon (IC), total carbon (TC) and total nitrogen (TN). In the field of CCS, it is often used to measure amount of CO_2 in a liquid sample (Bernhardsen et al., 2019; Knudsen et al., 2014).

The analyses happens over three steps, namely acidification, oxidation, and non-dispersive infrared (NDIR) detection. In the acidification step, acid is added, which then converts all bicarbonate and carbonate ions to carbon dioxide. The measurement of the resulting gas gives the amount of IC in the sample, corresponding to the CO_2 loading. Catalytic combustion oxidises all carbon in the sample to CO_2, so that this also can be quantified by NDIR. Other oxidation processes are also available for the quantification of organic carbon (Shimadzu, 2014).

Fast Mobility Particle Sizer (FMPS) is a fast response technique, enabling rapid detection of particle size distribution of aerosols. The gas-streams carrying aerosols is let into the FMPS and through a cyclone that removes particles bigger than 1 µm. The aerosols then continues through a region, in which they are charged with a known charge. The positively charged particles are then separated in an electric field based on their diameter and charge-state. The size distribution is measured in 32 channels, ranging from 5.6 to 560 nm (Jeong and Evans, 2009; Levin et al., 2015). Disadvantages of this technique is that it is not very robust in very demanding industrial surroundings (Kero and Jørgensen, 2016).

Optical Particle Counter (OPC) is an online measuring technique that is used to find aerosol size distribution and total particle number. In the OPC, particles are passed through a laser-light, which results in scattering of this light. The scattering is then classified and this gives a size spectrum (Burkart et al., 2010). OPCs can detect particles as small as 50 nm in diameter, and for smaller particles than this is simply not detected. Particles with a diameter of several hundred µm can also be detected, though not with the same instrument. If the particle size exceeds the detection limit for a certain instrument, it will simply be counted as the maximum diameter (Eliasson et al., 2016; Welker, 2012). A drawback of this method is that properties of the aerosols, such as density, shape, refractive index and absorption, is not accounted for (Welker, 2012).

Scanning Electron Microscope with Energy Dispersive X-ray Microanalysis (SEM/EDX) is an elemental microanalysis technique. The SEM part of the instrument is a microscope that can magnify from about 10 to 3 000 000 times. It is an offline method, so samples must first be collected from for example filters or films (Byers et al., 1971; Li and Shao, 2009). The surface of your sample is scanned with a focused beam of electrons. These electrons react with the atoms in the sample, resulting in various signals. The detection of these by SEM and by EDX can map out both the composition and the topography of the sample surface (Goldstein et al., 2017; Newbury and Ritchie, 2013). The resulting SEM image is quite analogous to normal vision (Byers et al., 1971), and the resulting image can give the structure, the size and the composition of solids in the aerosol particles. It can also be processed with different approaches to give size distribution (Brostrøm et al., 2020; Goldstein et al., 2017; Moser et al., 2017; Sun et al., 2012).

Electron Low Pressure Impactor (ELPI+) is a real-time particle detection technique, which combines electrical detection of charged particles and a 15-stage cascade impactor. When the aerosol enters the ELPI+, a unipolar diffusion charger first charges the particles of the aerosol. The unipolarly charged particles are then deposited in the various impactor stages depending on their aerodynamic size. In the impactor stages, electrometers are used to measure signals from the charged particles, which can then be converted to particle size distribution. In the end, this measurement gives particle number concentration and size distribution in real-time. The particle size distribution ranges from 6 nm to 10 µm (Järvinen et al., 2014; Lamminen, 2011).

Iso-kinetic sampling using impingers is the most common way of manual sampling of emissions (Bade et al., 2014; Gjernes et al., 2017; Lombardo et al., 2017; Mertens et al., 2012; Mertens et al., 2013; Morken et al., 2014; Morken et al., 2017). Typically, multiple impingers are installed in series to avoid breakthrough. The first impinger is often empty, whereas in the following impingers different absorbents, like dilute sulphuric acid or 2,4-dinitrophenylhydrazine (DNPH), are used. Sulphuric acid is often used for collection ammonia and amine samples, while 2,4-dinitrophenylhydrazine is used to sample acetaldehyde and formaldehyde (Bade et al., 2014; Mertens et al., 2012; Mertens et al., 2013). A good overview of standard methods for manual sampling, mainly developed for monitoring of the working environment, can be found elsewhere (Azzi et al., 2010; SEPA, 2015; Wittgens et al., 2010). A disadvantage of the iso-kinetic sampling is that it is a offline method, used periodically. FTIR, discussed earlier, is therefore often used to continuously monitor amine and ammonia emissions in the gas phase.

4 Results

4.1 Solvent Stability and Corrosion

Both oxidative and thermal degradation may take place with the carbamates formed in a reversible reaction between amine and CO_2. In the case of thermal degradation the mechanism often goes through carbamate polymerisation reactions (Davis and Rochelle, 2009; Lepaumier et al., 2009a; Rochelle, 2012). Oxidative degradation mechanisms, which are widely studied but extremely complex and therefore less understood, are assumed to start with radical reactions on the amine or carbamate. Once the reactions have initiated and primary degradation compounds are formed, these can react further with other degradation compounds, carbamates and amine in the solution to form secondary degradation compounds (Bello and Idem, 2005; Eide-Haugmo et al., 2011; Lepaumier et al., 2009a). These reactions are catalysed by the presence of dissolved metals in the aqueous amine solvent (Blachly and Ravner, 1963; Goff, 2005). The chemical structure of some typical degradation compounds identified and/or quantified in pilot plant and lab scale studies can be found in the appendix, in Table S3.

*Table 3.1: Summary of the main analytical methods used. *offline measurement*

Method	**Compounds analysed**	**Solvent amine**	**Water wash liquid**	**Emission**	**Remarks**
LC-MS	Amine and amine degradation products.	x	x	x*	The equipment and maintenance are costly, Requires skilled operator, often off site. However, up-concentration possible and is able to detect compounds in low concentration.
GC-MS	Amine and amine degradation products.	x	x	x*	The compounds need to have boiling point below 300-500 °C and the analytes have to be stable at these high temperatures. High-quality spectra achieved and extensive library of pure compounds available to compare against.
IC	Amine and amine degradation products.	x	x		Relatively inexpensive but requires regular use and maintenance. Only ionic compound could be analysed.
FT-IR	Amine gas effluents e.g. aldehydes, ammonia, water NO_X, SO_X, CO and CO_2	x	x	x	Online CO_2 analysis possible; both liquid and gas phase analysis possible, often preferred for emission monitoring; Liquid phase analyses more challenging due to degradation; Also used for speciation.
Titration	Total alkalinity in the solvent and in the water wash liquid; the CO_2-loading analyses; heat stable salts (HSS) analyses	x	x		Simple method and inexpensive.
PTR-MS	Amine and volatile organic compounds (VOCs).			x	Gas phase - could be used online; Quantitative data obtained without gas standard and calibration; High detection sensitivity (pptV range)
ICP-MS	Atoms	x			ppm levels can be measured; expensive instrument with high operation cost
TOC/TN	Carbon and nitrogen	x	x		Relatively simple and inexpensive; Could be placed onsite; often used to measure CO_2 in a liquid sample
FMPS	Particle size distribution			x	Fast response; Not robust in demanding industrial surroundings
OPC	Particle size distribution and total particle number			x	Detects particles down to 50 nm in diameter; Properties of aerosol like density and shape not accounted for
SEM/EDX	Particle size distribution and structure, size and composition of solids in the aerosol particles			x*	Offline method
ELPI+	Particle size distribution and particle number concentration			x	Offline method

A total of 29 individual campaigns in 18 different pilot plants, where solvent degradation was studied, were found. 30wt% MEA (aq.) was used in 19 of these (Table 4.1) and 10 were campaigns testing proprietary or other amine solvents (Table 4.2). A total of about 40 different compounds or compound groups were found measured in the liquid phase of the different campaigns, some just once, while others reoccur in several studies. A summary of the most frequently occurring liquid phase degradation components, as well as in which campaigns they have been analysed, can be found in Table 3.1 for campaigns using 30wt% MEA (aq.) and Table 4.1 for other, including proprietary, solvents.

Despite of pretreating the flue gas to remove reactive contaminants, amine degradation does take place in large scale CO_2 capture. This is sometimes a terminal problem, resulting in the need for solvent replacement and interrupted operation. Some technologies are being studied, to limit degradation after it has began to take place, such as solvent reclaiming, removing irreversibly formed heat stable salts. Reclaiming technologies aim to keep as much of the non-degraded amine as possible and only remove formed contaminants from the solvent. Reclaiming can typically be either thermal, by ion exchange or through electrodialysis and may be performed on- or offline (Kentish, 2016; Wang et al., 2015). The "Bleed and Feed" strategy involves the removal of parts of the degraded solvent and replacing it with fresh solvent (Moser et al., 2020). If any known degradation limiting technologies have been applied throughout the campaign, this is also given in Table 4.1.

Table 4.1: List of all the 30wt% MEA (aq.) campaigns studied in this review.

Location	**Time [h]**	**Remarks**	**Campaign focus**	**References**
Brindisi	550	40 m^3 of 30wt% MEA added during campaign. Typically, 1 mg m_N^{-3} of particulate matter at inlet.	Assessment of different operation modes and conditions. Establish guidelines with relevant data on emissions, HSE, and other operability, flexibility and cost aspects.	Mangiaracina et al. (2014); (Rieder et al., 2017)
CAER 0.1 MWth	100		Comparison of MEA 30wt% and the proprietary solvent CAER B2	(Thompson et al., 2014)
CAER 0.7 MWe	1316	Thermal reclaiming was performed from 880 to 970 hours.	Understand the impact on the solvent of flue gas constituents and potential higher oxygen content in the solvent due to secondary air stripper	(Thompson et al., 2017a; Thompson et al., 2017c; Thompson et al., 2017d)

Location	Time [h]	Remarks	Campaign focus	References
Changchun	1063		Performance trials; comparison with different solvent blends.	(Feron et al., 2015; Feron et al., 2014)
Esbjerg (a)	6000	Samples analysed after 500 hours. Solvent partly degraded before start (0.5wt% HSS content). 6 ppm S in flue gas.	Demonstrate the post combustion capture technology in conjunction with a coal-fired power station. Comparison with CASTOR 2, additionally comparing sulphur accumulation properties.	(Dhingra et al., 2017; Knudsen et al., 2009)
Esbjerg (b)	3360	Samples from 1850 hours (11 weeks) studied in degradation study.	Test campaign.	(da Silva et al., 2012)
Ferrybridge	>600		Benchmarking with MEA, before testing of a proprietary solvent. Assessment of solvent durability, perform process optimisation and to provide data on plant design and scale-up.	(Fitzgerald et al., 2014)
Heilbronn (a)	1600	Campaign in 2011.	Benchmarking campaign.	(Dhingra et al., 2017; Rieder and Unterberger, 2013)
Heilbronn (b)	1500	760 kg MEA added after 952 hours, water added at end, reducing the MEA concentration to ~25wt%. Concentrations of degradation products given here are from sampling at 535 hours. Campaign took place in 2013/14.	Establish guidelines with relevant data on emissions, HSE, and other operability, flexibility and cost aspects. ED reclaiming tests performed offline, with degraded solution.	(Bazhenov et al., 2015; Bazhenov et al., 2014; Rieder et al., 2017)
Longannet, MTU	Ca. 4400	Reclaiming after 3 months, total time 6 months		(da Silva et al., 2012)
Loy Yang	834	MEA pre-used 639 or 700 hours, for capture of CO_2 from a black coal-fired power plant (Tarong).	Performance trials; comparison with different solvent blends.	(Artanto et al., 2012; Dhingra et al., 2017; Reynolds et al., 2015b)
Maasvlakte (a)	3500	Reclaimed after 3000 hours	Study corrosion in relation to solvent degradation and ammonia emissions.	(Dhingra et al., 2017; Khakharia et al., 2015a)

Location	**Time [h]**	**Remarks**	**Campaign focus**	**References**
Maasvlakte (b)	890		Establish guidelines with relevant data on emissions, HSE, and other operability, flexibility, and cost aspects.	(Rieder et al., 2017)
Niederaussem (a)	5000		Performance validation and investigation of time-dependence of MEA degradation and organic acid formation. Test of optimised process configurations.	(Moser et al., 2011a)
Niederaussem (b)	12 000		Study solvent degradation.	(Moser et al., 2018)
Niederaussem (c)	13 000		Study time-dependent degradation products and trace components and how they can act as catalysts for degradation. Confirm threshold concentrations of iron from literature. Testing of "Bleed and Feed" as a degradation management strategy.	(Moser et al., 2020)
TCM (a)	2162	Campaign duration 20.11.13-24.02.14	Verify Aker Solutions' Advanced Carbon Capture® process including two proprietary advanced amine solvents.	(Gorset et al., 2014; Morken et al., 2014)
TCM (b)	2000	Reclaimed after 1852 hours	Demonstrate and document the performance of the TCM DA Amine Plant.	(Morken et al., 2017)
Tiller	2350		Benchmarking campaign.	(da Silva et al., 2012; Mejdell et al., 2011)

Formate, as well as other organic acids, have long been regarded as primary indicators of oxidative degradation in the liquid phase and are therefore among the most reported degradation compounds of MEA degradation. Of the 19 campaigns shown in Table 4.3, formate is quantified in nearly two thirds, and half of the campaigns also analysed for oxalate. These two as well as acetate and glycolate, are formed in the first steps of the degradation process by electron or hydrogen abstraction before they react with the amine or other degradation products to form other degradation compounds (Rooney et al., 1998).

Table 4.2: List of all the campaigns using proprietary or other solvents than MEA 30wt% (aq.) studied in this review.

Location	Time [h]	Solvent	Remarks	Reference(s)
Austin		8m PZ		(Nielsen et al., 2013)
CAER 0.1 MWth	185	CAER B2		(Thompson et al., 2014)
Changchun	306	blend 5		(Feron et al., 2014)
Esbjerg	1000	CASTOR 2	Sampling after 500 h, stripper pressure 2.0 bar	(Knudsen et al., 2009)
Ferrybridge	>600	RS-2®		(Fitzgerald et al., 2014)
Łaziska		40wt% AEEA		(Spietz et al., 2018)
Mikawa	840	Solvent A	Sterically hindered, secondary amine	(Saito et al., 2014; Saito et al., 2015)
Mikawa	740	TS-1		(Saito et al., 2014)
TCM	4029	S21	03.10.12-01.04.13, Reclaiming after 3600 hours	(Gorset et al., 2014)
TCM	3507	S26	03.03.14-16.08.14, Reclaiming after 3300 hours	(Gorset et al., 2014)

A summary of reported concentrations of organic acids can be seen in Figure 4.1, as well as total concentration of other (in some cases unknown) HSS, where that has been reported. One MEA-campaign from the 0.1 MWth CAER pilot (Thompson et al., 2014) of only 100 hours and one campaign from the Esbjerg pilot (Knudsen et al., 2009) of unclear total operation time prior to HSS analysis, were omitted. Figure 4.1 shows a large span in the concentrations of heat stable salts found in various 30wt% MEA (*aq.*) campaigns when normalised per time in operation. Normalisation of this data does not give a complete picture of the degradation processes and may not be an ideal way of comparing different pilot campaigns and locations to one another, but it gives a visual representation of the degradation compounds observed. Surprisingly, one of the highest HSS concentrations is actually found in the shortest campaigns. A correlation between the amount of pretreatment technologies applied prior to CO_2 removal is apparent, when comparing Figure 4.1 with Table 2.2. A summary of the flue gas sources and compositions at different locations, where post-combustion CO_2 capture campaigns have been performed. SR: SO_X removal, NR: NO_X, PR: particle removal. Further details on pretreatment can be found in the appendix, Table S1. Esbjerg, Heilbronn and Niederaussem all operate with coal as their flue gas sources and have an extensive pretreatment setup. TCM also observe relatively low concentrations of HSS. The flue gas originates from sources with less contaminants and the degradation here is comparable to pretreated flues gas from coal-fired power plants.

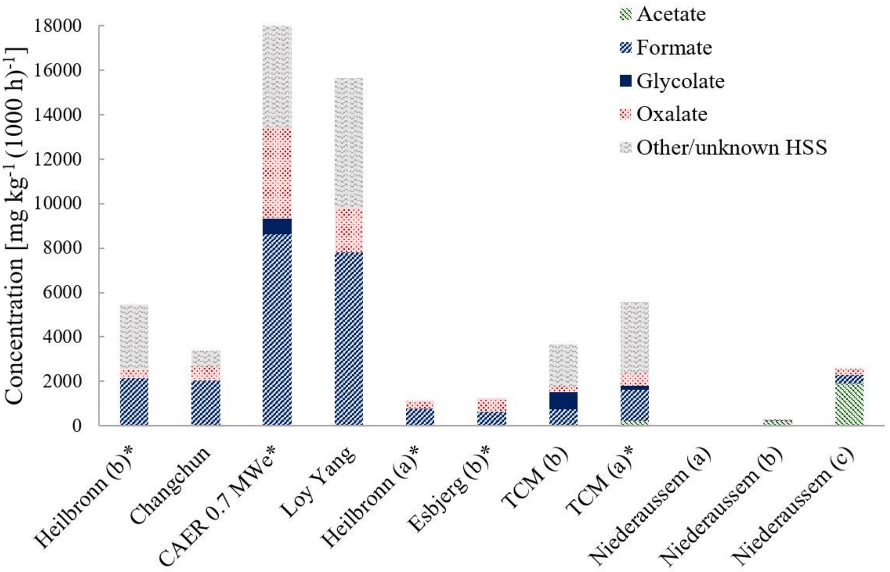

*Figure 4.1: Heat stable salt/organic acid concentrations measured in post-combustion CO_2 capture pilot campaigns using 30wt% MEA, at the end of the campaign or right before reclaiming the solvent. Concentrations converted to concentration per 1000 hours, to facilitate comparison of different campaigns and pilots. Keep in mind that where no concentration is given, reported data for the given compounds is not available. All references are given in Table 4.3. *Mass concentration converted to mass fraction under the assumption that $\rho = 1$ kg L^{-1}.*

Furthermore, it can be observed that most campaigns see relatively high concentrations of organic acids and HSS at the campaign end, or when samples have been analysed before solvent reclaiming has taken place, but that the ratio between the four organic acids are inconsistent. Acetate and formate are most often the dominant degradation product of those analysed, but it varies which one of the two is found in the highest concentrations. It therefore seems like process conditions play a very important role for which degradation pathways will take place within the solvent. The average concentration of liquid phase formate in Figure 4.1 is 2500 mg kg^{-1} (1000 h)$^{-1}$, whereas acetate, oxalate and glycolate both have an average of 800 and glycolate of 500 mg kg^{-1} (1000 h)$^{-1}$, respectively.

All the compounds previously discussed are typical products of oxidative degradation. Thermal degradation products have been reported in many campaigns and include *N*-(2-hydroxyethyl)-2-imidazolidione (HEIA), which is a product of a carbamate polymerization reaction, and 2-(2-hydroxyethylamino)ethanol (HEEDA), which is a product of an addition reaction. These degradation compounds are typically seen in lower concentrations than the oxidative degradation products. Measured concentrations of thermal (HEIA), as well as secondary oxidative degradation compounds (HEA, HEF, HEI, HEGly, HEPO, OZD, BHEOX) in MEA-campaigns are summarised in Table 4.5, the degradation product bicine is also presented here, assumed to be formed upon oxidation of DEA/MDEA or TEA derivatives (Gouedard et al., 2014; Lepaumier et al., 2009b). It is evident that secondary oxidative degradation compounds, formed when primary degradation compounds proceed to react, also occur in relatively high concentrations, especially HEF, HEGly and HEPO. The average concentrations of both HEGly and HEPO are twice that of formate when considering all campaigns, with about 5000 and 7000 mg kg^{-1} $(1000\ h)^{-1}$, respectively. This same trend, of much higher concentrations of HEPO and HEGly in the solvent than formate, is seen also in studies with synthetic flue gas (Chahen et al., 2016; Knuutila et al., 2014b).

Thermal degradation compounds tend, however, to occur in lower concentrations. For example, the concentration of HEEDA are very low and rarely reported, and it has not been included in this table. The highest reported concentration of HEEDA is 246 mg L^{-1}, in one of the MEA 30wt% (*aq.*) pilot campaigns (Thompson et al., 2017a). Some pilot campaigns even observe that the concentrations of some thermal degradation compounds (HEIA and HEEDA) decline after an initial increase, throughout the operation time, making it apparent that they further react, or degrade themselves (Moser et al., 2020; Thompson et al., 2017a). A campaign using synthetic flue gas and 30wt% MEA (*aq.*), also saw OZD reaching a threshold concentration after a certain time of operation, and thereafter no further change, despite of the overall degradation rate sustaining (Chahen et al., 2016). Equally for Pz, thermal degradation products such as ethylenediamine and *N*-(hydroxyethyl)-piperazine have been found to initially increase and then decrease (Nielsen et al., 2013).

Inorganic compounds originating from the flue gas or construction material, like oxidised metal ions and elementary sulphur, are also found in the degraded solvents. Keeping track of dissolved metal concentrations allows for a simple assessment of corrosion of the equipment. The presence of NO_X, SO_2, and chlorine in the flue gas are the reasons why these are found in the solvent. The accumulation of these species is likely to influence degradation rates and mechanisms and therefore give valuable insights about the processes taking place within the degrading solvent. Figure 4.2

shows that there is no immediate correlation between operation time and the accumulation of iron in the MEA solvent.

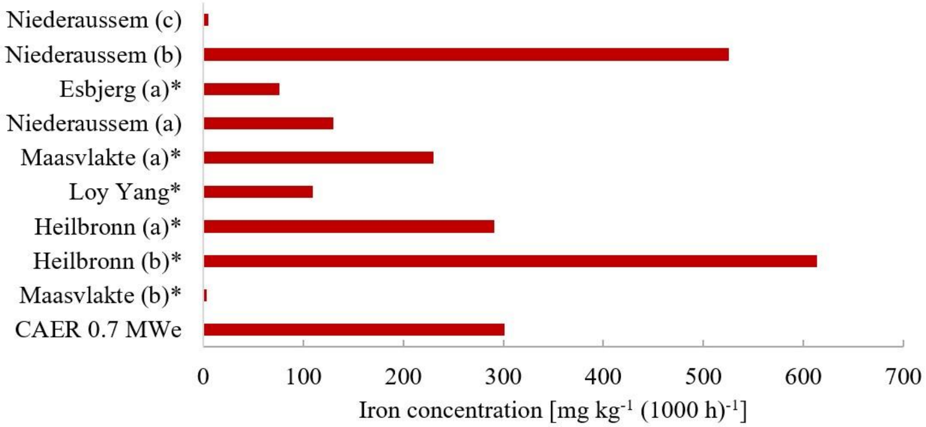

*Figure 4.2: Accumulated concentrations of iron during pilot campaigns using MEA 30wt% (aq.). All references are given in Table 4.3. *Mass concentration in original publication converted to mass fraction under the assumption that* $\rho = 1$ *kg* L^{-1}.

NO_X are known to form nitrosamines with several amine species. Nitrosamines are toxic already in low concentrations and have therefore been of great concern for the operation of an amine-based CO_2 capture process. They are, however, readily degradable in sunlight (de Koeijer et al., 2013). The formation of nitrosamines in pilot plants has been a concern, both with NO_X present in the flue gas and particularly when using secondary amines, which are known to be highly prone to the formation of nitrosamines (Fine, 2015; Knuutila et al., 2014a). A thorough lab-scale pilot test of addition of NO and NO_2 to MEA (primary amine) and diethanolamine (DEA; secondary amine) showed this, also testing the UV-radiation as a removal technology (Table 4.8) (Knuutila et al., 2014a; Knuutila et al., 2014b). Where measured, the concentrations of the nitrosamine NDELA is found in Table 4.5. Other nitrosamines, which are quantified less often than NDELA in the liquid phase and gas phase emissions in pilot campaigns are No-HEGly and NDMA. Morken et al. (2014) found 15 times more No-HEGly than NDELA, accounting for about half of the total nitrosamine (TONO) content. This finding indicates that the focus when studying nitrosamines in the amine solutions may not have been on the right compounds. Furthermore, a comparative study quantifying nitrosamines in identical solutions, a large variation in results from different laboratories has been reported (Fraboulet et al., 2016).

Table 4.3: An overview of the campaigns, which have studied degradation in MEA 30wt% (aq.) and which degradation product and dissolved inorganic compound concentrations have been reported. x = identified and quantified, nd = not detected, t= tentative

Campaign	**Total HSS**	**Acetate**	**Formate**	**Glycolate**	**Oxalate**	**HEA**	**HEI**	**HEF**	**HEGly**	**HEIA**	**HEPO**	**BHEOX**	**OZD**	**NDELA**	**HEEDA**	**Bicine**	**DEA**	**Fe**	**Ni**	**Cl-**	**SO_4^{2-}**	**NO_3^-**	**Reference**
Brindisi																		x					(Mangiaracina et al., 2014; Rieder et al., 2017)
CAER 0.1 MWth	x		x																	x	x	x	(Thompson et al., 2014)
CAER 0.7 MWe	x	x	x	x	x		x		x	x			x		x			x	x	x	x	x	(Thompson et al., 2017c; Thompson et al., 2017d)
Changchun	x		x		x																		(Feron et al., 2015; Feron et al., 2014)
Esbjerg (a)	x																	x					(Dhingra et al., 2017; Knudsen et al., 2009)
Esbjerg (b)			x		x	x	x	x	x		x	nd	nd								x		(da Silva et al., 2012)
Heilbronn (a)			x		x													x	x	x		x	(Dhingra et al., 2017; Rieder and Unterberger, 2013)
Heilbronn (b)	x	x	x	x	x													x		x	x	x	(Bazhenov et al., 2015; Rieder et al., 2017)
Longannet, MTU							x	x					x										(da Silva et al., 2012)
Loy Yang	x	x	x		x		x		t	x	t	x	x		nd	x	nd						(Artanto et al., 2012; Dhingra et al., 2017; Reynolds et al., 2015b)
Maasvlakte (a)																		x					(Dhingra et al., 2017; Khakharia et al., 2015a)
Maasvlakte (b)																		x					(Rieder et al., 2017)
Niederaussem (a)		x	x							x								x	x	x			(Moser et al., 2011a)
Niederaussem (b)		x	x															x	x	x	x		(Moser et al., 2018)
Niederaussem (c)		x	x		x					x			x		x			x	x	x	x	x	(Moser et al., 2020)
TCM (a)	x		x	x	x																		(Gorset et al., 2014; Morken et al., 2014)
TCM (b)	x	x	x	x	x	x	x	x	x	x	x	x	x	x	x	x	x				x	x	(Morken et al., 2017)
Tiller						x	x	x	x		x	x	x	x	x	x	nd						(da Silva et al., 2012; Mejdell et al., 2011)
SUM	8	7	12	4	10	4	7	5	5	5	5	4	7	3	5	3	3	10	5	7	8	7	

Table 4.4: An overview of the campaigns, which have studied degradation in various solvents (aq.) and which degradation product and dissolved inorganic compound concentrations have been reported.

Pilot	**Solvent**	**Degradation comp.**	**Inorganics**	**Reference(s)**
Austin	8m PZ	Formate, acetate, oxalate + more	Cr^{3+}, Fe^{2+}, Ni^{2+}, Cu^{2+}	(Nielsen et al., 2013)
CAER 0.1 MWth	CAER-B2	Total HSS and formate	SO_4^{2-}	(Thompson et al., 2014)
Esbjerg	CASTOR 2	Total HSS	S	(Knudsen et al., 2009)
Changchun	"blend 5"	Formate	SO_4^{2-}	(Feron et al., 2015)
TCM	S21	Total HSS and TONO		(Gorset et al., 2014)
TCM	S26	Total HSS and TONO		(Gorset et al., 2014)
Mikawa	"tertiary solvent A"	Formate, acetate and oxalate		(Saito et al., 2014)
Mikawa	"TS-1"	Formate		(Saito et al., 2014)

*Table 4.5: Measured concentrations of degradation compounds in mg L^{-1}, which are not inorganic components nor organic acids, in post-combustion CO_2 capture pilot campaigns using 30wt% MEA, at the end of the campaign or right before reclaiming of the solvent. *Mass fraction in original publication converted to mass concentration under the assumption that $\rho = 1$ kg L^{-1}.*

Campaign	**HEA**	**HEF**	**HEI**	**HEGly**	**HEPO**	**BHEOX**	**OZD**	**HEIA**	**NDELA**	**Bicine**	**Reference**
CAER 0.7 MWe			4800	1047			< 10	1712			(Thompson et al., 2017c)
Esbjerg (b)	590	440	440	7610	2320						(da Silva et al., 2012)
Longannet		8580	160				23				(da Silva et al., 2012)
Loy Yang			2030*			3400*	350*	960*		270*	(Reynolds et al., 2015b)
Niederaussem (a)								200*			(Moser et al., 2011a)
Niederaussem (c)							96*	380*			(Moser et al., 2020)
TCM (a)	4580	5200	2070	8000	11 140		150		31 µmol L^{-1}		(Morken et al., 2014)
TCM (b)	4963	5062	1826	18 922	18 788	274	82	181	4.9	62	(Morken et al., 2017)
Tiller	731	721	1758	7295	27 691	35.2	8.7		0.536	32.6	(da Silva et al., 2012)
Average/1000 h	1321	1505	839	4821	6940	672	131	435	1	32	

*Table 4.6: Measured concentrations of inorganic compounds in mg kg^{-1}, including metals, in post-combustion CO_2 capture pilot campaigns using 30wt% MEA as solvent, at the end of the campaign or right before reclaiming of the solvent. *Mass concentration in original publication converted to mass fraction under the assumption that ρ = 1 kg L^{-1}.*

Campaign	**Nitrate (NO_3^-)**	**Sulphate (SO_4^{2-})**	**Chloride (Cl^-)**	**Nickel (Ni)**	**Sulphur (S)**	**Reference**
CAER 0.1 MWth	720	3400	40			(Thompson et al., 2014)
CAER 0.7 MWe	1115*	3640*	193*	28		(Thompson et al., 2017c; Thompson et al., 2017d)
Esbjerg (b)		5100*				(da Silva et al., 2012)
Heilbronn (a)	150*	370*	10*	180*		(Rieder and Unterberger, 2013)
Heilbronn (b)	600*	820*	70*			(Bazhenov et al., 2014)
Niederaussem (a)			1800	200	100	(Moser et al., 2011a)
Niederaussem (b)	270	85	8300		20	(Moser et al., 2018)
Niederaussem (c)	2200	800	83	0	200	(Moser et al., 2020)
TCM (b)	1173*	70*				(Morken et al., 2017)

The reported concentrations of inorganic compounds quantified in the solvent during pilot campaigns are summarised in Table 4.6 for MEA and Table 4.7 for other amines and proprietary solvents. Some additional compounds, in addition to those given in Table 4.3 and Table 4.4, can be found quantified for the campaigns described in da Silva et al. (2012), Morken et al. (2017), Thompson et al. (2014), Reynolds et al. (2015b), Rieder and Unterberger (2013) and Saito et al. (2014). Since these compounds are not widely analysed and thus cannot not be used in search for general trends, they are not given here.

Dhingra et al. (2017) already showed that the concentration of dissolved iron in the 30wt% (*aq.*) solvent tends to reach a sudden spike over a short period of time in four different pilot campaigns. It therefore comes as no surprise, that there is no correlation between operation time and iron concentration in the solvent when studying Figure 4.2. The campaigns at Niederaussem (c) (Moser et al., 2020) and at Maasvlakte (b) (Rieder et al., 2017) have significantly lower iron concentrations compared to the seven other campaigns where data is available, despite of at least the pilots in Maasvlakte, Loy Yang and Esbjerg all being constructed in stainless steel 304/316L (Dhingra et al., 2017). These numbers indicate that no severe corrosion had taken place during the campaign. Comparing the seven campaigns with relatively high iron concentrations, we may still not be able to say much about degradability and corrosivity of the system, since degradation and corrosivity do not increase linearly, instead we can expect a rapid spike after corrosion and solvent degradation have reached a certain level.

When comparing the degradation of the proprietary solvents in Table 4.7, specific characteristics of the solvent have to be compared to MEA. Formed degradation compounds are solvent specific, making it impossible to compare solvents of unknown amines to any benchmark by comparing single degradation components. However, the formation of HSS over time makes an interesting comparison since total HSS -measurement takes into account all different HSS compounds that are present. For example, HSS formation rate appears to be halved with CAER-B2 compared to 30wt% MEA (*aq.*) under the same conditions in a 0.1 MWth pilot plant (Thompson et al., 2014), whereas when CASTOR-2 is compared to 30wt% MEA (aq.), it is reduced to a fourth (Knudsen et al., 2009). In "Blend 5" tested at Changchun, the HSS formation rate is more or less the same as for 30wt% MEA (*aq.*) (Feron et al., 2015). It should be remembered that comparing total HSS, or solvent make-up-rate, discussed earlier, does not tell anything about the formation of potentially toxic degradation compounds or the formation of volatile degradation products, which can have a huge effect on the design of emission countermeasures and monitoring emissions. A detailed understanding of the degradation compounds formed for all amines is always needed.

*Table 4.7: Accumulated concentrations of degradation compounds and sulphate during pilot campaigns using other solvents and blends than MEA 30wt%. *Mass concentration in original publication converted to mass fraction under the assumption that ρ = 1 kg L^{-1}. **Sum of formate, oxalate and acetate.*

Pilot	**Solvent**	**HSS [mg kg^{-1} (1000 h)$^{-1}$]**	**Formate [mg kg^{-1}]**	**Sulfate (SO_4^{-2}) [mg kg^{-1}]**	**Reference**
Austin	8m Pz	5648**	3273		(Nielsen et al., 2013)
CAER 0.1 MWth	CAER-B2	22 162	1694	2929	(Thompson et al., 2014)
Changchun	Blend 5	4085	215	980	(Feron et al., 2015)
Esbjerg	CASTOR-2	4000			(Knudsen et al., 2009)
Mikawa	Tertiary solvent A	313*	5*		(Saito et al., 2014)
Mikawa	TS-1	644*			(Saito et al., 2014)
TCM	S21	28 mmol/mg			(Gorset et al., 2014)
TCM	S26	6 mmol/mg			(Gorset et al., 2014)

Table 4.8: An overview of some relevant pilot studies using synthetic flue gas and aqueous amine solutions.

Pilot	**Solvent**	**Time [h]**	**Compounds studied**	**Campaign focus**	**Reference(s)**
Austin (SRP)	8m Pz	1350	Formate, oxalate, acetate, Cr^{3+}, Fe^{2+}, Ni^{2+}, Cu^{2+} + more		(Nielsen et al., 2013)
IFPEN	30wt% MEA	1700	Formate, glycolate, acetate, SO_4^{2-}, NO_3^-, NO_2^-, HEGly, DEA, OZD, HEF, HEA, HEI, HEPO + more	Study MEA degradation and predict degradation product emissions.	(Chahen et al., 2016)
Gløshaugen	30wt% MEA	990	Formate, NO_3^-, HEGly, DEA, OZD, HEF, HEPO, HEA, NDELA		(Knuutila et al., 2014a; Knuutila et al., 2014b)
Gløshaugen	50wt% DEA	410	OZD, HEF, HEPO, HEA, HEI, NDELA	Study formation and destruction of nitrosamines.	(Knuutila et al., 2014a; Knuutila et al., 2014b)

4.2 Emissions

In a CO_2 capture plant, it can be distinguished between three different types of emissions; gas-phase (vapour), liquid entrainment, and aerosol/mist emission (Knudsen et al., 2013; Spietz et al., 2018). Factors influencing the gas-phase emission are the volatility of the amine, CO_2 loading, and gas temperature. Often, a well-designed water wash is enough to minimise these emissions. Liquid entrainment emissions are liquid droplets that are carried by the gas flow, however, water wash sections can remove these. Aerosols and mist are small droplets suspended in the gas. The formation of these depend to a large extent on the flue gas composition upstream the CO_2 capture plant and on the capture plant's operation conditions (Mertens et al., 2015) and presence of condensation nuclei (<1 µm) as for example particulate matter, soot, SO_2, SO_3, NO_2 or H_2SO_4 (Mertens et al., 2012; Moser et al., 2015; Spietz et al., 2018). When formed, mist penetrates wash sections and conventional demisters, and therefore, additional mitigation techniques are required.

Several studies have been conducted in the last years to better understand and control emissions and mist/aerosol formation. A summary of the components contained in emissions can be found in Table 4.9. The table shows that the most commonly monitored emission is the solvent amine, followed by ammonia. Ammonia is one of the primary degradation compounds of MEA and is highly volatile. Nitrosamine concentrations are also often monitored due to their harmful nature. Concentration of nitramines in water wash have also been measured, but in both of them the nitramines were below the detection limit in the water wash water (Khakharia et al., 2014a;

Morken et al., 2014). Further volatile degradation compounds, such as allylamines, (form)aldehydes, and some ketones, have been studied only in a few campaigns.

Table 4.9: Emissions monitored at different pilot locations/campaigns. Emission monitoring given here does not necessarily mean that concentrations of emissions are published.

Pilot plant	**Solvent amine**	**NH_3**	**Nitrosamine**	**Aldehydes**	**Alkylamine**	**Nitramine**	**Ketones**	**Reference(s)**
CAER 0.7 MWe	x	x	x	x			x	(Thompson et al., 2017a; Thompson et al., 2017d)
Esbjerg	x	x		x				(Khakharia et al., 2014b; Mertens et al., 2012; Mertens et al., 2013; Aas and da Silva, 2010)
Ferrybridge	x	x	x					(Fitzgerald et al., 2014)
Łaziska		x		x				(Spietz et al., 2018)
Maasvlakte	x	x	x			x		(da Silva et al., 2013; Khakharia et al., 2014a)
Mitsubishi		x						(Kamijo et al., 2013)
MTU - Brevik	x	x	x					(Knudsen et al., 2014)
MTU - Longannet	x							(Graff, 2010)
MTU - NCCC	x	x			x			(Knudsen et al., 2013)
NCCC	x	x	x	x	x			(Dahlin et al., 2013)
Niederaussem	x							(Moser et al., 2014; Moser et al., 2013; Moser et al., 2017)
TCM	x	x	x	x		x	x	(Bade et al., 2014; Gorset et al., 2014; Lombardo et al., 2017; Morken et al., 2014; Morken et al., 2017)
Tiller	x	x	x		x			(Mejdell et al., 2011)
Toshiba	x							(Fujita et al., 2013)

The concentrations of the main degradation species detected in the gas phase can be found in Table 4.10, where it can be observed that there is no universal standard for the reporting of concentrations of compounds in emissions. Variation in practice, insufficient information and the different units makes it challenging to compare the results in detail. The MEA emissions are below one ppm in three out of the six campaigns. In the pilot campaigns with high MEA emissions, the emissions are measured after the absorber and no water wash sections are used. For proprietary solvents, the solvent emissions are, in all cases, lower compared to those of MEA campaigns. This could mean that the proprietary solvent components are less volatile than MEA, or well-designed emission mitigation methods are used.

Ammonia emissions, as seen in Table 4.10, are larger than MEA emissions due to the high volatility of ammonia. Also ammonia emissions can be controlled with water wash systems, partly explaining the lower emissions at TCM, Tiller, Maasvlakte and Mitsubishi compared to CAER. Furthermore, as the ammonia concentrations are often at ppm-levels in the gas phase, it is an attractive compound to monitor as a sign of degradation. Proprietary solvents seem to degrade less to ammonia as, in all cases, the ammonia emissions are significantly lower than those of MEA. However, since ammonia is highly volatile, the ammonia emissions are very dependent on the operating time, temperatures in the water wash sections and process conditions. The solvent degradation also influences emissions. As solvent degradation increases, the emission of ammonia has been reported to increase in MEA (Mertens et al., 2012; Mertens et al., 2013). However, no dedicated studies were found looking at the effect of degradation on emissions.

As seen in Table 4.10, nitrosamines are generally observed only in the lower ppm to ppb range. The same is true for aldehydes with one exception: a laboratory pilot study by Chahen et al. using 30wt% MEA (*aq.*) and a synthetic flue gas. In this study, acetaldehyde was measured in the range of 1 mg m^{-3}. This is a nearly 80 times higher concentration than formaldehyde in this particular study. This study also found relatively high concentrations of ethylene glycol and the nitrosamine NDMA, but these in the range of <0.5 mg m^{-3} (Chahen et al., 2016).

Based on the pilot results it is clear that for MEA, the wash water section can limit the MEA emission to a few hundred ppb, ammonia in the low ppm range, methylamine at low ppb range in case no mist is present (Gjernes et al., 2017; Lombardo et al., 2017; Morken et al., 2017). Furthermore, in these cases, there is no observation of nitrosamine and nitramine emissions over the detection limit. The solvent emissions of the tested proprietary solvents can be controlled to similar levels as seen with 30wt% MEA (*aq.*). This is in line with reported numbers for commercially available proprietary solvents (Feron et al., 2020; Singh and Stéphenne, 2014).

*Table 4.10: Concentrations of emissions in different campaigns and locations, where given in literature. *Reclaiming was, or may have been, performed in the duration of the campaign. [a] Reduced after water wash and BDU. [b] Reduced with ACC™ emission control system. [c] Reduced by cooling lean temperature. [d] Reduced by higher lean temperature and two-stage water wash [e] µmol* m_N^{-3} *nd = not detected.*

Pilot plant	Solvent	Solvent amine	NH_3	TONO	Formaldehyde	Reference(s)
Mitsubishi [ppm]	MEA		14			(Kamijo et al., 2013)
TCM [ppm]	MEA	<1	20	$<8\times10^{-8}$		(Morken et al., 2014)
Tiller [ppm]	MEA	<0.4	20	[d]		(Mejdell et al., 2011)
CAER 0.7 MWe* [ppmV]	MEA	5-1385	12-282	< LOQ	35-73	(Thompson et al., 2017a; Thompson et al., 2017d)
MTU - NCCC [ppmV]	MEA	10-50 / 0[b]	10-40			(Knudsen et al., 2013)
NCCC [ppmV]	MEA (water wash)	2.13	1.74		0.0031	(Dahlin et al., 2013)
NCCC [ppmV]	MEA (acid wash)	3.02	4.75		0.0020	(Dahlin et al., 2013)
Ferrybridge* [mg m_N^{-3}]	MEA			0.020		(Fitzgerald et al., 2014)
Maasvlakte [mg m_N^{-3}]	MEA	250 / 1[a]	10-70	$(5 \text{ to } 75)\times10^{-6}$		(da Silva et al., 2013; Khakharia et al., 2014a)
MTU - Longannet* [mg m_N^{-3}]	MEA	<4	50-80			(Graff, 2010)
Łaziska [ppm]	AEEA		27-50		0.11	(Spietz et al., 2018)
Mitsubishi [ppm]	KS-1		<1.5			(Kamijo et al., 2013)
MTU - NCCC [ppmV]	ACC novel solvent	20 / 0[b]	1-4			(Knudsen et al., 2013)
Toshiba [ppmV]	TS-1		18 / 5.6[c]			(Fujita et al., 2013)
Esbjerg [mg m_N^{-3}]	CASTOR/CESAR	0.02-0.7			0.059-1.1	(Khakharia et al., 2014b; Mertens et al., 2012; Aas and da Silva, 2010)
MTU - Breivik [mg m_N^{-3}]	S26	<0.46[b]	<4.0[b]	<0.03[b,d]		(Knudsen et al., 2014)
MTU - TCM* [mg m_N^{-3}]	S21	0.031	0.14	<0.83[e]		(Gorset et al., 2014)
MTU - TCM* [mg m_N^{-3}]	S26	0.09[b]	0.01[b]	<0.05[e]		(Gorset et al., 2014)
NCCC [ppm]	Pz	<1[d]	3.1	<0.34[e]		(Akinpelumi et al., 2019)
TCM* [mg m_N^{-3}]	S21	0.5	3.1	<0.34[e]		(Gorset et al., 2014)
TCM* [mg m_N^{-3}]	S26	1.8 / 0.09[b]	1.9 / 0.01[b]	<0.02[e]		(Gorset et al., 2014)

As mentioned earlier, the presence of mist can increase the emissions significantly and thus, extensive work has been conducted to study aerosol emissions, their formation, mechanisms, and countermeasures. Mist can be formed via two different nucleation mechanisms, homogeneous and heterogeneous (Kolderup et al.) and both mechanisms are important. Avoiding homogeneous nucleation by removing SO_3 and avoiding H_2SO_4 will not entirely eliminate aerosol formation, since heterogeneous nucleation and growth by condensation have been reported to be the main mechanisms leading to aerosol-based emissions in a CO_2 capture column (Khakharia et al., 2015a; Kolderup et al.; Moser et al., 2011b; Moser et al., 2014). Also, both the concentration of particles and sulphuric acid has an impact on the formation of aerosol emissions (Khakharia et al., 2015a; Khakharia et al., 2013). For cases with low particle numbers before the absorber, typically seen for natural gas-fired power plants, mist is often not detected (Morken et al., 2017). For TCM, a 500 000 particles cm^{-3} was deemed acceptable to stay below the local emission permit (Lombardo et al., 2017). Several publications discuss the influence of flue gas cleaning before the absorption column (Khakharia et al., 2013; Knudsen et al., 2013) and different process changes (Khakharia et al., 2015a; Khakharia et al., 2013; Khakharia et al., 2014b; Moser et al., 2011b; Moser et al., 2014; Moser et al., 2013) as the flue gas composition and operational settings influence the particle number, size, size distribution, composition, and physical/chemical properties of the mist

Effects of water wash temperature, acid wash, dry bed, flue gas pretreatment, and wet electric precipitator have been tested alone or in coupled operation. They all showed a reduction up to an order of magnitude of amine emission (Moser et al., 2014). A wet electrostatic precipitator (WESP), often seen as an option to avoid mist formation, could also cause aerosol formation by increasing the number concentration of ultra-fine particles or droplets in the flue gas (Moser et al., 2015). A gas-gas heater installed up- or downstream of the wet flue gas desulphurisation (WFGD) prevents amine mist formation inside the absorber (Harsha et al., 2019; Khakharia et al., 2015b; Khakharia et al., 2014b; Lombardo et al., 2017; Majeed et al., 2017; Mertens et al., 2015).

Having a dry bed between the absorber and the water wash reduces the emission of amine compounds (Moser et al., 2014). Furthermore, lean MEA inlet temperature to the absorber influencing the absorber temperature profile and flue gas temperature at the top of the absorber, flue gas temperature difference over the washing section, flow rate of water in wash sections as well as the amount of make-up water to these sections have a significant impact on the amine and ammonia emissions (Akinpelumi et al., 2019; Lombardo et al., 2017; Spietz et al., 2018). Demisters are an efficient way to reduce amine emissions when mist is present, and further testing of impaction candles and high efficiency demisters is proposed to identify options with low pressure drop and high efficiency (Lombardo et al., 2017). Finally, proprietary emission control concept (ACC), combining a novel absorber design to prevent amine mist formation and a final pH-controlled wash stage is reported to reduce the emission of alkylamines, ammonia and solvent amine(s) (Bade et al., 2014; Knudsen et al., 2013).

4.3 Analytical Methods

For the monitoring of both the solvent degradation and the emissions in the pilot plants, many different analytical methods are being deployed. The amount of information given about these, however, is varying. How much information is given can for example be dependent on the purpose of the given paper/report, if the analysis is done internally or externally, or if the specific method used is disclosed or not. In this section, the analytical methods that are most frequently deployed in the pilots and how they are used will be presented. These include FT-IR, LC-MS, GC-MS, IC, titration, PTR-MS and ICP-MS/-OES. Note that results from papers that only reports their findings, without stating which analytical method is being used, are not included.

When monitoring the emissions from the pilot plants, online FT-IR is often the preferred method (Artanto et al., 2012; Bade et al., 2014; de Koeijer et al., 2011; Fitzgerald et al., 2014; Khakharia et al., 2013; Khakharia et al., 2014a; Knudsen et al., 2013; Knudsen et al., 2014; Mertens et al., 2012; Moser et al., 2018; Thompson et al., 2017a). Here, the FT-IR is used to analyse the emissions from the absorber, and can detect and quantify various amines and aldehydes, water content, as well as standard inorganic components such as NH_3, SO_2, NO_X, etc.. The detection limit is usually 1 ppmv. When the solvent amine emission concentration dips below this limit, manual sampling campaigns have been conducted (Gorset et al., 2014).

LC-MS has also been frequently used to monitor emissions in many of the pilot plants (Bade et al., 2014; da Silva et al., 2012; Fujita et al., 2013; Khakharia et al., 2014a; Knudsen et al., 2013; Knudsen et al., 2014). This is however not done online, but through absorption in impingers. Different absorption medias are utilised, but sulphuric and sulfamic acid are the most common. At Norcem, DNPH cartridges was also used (Knudsen et al., 2014). These can capture condensate and aldehydes/ketones which is not captured in the acid absorbers. Sampling in the impingers are usually done for 1-2 hours. The impinger methods used are often well documented in the publications. The LC-MS results are, also, often used to verify

FT-IR results. As manual sampling combined with LC-MS analyses is based on up-concentrating the degradation compounds into the impingers, it can be used to detect compounds present in low concentrations, and can therefore give a more overall picture of the composition of the emissions. LC-MS is also used to study the solvent degradation and quantify degradation components (Knuutila et al., 2014a; Moser et al., 2020; Thompson et al., 2017c). Unfortunately, in general very little information is given about the LC-MS methods used by the pilot plants.

Like LC-MS, GC-MS is also used to monitor both the emissions and the solvent degradation in various pilots (Artanto et al., 2012; da Silva et al., 2012; Fujita et al., 2013; Knudsen et al., 2013; Knudsen et al., 2009; Moser et al., 2011b; Thompson et al., 2017c). The samples are often the same as the ones analysed with LC-MS, and so these two methods combined gives a comprehensive overview of the sample composition. But like with LC-MS, the methods used is in most cases under reported or not reported at all. There are however exceptions, where the method used is thoroughly rendered (Reynolds et al., 2015b).

Compared to the methods mentioned above, the information gained from IC is restricted to ionic species. This results in that that its use varies a lot in the different pilot plants. In some cases, it is used to analyse HSS in the solvent samples (da Silva et al., 2012; Fitzgerald et al., 2014; Moser et al., 2020; Reynolds et al., 2015b; Thompson et al., 2017c; Thompson et al., 2017d; Thompson et al., 2014), while in some cases only inorganic anions such as sulphate is analysed (Knuutila et al., 2014a; Mertens et al., 2015; Moser et al., 2020). How well the methods are rendered seems to depend on where the analysis has been conducted. For the ones performed in-house, the method is described well, while when external laboratories have been used it is usually not described.

Titration is a quick and cheap method, but is nevertheless not extensively used in the pilots. Under titration measurements of total amine concentration (total alkalinity), masurement of the CO_2-loading, or measurement of HSS is included. When titration is used to analyse samples from the pilots, many or all of these are usually performed (Fitzgerald et al., 2014; Knudsen et al., 2014; Knudsen et al., 2009; Moser et al., 2011a).

The last two analytical methods included is PTR-MS and ICP-MS/-OES. PTR-MS is used in some of the plants as an online analysis tool for amine concentration and volatile components (Bumb et al., 2017; Moser et al., 2014). In these cases, it is often used to study volatile degradation products in the emission stream (Fujita et al., 2013). ICP-MS/-OES is an offline method, and is used by some pilots to detect and quantify metals and trace elements in a solution (Knudsen et al., 2014; Moser et al., 2020; Thompson et al., 2017c). Little information is shared about the instruments or methods being used for both these analyses.

5 Discussion and Recommendations

Most of the pilots are not in continuous operation. Furthermore, the different campaigns typically focus on various aspects of the process to reduce risk, costs, and close knowledge gaps. As the pilot campaigns are costly, data on a lot of different aspects of the process is collected simultaneously. The campaign's focus may be on process performance of a promising solvent or solvent blend, and large changes in the process parameters are done throughout the campaign duration. At the same time as the process itself is optimised, data related to solvent degradation can be collected for stability assessment. These different focus points of the different campaigns make it more challenging to compare them to one another, when it comes to degradation and emission. Degradation depends on many factors as well as process parameters, including flue gas composition, temperatures in the absorber and desorber, construction material of the plant, and the solvent residence times in the absorber and desorber. This means that for a clear and unambiguous comparison, all these factors need to be taken into consideration, when they mostly are reported in varying detail, depending on the campaign emphasis. Finally, the reported degradation, the analytical methods, sampling frequency and type of compounds analysed, also vary a lot from campaigns to campaign. All these factors lead to a situation, where a comparison of degradation in different campaigns, even when operated with the same solvent, is intricate. The gathered learning from all these campaigns together does, however, give an overall picture of the degradation that has been and can be observed when operating a post-combustion CO_2 capture plant using MEA.

Below, the main findings related to flue gas treatment, degradation and emission are discussed.

Flue gas pretreatment. Sufficient flue gas pretreatment before entering the absorber column plays a vital role in the solvent stability in connection with coal-fired power plants. For example, the pilot plants in Niederaussem, Esbjerg and Heilbronn, which have extensive setups for pretreatment, have much lower formation rates of HSS than those, like Loy Yang and the 0.1 MWth CAER pilot, where more limited flue gas pretreatment is performed. There is a good agreement that removing SO_X, NO_X and particulates from the flue gas a positive effect on solvent degradation and therefore emissions of degradation compounds.

Solvent degradation. When reading the summaries of degradation and corrosion products quantified in Table 4.3 to Table 4.7 it is important to keep in mind that a plethora of process conditions may play decisive roles in the degradation mechanisms and rates that take place. Usually, limited information is reported when it comes to changes in process conditions during the campaign, and detailed process design, like residence time of the solvent in the absorber sump. Knowledge of these details could give additional insights on what influences solvent stability.

Organic acids have often been used as an indication of MEA degradation, but no studies have yet found a direct correlation between their concentration and the total degradation in an arbitrary MEA campaign. In addition to the organic acids being precursors for the formation of other degradation compounds, HEF being formed from formic acid, HEA from acetic acid etc., different campaigns have showed different acids as primary degradation products. At the pilot plant in Niederaussem, acetate is measured in higher concentrations than formate (Moser et al., 2011a; Moser et al., 2018; Moser et al., 2020), but in the Loy Yang and TCM pilots the opposite is seen (Morken et al., 2017; Reynolds et al., 2015b) (Figure 4.1). Furthermore, as some (thermal) degradation compounds tend to increase in concentration in the beginning of a campaign and then steadily decrease later in the campaign (Moser et al., 2020), reacting to further degradation compounds or decomposing, it is important to be aware of what one is measuring. These compounds should therefore not be used for assessing the state of the amine solvent.

Because organic acids react further to form other degradation compounds throughout the operation time, their concentrations do not always increase linearly. It is less common to quantify other degradation compounds, since they typically require more complicated analytical methods, which are time-consuming and costly. Based on the results of the studied pilot campaigns, there doesn’t seem to be any single degradation product that quantitatively correlates with the overall amine degradation. Despite of some of the HSS being of inorganic origin, coming from the flue gas itself (SO_4^{2-}, Cl^-, NO_3^-, etc.) and some from the degradation of the amine, it is still an important

parameter so consider when assessing the state of the solvent. It has been seen that despite of extensive flue gas pretreatment, remaining concentrations of inorganic contaminants increases steadily with operation time (Thompson et al., 2017c). However, in several cases the total amount of heat stable salts (HSS) in the solvent increases nearly linearly throughout the operation time, regardless of other process parameters and this might give a good indication of the solvent degradation rate (Feron et al., 2015; Reynolds et al., 2015b; Thompson et al., 2014). The total amount of HSS is often not given in articles describing pilot campaigns and instead, the monitoring focuses on selected organic acids. In these cases, knowing how well the monitored compounds describe the solvent's degree of degradation can be challenging. If one still wants to study single organic acids, an assessment should probably still be made to the total amount of HSS.

Also, although organic acids are some of the typical main degradation products of MEA, this is most likely not the same for other amines. Despite of these products often being denominated as *primary* degradation products, this does not state anything about their importance, merely the order in which they are formed. Using an organic acid, such as i.e. formic acid as a proxy to assess overall degradation should therefore be done with caution, regardless of which amine is studied. Nevertheless, the concentrations of heat stable salts and inorganics from the flue gas and corrosion can still indicate the properties and stability of the different solvents. Iron is a frequently monitored inorganic species in the solvent and a correlation between ammonia formation and iron concentration in the solvent has been clearly observed (Dhingra et al., 2017). Despite of this correlation, it is not clear which effects cause this, whether it is the increasing corrosivity with increasing degradation or an increased iron solubility caused by pH changes (Nordstrom and Alpers, 1997) or iron complex formation with a more degraded solution. A combination of these explanations is also likely. An explanation for the rapid spike observed both for ammonia formation and iron concentration has not been found. Further and thorough analytical work will be needed to fully understand these phenomena in degraded amine solvents.

Most studies choose a factor to compare a new solvent blend to benchmark 30wt% MEA (*aq.*), like total concentration of HSS or total concentration of nitrosamines in the solvent (TONO). These give insights about specific degradation properties of the solvent and is useful for solvent stability assessment. Comparing single property of solvent, like TONO-concentration can be a way to address specific issues, like safety of the operators. However, it does not say anything about the overall solvent stability. Comparing the amount of dissolved inorganic components in the same pilot but for different solvent systems may indicate the suitability of a certain solvent in certain application (Feron et al., 2015; Thompson et al., 2014).

There is no guideline for how to monitor amine degradation in a carbon capture plant. This has resulted in the use of various methods in different pilot campaigns, with no common consensus in terms of what compounds to analyse for and how this is done. A determining factor in the choice of analytical method is often the availability and cost of the analytical methods. Some methods might be more readily available but give less information, for example total alkalinity, while others are very costly and unavailable, and might therefore not be chosen, like for example LC-MS.

Combination of measurement of NH_3 by FT-IR combined with determination of NH_3 concentrating in the water wash, as well as total HSS concentration in the liquid solvent could be a relatively easy and solvent independent way of monitoring the state of degradation in the plant. It should be remembered that specific analyses should be performed to monitor the accumulation of toxic and harmful degradation compounds in the solvent loop. Additionally, specific methods to monitor the emission of volatile degradation compounds and solvent amine will always be needed.

Analytical methods. Few of the analytical methods applied in monitoring the amine degradation have been sufficiently validated. Validation of a method ensures that the analytical system used is suitable for its purpose and that it provides legitimate data. Ideally, an analytical method should be validated against another method, which is independent of its measurement principle. For instance, the quantification of MEA by LC-MS should agree with the concentration measured by cation IC, as these methods depend on entirely different measurement principles.

Furthermore, in many cases, very little information has been published regarding the parameters of the analytical methods used, e.g. flow rate and retention time, in the chromatographic methods. This is unfortunate, as it makes it impossible for others to validate the reliability of the claims given regarding the results of these analyses. In combination with, and maybe as a result of, the restricted information given about the analytical methods is the under-reporting of uncertainties and detection limits. Both of these parameters are important in handling the data given, and the lack thereof therefore impairs the results.

It is widely seen that some external laboratories are processing the samples from different campaigns and pilots. In these cases, accredited, validated methods for the specific compounds in question are crucial. Use of round robin tests could be an effective way to ensure the consistence of the reported analyses of degradation compounds. Published round robin tests have, for example, highlighted the challenges in analyses of nitrosamines (Fraboulet et al., 2016).

Emissions. As emissions are site and solvent specific, direct comparison of actual emissions from different pilot plants is therefore not an option. The emission of highly volatile degradation compounds, like ammonia, can usually be controlled with water or acid wash (Knudsen et al., 2013; Mertens et al., 2013). The same applies to many solvent compounds, as long as the aerosol formation is limited. For example, the gaseous MEA emission could be abated by single well-designed water wash (Mertens et al., 2012; Mertens et al., 2013). In the presence of aerosol, the solvent emissions can be significant, and aerosol mitigation techniques are needed to reduce the emissions to acceptable levels. The emissions through aerosol particles can be reduced by eliminating the mist precursors upstream from the absorber, or by controlling the growth of the aerosol particles in the absorber. The proposed ways to control the aerosol growth, are reducing the temperature gradients in the absorber or accelerating the particle growth to form large, easily removable aerosols (Knudsen et al., 2013; Mertens et al., 2013; Moser et al., 2014). Operation of the presence of some upstream equipment like wet flue gas desulphurisation unit, gas heater, and wet electrostatic precipitator can have a crucial influence on the aerosol formation (Mertens et al., 2015; Moser et al., 2015). In general, the installation of a Brownian demister unit reduces the aerosol emissions (Bade et al., 2014; Khakharia et al., 2014a; Lombardo et al., 2017).

Emissions of both the solvent itself and its degradation products has to be considered and monitored, but the available information about the pilots and performed campaigns varies. For example, data related to solvent emissions and descriptions of emission reduction technologies are often missing. Besides, the emission reduction technologies used are sometimes proprietary, and details are therefore not given in the publication. A reliable monitoring strategy is required to keep track of the degradation and emission in pilot-plants. There is, however, no set standard to follow. Instead, multiple analytical methods are being used, and this choice is often dependent on the desired information, available resources and know-how as well as the availability of equipment.

Finally, all full-scale plants will need an emission permit, and these depend on local regulations where the plant is located. In Norway, for example, the emission permit for TCM regulates the emission levels for solvent amine, alkylamines aldehydes and ammonia (Morken et al., 2014). The regulation also includes nitrosamine and nitramine.

The following take-home-messages and trends summarise the main findings:

- Flue gas pretreatment including SO_X, NO_X and particle removal significantly increases solvent stability. Pilot plants containing an excessive flue gas pretreatment system tend to experience significantly less degradation than those with a limited or no such system. However, the type of flue gas pre- treatment also impacts the emissions, as some flue gas pretreatments can increase the risk of amine mist formation by increasing the presence of nuclei in the flue gas.

- Monitoring of any single known degradation compound is not a universal way of assessing solvent stability, not even for the comprehensively studied MEA. The organic compounds formate and acetate, for example, seem to vary in their relative abundance in different pilot plants and campaigns. Some compounds even decrease in concentration after a certain time of operation and therefore, the monitoring of single compounds should be done with caution and this knowledge in mind.
- A relatively simple, and to some extent, solvent independent method to monitor solvent degradation could be a combination of measurement of gas-phase NH_3 by FT-IR with total HSS concentration in the liquid solvent. However, monitoring of NH_3 or the total HSS concentration is not always the best solution. But for solvents that produce NH_3 and HSS as one of their primary degradation compounds,such as MEA, this is a straight-forward and informative monitoring approach. Knowledge of the main degradation compounds are therefore always needed.
- There is no universal standard for measurement of emission from large-scale capture plant. An international standard is also lacking for sampling, conditioning, and analysis of volatile trace elements in flue gas, leaving the CO_2 capture plant (Moser et al., 2013). These issues should be addressed in future works and development of such a standard would enhance the comparability and certainty in the measurements on site.
- There is a general lack in reporting of analytical methods and their uncertainties, when emission and degradation data is published. To facilitate reproducible and comparable results, documented methods should be applied for the quantification of species both in gas and liquid phase, including all parameters for chromatographic analyses.

Acknowledgement

This publication has been produced with support from the NCCS Centre, performed under the Norwegian research program Centres for Environment-friendly Energy Research (FME). The authors acknowledge the following partners for their contributions: Aker Solutions, Ansaldo Energia, Baker Hughes, CoorsTek Membrane Sciences, EMGS, Equinor, Gassco, Krohne, Larvik Shipping, Lundin, Norcem, Norwegian Oil and Gas, Quad Geometrics, Total, Vår Energi, and the Research Council of Norway (257579/E20).

The LAUNCH project funded through the ACT programme (Accelerating CCS Technologies, Horizon2020 Project No 294766). Financial contributions are made from: Netherlands Enterprise Agency (RVO), Netherlands; Bundesministerium für Wirtschaft und Energie (BMWi), Germany; Gassnova SF (GN), Norway; Department for Business, Energy & Industrial Strategy (BEIS) together with extra funding from NERC and EPSRC research councils, United Kingdom; US-Department of Energy (US-DOE), USA.

References

Akinpelumi, K., Saha, C., Rochelle, G.T., 2019. Piperazine aerosol mitigation for post-combustion carbon capture. International Journal of Greenhouse Gas Control 91, 102845.

Aronu, U.E., Lauritsen, K.G., Grimstvedt, A., Mejdell, T., 2014. Impact of heat stable salts on equilibrium CO_2 absorption, Energy Procedia. Elsevier Ltd, pp. 1781-1794.

Artanto, Y., Jansen, J., Pearson, P., Do, T., Cottrell, A., Meuleman, E., Feron, P., 2012. Performance of MEA and amine-blends in the CSIRO PCC pilot plant at Loy Yang Power in Australia. Fuel 101, 264-275.

Azzi, M., Day, S., French, D., Halliburton, B., Jackson, P., Lavrencic, S., Riley, K., Tibbett, A., 2010. CO_2 Capture Mongstad-Project A-Establishing sampling and analytical procedures for potentially harmful components from post-combustion amine based CO_2 capture Task 2: Procedures for Manual Sampling.

Bade, O.M., Knudsen, J.N., Gorset, O., Askestad, I., 2014. Controlling amine mist formation in CO_2 capture from Residual Catalytic Cracker (RCC) flue gas, Energy Procedia. Elsevier Ltd, pp. 884-892.

Bazhenov, S., Rieder, A., Schallert, B., Vasilevsky, V., Unterberger, S., Grushevenko, E., Volkov, V., Volkov, A., 2015. Reclaiming of degraded MEA solutions by electrodialysis: Results of ED pilot campaign at post-combustion CO_2 capture pilot plant. International Journal of Greenhouse Gas Control 42, 593-601.

Bazhenov, S., Vasilevsky, V., Rieder, A., Unterberger, S., Grushevenko, E., Volkov, V., Schallert, B., Volkov, A., 2014. Heat Stable Salts (HSS) Removal by Electrodialysis: Reclaiming of MEA Used in Post-combustion CO_2-Capture. Energy Procedia 63, 6349-6356.

Bello, A., Idem, R.O., 2005. Pathways for the formation of products of the oxidative degradation of CO_2-loaded concentrated aqueous monoethanolamine solutions during CO_2 absorption from flue gases. Industrial & engineering chemistry research 44, 945-969.

Bernhardsen, I.M., Trollebø, A.A., Perinu, C., Knuutila, H.K., 2019. Vapour-liquid equilibrium study of tertiary amines, single and in blend with 3-(methylamino) propylamine, for post-combustion CO_2 capture. The Journal of Chemical Thermodynamics 138, 211-228.

Blachly, C., Ravner, H., 1963. The effect of trace amounts of copper on the stability of monoethanolamine scrubber solutions. Naval Research Lab Washington DC.

Brigman, N., Shah, M.I., Falk-Pedersen, O., Cents, T., Smith, V., De Cazenove, T., Morken, A.K., Hvidsten, O.A., Chhaganlal, M., Feste, J.K., Lombardo, G., Bade, O.M., Knudsen, J., Subramoney, S.C., Fostås, B.F., de Koeijer, G., Hamborg, E.S., 2014. Results of Amine Plant Operations from 30 wt% and 40 wt% Aqueous MEA Testing at the CO_2 Technology Centre Mongstad. Energy Procedia 63, 6012-6022.

Brostrøm, A., Kling, K.I., Hougaard, K.S., Mølhave, K., 2020. Complex Aerosol Characterization by Scanning Electron Microscopy Coupled with Energy Dispersive X-ray Spectroscopy.

Brown, N., Heller, G., Staab, G., Silverman, T., Kupfer, R., Brown, R., Brown, A., 2017. Novel Advanced Solvent-based Carbon Capture Pilot Demonstration at the National Carbon Capture Center. Energy Procedia 114, 1075-1086.

Bui, M., Gunawan, I., Verheyen, V., Feron, P., Meuleman, E., 2016. Flexible operation of CSIRO's post-combustion CO_2 capture pilot plant at the AGL Loy Yang power station. International Journal of Greenhouse Gas Control 48, 188-203.

Bumb, P., Patkar, P.E.A., Mather, R., Kumar, R., Hall, J., Morton, F., Anthony, J., 2017. Field Demonstration of Advanced CDRMax Solvent at the US-DOE's National Carbon Capture Centre and the CO_2 Technology Centre Mongstad DA, Norway, Energy Procedia. Elsevier Ltd, pp. 1087-1099.

Burkart, J., Steiner, G., Reischl, G., Moshammer, H., Neuberger, M., Hitzenberger, R., 2010. Characterizing the performance of two optical particle counters (Grimm OPC1.108 and OPC1.109) under urban aerosol conditions. Journal of Aerosol Science 41, 953-962.

Byers, R.L., Davis, J.W., White, E.W., McMillan, R.E., 1971. Computerized method for size characterization of atmospheric aerosols by the scanning electron microscope. Environmental Science & Technology 5, 517-521.

Chahen, L., Huard, T., Cuccia, L., Cuzuel, V., Dugay, J., Pichon, V., Vial, J., Gouedard, C., Bonnard, L., Cellier, N., Carrette, P.-L., 2016. Comprehensive monitoring of MEA degradation in a post-combustion CO_2 capture pilot plant with identification of novel degradation products in gaseous effluents. International Journal of Greenhouse Gas Control 51, 305-316.

Chi, S., Rochelle, G.T., 2002. Oxidative Degradation of Monoethanolamine. Industrial & Engineering Chemistry Research 41, 4178-4186.

Cousin, A., Cottrell, A., Huang, S., Feron, P.H.M., Lawson, A., 2012. Tarong CO_2 capture pilot plant. Energy Generation, 16-17.

Cousins, A., Wardhaugh, L., Cottrell, A., 2016. Pilot plant operation for liquid absorption-based post-combustion CO_2 capture. Elsevier Inc.

Cuccia, L., Dugay, J., Bontemps, D., Louis-Louisy, M., Vial, J., 2018. Analytical methods for the monitoring of post-combustion CO_2 capture process using amine solvents: A review. International Journal of Greenhouse Gas Control 72, 138-151.

Cuzuel, V., Brunet, J., Rey, A., Dugay, J., Vial, J., Pichon, V., Carrette, P.-L., 2014. Validation of a liquid chromatography tandem mass spectrometry method for targeted degradation compounds of ethanolamine used in CO_2 capture: application to real samples. Oil & Gas Science and Technology–Revue d’IFP Energies nouvelles 69, 821-832.

da Silva, E.F., Kolderup, H., Goetheer, E., Hjarbo, K.W., Huizinga, A., Khakharia, P., Tuinman, I., Mejdell, T., Zahlsen, K., Vernstad, K., Hyldbakk, A., Holten, T., Kvamsdal, H.M., Van Os, P., Einbu, A., 2013. Emission studies from a CO_2 capture pilot plant, Energy Procedia. Elsevier Ltd, pp. 778-783.

da Silva, E.F., Lepaumier, H., Grimstvedt, A., Vevelstad, S.J., Einbu, A., Vernstad, K., Svendsen, H.F., Zahlsen, K., 2012. Understanding 2-ethanolamine degradation in postcombustion CO_2 capture. Industrial & Engineering Chemistry Research 51, 13329-13338.

Dahlin, R.S., Landham, E.C., Kelinske, M.L., Wheeldon, J.M., Love, D.H., 2013. Amine Losses and Formation of Degradation Products in Post-Combustion CO_2 Capture, 38th International Technical Conference on Clean Coal & Fuel Systems 2013: The Clearwater Clean Coal Conference.

Davis, J., Rochelle, G., 2009. Thermal degradation of monoethanolamine at stripper conditions, Energy Procedia, pp. 327-333.

de Koeijer, G., Enge, Y., Sanden, K., Graff, O.F., Falk-Pedersen, O., Amundsen, T., Overå, S., 2011. CO_2 Technology Centre Mongstad–Design, functionality and emissions of the amine plant. Energy Procedia 4, 1207-1213.

de Koeijer, G., Talstad, V.R., Nepstad, S., Tønnessen, D., Falk-Pedersen, O., Maree, Y., Nielsen, C., 2013. Health risk analysis for emissions to air from CO_2 Technology Centre Mongstad. International Journal of Greenhouse Gas Control 18, 200-207.

Dhingra, S., Khakharia, P., Rieder, A., Cousins, A., Reynolds, A., Knudsen, J., Andersen, J., Irons, R., Mertens, J., Abu Zahra, M., Van Os, P., Goetheer, E., 2017. Understanding and Modelling the Effect of Dissolved Metals on Solvent Degradation in Post Combustion CO_2 Capture Based on Pilot Plant Experience. Energies 10.

Diab, F., Provost, E., Laloué, N., Alix, P., Souchon, V., Delpoux, O., Fürst, W., 2012. Quantitative analysis of the liquid phase by FT-IR spectroscopy in the system CO_2/diethanolamine (DEA)/H_2O. Fluid Phase Equilibria 325, 90-99.

Eide-Haugmo, I., Lepaumier, H., da Silva, E.F., Einbu, A., Vernstad, K., Svendsen, H.F., 2011. A study of thermal degradation of different amines and their resulting degradation products, 1st Post Combustion Capture Conference, pp. 17-19.

Eliasson, J., Watson, I.M., Weber, K., 2016. Chapter 5 - In Situ Observations of Airborne Ash From Manned Aircraft, in: Mackie, S., Cashman, K., Ricketts, H., Rust, A., Watson, M. (Eds.), Volcanic Ash. Elsevier, pp. 89-98.

Enaasen, N., Zangrilli, L., Mangiaracina, A., Mejdell, T., Kvamsdal, H.M., Hillestad, M., 2014. Validation of a dynamic model of the brindisi pilot plant, Energy Procedia. Elsevier, pp. 1040-1054.

Feron, P., Conway, W., Puxty, G., Wardhaugh, L., Green, P., Maher, D., Fernandes, D., Cousins, A., Cottrell, A., Li, K., Shiwang, G., Lianbo, L., Hongwei, N., Hang, S., Jinyi, W., Shiqing, W., Dongfang, G., Maeder, M., Clifford, S., 2015. Comparative evaluation of a new liquid absorbent in a PCC pilot plant in China, PCCC3, Regina SK, Canada.

Feron, P., Conway, W., Puxty, G., Wardhaugh, L., Green, P., Maher, D., Fernandes, D., Cousins, A., Gao, S.W., Liu, L.B., Niu, H.W., Shang, H., 2014. Amine based post-combustion capture technology advancement for application in Chinese coal fired power stations. 12th International Conference on Greenhouse Gas Control Technologies, Ghgt-12 63, 1399-1406.

Feron, P.H.M., Cousins, A., Jiang, K., Zhai, R., Garcia, M., 2020. An update of the benchmark post-combustion CO_2-capture technology. Fuel 273, 117776.

Fine, N.A., 2015. Nitrosamine management in aqueous amines for post-combustion carbon capture.

Fitzgerald, F.D., Hume, S.A., McGough, G., Damen, K., 2014. Ferrybridge CCPilot100+ operating experience and final test results, Energy Procedia. Elsevier Ltd, pp. 6239-6251.

Fraboulet, I., Chahen, L., Lestremau, F., Grimstvedt, A., Schallert, B., Moeller, B.C., Järvinen, E., 2016. Round robin tests on nitrosamines analysis in the effluents of a CO_2 capture pilot plant, Energy Procedia. Elsevier Ltd, pp. 252-261.

Freeman, S.A., 2011. Thermal degradation and oxidation of aqueous piperazine for carbon dioxide capture, Energy Procedia.

Frimpong, R.A., Johnson, D., Richburg, L., Hogston, B., Remias, J.E., Neathery, J.K., Liu, K., 2013. Comparison of solvent performance for CO_2 capture from coal-derived flue gas: A pilot scale study. Chemical Engineering Research and Design 91, 963-969.

Fujita, K., Muraoka, D., Ogawa, T., Kitamura, H., Suzuki, K., Saito, S., 2013. Evaluation of amine emissions from the post-combustion CO_2 capture pilot plant, Energy Procedia. Elsevier Ltd, pp. 727-734.

Gao, T., Selinger, J.L., Rochelle, G.T., 2019. Demonstration of 99% CO_2 removal from coal flue gas by amine scrubbing. International Journal of Greenhouse Gas Control 83, 236-244.

Gjernes, E., Pedersen, S., Cents, T., Watson, G., Fostås, B.F., Shah, M.I., Lombardo, G., Desvignes, C., Flø, N.E., Morken, A.K., De Cazenove, T., Faramarzi, L., Hamborg, E.S., 2017. Results from 30 wt% MEA Performance Testing at the CO_2 Technology Centre Mongstad, Energy Procedia. Elsevier Ltd, pp. 1146-1157.

Goff, G.S., 2005. Oxidative Degradation of Aqueous Monoethanolamine in CO_2 Capture Processes: Iron and Copper Catalysis, Inhibition, and O_2 Mass Transfer.

Goldstein, J.I., Newbury, D.E., Michael, J.R., Ritchie, N.W., Scott, J.H.J., Joy, D.C., 2017. Scanning electron microscopy and X-ray microanalysis. Springer.

Gorset, O., Knudsen, J.N., Bade, O.M., Askestad, I., 2014. Results from testing of Aker Solutions advanced amine solvents at CO_2 Technology Centre Mongstad, Energy Procedia. Elsevier Ltd, pp. 6267-6280.

Gouedard, C., Rey, A., Cuzuel, V., Brunet, J., Delfort, B., Picq, D., Dugay, J., Vial, J., Pichon, V., Launay, F., 2014. Amine degradation in CO_2 capture. 3. New degradation products of MEA in liquid phase: amides and nitrogenous heterocycles. International Journal of Greenhouse Gas Control 29, 61-69.

Graff, O.F., 2010. Advanced CO_2 capture with Bio Aker Clean Carbon-Emission measurement and analysis from Mobile Carbon Capture Test Facility.

Grimstvedt, A., Wiig, M., Einbu, A., Vevelstad, S.J., 2019. Multi-component analysis of monethanolamine solvent samples by FTIR. International Journal of Greenhouse Gas Control 83, 293-307.

Hansel, A., Jordan, A., Holzinger, R., Prazeller, P., Vogel, W., Lindinger, W., 1995. Proton transfer reaction mass spectrometry: on-line trace gas analysis at the ppb level. International Journal of Mass Spectrometry and Ion Processes 149-150, 609-619.

Harsha, S., Khakharia, P., Huizinga, A., Monteiro, J., Goetheer, E., Vlugt, T.J.H., 2019. In-situ experimental investigation on the growth of aerosols along the absorption column in post combustion carbon capture. International Journal of Greenhouse Gas Control 85, 86-99.

Hilliard, M.D., 2008. A Predictive Thermodynamic Model for an Aqueous Blend of Potassium Carbonate, Piperazine, and Monoethanolamine for Carbon Dioxide Capture from Flue Gas.

Idem, R., Supap, T., Shi, H., Gelowitz, D., Ball, M., Campbell, C., Tontiwachwuthikul, P., 2015. Practical experience in post-combustion CO_2 capture using reactive solvents in large pilot and demonstration plants. International Journal of Greenhouse Gas Control 40, 6-25.

Jeong, C.-H., Evans, G.J., 2009. Inter-Comparison of a Fast Mobility Particle Sizer and a Scanning Mobility Particle Sizer Incorporating an Ultrafine Water-Based Condensation Particle Counter. Aerosol Science and Technology 43, 364-373.

Jordan, A., Haidacher, S., Hanel, G., Hartungen, E., Herbig, J., Märk, L., Schottkowsky, R., Seehauser, H., Sulzer, P., Märk, T.D., 2009. An online ultra-high sensitivity Proton-transfer-reaction mass-spectrometer combined with switchable reagent ion capability (PTR+SRI−MS). International Journal of Mass Spectrometry 286, 32-38.

Järvinen, A., Aitomaa, M., Rostedt, A., Keskinen, J., Yli-Ojanperä, J., 2014. Calibration of the new electrical low pressure impactor (ELPI+). Journal of Aerosol Science 69, 150-159.

Kadnar, R., Rieder, J., 1995. Determination of anions in amine solutions for sour gas treatment. Journal of Chromatography A 706, 339-343.

Kamijo, T., Sorimachi, Y., Shimada, D., Miyamoto, O., Endo, T., Nagayasu, H., Mangiaracina, A., 2013. Result of the 60 tpd CO_2 capture pilot plant in European coal power plant with KS-1™ solvent, Energy Procedia. Elsevier Ltd, pp. 813-816.

Kentish, S.E., 2016. Reclaiming of amine-based absorption liquids used in post-combustion capture, Absorption-Based Post-Combustion Capture of Carbon Dioxide, pp. 426-438.

Kero, I.T., Jørgensen, R.B., 2016. Comparison of Three Real-Time Measurement Methods for Airborne Ultrafine Particles in the Silicon Alloy Industry. International Journal of Environmental Research and Public Health 13.

Khakharia, P., Brachert, L., Mertens, J., Anderlohr, C., Huizinga, A., Fernandez, E.S., Schallert, B., Schaber, K., Vlugt, T.J.H., Goetheer, E., 2015a. Understanding aerosol based emissions in a Post Combustion CO_2 Capture process: Parameter testing and mechanisms. International Journal of Greenhouse Gas Control 34, 63-74.

Khakharia, P., Brachert, L., Mertens, J., Huizinga, A., Schallert, B., Schaber, K., Vlugt, T.J.H., Goetheer, E., 2013. Investigation of aerosol based emission of MEA due to sulphuric acid aerosol and soot in a Post Combustion CO_2 Capture process. International Journal of Greenhouse Gas Control 19, 138-144.

Khakharia, P., Kvamsdal, H.M., Da Silva, E.F., Vlugt, T.J.H., Goetheer, E., 2014a. Field study of a Brownian Demister Unit to reduce aerosol based emission from a

Post Combustion CO_2 Capture plant. International Journal of Greenhouse Gas Control 28, 57-64.

Khakharia, P., Mertens, J., Huizinga, A., De Vroey, S., Sanchez Fernandez, E., Srinivasan, S., Vlugt, T.J.H., Goetheer, E., 2015b. Online corrosion monitoring in a postcombustion CO_2 capture pilot plant and its relation to solvent degradation and ammonia emissions. Industrial and Engineering Chemistry Research 54, 5336-5344.

Khakharia, P., Mertens, J., Vlugt, T.J.H., Goetheer, E., 2014b. Predicting aerosol based emissions in a post combustion CO_2 capture process using an aspen plus model, Energy Procedia. Elsevier Ltd, pp. 911-925.

Knudsen, J.N., Bade, O.M., Anheden, M., Bjorklund, R., Gorset, O., Woodhouse, S., 2013. Novel concept for emission control in post combustion capture, Energy Procedia. Elsevier Ltd, pp. 1804-1813.

Knudsen, J.N., Bade, O.M., Askestad, I., Gorset, O., Mejdell, T., 2014. Pilot plant demonstration of CO_2 capture from cement plant with advanced amine technology, Energy Procedia. Elsevier Ltd, pp. 6464-6475.

Knudsen, J.N., Jensen, J.N., Vilhelmsen, P.-J., Biede, O., 2009. Experience with CO_2 capture from coal flue gas in pilot-scale: Testing of different amine solvents, Energy Procedia, pp. 783-790.

Knuutila, H., Asif, N., Vevelstad, S.J., Svendsen, H.F., 2014a. Formation and Destruction of NDELA in 30 wt% MEA (Monoethanolamine) and 50 wt% DEA (Diethanolamine) Solutions. Oil & Gas Science and Technology–Revue d'IFP Energies nouvelles 69, 805-820.

Knuutila, H., Svendsen, H.F., Asif, N., 2014b. Decomposition of nitrosamines in aqueous monoethanolamine (MEA) and diethanolamine (DEA) solutions with UV-radiation. International Journal of Greenhouse Gas Control 31, 182-191.

Kohl, A.L., Nielsen, R.B., 1997. Chapter 3 - Mechanical Design and Operation of Alkanolamine Plants, in: Kohl, A.L., Nielsen, R.B. (Eds.), Gas Purification (Fifth Edition). Gulf Professional Publishing, Houston, pp. 187-227.

Kolderup, H., da Silva, E., Mejdell, T., Tobiesen, A., Haugen, G., Hoff, K.A., Josefsen, K., Strøm, T., Furuseth, O., Hanssen, K.F., Myhrvold, T., Johnsen, K., SINTEF REPORT Emission Reducing Technologies H&ETQP Amine6 SINTEF Materials and Chemistry.

Lamminen, E., 2011. Accurate measurement of nanoparticle charge, number and size with the ELPI+™ instrument, Journal of Physics: Conference Series. IOP Publishing, p. 012064.

Léonard, G., Voice, A., Toye, D., Heyen, G., 2014. Influence of dissolved metals and oxidative degradation inhibitors on the oxidative and thermal degradation of monoethanolamine in postcombustion CO_2 capture. Industrial & Engineering Chemistry Research 53, 18121-18129.

Lepaumier, H., Grimstvedt, A., Vernstad, K., Zahlsen, K., Svendsen, H.F., 2011. Degradation of MMEA at absorber and stripper conditions. Chemical engineering science 66, 3491-3498.

Lepaumier, H., Picq, D., Carrette, P.L., 2009a. New amines for CO_2 Capture. I. Mechanisms of amine degradation in the presence of CO_2. Industrial and Engineering Chemistry Research 48, 9061-9067.

Lepaumier, H., Picq, D., Carrette, P.L., 2009b. New amines for CO_2 Capture. II. Oxidative degradation mechanisms. Industrial and Engineering Chemistry Research 48, 9068-9075.

Levin, M., Gudmundsson, A., Pagels, J.H., Fierz, M., Mølhave, K., Löndahl, J., Jensen, K.A., Koponen, I.K., 2015. Limitations in the Use of Unipolar Charging for Electrical Mobility Sizing Instruments: A Study of the Fast Mobility Particle Sizer. Aerosol Science and Technology 49, 556-565.

Li, W., Shao, L., 2009. Transmission electron microscopy study of aerosol particles from the brown hazes in northern China. Journal of Geophysical Research Atmospheres 114.

Lindinger, W., Hansel, A., Jordan, A., 1998. On-line monitoring of volatile organic compounds at pptv levels by means of proton-transfer-reaction mass spectrometry (PTR-MS) medical applications, food control and environmental research. International Journal of Mass Spectrometry and Ion Processes 173, 191-241.

Lombardo, G., Fostås, B.F., Shah, M.I., Morken, A.K., Hvidsten, O.A., Mertens, J., Hamborg, E.S., 2017. Results from Aerosol Measurement in Amine Plant Treating Gas Turbine and Residue Fluidized Catalytic Cracker Flue Gases at the CO_2 Technology Centre Mongstad, Energy Procedia. Elsevier Ltd, pp. 1210-1230.

Lundanes, E., Reubsaet, L., Greibrokk, T., 2013. Chromatography: basic principles, sample preparations and related methods. John Wiley & Sons.

Macbride, D.M., Malone, C.G., Hebb, J.P., Cravalho, E.G., 1997. Effect of Temperature Variation on FT-IR Spectrometer Stability, APPLIED SPECTROSCOPY.

Majeed, H., Knuutila, H., Hillestad, M., Svendsen, H.F., 2017. Effect of Amine Volatility on Aerosol Droplet Development in Absorption Columns, Energy Procedia. Elsevier Ltd, pp. 977-986.

Mangiaracina, A., Zangrilli, L., Robinson, L., Kvamsdal, H.M., Os, P.V., 2014. OCTAVIUS: Evaluation of flexibility and operability of amine based post combustion CO_2 capture at the Brindisi Pilot Plant, Energy Procedia. Elsevier Ltd, pp. 1617-1636.

Matin, N.S., Remias, J.E., Neathery, J.K., Liu, K., 2012. Facile Method for Determination of Amine Speciation in CO_2 Capture Solutions. Industrial & Engineering Chemistry Research 51, 6613-6618.

Mejdell, T., Haugen, G., Rieder, A., Kvamsdal, H.M., 2017. Dynamic and Control of an Absorber - Desorber Plant at Heilbronn, Energy Procedia, pp. 1231-1244.

Mejdell, T., Vassbotn, T., Juliussen, O., Tobiesen, A., Einbu, A., Knuutila, H., Hoff, K.A., Andersson, V., Svendsen, H.F., 2011. Novel full height pilot plant for solvent development and model validation, Energy Procedia. Elsevier Ltd, pp. 1753-1760.

Mertens, J., Bruns, R., Schallert, B., Faniel, N., Khakharia, P., Albrecht, W., Goetheer, E., Blondeau, J., Schaber, K., 2015. Effect of a gas-gas-heater on H_2SO_4

aerosol formation: Implications for mist formation in amine based carbon capture. International Journal of Greenhouse Gas Control 39, 470-477.

Mertens, J., Knudsen, J., Thielens, M.L., Andersen, J., 2012. On-line monitoring and controlling emissions in amine post combustion carbon capture: A field test. International Journal of Greenhouse Gas Control 6, 2-11.

Mertens, J., Lepaumier, H., Desagher, D., Thielens, M.L., 2013. Understanding ethanolamine (MEA) and ammonia emissions from amine based post combustion carbon capture: Lessons learned from field tests. International Journal of Greenhouse Gas Control 13, 72-77.

Meuleman, E., Cottrell, A., Ghayur, A., 2016. Treatment of flue-gas impurities for liquid absorbent-based post-combustion CO_2 capture processes, Absorption-Based Post-Combustion Capture of Carbon Dioxide. Woodhead Publishing, pp. 519-551.

Morken, A.K., Nenseter, B., Pedersen, S., Chhaganlal, M., Feste, J.K., Tyborgnes, R.B., Ullestad, Ø., Ulvatn, H., Zhu, L., Mikoviny, T., Wisthaler, A., Cents, T., Bade, O.M., Knudsen, J., De Koeijer, G., Falk-Pedersen, O., Hamborg, E.S., 2014. Emission results of amine plant operations from MEA testing at the CO_2 Technology Centre Mongstad, Energy Procedia. Elsevier Ltd, pp. 6023-6038.

Morken, A.K., Pedersen, S., Kleppe, E.R., Wisthaler, A., Vernstad, K., Ullestad, Ø., Flø, N.E., Faramarzi, L., Hamborg, E.S., 2017. Degradation and Emission Results of Amine Plant Operations from MEA Testing at the CO_2 Technology Centre Mongstad. Energy Procedia 114, 1245-1262.

Morton, F., Laird, R., Northington, J., 2013. The National Carbon Capture Center: Cost-effective test bed for carbon capture R&D. Energy Procedia 37, 525-539.

Moser, P., Schmidt, S., Sieder, G., Garcia, H., Stoffregen, T., 2011a. Performance of MEA in a long-term test at the post-combustion capture pilot plant in Niederaussem. International Journal of Greenhouse Gas Control 5, 620-627.

Moser, P., Schmidt, S., Sieder, G., Garcia, H., Stoffregen, T., Stamatov, V., 2011b. The post-combustion capture pilot plant Niederaussem–results of the first half of the testing programme. Energy Procedia 4, 1310-1316.

Moser, P., Schmidt, S., Stahl, K., Vorberg, G., Lozano, G.A., Stoffregen, T., Richter, T., 2015. The wet electrostatic precipitator as a cause of mist formation-Results from the amine-based post-combustion capture pilot plant at Niederaussem. International Journal of Greenhouse Gas Control 41, 229-238.

Moser, P., Schmidt, S., Stahl, K., Vorberg, G., Lozano, G.A., Stoffregen, T., Rösler, F., 2014. Demonstrating emission reduction - Results from the post-combustion capture pilot plant at niederaussem, Energy Procedia. Elsevier Ltd, pp. 902-9

Moser, P., Schmidt, S., Wallus, S., Ginsberg, T., Sieder, G., Clausen, I., Palacios, J.G., Stoffregen, T., Mihailowitsch, D., 2013. Enhancement and long-term testing of optimised post-combustion capture technology - Results of the second phase of the testing programme at the Niederaussem pilot plant, Energy Procedia. Elsevier Ltd, pp. 2377-2388.

Moser, P., Wiechers, G., Schmidt, S., Elsen, R., Khakharia, P., Garcia, J., Monteiro, M.-S., Jens, K.-J., Solli, K.-A., Sanchez Fernandez, E., Garcia, S., Maroto-Valer, M., Barrio, J., Kvamsdal, M., 2018. MEA consumption-ALIGN-CCUS: Comparative long-term testing to answer the open questions, GHGT-14, Melbourne, Australia.

Moser, P., Wiechers, G., Schmidt, S., Garcia Moretz-Sohn Monteiro, J., Charalambous, C., Garcia, S., Sanchez Fernandez, E., 2020. Results of the 18-month test with MEA at the post-combustion capture pilot plant at Niederaussem – new impetus to solvent management, emissions and dynamic behaviour. International Journal of Greenhouse Gas Control 95, 102945.

Moser, P., Wiechers, G., Stahl, K., Stoffregen, T., Vorberg, G., Lozano, G.A., 2017. Solid Particles as Nuclei for Aerosol Formation and Cause of Emissions - Results from the Post-combustion Capture Pilot Plant at Niederaussem, Energy Procedia. Elsevier Ltd, pp. 1000-1016.

Nakamura, S., Yamanaka, Y., Matsuyama, T., Okuno, S., Sato, H., 2013. IHI s Amine-Based CO_2 Capture Technology for Coal Fired Power Plant. Energy Procedia 37, 1897-1903.

Nakamura, S., Yamanaka, Y., Matsuyama, T., Okuno, S., Sato, H., Iso, Y., Huang, J., 2014. Effect of Combinations of Novel Amine Solvents, Processes and Packing at IHI's Aioi Pilot Plant. Energy Procedia 63, 687-692.

Newbury, D.E., Ritchie, N.W.M., 2013. Is Scanning Electron Microscopy/Energy Dispersive X-ray Spectrometry (SEM/EDS) Quantitative? Scanning 35, 141-168.

Nicol, K., 2013. Recent developments in particulate control, pp. 1-54.

Nielsen, P.T., Li, L., Rochelle, G.T., 2013. Piperazine degradation in pilot plants, Energy Procedia. Elsevier Ltd, pp. 1912-1923.

Nordstrom, D.K., Alpers, C.N., 1997. The environmental geochemistryof mineral deposits. Reviews in economic geology 6A, 133-160.

Okuno, S., Nakamura, S., Yamanaka, Y., Matsuyama, T., Sato, H., Ikeda, R., 2017. Demonstration Results on Advanced Amine Solvents, Packings and Process at IHI's AIOI PILOT PLANT, Energy Procedia. Elsevier Ltd, pp. 1282-1287.

Reynolds, A.J., Verheyen, T.V., Adeloju, S.B., Chaffee, A.L., Meuleman, E., 2015a. Evaluation of methods for monitoring MEA degradation during pilot scale post-combustion capture of CO_2. International Journal of Greenhouse Gas Control 39, 407-419.

Reynolds, A.J., Verheyen, T.V., Adeloju, S.B., Chaffee, A.L., Meuleman, E., 2015b. Monoethanolamine Degradation during Pilot-Scale Post-combustion Capture of CO_2 from a Brown Coal-Fired Power Station. Energy & Fuels 29, 7441-7455.

Richner, G., Puxty, G., 2012. Assessing the Chemical Speciation during CO_2 Absorption by Aqueous Amines Using in Situ FTIR. Industrial & Engineering Chemistry Research 51, 14317-14324.

Rieder, A., Dhingra, S., Khakharia, P., Zangrilli, L., Schallert, B., Irons, R., Unterberger, S., van Os, P., Goetheer, E., 2017. Understanding solvent degradation: A study from three different pilot plants within the OCTAVIUS project. Energy Procedia 114, 1195-1209.

Rieder, A., Unterberger, S., 2013. EnBW's Post-Combustion Capture Pilot Plant at Heilbronn–Results of the First Year's Testing Programme. Energy Procedia 37, 6464-6472.

Rochelle, G., Bishnoi, S., Chi, S., Dang, H., Santos, J., 2001. Research needs for CO_2 capture from flue gas by aqueous absorption/stripping, Research Report for P.O.: No. DE-AF26-99FT01029 of U.S. Department of Energy.

Rochelle, G.T., 2012. Thermal degradation of amines for CO_2 capture. Current Opinion in Chemical Engineering 1, 183-190.

Rogelj, J., Shindell, D., Jiang, K., Fifita, S., Forster, P., Ginzburg, V., Handa, C., Kheshgi, H., Kobayashi, S., Kriegler, E., Mundaca, L., Séférian, R., Vilariño, M.V., 2018. Mitigation Pathways Compatible with 1.5°C in the Context of Sustainable Development. In: *Global Warming of 1.5°C. An IPCC Special Report on the impacts of global warming of 1.5°C above pre-industrial levels and related global greenhouse gas emission pathways, in the context of strengthening the global response to the threat of climate change, sustainable development, and efforts to eradicate poverty*. IPCC.

Rooney, P., Dupart, M., Bacon, T., 1998. Oxygen's role in alkanolamine degradation. Hydrocarbon processing (International ed.) 77, 109-113.

Saito, S., Udatsu, M., Kitamura, H., Murai, S., Kato, Y., Maezawa, Y., Watando, H., 2014. Development and Evaluation of a New Amine Solvent at the Mikawa CO_2 Capture Pilot Plant. Energy Procedia 51, 176-183.

Saito, S., Udatsu, M., Kitamuraa, H., Murai, S., 2015. Absorption-Based Post-Combustion Capture of Carbon Dioxide, PCCC-3. IEAGHG, Regina SK, Canada.

SEPA, 2015. Review of amine emissions from carbon capture systems, Version 2.01.
Sexton, A.J., 2008. Amine Oxidation in CO_2 Capture Processes.

Shah, M.I., Lombardo, G., Fostås, B., Benquet, C., Kolstad Morken, A., De Cazenove, T., 2018. CO_2 capture from RFCC flue gas with 30 wt% MEA at Technology Centre Mongstad, process optimization and performance comparison, 14th International Conference on Greenhouse Gas Control Technologies, GHGT-14.

Sheppard, B.S., Shen, W.-L., Davidson, T.M., Caruso, J.A., 1990. Helium-argon inductively coupled plasma for plasma source mass spectrometry. Journal of Analytical Atomic Spectrometry 5, 697-700.

Shimadzu, 2014. Manual TOC Shimadzu.

Singh, A., Stéphenne, K., 2014. Shell Cansolv CO_2 capture technology: Achievement from first commercial plant, Energy Procedia. Elsevier B.V., pp. 1678-1685.

Somridhivej, B., Boyd, C.E., 2016. An assessment of factors affecting the reliability of total alkalinity measurements. Aquaculture 459, 99-109.

Spietz, T., Chwoła, T., Krótki, A., Tatarczuk, A., Więcław-Solny, L., Wilk, A., 2018. Ammonia emission from CO_2 capture pilot plant using aminoethylethanolamine. International Journal of Environmental Science and Technology 15, 1085-1092.

Strazisar, B.R., Anderson, R.R., White, C.M., 2003. Degradation pathways for monoethanolamine in a CO_2 capture facility. Energy & fuels 17, 1034-1039.

Sun, K., Lu, L., Jiang, H., 2012. Experimental study of aerosol distribution and concentration variation through curved ducts. Thermal Science 16, 1437-1441.

Tanthapanichakoon, W., Veawab, A., McGarvey, B., 2006. Electrochemical Investigation on the Effect of Heat-stable Salts on Corrosion in CO_2 Capture Plants Using Aqueous Solution of MEA. Industrial & Engineering Chemistry Research 45, 2586-2593.

Thomas, R., 2013. Practical guide to ICP-MS: a tutorial for beginners.

Thompson, J., Nikolic, H., Combs, M., Bhatnagar, S., Pelgen, J., Abad, K., Liu, K., 2017a. Solvent Degradation and Emissions from a 0.7MWe Pilot CO_2 Capture System with Two-stage Stripping. Energy Procedia 114, 1297-1306.

Thompson, J., Richburg, H., Liu, K., 2017b. Thermal Degradation Pathways of Aqueous Diamine CO_2 Capture Solvents. Energy Procedia 114, 2030-2038.

Thompson, J.G., Bhatnagar, S., Combs, M., Abad, K., Onneweer, F., Pelgen, J., Link, D., Figueroa, J., Nikolic, H., Liu, K., 2017c. Pilot testing of a heat integrated 0.7 MWe CO_2 capture system with two-stage air-stripping: Amine degradation and metal accumulation. International Journal of Greenhouse Gas Control 64, 23-33.

Thompson, J.G., Combs, M., Abad, K., Bhatnagar, S., Pelgen, J., Beaudry, M., Rochelle, G., Hume, S., Link, D., Figueroa, J., 2017d. Pilot testing of a heat integrated

0.7 MWe CO_2 capture system with two-stage air-stripping: Emission. International Journal of Greenhouse Gas Control 64, 267-275.

Thompson, J.G., Frimpong, R., Remias, J.E., Neathery, J.K., Liu, K., 2014. Heat stable salt accumulation and solvent degradation in a pilot-scale CO_2 capture process using coal combustion flue gas. Aerosol and Air Quality Research 14, 550-558.

Todoli, J.-L., Mermet, J.-M., 2011. Liquid sample introduction in ICP spectrometry: A practical guide. Elsevier.

Vega, F., Sanna, A., Navarrete, B., Maroto-Valer, M.M., Cortés, V.J., 2014. Degradation of amine-based solvents in CO_2 capture process by chemical absorption. Greenhouse Gases: Science and Technology 4, 707-733.

Vevelstad, S.J., Grimstvedt, A., Elnan, J., da Silva, E.F., Svendsen, H.F., 2013. Oxidative degradation of 2-ethanolamine: The effect of oxygen concentration and temperature on product formation. International Journal of Greenhouse Gas Control 18, 88-100.

Wang, T., Hovland, J., Jens, K.J., 2015. Amine reclaiming technologies in post-combustion carbon dioxide capture. Journal of Environmental Sciences 27, 276-289.

Wang, T., Jens, K.-J., 2012. Oxidative Degradation of Aqueous 2-Amino-2-methyl-1-propanol Solvent for Postcombustion CO_2 Capture. Industrial & Engineering Chemistry Research 51, 6529-6536.

Welker, R.W., 2012. Chapter 4 - Size Analysis and Identification of Particles, in: Kohli, R., Mittal, K.L. (Eds.), Developments in Surface Contamination and Cleaning. William Andrew Publishing, Oxford, pp. 179-213.

Wittgens, B., Einbu, A., Brunsvik, A., Zahlsen, K., 2010. H&E TQP 1D1: Establish sampling and analytical procedures for potentially harmful components post combustion amine based CO_2 capture. Subtask 3: Online sampling and analysis. FM07-AJZ00-Z-RA-0002-03.

Zhu, Q., 2010. Non-calcium desulphurisation technologies, pp. 1-42.

Aas, N., da Silva, E.F., 2010. Emission measurements at Dong's Emission measurements at Dong s pilot plant for CO_2 capture in Esbjerg, Oslo.

Supporting Information

A review of degradation and emissions in post-combustion CO_2 capture pilot plants

Vanja Buvik[a], Karen K. Høisæter[a], Solrun J. Vevelstad[b], Hanna K. Knuutila[a]*

[a] Department of Chemical Engineering, NTNU, NO-7491 Trondheim, Norway

[b] SINTEF Industry, NO-7465 Trondheim, Norway

* Corresponding author: hanna.knuutila@ntnu.no

Table S1: A more detailed summary of the different pretreatment technologies applied at the different pilot campaign locations.

Location	**Pretreatment**
Austin, Texas	SCR, FGD
Brindisi, Italy	DeNOx, WESP/ESP/FF, DeSOx
CAER 0.1 MWth, USA	WFGD, high-temperature cyclone, knock-out drum
CAER 0.7 MWe, USA	WFGD, low NO_X, ESP
Changchun, China	PR, FGD, SCR, denitrification
Esbjerg, Denmark	SCR, deNOx, ESP, FGD
Ferrybridge, UK	FGD, in-furnace NO_X reduction
Heilbronn, Germany	deep SO_2 removal, pre-scrubber, DeNOx, ESP
Łaziska, Poland	Water scrubber, FGD
Loy Yang, Australia	knock-out drum, caustic wash
Maasvlakte, The Netherlands	BDU, FGD, caustic wash
Mikawa, Japan	ESP, FGD
Niederaussem, Germany	FGD, SCR, Caustic wash
Tarong, Australia	PR, caustic wash
TCM, Norway	FGD, BD filter
Tiller, Norway	water scrubber
Wilsonville, USA	particulate filter, SCR, ESP, WFGD

Table S2: Measured concentrations of total amount of heat stable salts (HSS) and organic acids in post-combustion CO_2 capture pilot campaigns using 30wt% MEA as their solvent, at the end of the campaign of right before reclaiming the solvent, in mg kg^{-1}. Hours of operation given in table indicates the time of sampling. *Mass concentration in original publication converted to mass fraction under the assumption that $\rho = 1$ kg L^{-1}.

Campaign	**HSS**	**Acetate**	**Formate**	**Glycolate**	**Oxalate**
Niederaussem (a)			200		
Niederaussem (b)		2500	530		240
Niederaussem (c)		25 000	5000		2700
CAER 0.1 MWth	4700		799		
CAER 0.7 MWe	17 677*	884*	7583*	619*	3643*
Loy Yang	24 000	5000	12 000		3000
Esbjerg (a)	13 000				
Esbjerg (b)			1200*		1100*
Heilbronn (a)			1260*		560*
Heilbronn (c)*	3482	350	1160	205	270
Changchun	3590		2160		700
TCM (a)	12 000	500*	3000*	400*	1200*
TCM (b)	6785 (0.12 mol kg^{-1})		1400	1440	520

Table S3: Chemical structures of compounds, which have been quantified in pilot campaigns. [a]Thermal degradation compounds, [b]Primary and [c]Secondary oxidative degradation compounds.

IUPAC name	Abbreviation	CAS-number	Chemical structure
Acetate	[b]	71-50-1	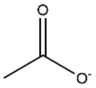
N-(2-Aminoethyl)-*N*'(2-hydroxyethl)-imidazolidione	AEHEIA	no CAS	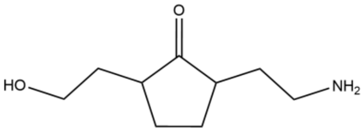
N,*N*'-Bis(2-hydroxy-ethyl)oxamide	BHEOX[c]	1871-89-2	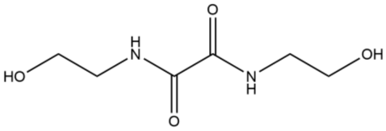
Bicine		150-25-4	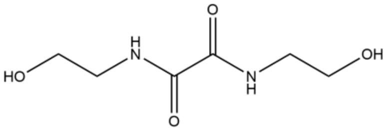
Diethanolamine	DEA[a]	109-89-7	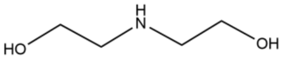
Ethylamine	EA[b]	75-04-7	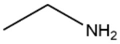
Formate	[b]	71-47-6	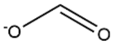
Glycolate	[b]	79-14-1	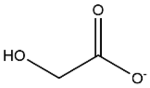
N-(2-Hydroxyethyl)-acetamide	HEA[c]	142-26-7	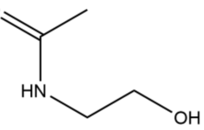
2-(2-Hydroxyethylamino)-ethanol	HEEDA[a] or AEEA	111-41-1	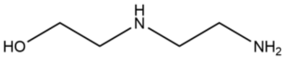
N-(2-Hydroxyethyl)-formamide	HEF[c]	693-06-1	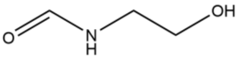

IUPAC name	Abbreviation	CAS-number	Chemical structure
N-(2-Hydroxyethyl)-glycine	HEGly[c]	5835-28-9	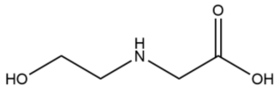
(*N*-(2-Hydroxyethyl)-(hydroxyethyl)-amino)acetamide	HEHEAA[c]	144236-39-5	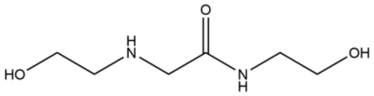
N-(2-Hydroxyethyl)-imidazole	HEI[c]	1615-14-1	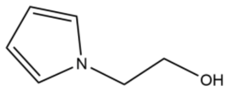
N-(2-Hydroxyethyl)-2-imidazolidione	HEIA[a]	3699-54-5	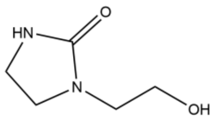
4-(2-Hydroxyethyl)-2-piperazinone	HEPO[c]	23936-04-1	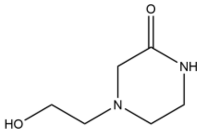
Monoethanolamine	MEA	141-43-5	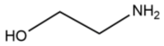
2-(Nitroamino)-ethanol	MEA-NO$_2$	74386-82-6	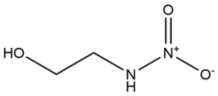
N-Nitrosodiethanolamine	NDELA	1116-54-7	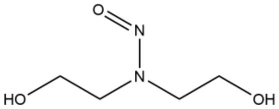
N-Nitrosodimethylamine	NDMA	62-75-9	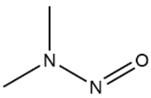
Nitroso-(2-hydroxy ethyl)-glycine	No-HEGly	80556-89-4	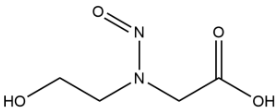

IUPAC name	**Abbreviation**	**CAS-number**	**Chemical structure**
Oxalate	b	338-70-5	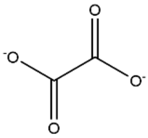
2-Oxazolidinone	OZD[c]	497-25-6	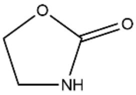
Piperazine	Pz	110-85-0	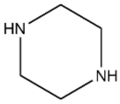

Chapter 5

The Impact of the Solvent on the Thermal Stability of Amines

The first part of this chapter contains a paper on the impact of the solvent on the thermal stability of amines. This has been published in Industrial & Engineering Chemistry Research journal in October 2022. The paper presents thermal degradation experiments of various amine solvents where the water is replaced either by increasing the amine concentration or by introducing an organic diluent as cosolvent. The effect on the thermal stability of the amine was studied. The second part of this chapter presents results from a corrosion study conducted on the samples included in the preceding publication.

5.1 The Impact of the Solvent on the Thermal Stability of Amines

Journal publication:

Høisæter, Karen K.; Vevelstad, Solrun; Braakhuis, Lucas & Knuutila, Hanna K. The Impact of the Solvent on the Thermal Stability of Amines. Ind. Eng. Chem. Res., Vol 61, 2022, 16179–16192.

The Impact of the Solvent on the Thermal Stability of Amines

Karen K. Høisæter[a], Solrun J. Vevelstad[b], Lucas Braakhuis[a], Hanna K. Knuutila[a]*

[a] Department of Chemical Engineering, NTNU, NO-7491 Trondheim, Norway

[b] SINTEF Industry, P.O.Box 4760 Torgarden, NO-7465, Norway

* Corresponding author: hanna.knuutila@ntnu.no

Abstract

Water-lean solvents have been proposed as a possible alternative to aqueous amine systems in postcombustion carbon capture. There is however little data available on how amine degradation is affected by different solvents. This study presents new insights on the effect of solvent on thermal degradation of alkanolamines from laboratory-scale degradation experiments. Replacing the water in aqueous monoethanolamine (MEA) solutions with organic diluents resulted in varying thermal degradation rates. Overall, all tested organic diluents (triethylene glycol, diethylene glycol, mono ethylene glycol, tetrahydrofurfuryl alcohol, *N*-formyl morpholine/water, and *N*-methyl-2-pyrrolidone) resulted in higher thermal degradation rates for loaded MEA. None of the proposed parameters, such as acid-base behavior, polarity, or relative permittivities, stood out as single contributing factors for the variation in degradation rates. The typical degradation compounds observed for an aqueous MEA solvent were also observed for MEA in various concentrations and with various organic diluents.

Keywords

CO_2 absorption, thermal degradation, amine solvents, water-lean solvent

1 Introduction

Greenhouse gas control is a key factor in reducing climate change. For postcombustion carbon capture, chemical absorption of carbon dioxide in aqueous amine solvents is a well-established technique and the current industry standard.[1] Flue gas containing CO_2 is brought into contact with an amine in an absorption column, with which it selectively reacts. Purified gas exits the system, while the separated CO_2 is released from the amine upon heating in a desorber column. Numerous amine systems have been experimentally investigated and maybe the most well-known systems are 30wt% aqueous monoethanolamine (MEA) and 40wt% piperazine (PZ)/amino-methyl-propanol (AMP).[2-4]

During the absorption/desorption process of carbon dioxide, the amines undergo unwanted irreversible reactions. This is due to the harsh environment they are exposed to in the cyclic system, such as exposure to reactive components in the flue gas, elevated temperatures, and contact with metals.[5,6] This amine degradation causes a significant operating expense and is one of the key issues with this technology. The compounds formed during degradation of the amines cause foaming, increased viscosity, corrosion of equipment, and fouling.[7,8] Also, emissions of hazardous degradation compounds and makeup cost for treatment of the old solvent are challenges for the process.[6,9,10] Therefore, reducing degradation is essential to make this technology acceptable for large emission industries, such as waste incineration, cement and steel production, and fossil-fuel-based energy production.[11]

To achieve this reduction, understanding the process behind the degradation is essential. Having an improved understanding of the underlying chemistry can help improve existing solvent systems, and, in addition, help in the development of new solvent systems. In this work, we will investigate the effect of solvent composition on thermal degradation. This has been done through a series of lab-scale experiments. First, we investigated how water in the solvent blends affected the degradation. This was done through thermal degradation experiments of various amine blends. Water was removed by changing the concentration of the amine. Thereafter, water was removed by switching the water with organic diluents. In this way, we could study the effect of both water and organic diluents on the thermal stability of amines. MEA was chosen as a reference system, as it is an already well-studied amine, and other amines were included based on their structure.

1.1 CO_2 Absorption

The chemical absorption of CO_2 is an acid–base reaction between carbon dioxide and the amine absorbent. Scheme 1 shows an overview of the reaction pathways for the formation of CO_2-carrying species upon loading an aqueous primary amine solution. For primary and secondary amines, the acidic CO_2 can react with two moles of amine forming an amine carbamate, possibly via a zwitterion, as shown in Scheme 1a.[12,13] The lifetime of this zwitterion is uncertain, but it is expected to be unstable.[14,15] Da Silva and Svendsen[16] found that the carbamate formation is likely to happen through a one-step reaction, where the zwitterion is entirely transient, or, if the zwitterion is formed as an intermediate, is likely to be short-lived. Tertiary amines cannot undergo this reaction to form carbamates as their three substituents make them unable to transition from the zwitterion to a stable carbamate.

The reaction between primary, secondary, or tertiary amines and CO_2 can also lead to the formation of bicarbonate and carbonate salts if water is present in the system. This can happen by hydrolysis from the amine carbamate, as shown in Scheme 1b, or through the formation and deprotonation of carbonic acid, as shown in Scheme 1c. This last case is the main route for tertiary amines reacting with CO_2. Generally, when an amine reacts with CO_2, protonated amines are formed as the counter ions to the CO_2-carrying products.[17,18] Physical absorption also occurs and is favored at high CO_2 pressures.

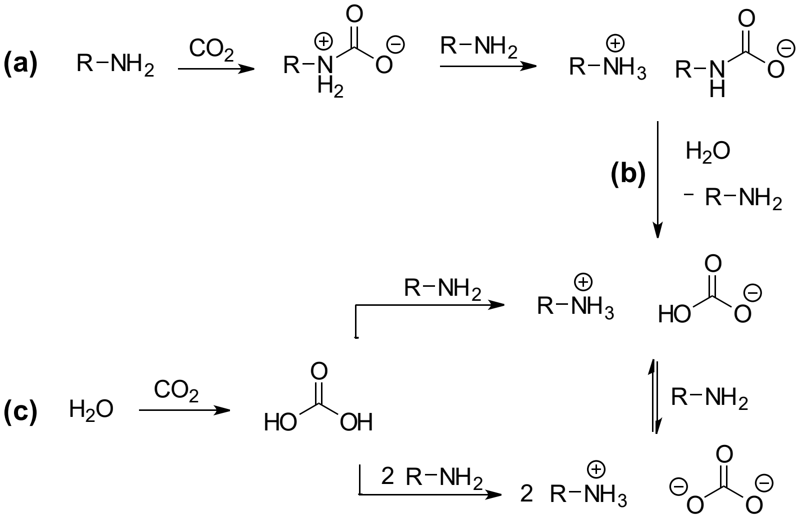

Scheme 1: CO_2 absorption pathways for primary aqueous amines.

Which CO_2-carrying species are formed is governed by the conditions of the system, e.g., choice of amine, amine concentration, pH of the solution, etc. A primary amine, such as MEA in an aqueous solution, would, for example, primarily form MEA carbamate.[17] The formation of carbonate, even though experimentally observed, is not considered significant for CO_2 absorption in aqueous MEA.[19]

1.2 Thermal Degradation Mechanism

Degradation of the amines is generally categorized as oxidative or thermal, either with or without the presence of CO_2. Little degradation has, however, been observed in aqueous amine solutions without CO_2, even at 200 °C.[20] Thermal degradation in the presence of CO_2 is dependent on temperature and therefore happens mainly in the stripper and reboiler. It has been studied experimentally for a long time,[21] and a polymerization reaction has been proposed.[22,23] The reaction rate has been found to increase with higher temperatures, pressures, and higher concentrations of CO_2.[5,24,25]

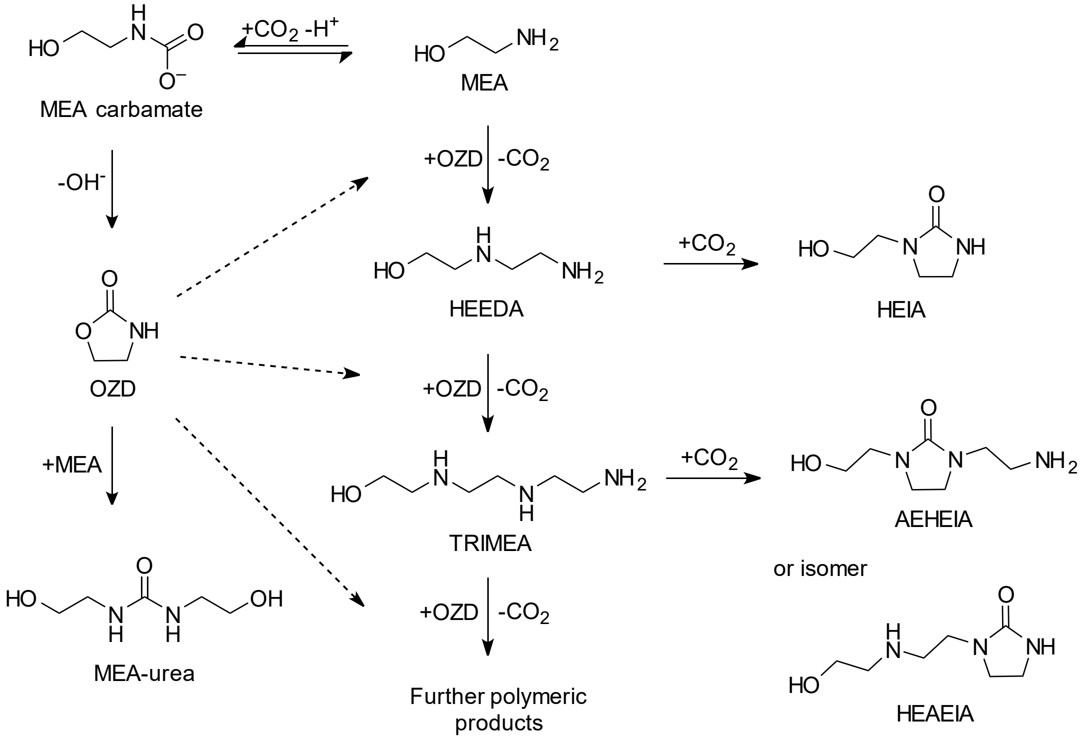

Scheme 2: Overview of proposed carbamate polymerization reaction of MEA at stripper conditions.[27]

Scheme 2 shows an example of the polymerization reaction for thermal degradation of MEA. When MEA reacts with CO_2, MEA carbamate is formed. The carbamate polymerization reaction is thought to be initiated by intramolecular cyclization of this carbamate or its protonated form, carbamic acid. The cyclization reaction results in the formation of 2-oxazolidone (OZD).[24,26] This reactive degradation compound is found only in small concentrations and is thought to be an intermediate product, reacting with MEA to form other identified degradation products, such as *N*-(2-hydroxyethyl)ethylenediamine (HEEDA/AEEA), 1-(2-hydroxyethyl)-2-imidazolidone (HEIA), 1,3-bis(2-hydroxyethyl)urea (MEA urea/BHEU), *N*-(2-hydroxyethyl)-diethylenetriamine (TRIMEA), etc. The order and by which mechanisms these are formed is not fully established, and different scenarios have been proposed.

The formation of OZD is believed to institute further amine degradation through the carbamate polymerization reaction. Initially, Polderman et al.[22] proposed that HEIA is formed when OZD reacts with MEA. From this, HEEDA was believed to form when HEIA expelled a CO_2 molecule. Davis[23] has later proposed that HEEDA is actually formed from OZD reacting with MEA. From experiments performed under stripper conditions, it was found that very little HEEDA is formed from HEIA, whereas HEIA is readily formed from HEEDA when exposed to CO_2. Degradation experiments have shown that, after an initial increase, the concentration of HEEDA has been found to stabilize, indicating that it acts as an intermediate. HEIA has been found to accumulate over time.[28,29] This supports the proposed mechanism by Davis.

Similar to HEEDA, MEA urea can also be formed from MEA reacting with OZD. Which of these degradation product, HEEDA or MEA urea, is formed depends on where on the OZD structure the ring is cleaved. The formation of HEEDA expels one CO_2 molecule, while for the formation of MEA urea, it is kept intact.

Further polymeric degradation products can be formed from HEEDA and OZD. Davis[23] found that HEEDA can react with OZD to form TRIMEA, likely following the same reaction mechanism as that of the formation of HEEDA itself. TRIMEA can then either react with another OZD, following the same reaction mechanism, to form further polymeric products or with CO_2 to form cyclic urea. This intramolecular ring closure gives rise to two possible degradation products, HEAEIA and AEHEIA. Since they are constitutional isomers and standards for MS analysis have not been commercially available, it is unknown which isomer is formed.

Tertiary amines do not degrade through the same reactions, simply because they do not form carbamate upon CO_2 loading. These need a preliminary step of dealkylation to form a primary or secondary amine before further degradation can occur. Because of this, tertiary amines are considerably more thermally stable than primary and secondary amines.[28]

1.3 Water-Lean Solvents

Water-lean, hybrid, or mixed solvents are common denominators of solvent systems, where the water content is reduced. In recent years, water-lean solvents have been proposed in the literature as an option to reduce the energy consumption for solvent regeneration.[30,31] In utilizing these solvents, the objective is to keep the high efficiency of aqueous alkanolamines but reduce unwanted properties.[32] Amongst others, this includes the high energy cost of the vaporization of the cosolvent, which for aqueous amine systems is the water.

The term water-lean solvent covers a broad array of solvents. In some cases, the amine concentration in aqueous amine blends is simply increased, thereby replacing the water with an amine. Some proposed solvents have water replaced in parts or in total by an organic diluent. In other cases, chemical classes with more complex binding mechanisms are proposed. In total, a considerable amount of solvent mixtures have been tested, ranging from blends with the typical organic cosolvents to the more advanced CO_2 binding organic liquids, known as CO_2BOLs.[19,32-40] Among these, there are some very promising solvents being tested at a pilot scale, such as RTI international's NAS, ION's advanced solvent, GE Global Research's GAP-TEG solvent system, and PNNL's EEMPA solvent.[41-44] These are examples of water-lean solvents systems where the positive traits of water-lean solvents have been maintained, while lower degradation compared to the standard aqueous MEA has been achieved. Thus, these solvents are providing a possible interesting future for CO_2 capture. Still, even though many water-lean solvent systems have been proposed and studied, there is still little data published on how the changes in composition of the solvent influence the degradation of the amines.[30]

2 Materials and Methods

2.1 Experimental Procedure

The chemicals used for this study are listed in Table 1. The effect of solvent on the thermal stability of amines was studied in the presence of CO_2. This has been done through four series of experiments. An overview of the experiments is given in Table 2.

Table 1: Details on the chemicals used in this study.

Chemical	Abbr.	Structure	CAS	Purity
Monoethanolamine [a]	MEA	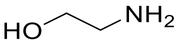	141-43-5	≥ 99%
Triethylene glycol [a]	TEG	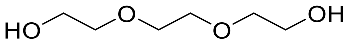	112-27-6	99%
Diethylene glycol [a]	DEG	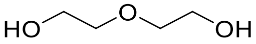	111-46-6	≥ 99%
Ethylene glycol [a]	MEG	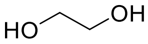	107-21-1	≥ 99%
Tetrahydrofurfuryl alcohol [a]	THFA	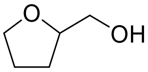	97-99-4	≥ 98%
N-Methyl-2-pyrrolidone [a]	NMP	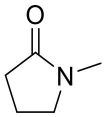	872-50-4	≥ 99%
N-Formyl morpholine [a]	NFM	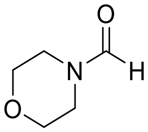	4394-85-8	99%
Sulfolane [a]	TMS	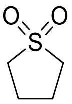	126-33-0	99%
Poly(ethylene glycol)dimethyl ether [a]	Selexol	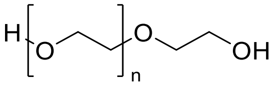	24991-55-7	M_n ~250

Propylene carbonate [a]	PC	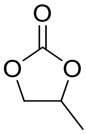	108-32-7	Anhydrous, 99.7%
3-Amino-propanol [a]	AP	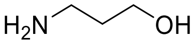	156-87-6	99%
2-(Methyl-amino)-ethanol [a]	MMEA	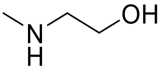	109-83-1	≥ 98%
2-(Ethyl-amino)-ethanol [a]	EAE	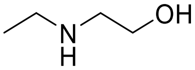	110-73-6	≥ 98%
2-Dimethyl-aminoethanol [a]	DMMEA	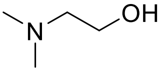	108-01-0	≥ 99.5%
2-(Diethyl-amino)-ethanol [a]	DEEA	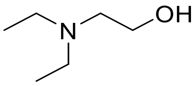	100-37-8	≥ 99.5%
3-Dimethyl-amino-1-propanol [a]	DMPA	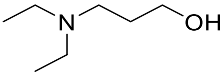	3179-63-3	99%
Carbon dioxide [b]	CO_2		124-38-9	99.9%

[a] Purchased from Sigma-Aldrich Norway AS/Merck Life Sciences.

[b] Purchased from AGA AB.

Variations in MEA and CO_2 Concentrations. Solutions with different ratios of MEA and deionized water were prepared. Three different sets of solutions were made by changing different parameters: (1) Solutions where the MEA concentration was kept constant (11mol%, 7 n_{MEA} kg_{H2O}^{-1}) and the loading was varied, (2) solutions where the MEA concentrations were varied, and the absolute CO_2 concentration was kept constant (0.19 mol CO_2 per 100 g unloaded solution), and (3) solutions where the MEA concentrations were varied while the loading was kept constant (0.1 mol CO_2 per mol MEA).

MEA in Varying Ratios of Triethylene Glycol (TEG) and Water. Solutions of 5 n_{MEA} $kg_{H2O+TEG}^{-1}$ in varying ratios of TEG and deionized water were prepared. The ratios of TEG and water ranged from 0−100%. All of the solutions were loaded to 0.5 mol CO_2 per mol MEA.

Other Amines in TEG and Water. Various amines were prepared in solutions (5 n_{MEA} $kg_{H2O+TEG}^{-1}$) with both pure deionized water and with 50mol% TEG in water. The amines studied were the primary amines MEA and AP, the secondary amines MMEA and EAE, and the tertiary amines DMMEA, DEEA, and DMPA. Solutions of primary and secondary amines were loaded to 0.5 mol CO_2 per mol amine, while solutions of tertiary amines were loaded to 0.3 mol CO_2 per mol amine. The loading of 0.3 for the tertiary amines was chosen because it was not possible to reach loadings of 0.5 in solutions containing TEG.

MEA in Various Organic Solvents. Solutions of 43mol% MEA in various organic solvents were prepared. MEA (43mol%) was chosen as this corresponds with the MEA concentration of the solution already studied for MEA in pure TEG. A wide array of diluents proposed as candidates for water-lean applications was tested.[30] The organic solvents chosen were monoethylene glycol (MEG), diethylene glycol (DEG), *N*-methyl-2-pyrrolidone (NMP), tetrahydrofurfuryl alcohol (THFA), *N*-formylmorpholine (NFM), sulfolane (TMS), poly(ethylene glycol) dimethyl ether (Selexol), and propylene carbonate (PC). However, both TMS and Selexol formed two phases upon loading, and MEA in PC could not be loaded above 0.1 mol CO_2 per mol MEA. MEA in pure NFM also resulted in phase separation, but here, the addition of water gave one phase. Therefore, a sample of MEA in 20mol% NFM in water was run. In conclusion, the solvents that were tested in thermal degradation experiments with MEA were monethylene glycol (MEG), diethylene glycol (DEG), triethylene glycol (TEG), tetrahydrofurfuryl alcohol (THFA), and *N*-methyl-2-pyrrolidone (NMP), as well as a mixture of 20mol% *N*-formylmorpholine (NFM) in water. All solutions were loaded to 0.5 mol CO_2 per mol MEA.

Table 2: Overview of thermal degradation experiments.

Amine	**Amine concentration**	**Loading [mol CO_2/mol amine]**	**Organic solvent**	**Organic solvent concentration [mol%]**
Variations of loaded MEA				
MEA	11mol%	0.1, 0.2, 0.3, 0.4	-	-
	8-100mol%	0.1-0.5 [a]	-	-
	11-73mol%	0.1	-	-
MEA in TEG and water				
MEA	$5\,\frac{n_{MEA}}{kg_{H_2O+TEG}}$	0.5	TEG	0-100
Various amines in TEG and water				
AP	$5\,\frac{n_{MEA}}{kg_{H_2O+TEG}}$	0.5	TEG	0, 50
MMEA				
EAE				
DMMEA		0.3		
DEEA				
DMPA				
MEA in various organic solvents				
MEA	43mol%	0.5	MEG	100
			DEG	
			TEG	
			THFA	
			NMP	
			NFM	20

[a] The loadings were chosen to obtain a constant absolute amount of CO_2 (0.19 mol CO_2 per 100 g unloaded solution) with the varying MEA concentration.

All solutions were made and loaded gravimetrically in batches, and loading was achieved by sparging CO_2 gas into the solutions. Both loading and amine concentration were checked with amine titration and total inorganic carbon (TIC) analysis, respectively. All solutions were initially slightly overloaded to allow correction of the concentrations by adding the fresh solvent to the batch before the experiments were run.

Thermal degradation of the solutions was conducted in 10 cm long 316 stainless steel cylinders, with an outer diameter of 1.3 cm and thickness of 0.1 cm and equipped with Swagelok end caps. For each solution, the same batch was loaded into a set of 10 cylinders, giving five data points over time and two parallels. The average relative standard deviation between the parallels was 0.49%. Within this, there were three parallels with a distinctly higher relative standard deviation of 2.0−3.5%. These are given in Supporting Information Table S1. For all series, the solution (8 mL) was loaded directly into the cylinders. The cylinders were closely sealed and placed in a forced convection oven at 135 °C. This temperature was chosen as it is the temperature frequently reported in other studies, which allows for comparison of degradation data with these publications.[24,26,45−48] For all series with primary and secondary amines, cylinders were extracted once a week, while for the series of tertiary amines, cylinders were extracted over a longer period. This was to ensure enough degradation from the more stable tertiary amines.

Metal cylinders opened for sampling were not returned for further degradation. All cylinders were weighed before and after the experiment to detect possible leakages. Leakages were detected in 7 of the 275 cylinders. An overview of the cylinder leakages is given in Supporting Information Table S2. For these solutions, the results reported are from only one parallel.

A selection of the solvent blends was also introduced into glass tubes (4 mL), which were then placed into new sets of cylinders. The glass tubes were used to prevent contact between the solvent and the metal walls of the cylinders. There was no significant difference in degradation rate for the experiments done with the solutions in direct contact with the cylinder compared to the ones with inserted glass walls – see comparison in Supporting Information Figure S1. Quantitatively and qualitatively, the formed degradation products were also the same in both cases − see comparison in Supporting Information Figure S2. This indicates that the degradation mechanisms are not influenced by the metal concentration in the solutions. This is in line with the literature.[49]

2.2 Analytical methods

Total alkalinity of the samples was found through amine titration with H_2SO_4.[50] Total inorganic carbon (TIC) measurements were used to determine the amount of CO_2 in the samples. For this, a Shimadzu TOCLCPH in TIC mode was used. Combining TIC results with the titration allowed us to monitor the loading of the solutions. Quantitative analyses of MEA and a selection of thermal degradation products by Liquid chromatography coupled with mass spectroscopy (LC-MSMS) were performed by SINTEF Industry on a UHPLC Agilent 1290 Infinity System with an Agilent 6490 triple quadrupole detector. For analyte separation, both Ascentis

Express Phenyl-Hexyl 2.7 µm HPLC column and a Discovery HS F5 HPLC column from Sigma-Aldrich Co. LLC were used.

The NMR experiments were performed at 26.8 °C on a Bruker 600 MHz Avance III HD equipped with a 5 mm cryogenic CP-TCI z-gradient probe. The obtained spectra were analyzed in the software Bruker TopSpin 4.0.7. Deuterated water was used as the "lock" solvent and TMSP (Tris(trimethylsilyl)phosphine) was used as an internal reference standard. The solution to be analyzed was placed in an NMR tube, and the "lock" solvent was placed in an inserted coaxial insert.

3 Results and Discussion

Our focus in this paper is to investigate what effect water and the solvent composition have on thermal degradation of amines. This has been done through four series of thermal degradation experiments. Results from the variations of loaded aqueous MEA will be presented in Section 3.1. In Section 3.2, results from both the series of MEA in different ratios of TEG and water and the series of various other amines in TEG and water will be presented. The last of the series will be presented in Section 3.3 and covers thermal degradation results of MEA in various organic solvents. The thermal degradation products found in the different series will be presented in Section 3.4.

The degradation trends of the solvent amine presented in this section will be derived from titration results. The titration results show the solvent's basicity, and since some degradation products are basic, the titration results will somewhat overpredict the actual concentration of the starting amine (e.g., MEA). However, even though titration measurements are not as accurate as other analytical methods, such as the LC-MS analysis, more data points are available due to the simplicity of the method. As the trends coincide well with the more accurate LC-MS results, titration data will be used when presenting the degradation trends. See the Supporting Information, Figure S3, for a comparison of titration and LC-MS data. All thermal degradation data presented in this section will be given as figures. Data for these and associated analyses will be provided in Supporting Information Tables S3−S11.

3.1 Variations of Loaded MEA

In the first series of experiments, our focus was on studying the effect of solvent composition in aqueous amine solutions. To achieve this, three variations on loaded aqueous MEA were studied. The three groups were solutions, where (1) the MEA concentration was kept constant and the loading was varied, (2) the MEA concentration was varied and the absolute CO_2 concentration was kept constant, and (3) the MEA concentration was varied while the loading was kept constant.

The first series of aqueous MEA were solutions of 11mol% MEA (30wt%) with increasing loadings (α = 0.1, 0.2, 0.3, and 0.4). Figure 1 shows the titration results from this experiment plotted together with LC-MS data from thermal degradation experiments performed under the same conditions by Davis and Rochelle.[24] Da Silva et al.[45] have also reported data showing the same trends but with distinctly higher degradation rates. The results show that thermal degradation increases with increased loading in all cases.

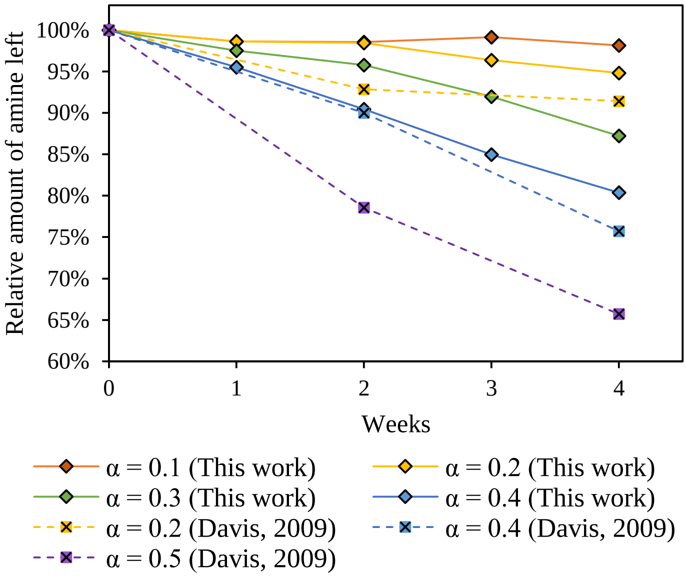

Figure 1: Effect of CO_2 loading (α) on the thermal degradation of MEA (11mol%, 135 °C). Data points from Davis and Rochelle[24] represent purely MEA left in the solutions as LC-MS was used for analysis.

The second series of solutions consisted of increasing ratios of MEA in deuterated water, ranging from 8−100mol% MEA before loading. All solutions were loaded with 0.19 mol CO_2 per 100 g unloaded solution, corresponding to the amount needed to load the 8mol% solution to 0.5 mol CO_2 per mol MEA. This means that while the loading decreases with the increase in MEA concentration, the concentration of CO_2 is the same for all solutions. Figure 2 shows the resulting amine loss and indicates that all solutions degrade at approximately the same rate. The absolute amine loss for all of the solutions lies within 0.81−1.14 mol/kg and is not following any trend. It, therefore, appears that the thermal degradation rates are closely tied to the absolute amount of CO_2. This is in line with literature findings.[51] From these results, and those from the previous experiment, it also appears that the thermal degradation rates do not seem to be affected much by MEA or water concentration.

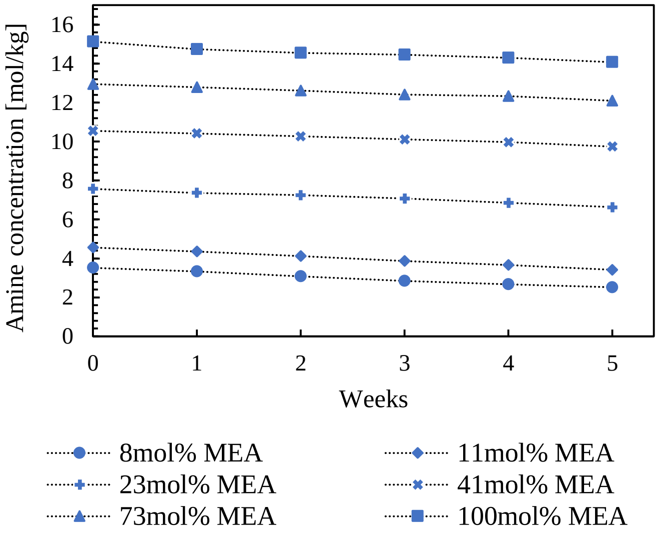

Figure 2: Effect of MEA start concentration on the thermal degradation of loaded MEA (0.19 mol CO_2/100 g unloaded solution, 135 °C).

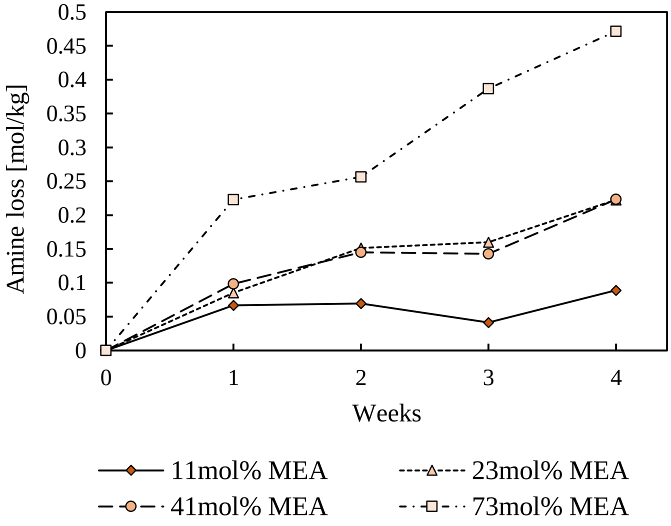

Figure 3: Effect of change in amine concentration on thermal degradation of loaded MEA (α=0.1, 135°C).

The third series of aqueous loaded MEA was solutions of increasing amounts of MEA with loadings of 0.1. This loading was chosen to avoid high pressures in the cylinders at high MEA concentrations, unfortunately at the expense of higher degradation rates. The results shown in Figure 3 are as expected. With higher MEA concentrations and, therefore, higher CO_2 concentrations, the amine loss was bigger.

From these three experiments, it seems like mainly the CO_2 concentration is accountable for the rate of thermal degradation. However, the change in loading should not necessarily be seen simply as changes in CO_2 concentration in the different solutions. As presented in Section 1.1, changes in the loading and/or solvent composition will change which CO_2-carrying species are being formed and in what quantities. Therefore, we plotted the equilibrium speciation of loaded predicted speciation for different loadings of 11mol% aqueous MEA at 135 °C. As expected for a primary aqueous amine, MEA carbamate is the predominant CO_2-carrying species formed upon loading. At low loadings, carbamate is almost exclusively forming, while as the loading increases, some fractions of CO_2 in the solutions form bicarbonate. Protonated MEA is formed as the counterion for both carbamate and bicarbonate and therefore increases steadily with the increase in loading.

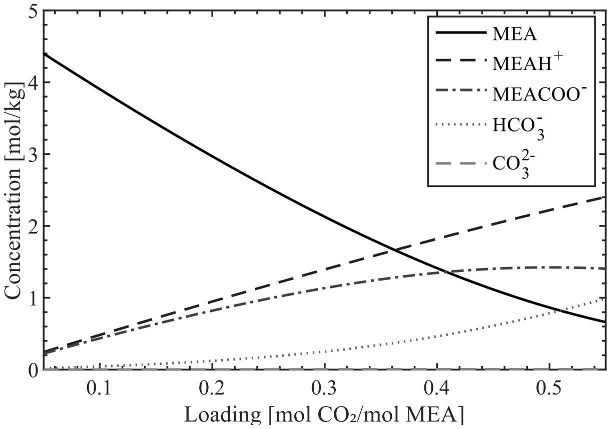

Figure 4: Speciation upon loading of 11mol% aqueous MEA. (Speciation given by ENRTL-RK model in Aspen Plus V10, 135 °C)

MEA carbamate is thought to play a prominent role in the initial carbamate polymerization reaction.[20] In Figure 1, it was seen from the experiment that increased loading resulted in increased thermal degradation. The degradation rate for the solution loaded to 0.5 is distinctly higher than that for the solution loaded to 0.4. At the same time, Figure 4 shows that the MEA carbamate concentration at loadings 0.4 and 0.5 is quite similar, indicating that the MEA carbamate concentration alone is not accountable for the reaction rate during thermal degradation. The degradation rates correlate to the total amount of CO_2 present, seemingly regardless of in which form, and thereby also to the concentration of protonated MEA. Regarding identifying a rate-limiting component, both total CO_2 concentration and protonated MEA concentration are viable possibilities.

Next, we look at the speciation of the solutions with increasing MEA concentration and constant absolute CO_2 concentration. Figure 5 shows the predicted speciation of the CO_2-carrying species in these solution compositions at 135 °C. Here, we see that at higher mole percentages of MEA, mainly the formation of carbamate and protonated MEA is expected. At the lower percentages, i.e., with the presence of more water, increasing amounts of bicarbonate take the place of carbamate. The thermal degradation results of these solutions, as presented in Figure 2, showed that the solutions with low MEA concentrations (e.g., 8mol%) degrade at the same rate as solutions with high MEA concentrations (e.g., 73mol%). Seeing these results in context with the predicted speciation of the system, the concentration of carbamate and bicarbonate is predicted to be approximately the same at 8mol% MEA, while it is predicted to only form carbamate at 73mol% MEA. Again, the MEA carbamate concentration alone does not seem to influence the degradation. Also, both the concentration of protonated MEA and the total concentration of CO_2-carrying species correlate better with the observed degradation rates. In the end, the correlations found from these results do not allow us to determine one species that governs the degradation rates. However, investigation of the impact of these species could be an interesting aspect for future work.

From these thermal degradation results of aqueous MEA solutions, it seems like the concentration of CO_2 in the solutions affects the degradation rates, while the concentration of water does not. To investigate this further, we then looked more closely for any effect of removing water. In the previous experiments, this was done by changing the ratios of MEA and water. Now, we wanted to look at the effect of replacing water with an organic solvent.

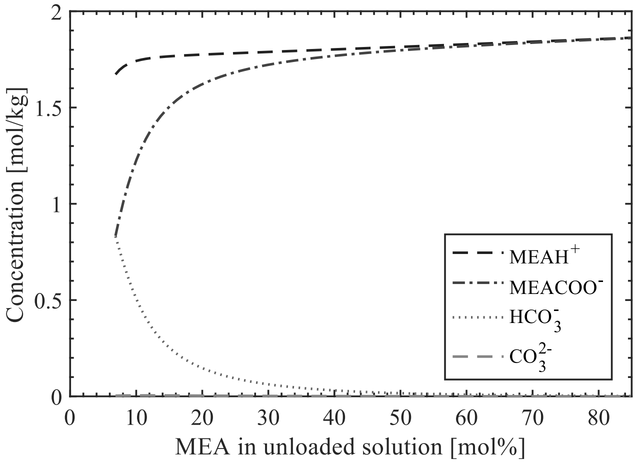

Figure 5: Speciation at increasing concentrations of MEA (Speciation given by ENRTL-RK model in Aspen Plus V10, 135 °C, [CO_2] = 1,9 mol/kg).

3.2 MEA and Other Amines in Various Ratios of TEG and Water

While switching water to an organic diluent allowed us to study the effect of the water, it also gave an insight into the stability of amines in nonaqueous and water-lean systems. Triethylene glycol (TEG) was chosen as the organic diluent in the first experiments because it was expected to be inert and stable under the given conditions. The effect of removing water was studied by comparing results for an aqueous solution with results for solutions, where increasing amounts of water were replaced with TEG.

Solvent blends with 5 n_{MEA} $kg_{H2O+TEG}^{-1}$ loaded to 0.5 mol CO_2 per mol MEA were prepared in TEG and deuterated water solutions ranging from 0−100mol% TEG. Figure 6 shows that higher ratios of TEG in the solvents resulted in increased thermal degradation rates of MEA.

Trying to explain the reduced stability in the organic diluent, we started by looking into the thermal stability of TEG itself. The idea behind this was that if TEG thermally degrades, compounds that are formed from this might enhance the degradation of MEA. This would explain the degradation rates observed. A thermal degradation experiment of pure TEG was therefore conducted with the same conditions that were used for the mixed solvent. After five weeks, a sample of the degraded TEG was analyzed using NMR spectroscopy. A comparison with a sample of pure, undegraded TEG showed that TEG had undergone virtually no thermal degradation. This explanation can then be ruled out. The comparison of the two NMR spectra is given in Supporting Information Figure S4.

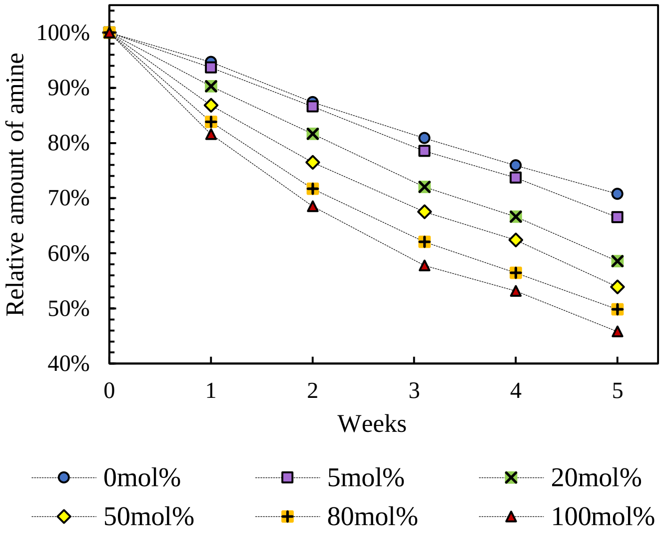

Figure 6: Effect of increasing ratios of TEG in water on thermal degradation of MEA (5 n_{MEA} $kg_{H2O+TEG}^{-1}$, α=0.5, 135 °C).

Looking into other possibilities for the increase in degradation with increased ratios of TEG, we then considered if the presence of TEG leads to the emergence of other degradation pathways. An indicator of this might be the presence of other degradation products than the ones expected through the carbamate polymerization reaction of aqueous MEA. We, therefore, analyzed for these degradation products to see if they would account for the amount of MEA lost during the degradation. Using LC-MS to search for the known thermal degradation products of MEA, 2-oxazolidone (OZD, CAS: 497-25-6), 1,3-bis(2-hydroxyethyl)urea (MEA urea, CAS: 15438-70-7), *N*-(2-hydroxyethyl)ethylenediamine (HEEDA, CAS: 111-41-1), and 3-(2-hydroxyethyl)-1,3-oxazolidin-2-one (HEIA, CAS: 3356-88-5) were observed. Results can be found in Section 3.4. The formation of further polymerized degradation products, e.g., tri-HEIA, was not explored, as an analytical method for this was not available. Moles of unknown degradation products, in relation to the amine loss in the solutions, were slightly higher in the solutions with TEG than the ones from the aqueous solution (8mol% MEA). Thus, these results do not clearly indicate that other degradation pathways are present. It is, however, clear that aqueous MEA solutions and MEA solutions with organic solvents, such as TEG, form many of the same degradation compounds. More details on the thermal degradation products formed in these experiments will be presented in Section 3.4.

In the case of the increasing degradation rates for solutions with TEG, we will lastly touch shortly upon two other possible explanations: first, the ratios between the CO_2-carrying species can be affected by the solvent change and, second, the solvent properties of the organic diluent have other effects on the species involved in the degradation mechanism.

As already stated in earlier discussions, the main CO_2-carrying products in aqueous MEA loaded to 0.5 are MEA carbamate and bicarbonate, both paired with protonated MEA. This is what we expect to be formed with the presence of water. Bicarbonate needs the presence of water to be formed. Removing water from the system, therefore, changes the speciation of the loaded solutions. Also, TEG is known to form alkylcarbonate in the presence of CO_2.[52] These are, however, not expected to form in significant amounts if carbamate can be formed. Unfortunately, we do not have a model for the speciation under these conditions to investigate this further.

The other effect of changing the solvent might be how well it stabilizes the different compounds involved in the carbamate polymerization reaction. Water is highly polar and is an excellent solvent for stabilizing ions. When switching to TEG, the ionic species, carbamate, and protonated MEA become less stabilized. The equilibrium between the ionic form and nonionic form of carbamate and protonated MEA might then be shifted toward the nonionic form. This results in higher concentrations of carbamic acid. If this protonation step is necessary for the reaction to form OZD, then this might be an explanation to why degradation rates are enhanced. Overall, it becomes clear from this that further studies are needed to explain the change in stability.

We also tested the thermal stability of some primary, secondary, and tertiary amines in solutions with 50mol% TEG in water. As presented in Section 1.2, primary and secondary amines that form carbamate are believed to degrade through the same mechanism as MEA. From the thermal degradation study done for AP, MMEA, and EAE in TEG (5, $\alpha = 0.5$), shown in Figure 7 and Figure 8, we saw loss in stability when water was replaced with TEG. This indicates that the trends seen for MEA are also expected for other primary and secondary amines. Tertiary amines do not form carbamate and therefore have a high thermal stability. Thermal degradation of DMMEA, DEEA, and DMPA in TEG (5 $n_{amine}\ kg_{H2O+TEG}^{-1}$, $\alpha = 0.3$) did not show any noticeable effect on the stability compared to aqueous solutions. The results from the thermal degradation experiments of the tertiary amines are presented in Supporting Information, Figures S5-S7.

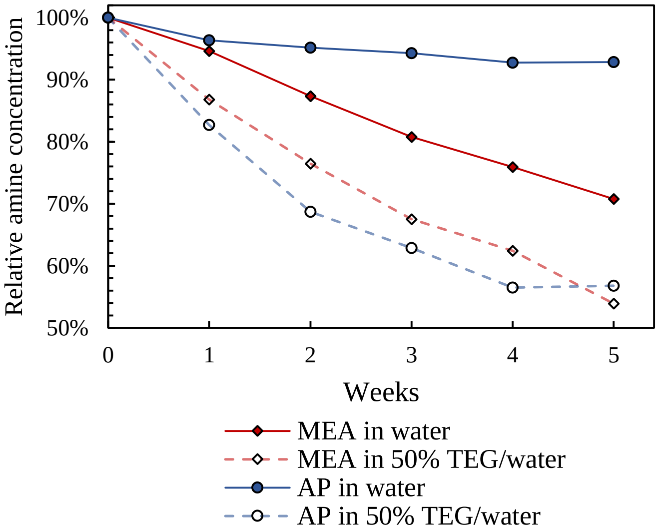

Figure 7: Effect of addition of TEG on thermal stability of primary amines MEA and AP (5 n_{amine} $kg_{H2O+TEG}$, $\alpha = 0.5$, 135 °C).

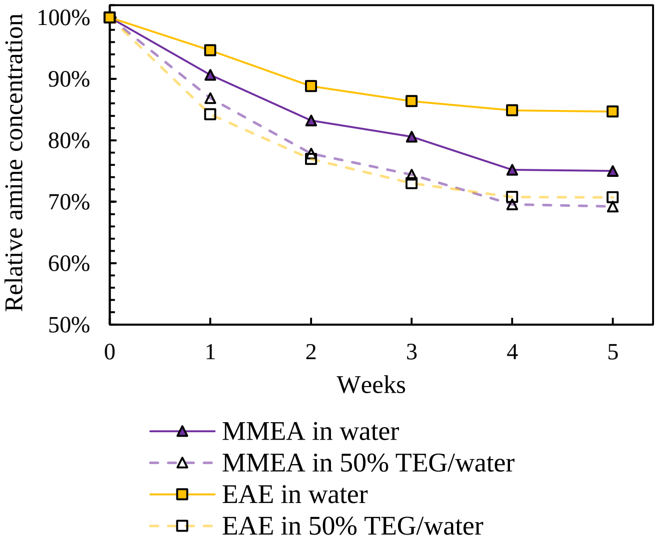

Figure 8: Effect of addition of TEG on thermal stability of secondary amines MMEA and EAE (5 n_{amine} $kg_{H2O+TEG}$, $\alpha = 0.5$, 135 °C).

3.3 MEA in Various Organic Solvents

Seeing how the degradation of the amines increased when using TEG as the diluent, we then expanded our study of the effect of the solvent on thermal degradation by including other organic diluents. In this series of experiments, solutions of 43mol% MEA in different organic diluents (DEG, MEG, THFA, NFM/water, and NMP, shown in Figure 9) were prepared and loaded to 0.5 mol CO_2 per mol MEA. The degradation trends for all of the tested solutions are shown in Figure 10. All of the organic diluents increased the degradation rates of MEA compared to pure water.

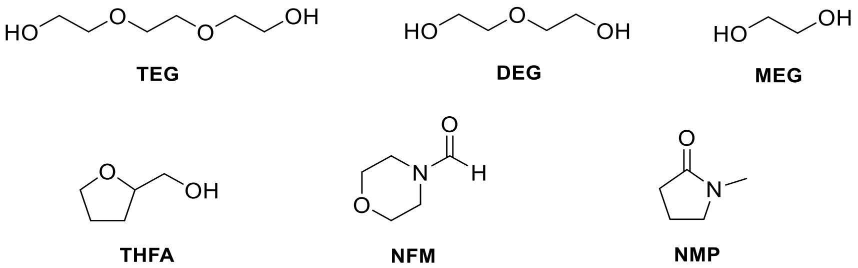

Figure 9: Structure of organic diluents.

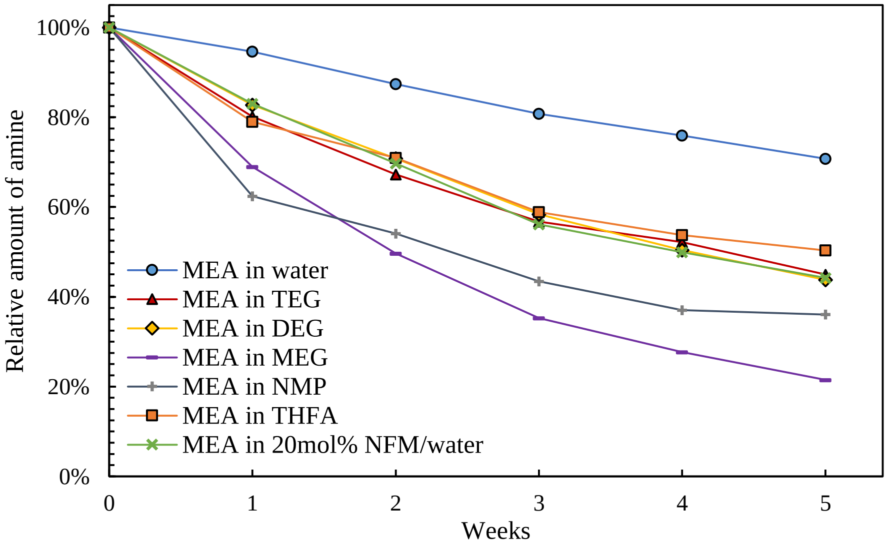

Figure 10: Overview of thermal degradation of loaded MEA in various organic diluents.

The same reasoning as to why MEA degrades more in TEG than in water might apply to the other organic solvents as well. The difference in the degradation rates between the different diluents, however, is harder to explain. The organic diluents were selected based on what solvents were proposed as possible water-lean diluents in the literature, not their chemical properties. From the chosen collection, however, it is still possible to investigate the possible effect of some parameters such as acid−base behavior, polarity, and relative permittivities.

The acid−base behavior of the solvents is described by their autoprotolysis constants, pKs, also called pK_{auto}. The pKs denote a solvent's ability to self-ionize. Small values indicate that the solvent can easily donate a proton, and vice-versa.[52,53] We only managed to find the pKs values of water, MEG, and NMP, as presented in Table 3. NMP is considered an aprotic solvent, as it does not hold a proton attached to a heteroatom. Autoionization is therefore quite disfavored, which is denoted by the exceptionally large pK value of this solvent. From the pK values found and the thermal degradation rates of MEA in these three solvents, there does not seem to be a correlation. Though water and MEA have similar pK values, the degradation rate of MEA in MEG is considerably higher than that of MEA in water. The degradation rate of MEA in NMP, however, is closer to that of MEA in MEG, even with their distinctly different pKs.

The polarity parameter was touched upon in the previous section, and as stated there, water is more polar than TEG. The relative polarity of the solvents is presented in Table 3. Though this could seem promising as a way of explaining the decreased stability of the amine in TEG, it falls short when including the other organic solvents, e.g., MEG. MEG has a higher polarity than TEG, so by that reasoning, MEA should be more stable in this solvent. As seen from Figure 10, however, MEA in MEG has the highest degradation rate of the solvents tested.

The relative permittivity of a solvent is given by its dielectric constant, ε_r. This value represents the solvent's ability to separate charges and orient its dipoles. It has been found to influence the ability a solvent has to stabilize charged species.[53,55−57] The dielectric constants for the studied solvents are presented in Table 3. There is again a mismatch between the investigated parameter and the observed thermal degradation rates. Suppose that a high dielectric constant allows the solvent to stabilize the MEA carbamate, thereby disfavoring the ring formation of OZD (see Section 1.2). The high dielectric constant of water is in line with this. The problem with this explanation arises when taking the glycols into account. MEA has a higher dielectric constant than DEG and TEG. However, it results in the highest degradation rate of MEA of the solvents studied.

Table 3: Solvent properties of pure solvents; autoprotolysis constant (pK_s), relative polarity (E_T^N) and dielectric constant (ε_r).

Solvent name	pK_s $[-lg(K_s/mol^2 * L^{-2})]$	E_T^N [-] [a]	ε_r [-] [a]
Water	14 [a]	1	78.36
MEG	15.84 [a]	0.79	37.70
DEG	-	0.713	31.69 (20 °C)
TEG	-	0.682	23.69 (20 °C)
NMP	≥24.2 [b]	0.355	32.2
NFM	-	-	-
THFA	-	-	-

a 53, b 54

None of the highlighted parameters give a satisfactory explanation for the degradation trends observed. The explanation thus might be a combination of different effects and might be specific to each solvent. As a final note, one can speculate if the reason for why MEA degrades faster in organic diluents than in water is an effect of the initial degradation reaction, the cyclization reaction forming OZD (see Section 1.2). In this reaction, a water molecule is expelled. This means that the formation of OZD should be more prone to happen in systems with lower water content. As OZD is considered the starting intermediate for the carbamate polymerization reaction, this increased formation rate would naturally lead to increased degradation rates for the system. The differences between the different organic diluents, however, is not explained by this.

Even though this study cannot give any exact mechanistic reasons for the increased degradation of the tested alkanolamines when water is replaced with the selected diluents, it does show why the degradation of water-lean solvents should be assessed in the early stage of solvent development work. It should also be remembered that most of the data in this work is on MEA-based water-learn solvent systems. Varying the amine (including the use of secondary and tertiary amines) would allow development of water-lean solvent systems with significantly lower degradation compared to aqueous 30wt% MEA.

3.4 Degradation Product Formation

Lastly, we will present the thermal degradation products in the solutions containing MEA. The degradation products included are OZD, HEEDA, HEIA, and MEA urea.

The other possible degradation products formed during thermal degradation of MEA shown in Scheme 2 were not analyzed as an analytical method was not available.

Figure 11 shows the thermal degradation products formed in solutions with varying ratios of loaded MEA in water (0.19 mol CO_2 per 100 g unloaded solution) after five weeks. All solutions have the same absolute amount of CO_2. The most drastic change when increasing the amine concentration is the steep increase in HEEDA. This can simply be because of the increasingly excessive amounts of MEA. OZD can thus readily react with MEA to form HEEDA. The high concentration of MEA also results in a shortage of free CO_2 available. This can explain the decrease in HEIA, as it is expected to form through the cyclization of the carbamate of HEEDA. The amount of MEA urea formed also increases with increasing concentrations of MEA, which can be attributed to the ready availability of MEA.

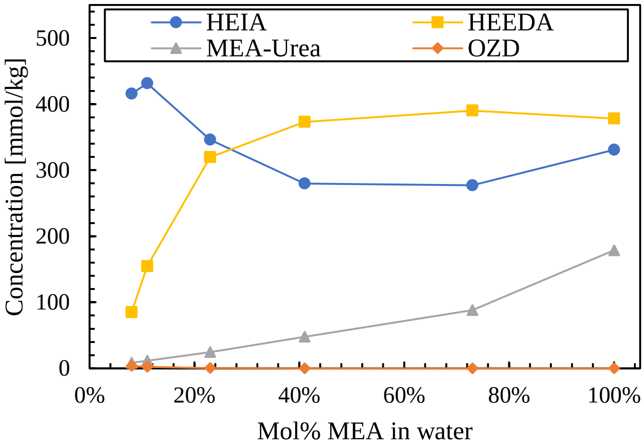

Figure 11: Thermal degradation products formed in solutions with increased concentrations of loaded MEA (0.19 mol CO_2 per 100 g unloaded solution) after 5 weeks.

Thermal degradation products formed after 4 weeks in aqueous solutions of MEA with different loadings are shown in Figure 12. The increase in loading resulted in a considerable increase in the formation of HEIA and a slight increase in the formation of HEEDA. HEIA formation is expected to be dependent on the amount of CO_2 available to form the carbamate of HEEDA. The increase in HEEDA can therefore be seen as a result of the increase in CO_2 concentration. This is in line with the results in Section 3.1, showing that increased loading resulted in increased thermal degradation.

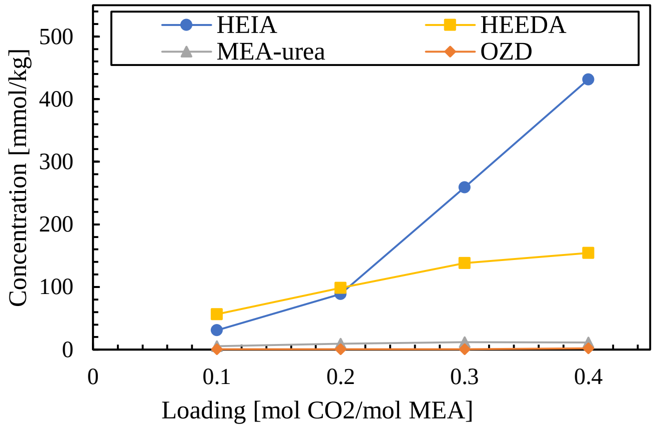

Figure 12: Thermal degradation products formed in solutions of loaded aqueous MEA (30wt%) with increasing loading after 4 weeks.

Aqueous MEA solutions with increasing amounts of MEA, all loaded to 0.1, gave thermal degradation products as presented in Figure 13. As the ratio between MEA and CO_2 is kept constant, the results shown here are the effect of reducing the water content. The overall degradation rates (Figure 3) showed that the increased MEA concentration resulted in increased degradation. The increase in formation of HEIA, HEEDA, and MEA urea mirrors this. They all stay within the same trend, with only some small variations in the ratio between them. The OZD concentration stays low even with the increased MEA concentration. This is as expected since OZD is considered a short-lived intermediate product. Overall, the water concentration does not seem to influence the formation of thermal degradation products.

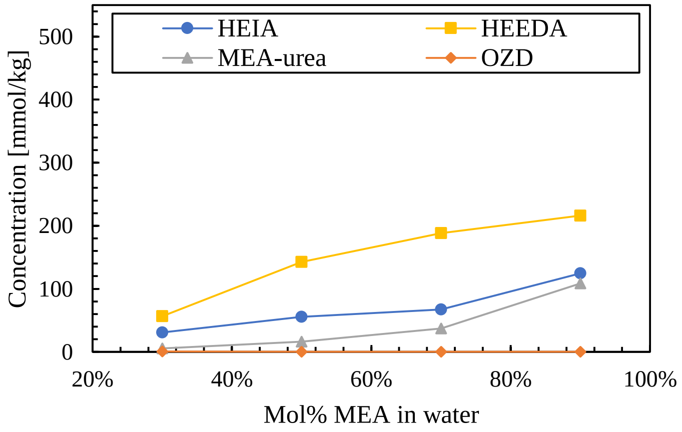

Figure 13: Thermal degradation products formed in solutions of loaded aqueous MEA ($\alpha = 0.1$) after 4 weeks.

Figure 14 shows the thermal degradation products that are present in the solutions with loaded MEA in varying ratios of TEG and water at week 5. The data points at 0mol% TEG correspond with the solution of 5 n_{MEA} kg_{H2O}^{-1} (8mol%) in water. Increasing the concentration of TEG, and thereby removing water, shows varying effects on the formation of thermal degradation products. HEEDA and MEA urea are only slightly affected and have a small decrease and increase, respectively. HEIA, however, is strongly influenced by the change in ratio. From solutions without TEG to solutions without water, the amount of HEIA produced is doubled.

When comparing this with MEA degraded in the other organic solvents, a similar result can be seen. Figure 15 shows the thermal degradation products formed during thermal degradation of loaded MEA ($\alpha = 0.5$) in various organic diluents. In all cases when switching water with another diluent, the amount of HEIA produced is nearly doubled. This indicates that it is the removal of water that results in the formation of HEIA being favored. This is especially interesting in the case of the NFM/water mixture, where the amount of HEIA is tripled from only changing 20mol% water to NFM. Another interesting point is the high formation of MEA urea in the loaded MEA degraded in NMP. It is not clear why these different degradation patterns take place. Overall, from these results, it becomes clear that further studies are needed to understand the degradation mechanisms.

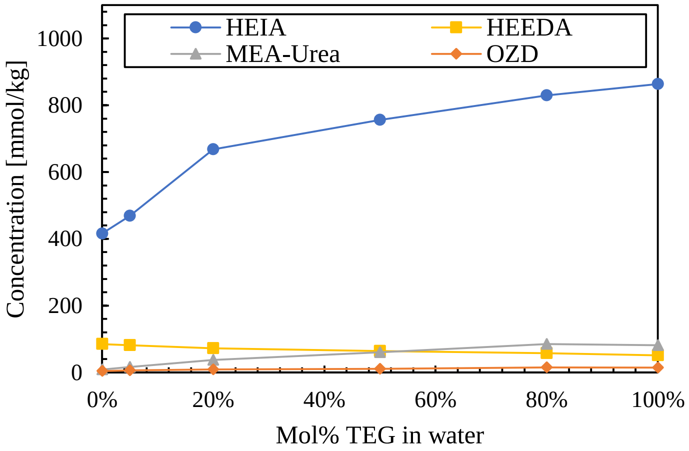

Figure 14: Thermal degradation products formed in solutions with loaded MEA (α = 0.5) in varying ratios of TEG and water after 5 weeks.

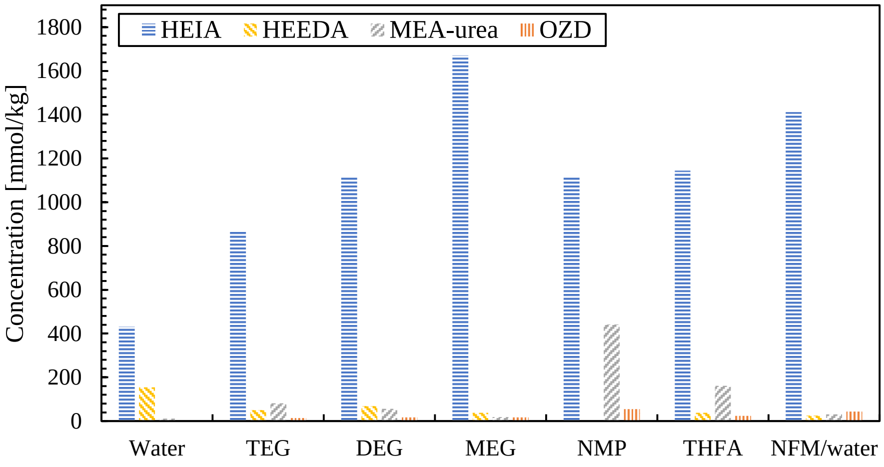

Figure 15: Thermal degradation products formed in solutions of loaded MEA (43mol%, α = 0.5) in various diluents after 5 weeks.

4 Conclusions

Water-lean solvents have been proposed as a possible alternative to aqueous amine systems in postcombustion carbon capture. There is however little data available on how amine degradation is affected by different solvents. This study presents new insights on the effect of solvent on thermal degradation of alkanolamines from laboratory-scale degradation experiments.

To investigate the effect of the water on thermal degradation, water was replaced by increasing amount of MEA in the first series of experiments. It was observed that the amine and water concentration did not affect the thermal degradation rate of the amine. An increase in the CO_2 concentration, however, resulted in increased thermal degradation. Which CO_2-carrying species is responsible for the increased degradation rates is not clear and it is an interesting topic for further investigations.

In the next experiments, water was replaced with the organic diluent TEG. Solutions of loaded MEA in TEG and water were prepared, and an increased ratio of TEG gave increased thermal degradation of MEA. Experiments with other primary and secondary amines (AP, MMEA, and EAE in TEG) gave the same outcome. It was not concluded whether the stability of tertiary amines (DMMEA, DEEA, and DMPA in TEG) was affected due to their high thermal stability.

Replacing the water in aqueous MEA solutions with organic diluents resulted in varying thermal degradation rates. Overall, all tested organic diluents (DEG, MEG, THFA, NFM/water, and NMP) resulted in higher thermal degradation rates for loaded MEA. None of the proposed parameters such as acid-base behavior, polarity, or relative permittivities, stood out as single contributing factors for the variation in degradation rates. The typical degradation compounds observed for an aqueous MEA solvent were also observed for MEA in various concentrations and with various organic diluents. In conclusion, it seems to be necessary to study each water-lean solvent system separately to rule out amine stability issues. Early-stage testing of new solvent systems is important.

Acknowledgement

The authors would like to acknowledge Ricardo Wanderley for running and analysing some of the degraded aqueous MEA series.

The LAUNCH project (Project No. 299662) is co-funded by the ERA-NET Accelerating CCS Technologies initiative, which supports the delivery of safe and cost-effective carbon capture, utilization, and storage. The governments of each participating country have contributed funding through the ACT2 initiative.

References

(1) Rochelle, G. T. Conventional Amine Scrubbing for CO_2 Capture. In *Absorption-Based Post-Combustion Capture of Carbon Dioxide*; Elsevier Inc., 2016; pp 35–67. https://doi.org/10.1016/B978-0-08-100514-9.00003-2.

(2) Moser, P.; Wiechers, G.; Schmidt, S.; Garcia Moretz-Sohn Monteiro, J.; Charalambous, C.; Garcia, S.; Sanchez Fernandez, E. Results of the 18-Month Test with MEA at the Post-Combustion Capture Pilot Plant at Niederaussem – New Impetus to Solvent Management, Emissions and Dynamic Behaviour. *Int. J. Greenh. Gas Control* **2020**, *95*, 102945. https://doi.org/10.1016/J.IJGGC.2019.102945.

(3) Feron, P. H. M.; Cousins, A.; Jiang, K.; Zhai, R.; Garcia, M. An Update of the Benchmark Post-Combustion CO_2-Capture Technology. *Fuel* **2020**, *273*, 117776. https://doi.org/10.1016/J.FUEL.2020.117776.

(4) Bernhardsen, I. M.; Knuutila, H. K. A Review of Potential Amine Solvents for CO_2 Absorption Process: Absorption Capacity, Cyclic Capacity and PKa. *Int. J. Greenh. Gas Control* **2017**, *61*, 27–48.

(5) Gouedard, C.; Picq, D.; Launay, F.; Carrette, P. L. Amine Degradation in CO_2 Capture. I. A Review. *Int. J. Greenh. Gas Control* **2012**, *10*, 244–270. https://doi.org/10.1016/j.ijggc.2012.06.015.

(6) Mazari, S. A.; Si Ali, B.; Jan, B. M.; Saeed, I. M.; Nizamuddin, S. An Overview of Solvent Management and Emissions of Amine-Based CO_2 Capture Technology. *Int. J. Greenh. Gas Control* **2015**, *34*, 129–140. https://doi.org/10.1016/j.ijggc.2014.12.017.

(7) Martin, S.; Lepaumier, H.; Picq, D.; Kittel, J.; de Bruin, T.; Faraj, A.; Carrette, P.-L. L. New Amines for CO_2 Capture. IV. Degradation, Corrosion, and Quantitative Structure Property Relationship Model. *Ind. Eng. Chem. Res.* **2012**, *51* (18), 6283–6289. https://doi.org/10.1021/ie2029877.

(8) Kennard, M. L.; Melserv, A. Mechanisms and Kinetics of Diethanolamine Degradation. *Ind. Eng. Chem. Fundam* **1985**, *24*, 129–140.

(9) Shao, R.; Stangeland, A. *Amines Used in CO_2 Capture-Health and Environmental Impacts*; 2009.

(10) Rao, A. B.; Rubin, E. S. A Technical, Economic, and Environmental Assessment of Amine-Based CO_2 Capture Technology for Power Plant Greenhouse Gas Control. *Environ. Sci. Technol.* **2002**, *36* (20), 4467–4475. https://doi.org/10.1021/es0158861.

(11) Bui, M.; Adjiman, C. S.; Bardow, A.; Anthony, E. J.; Boston, A.; Brown, S.; Fennell, P. S.; Fuss, S.; Galindo, A.; Hackett, L. A.; Hallett, J. P.; Herzog, H. J.; Jackson, G.; Kemper, J.; Krevor, S.; Maitland, G. C.; Matuszewski, M.; Metcalfe, I. S.; Petit, C.; Puxty, G.; Reimer, J.; Reiner, D. M.; Rubin, E. S.; Scott, S. A.; Shah, N.; Smit, B.; Trusler, J. P. M.; Webley, P.; Wilcox, J.; Mac Dowell, N. Carbon Capture and Storage (CCS): The Way Forward. *Energy Environ. Sci.* **2018**, *11* (5), 1062–1176. https://doi.org/10.1039/c7ee02342a.

(12) Danckwerts, P. V. The Reaction of CO_2 with Ethanolamines. *Chem. Eng. Sci.* **1979**, *34* (4), 443–446. https://doi.org/10.1016/0009-2509(79)85087-3.

(13) Johnson, S. L.; Morrison, D. L. Kinetics and Mechanism of Decarboxylation of *N*-Arylcarbamates. Evidence for Kinetically Important Zwitterionic Carbamic Acid Species of Short Lifetime. *J. Am. Chem. Soc.* **2002**, *94* (4), 1323–1334. https://doi.org/10.1021/JA00759A045.

(14) Ohno, K.; Inoue, Y.; Yoshida, H.; Matsuura, H. Reaction of Aqueous 2-(*N*-Methylamino)Ethanol Solutions with Carbon Dioxide. Chemical Species and

Their Conformations Studied by Vibrational Spectroscopy and Ab Initio Theories. *J. Phys. Chem. A* **1999**, *103* (21), 4283–4292. https://doi.org/10.1021/JP984821Q.

(15) Da Silva, E. F.; Svendsen, H. F. Ab Initio Study of the Reaction of Carbamate Formation from CO_2 and Alkanolamines. *Ind. Eng. Chem. Res.* **2004**, *43* (13), 3413–3418. https://doi.org/10.1021/IE030619K.

(16) Da Silva, E. F.; Svendsen, H. F. Computational Chemistry Study of Reactions, Equilibrium and Kinetics of Chemical CO_2 Absorption. *Int. J. Greenh. Gas Control* **2007**, *1* (2), 151–157. https://doi.org/10.1016/S1750-5836(07)00022-9.

(17) Kortunov, P. V; Siskin, M.; Baugh, L. S.; Calabro, D. C. In Situ Nuclear Magnetic Resonance Mechanistic Studies of Carbon Dioxide Reactions with Liquid Amines in Aqueous Systems: New Insights on Carbon Capture Reaction Pathways. *Energy and Fuels* **2015**, *29* (9), 5919–5939. https://doi.org/10.1021/acs.energyfuels.5b00850.

(18) Park, J. Y.; Yoon, S. J.; Lee, H. Effect of Steric Hindrance on Carbon Dioxide Absorption into New Amine Solutions: Thermodynamic and Spectroscopic Verification through Solubility and NMR Analysis. *Environ. Sci. Technol.* **2003**, *37* (8), 1670–1675. https://doi.org/10.1021/es0260519.

(19) Barzagli, F.; Lai, S.; Mani, F. Novel Non-Aqueous Amine Solvents for Reversible CO_2 Capture. In *Energy Procedia*; Elsevier Ltd, 2014; Vol. 63, pp 1795–1804. https://doi.org/10.1016/j.egypro.2014.11.186.

(20) Lepaumier, H.; Picq, D.; Carrette, P. L. Degradation Study of New Solvents for CO_2 Capture in Post-Combustion. *Energy Procedia* **2009**, *1* (1), 893–900. https://doi.org/https://doi.org/10.1016/j.egypro.2009.01.119.

(21) Kohl, A. L.; Nielsen, R. B. Alkanolamines for Hydrogen Sulfide and Carbon Dioxide Removal. In *Gas Purification*; 1997; pp 40–186. https://doi.org/10.1016/b978-088415220-0/50002-1.

(22) Polderman, L. D.; Dillon, C. P.; Steele, A. B. Why Monoethanolamine Solution Breaks down in Gas-Treating Service. *Oil Gas J.* **1955**, *53* (No. 2), 180–183.

(23) Davis, J. D. Thermal Degradation of Aqueous Amines Used for Carbon Dioxide Capture. PhD Thesis., 2009, Vol. 2.

(24) Davis, J.; Rochelle, G. Thermal Degradation of Monoethanolamine at Stripper Conditions. In *Energy Procedia*; 2009; Vol. 1, pp 327–333. https://doi.org/10.1016/j.egypro.2009.01.045.

(25) Freeman, S. A.; Rochelle, G. T. Thermal Degradation of Aqueous Piperazine for CO_2 Capture. 1. Effect of Process Conditions and Comparison of Thermal Stability of CO 2 Capture Amines. *Ind. Eng. Chem. Res.* **2012**, *51* (22), 7719–7725. https://doi.org/10.1021/ie201916x.

(26) Lepaumier, H.; Da Silva, E. F.; Einbu, A.; Grimstvedt, A.; Knudsen, J. N.; Zahlsen, K.; Svendsen, H. F. Comparison of MEA Degradation in Pilot-Scale with Lab-Scale Experiments. In *Energy Procedia*; Elsevier Ltd, 2011; Vol. 4, pp 1652–1659. https://doi.org/10.1016/j.egypro.2011.02.037.

(27) Braakhuis, L.; Høisæter, K. K.; Knuutila, H. K. Modeling the Formation of Degradation Compounds during Thermal Degradation of MEA. *Ind. Eng. Chem. Res.* **2022**, *61* (7), 2867–2881. https://doi.org/10.1021/acs.iecr.1c04496.

(28) Lepaumier, H.; Picq, D.; Carrette, P. L. New Amines for CO 2 Capture. I. Mechanisms of Amine Degradation in the Presence of CO 2. *Ind. Eng. Chem. Res.* **2009**, *48* (20), 9061–9067. https://doi.org/10.1021/ie900472x.

(29) Sexton, A. J.; Rochelle, G. T. Catalysts and Inhibitors for MEA Oxidation. In *Energy Procedia*; 2009; Vol. 1, pp 1179–1185. https://doi.org/10.1016/j.egypro.2009.01.155.

(30) Wanderley, R. R.; Pinto, D. D. D.; Knuutila, H. K. From Hybrid Solvents to Water-Lean Solvents – A Critical and Historical Review. *Sep. Purif. Technol.* **2021**, *260*, 1383–5866. https://doi.org/10.1016/j.seppur.2020.118193.

(31) Heldebrant, D. J.; Koech, P. K.; Glezakou, V.-A.; Rousseau, R.; Malhotra, D.; Cantu, D. C. Water-Lean Solvents for Post-Combustion CO Capture: Fundamentals, Uncertainties, Opportunities, and Outlook. *Chem. Rev.* **2017**, *117* (14), 9594. https://doi.org/10.1021/acs.chemrev.6b00768.

(32) Barzagli, F.; Mani, F.; Peruzzini, M. Efficient CO_2 Absorption and Low Temperature Desorption with Non-Aqueous Solvents Based on 2-Amino-2-Methyl-1-Propanol (AMP). *Int. J. Greenh. Gas Control* **2013**, *16*, 217–223. https://doi.org/10.1016/J.IJGGC.2013.03.026.

(33) Zheng, C.; Tan, J.; Wang, Y. J.; Luo, G. S. CO 2 Solubility in a Mixture Absorption System of 2-Amino-2-Methyl-1-Propanol with Glycol. *Ind. Eng. Chem. Res.* **2012**, *51* (34), 11236–11244. https://doi.org/10.1021/IE3007165.

(34) Karlsson, H. K.; Sanku, M. G.; Svensson, H. Absorption of Carbon Dioxide in Mixtures of *N*-Methyl-2-Pyrrolidone and 2-Amino-2-Methyl-1-Propanol. *Int. J. Greenh. Gas Control* **2020**, *95*, 102952. https://doi.org/10.1016/j.ijggc.2019.102952.

(35) Karlsson, H. K.; Drabo, P.; Svensson, H. Precipitating Non-Aqueous Amine Systems for Absorption of Carbon Dioxide Using 2-Amino-2-Methyl-1-Propanol. *Int. J. Greenh. Gas Control* **2019**, *88*, 460–468.

(36) Garcia, M.; Knuutila, H. K.; Aronu, U. E.; Gu, S. Influence of Substitution of Water by Organic Solvents in Amine Solutions on Absorption of CO_2. *Int. J. Greenh. Gas Control* **2018**, *78*, 286–305. https://doi.org/10.1016/J.IJGGC.2018.07.029.

(37) Wanderley, R. R.; Knuutila, H. K. Mapping Diluents for Water-Lean Solvents: A Parametric Study. *Ind. Eng. Chem. Res.* **2020**, *59* (25), 11656–11680. https://doi.org/10.1021/acs.iecr.0c00940.

(38) Skylogianni, E.; Perinu, C.; Cervantes Gameros, B. Y.; Knuutila, H. K. Carbon Dioxide Solubility in Mixtures of Methyldiethanolamine with Monoethylene Glycol, Monoethylene Glycol–Water, Water and Triethylene Glycol. *J. Chem. Thermodyn.* **2020**, *151*, 106176. https://doi.org/10.1016/j.jct.2020.106176.

(39) Pakzad, P.; Mofarahi, M.; Izadpanah, A. A.; Afkhamipour, M.; Lee, C. H. An Experimental and Modeling Study of CO_2 Solubility in a 2-Amino-2-Methyl-1-Propanol (AMP) + *N*-Methyl-2-Pyrrolidone (NMP) Solution. *Chem. Eng. Sci.* **2018**, *175*, 365–376. https://doi.org/10.1016/j.ces.2017.10.015.

(40) Barzagli, F.; Giorgi, C.; Mani, F.; Peruzzini, M. Reversible Carbon Dioxide Capture by Aqueous and Non-Aqueous Amine-Based Absorbents: A Comparative Analysis Carried out by ^{13}C NMR Spectroscopy. *Appl. Energy* **2018**, *220*, 208–219. https://doi.org/10.1016/j.apenergy.2018.03.076.

(41) RTI International. *Testing of RTI's Non-Aqueous Solvent CO_2 Capture Process at NCCC Using the SSTU*; 2018.

(42) Freeman, C. *Molecular Refinement of Transformational Solvents for CO_2 Separations*; 2019.

(43) Brown, A. “Buz”; Awtry, A.; Meuleman, E. *ION Advanced Solvent CO_2 Capture Pilot Project*; Pittsburgh, PA, and Morgantown, WV (United States), 2018. https://doi.org/10.2172/1484045.

(44) Hancu, D. *Large Pilot-Scale Carbon Dioxide (CO_2) Capture Project Using Aminosilicone Solvent*; Pittsburgh, PA, and Morgantown, WV (United States), 2017. https://doi.org/10.2172/1414342.

(45) Da Silva, E. F.; Lepaumier, H.; Grimstvedt, A.; Vevelstad, S. J.; Einbu, A.; Vernstad, K.; Svendsen, H. F.; Zahlsen, K. Understanding 2-Ethanolamine Degradation in Postcombustion CO 2 Capture. *Ind. Eng. Chem. Res.* **2012**, *51*, 13329–13338. https://doi.org/10.1021/ie300718a.

(46) Shoukat, U.; Baumeister, E.; Pinto, D. D. D.; Knuutila, H. K. Thermal Stability and Corrosion of Tertiary Amines in Aqueous Amine and Amine-Glycol-Water Solutions for Combined Acid Gas and Water Removal. *J. Nat. Gas Sci. Eng.* **2019**, *62*, 26–37. https://doi.org/https://doi.org/10.1016/j.jngse.2018.11.025.

(47) Lepaumier, H.; Grimstvedt, A.; Vernstad, K.; Zahlsen, K.; Svendsen, H. F. Degradation of MMEA at Absorber and Stripper Conditions. *Chem. Eng. Sci.* **2011**, *66* (15), 3491–3498. https://doi.org/10.1016/j.ces.2011.04.007.

(48) Fytianos, G.; Grimstvedt, A.; Knuutila, H.; Svendsen, H. F. Effect of MEA’s Degradation Products on Corrosion at CO_2 Capture Plants. In *Energy Procedia*; Elsevier Ltd, 2014; Vol. 63, pp 1869–1875. https://doi.org/10.1016/j.egypro.2014.11.195.

(49) Eide-Haugmo, I. Environmental Impacts and Aspects of Absorbents Used for CO_2 Capture, 2011.

(50) Ma’mun, S.; Jakobsen, J. P.; Svendsen, H. F.; Juliussen, O. Experimental and Modeling Study of the Solubility of Carbon Dioxide in Aqueous 30 Mass% 2-((2-Aminoethyl)Amino)Ethanol Solution. *Ind. Eng. Chem. Res.* **2006**, 44, 8, 2505–2512. https://doi.org/10.1021/ie0505209.

(51) Lepaumier, H.; Picq, D.; Carrette, P. New Amines for CO_2 Capture. II. Oxidative Degradation Mechanisms. *Ind. Eng. Chem. Res.* **2009**, *48* (20), 9068–9075. https://doi.org/10.1021/ie9004749.

(52) Wanderley, R. R.; Høisæter, K. K.; Knuutila, H. K. Signs of Alkylcarbonate Formation in Water-Lean Solvents: VLE-Based Understanding of PKa and

PKs Effects. *Int. J. Greenh. Gas Control* **2021**, *109*, 103398. https://doi.org/10.1016/J.IJGGC.2021.103398.

(53) Reichardt, C.; Welton, T. *Solvents and Solvent Effects in Organic Chemistry: Fourth Edition*; Wiley-VCH, 2010. https://doi.org/10.1002/9783527632220.

(54) Izutsu, K. Potentiometry in Non-Aqueous Solutions. In *Electrochemistry in Nonaqueous Solutions*; Wiley-VCH Verlag GmbH & Co. KGaA: Weinheim, FRG, 2002; pp 167–200. https://doi.org/10.1002/3527600655.ch6.

(55) Wanderley, R. R.; Yuan, Y.; Rochelle, G. T.; Knuutila, H. K. CO_2 Solubility and Mass Transfer in Water-Lean Solvents. *Chem. Eng. Sci.* **2019**, *202*, 403–416. https://doi.org/https://doi.org/10.1016/j.ces.2019.03.052.

(56) Hamborg, E. S.; van Aken, C.; Versteeg, G. F. The Effect of Aqueous Organic Solvents on the Dissociation Constants and Thermodynamic Properties of Alkanolamines. *Fluid Phase Equilib.* **2010**, *291* (1), 32–39. https://doi.org/10.1016/J.FLUID.2009.12.007.

(57) Leites, I. L. Thermodynamics of CO_2 Solubility in Mixtures Monoethanolamine with Organic Solvents and Water and Commercial Experience of Energy Saving Gas Purification Technology. *Energy Convers. Manag.* **1998**, *39* (16–18), 1665–1674. https://doi.org/10.1016/S0196-8904(98)00076-4.

Supporting Information

The Impact of the Solvent on the Thermal Stability of Amines

Karen K. Høisæter[a], Solrun J. Vevelstad[b], Lucas Braakhuis[a], Hanna K. Knuutila[a]*

[a] Department of Chemical Engineering, NTNU, NO-7491 Trondheim, Norway
[b] SINTEF Industry, P.O.Box 4760 Torgarden, NO-7465, Norway

* Corresponding author: Hanna.knuutila@ntnu.no

Additional experimental details, and extensive experimental results.

Table S1: Overview of samples with higher RSD.

Week	Solution composition	RSD
6	$5 \frac{n_{amine}}{kg_{H_2O + TEG}}$ DMPA in 50mol% TEG in water	2.0%
9	$5 \frac{n_{amine}}{kg_{H_2O + TEG}}$ DEEA in water	3.5%
12	$5 \frac{n_{amine}}{kg_{H_2O + TEG}}$ DMMEA in water	2.5%

Table S2: Overview of cylinder leakages.

Week	Solution composition
1	30% MEA in THFA
1	30% MEA in NMP
2	30% MEA in MEG
2	30% MEA in DEG
2	30% MEA in TEG
3	30% MEA in MEG
5	90% MEA in water, α = 0.1

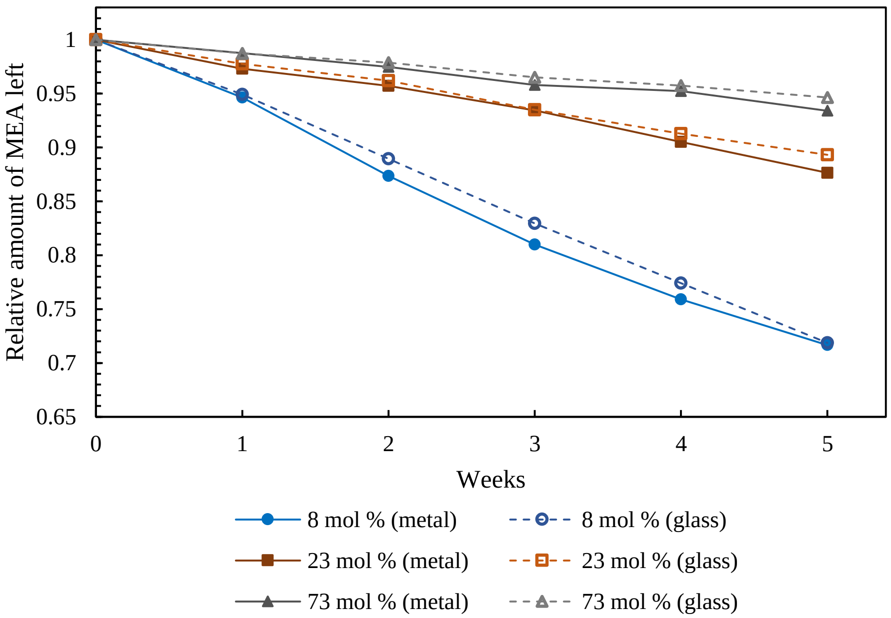

Figure S1: Comparison of thermal degradation results of metal and glass cylinders with loaded MEA (0.19 mol CO_2 per 100 g unloaded solution).

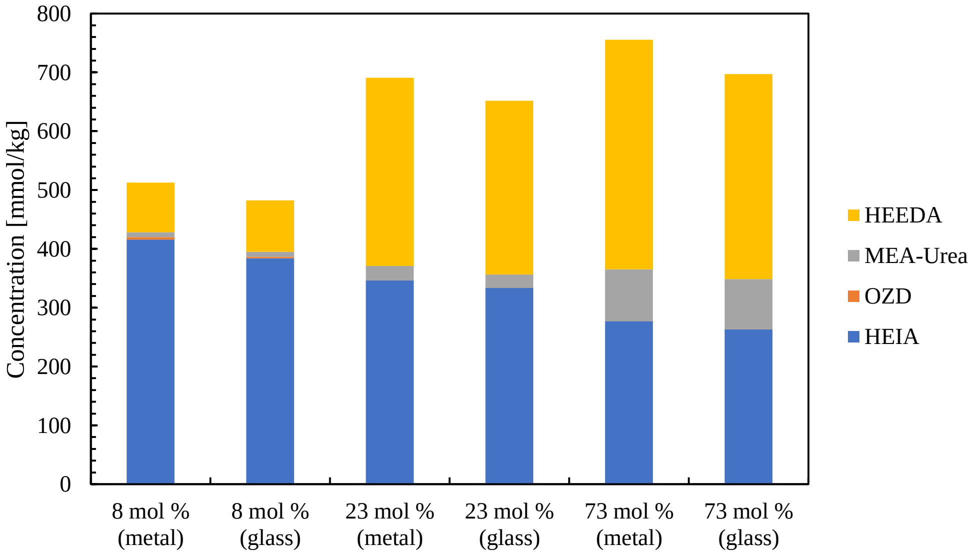

Figure S2: Thermal degradation products of a selection of concentrations of aqueous MEA (0.19 mol CO_2 per 100 g unloaded solution) formed after 5 weeks with metal and glass walls.

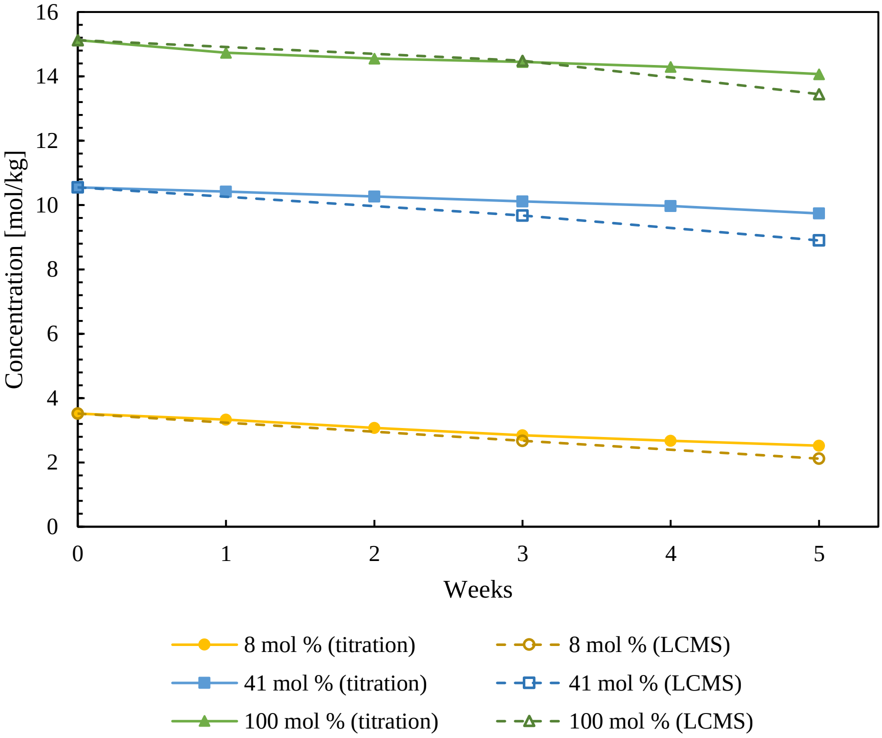

Figure S3: LCMS results vs titration results for comparison.

Table S3: Titration results [mol/kg] for thermal degradation experiments of aqueous MEA conducted in metal cylinders at 135°C.

Week	***0***	***1***	***2***	***3***	***4***	***5***
11mol% MEA α=0.1	4.81	4.75	4.74	4.77	4.72	4.75
11mol% MEA α=0.2	4.71	4.64	4.63	4.54	4.46	4.47
11mol% MEA α=0.3	4.62	4.51	4.42	4.25	4.03	4.09
11mol% MEA α=0.4	4.56	4.35	4.12	3.87	3.66	3.42
8mol% MEA α=0.5	3.52	3.33	3.07	2.85	2.67	2.52
23mol% MEA α=0.23	7.57	7.37	7.24	7.07	6.85	6.63
41mol% MEA α=0.17	10.55	10.41	10.26	10.11	9.97	9.74
73mol% MEA α=0.13	12.95	12.78	12.62	12.40	12.33	12.09
100mol% MEA α=0.12	15.13	14.73	14.55	14.45	14.30	14.07
23mol% MEA α=0.1	7.93	7.85	7.78	7.77	7.71	7.73
41mol% MEA α=0.1	10.87	10.77	10.72	10.73	10.65	10.65
73mol% MEA α=0.1	13.75	13.53	13.49	13.36	13.28	13.34

Table S4: Titration results [mol/kg] for thermal degradation experiments of aqueous MEA conducted in cylinders with glass walls at 135°C.

Week	***0***	***1***	***2***	***3***	***4***	***5***
8mol% MEA α=0.5	3.52	3.34	3.13	2.92	2.72	2.53
23mol% MEA α=0.23	7.57	7.40	7.28	7.08	6.91	6.76
73mol% MEA α=0.13	12.95	12.78	12.67	12.49	12.39	12.25

Table S5: Titration results [mol/kg] for thermal degradation experiments of MEA (5 $\frac{n_{MEA}}{kg_{H_2O+TEG}}$, α=0.5) in TEG and water conducted in metal cylinders at 135°C.

Week	***0***	***1***	***2***	***3.1***	***4***	***5***
Water	3.52	3.33	3.07	2.84	2.67	2.49
5mol% TEG	3.58	3.36	3.10	2.81	2.64	2.38
20mol% TEG	3.60	3.25	2.94	2.59	2.40	2.11
50mol% TEG	3.56	3.09	2.73	2.41	2.22	1.92
80mol% TEG	3.58	3.00	2.57	2.22	2.02	1.78
TEG	3.54	2.88	2.42	2.04	1.88	1.62

Table S6: Titration results [mol/kg] for thermal degradation experiments of primary amine AP and secondary amines MMEA and EAE in water and TEG (5 $\frac{n_{amine}}{kg_{H_2O+TEG}}$, α=0.5) conducted in metal cylinders at 135°C.

Week	***0***	***1***	***2***	***3***	***4***	***5***
AP in water	3.36	3.24	3.20	3.17	3.12	3.12
MMEA in water	3.27	2.97	2.72	2.64	2.46	2.45
EAE in water	2.90	2.75	2.58	2.51	2.46	2.46
AP in 50mol% TEG	3.34	2.76	2.30	2.10	1.89	1.90
MMEA in 50mol% TEG	3.32	2.88	2.58	2.47	2.31	2.30
EAE in 50mol% TEG	3.08	2.59	2.37	2.25	2.18	2.18

Table S7: Titration results [mol/kg] for thermal degradation experiments of tertiary amines DMMEA, DEEA and DMPA in water and TEG (5 $\frac{n_{amine}}{kg_{H_2O+TEG}}$, α=0.3) conducted in metal cylinders at 135°C.

Week	***0***	***2***	***4***	***6***	***9***	***12***
DMMEA in water	3.02	2.99	3.08	2.96	2.97	2.94
DEEA in water	2.60	2.58	2.57	2.54	2.56	2.46
DMPA in water	2.93	2.96	2.93	2.96	2.89	2.85
DMMEA in 50mol% TEG	3.00	3.01	2.99	2.98	2.94	2.93
DEEA in 50mol% TEG	2.95	3.08	2.95	2.94	2.90	2.89
DMPA in 50mol% TEG	2.98	2.95	2.96	3.07	2.95	2.97

Table S8: Titration results [mol/kg] for thermal degradation experiments of MEA (43mol%, α=0.5) in organic diluents conducted in metal cylinders at 135°C.

Week	***0***	***1***	***2***	***3***	***4***	***5***
Water	3.52	3.33	3.07	2.84	2.67	2.49
MEG	5.94	4.10	2.95	2.10	1.65	1.28
DEG	4.42	3.66	3.13	2.58	2.23	1.93
TEG	3.60	2.88	2.42	2.04	1.88	1.62
20mol% NFM in water	7.95	6.60	5.54	4.46	3.97	3.51
NMP	4.38	2.73	2.37	1.90	1.62	1.58
THFA	4.39	3.47	3.12	2.58	2.36	2.21

Table S9: LCMS results [mmol/kg] for thermal degradation experiments of aqueous MEA in metal cylinders at 135°C.

Mol%	***α***	***Week***	***MEA***	***HEIA***	***OZD***	***MEA-urea***	***HEEDA***
11	**0.1**	**3**	4823	14.5	0.47	5.36	29.7
11	**0.2**		4368	53.9	0.57	10.33	88.9
11	**0.3**		3991	152.6	1.27	14.50	128.8
11	**0.1**	**4**	4807	30.8	0.58	5.47	56.5
11	**0.2**		4238	88.5	0.70	9.66	98.4
11	**0.3**		3525	258.9	0.76	11.91	138.3
8	**0.5**	**3**	2670	266.2	4.76	12.29	94.2
41	**0.17**		9676	153.4	0.11	56.37	274.2
100	**0.12**		14482	164.5	0.06	203.13	253.4
8	**0.5**	**5**	2116	415.8	3.87	8.47	84.6
11	**0.4**		2894	431.4	2.07	11.41	154.4
23	**0.23**		5803	346.3	0.23	24.48	319.8
41	**0.17**		8899	279.6	0.09	47.70	373.0
73	**0.13**		11332	277.1	0.05	88.25	390.1
100	**0.12**		13447	330.7	0.02	178.69	378.3
23	**0.1**	**4**	7331	55.7	< 0.13	16.00	142.4
41	**0.1**		10568	67.2	< 0.13	37.06	188.1
73	**0.1**		12983	124.5	< 0.13	108.46	216.1

Table S10: LCMS results [mmol/kg] for thermal degradation experiments of MEA (5 $\frac{n_{MEA}}{kg_{H_2O+TEG}}$, α=0.5) in TEG and water in metal cylinders at 135°C.

Mol% TEG	*Week*	*MEA*	*HEIA*	*OZD*	*MEA-Urea*	*HEEDA*
50	**3**	2203	476.7	14.01	92.99	75.2
100		1946	599.2	19.7	131.22	61.4
5	**5**	2056	469	5.63	15.93	81.1
20		1785	668.1	8.46	37.14	72.4
50		1708	756.2	11.1	60.43	64.0
80		1592	829.6	14.91	84.89	57.6
100		1397	863.6	14.54	81.38	51.1

Table S11: LCMS results [mmol/kg] for thermal degradation experiments of MEA (43mol%, α=0.5) in organic diluents in metal cylinders at 135°C.

Solvent	*Week*	*MEA*	*HEIA*	*OZD*	*MEA-urea*	*HEEDA*
TEG	**3**	1946	599.2	19.7	131.22	61.4
DEG		2188	818.5	22.29	102.46	94.83
MEG		1356	1486.8	22.98	56.44	83.41
NMP		1829	729.8	60.58	587.22	1.47
THFA		2427	821.5	28.84	217.59	50.06
20mol%NFM in water		1861	1102.5	45.40	71.32	53.68
TEG	**5**	1397	863.6	14.54	81.38	51.09
DEG		1519	1115.0	17.31	56.70	69.37
MEG		613	1671.2	16.48	18.89	38.35
NMP		1400	1119.6	54.21	441.11	0.52
THFA		1973	1144.7	24.28	161.23	38.07
20mol% NFM in water		904	1412.0	42.87	30.66	25.63

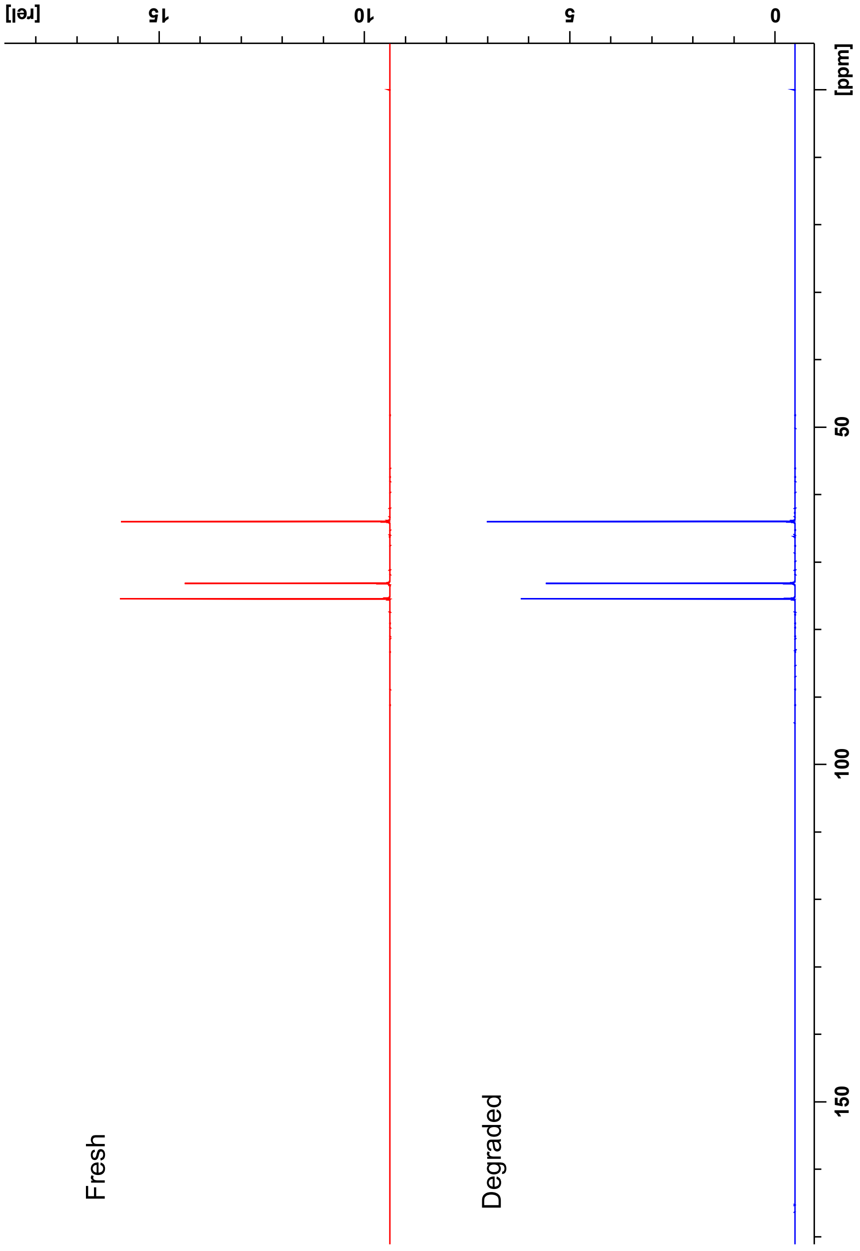

Figure S4: NMR spectra for comparison of pure TEG thermally degraded for 5 weeks and fresh, undegraded TEG.

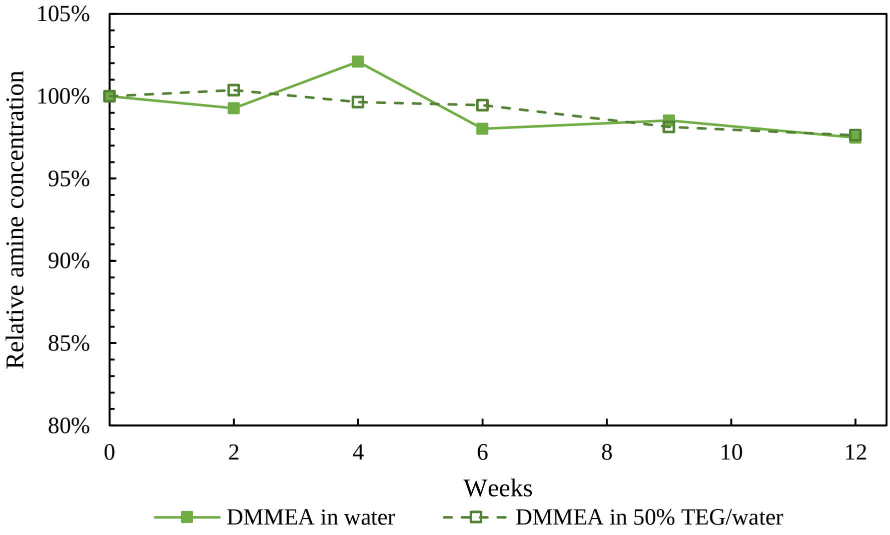

Figure S5: Effect of addition of TEG on thermal stability of tertiary amine DMMEA (5 $\frac{n_{amine}}{kg_{H_2O+TEG}}$*,*
α = 0.3, 135 °C).

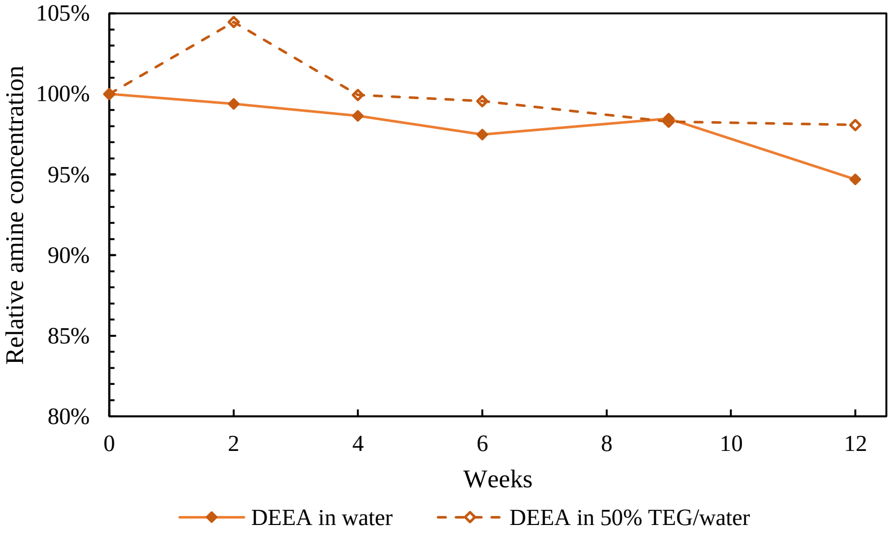

Figure S6: Effect of addition of TEG on thermal stability of tertiary amine DEEA (5 $\frac{n_{amine}}{kg_{H_2O+TEG}}$*,*
α = 0.3, 135 °C).

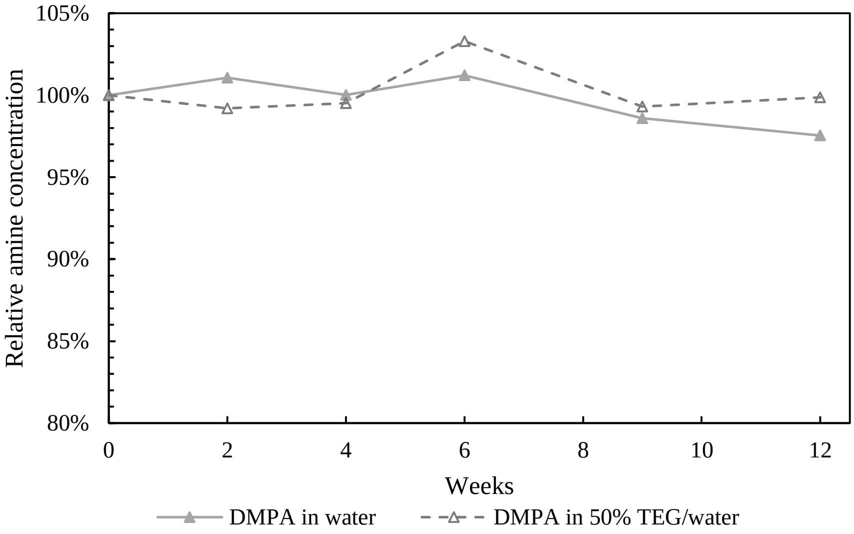

Figure S7: Effect of addition of TEG on thermal stability of tertiary amine DMPA (5 $\frac{n_{amine}}{kg_{H_2O+TEG}}$*, α = 0.3, 135 °C).*

5.2 Corrosion Effects in Water-Lean Solvents

In addition to the analysis presented in the first part of this chapter, a short corrosion study of the degraded solvents was performed as a side study. This was done to gain insights into the corrosivity of the solvents. The results, however, were not included in the publication as the presence of metals is not expected to affect the thermal degradation mechanism of amines.[1] In addition, the results did not show any clear trends. In the following subsection, a short overview of corrosion in CCS will be presented, followed by the result from the metal analysis and some considerations of these.

Alongside degradation, corrosion can be a severe problem when operating a CO_2 absorption process.[2] Although a lot of research has been done in the field and valuable insights have been gained, the corrosion process that takes place in post-combustion capture plants is not well understood.

Overall, corrosion is a complex problem, and it has been found that multiple factors contribute, including the composition of the amine solution, temperature, acid gases, and flue gas impurities. Carbon steel corrodes by a charge transfer reaction between the metal surface and the surroundings, accompanied by a reduction. Stainless steel has the important ability to form $Ni(OH)_2$ and Cr_2O_3 on the surface. At high pH levels, these will work as a protective layer for the metal underneath. However, if the system experience sufficiently oxidizing conditions, the protective layer will become inactive and corrosion will occur similarly to carbon steel corrosion.[3] Most of the electrochemical reactions involved in corrosion are thermally activated.[4,5] This is in line with what has been observed and reported in the literature, where increased temperature has been reported to result in increased corrosion rates.[2,6,7]

The composition of the amine solution also influences the corrosion rates. Generally, amines by themselves are not corrosive.[8] Increased loading of the amine, however, results in increased corrosivity.[2,6] At areas with the combination of high loading and high temperature, the likelihood of excessive corrosion is, therefore, high. Such a point can be found in the rich amine line between the heat exchanger and the stripper.[4]

The choice of amine does not affect corrosion rates if the amine is not loaded. When the amine is loaded, however, the choice of amine becomes highly influential.[4] The corrosion potential of the amine classes is proposed to go from most to least corrosive in the order primary > secondary > tertiary.[9] However, the variation within a class can be very large. Studies have suggested that the corrosivity of the amine solution is linked to the rate of carbamate formation.[7] Also, sterically hindered amines are not very corrosive, as they form a protective layer of iron carbonate ($FeCO_3$) on the metal surface. Both sterically hindered amines and tertiary amines are capable of this, as they are both a source of the carbonate species needed for this formation.[9] A consensus on the effect of the amine concentration has not been reached.[4]

As the amine degrades during operating hours, the formation of degradation products will also contribute to the corrosion problem. Some basic degradation products have been found to increase corrosion rates, but heat-stable salts (HSS) are generally considered the main contributors.[2,10–13] The higher the concentration of these components, the higher the corrosion rates. The reason why, and by which mechanisms this happens, is not understood.

Studying corrosion is usually done using coupons. Here, the weight loss is measured,[2,14] and in some cases, visual inspection of the surface of the coupons is also conducted.[15] Metal concentration in the solvent can also give insight into the state of the solvent concerning corrosion. These are measured using ICP-MS/-OES.[16] These are, however, not considered proper corrosion tests but can indicate the corrosivity of the actual systems.

In this study, the analyses were performed externally at the Department of Chemistry, NTNU, as described in the Methodology Section of the thesis. The metals quantified were Mo, Cr, Ni, and Fe, and the solvent systems studied were the same as presented in the publication in the first part of this chapter. An overview of these is presented below.

a. Increasing concentrations of loaded monoethanol amine (MEA) in water with a constant absolute concentration of CO_2 (0.19 mol CO_2/100 g unloaded solution).

b. Loaded MEA (5 Molal, α=0.5) in changing ratios of triethylene glycol (TEG) and water.

c. Loaded primary (5 Molal, α=0.5), secondary (5 Molal, α=0.5), and tertiary (5 Molal, α=0.3) amines in solutions of TEG and water. Amines included were 3-amino-propanol (AP, 1°), 2-(methyl-amino)-ethanol (MMEA, 2°), 2-(ethyl-amino)-ethanol (EAE, 2°), 2-dimethyl-amino-ethanol (DMMEA, 3°), and 2-(diethyl-amino)-ethanol (DEEA, 3°).

d. Loaded MEA (5 Molal, α=0.5) in organic solvents TEG, diethylene glycol (DEG), monoethylene glycol (MEG) and a 20mol% *N*-Formyl morpholine/water solution (NFM).

a. The results for the solutions with increasing concentrations of loaded aqueous MEA are shown in Figure 5.2.1. In these experiments, the MEA concentration was varied, while the absolute concentration of CO_2 was kept constant. The result from the thermal degradation experiments indicated that all these solutions degraded at approximately the same rate. From the analysis of the metal concentrations, some unexpected results were observed. At low concentrations of MEA, the metal concentration increased with the increase in MEA. At the midrange concentrations, the concentration of metals stabilized, before decreasing as the concentration increased further. Though the concentrations of the separate metals were not the same, the total amount of metals was found to be the same for the solutions with 8mol% and 100mol% MEA. In the literature, no consensus has been reached with regard to the effect of amine concentration on corrosion. From these results, it seems to have an effect, though it is not a clear trend.

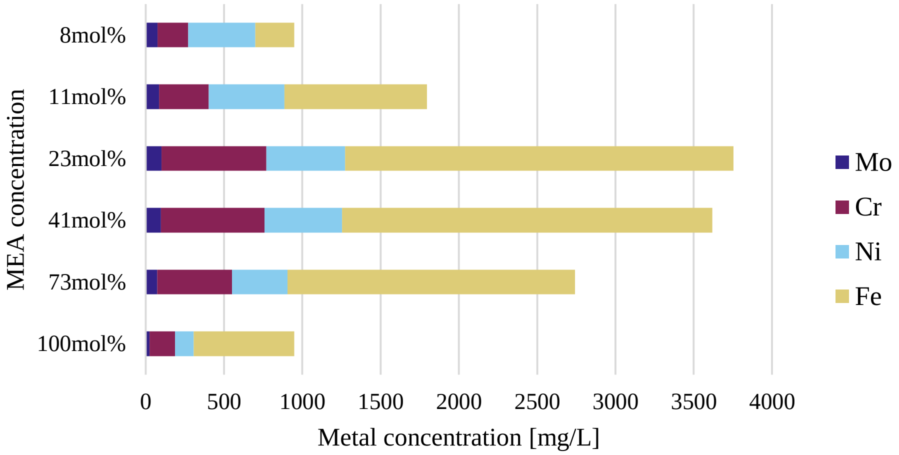

Figure 5.2.1: Metal concentrations in thermally degraded solutions (5 weeks, 135 °C) of loaded aqueous MEA (0.19 mol CO_2/100 g unloaded solution) with increasing MEA concentrations.

b. In the solutions with loaded MEA in various ratios of TEG in water, the increase in the concentration of TEG showed an increase in the thermal degradation rates of MEA. The metal concentration in these solutions is shown in Figure 5.2.1. It is worth noticing that the 0mol% TEG in Figure 5.2.2 corresponds to the 8mol% MEA in Figure 5.2.1. Figure 5.2.2 shows that, at lower concentrations of TEG, the metal concentration increases with an increasing ratio of TEG. Between 20mol% and 50mol%, however, there is a sharp change and all the solutions with high TEG content have very low metal concentrations. Higher TEG concentrations, therefore, might have an inhibitory effect on corrosion. The change in metal content might also be due to insufficient solubility of the metal ions in TEG. We have unfortunately not found any published data on the solubility of any of the measured metals in TEG.

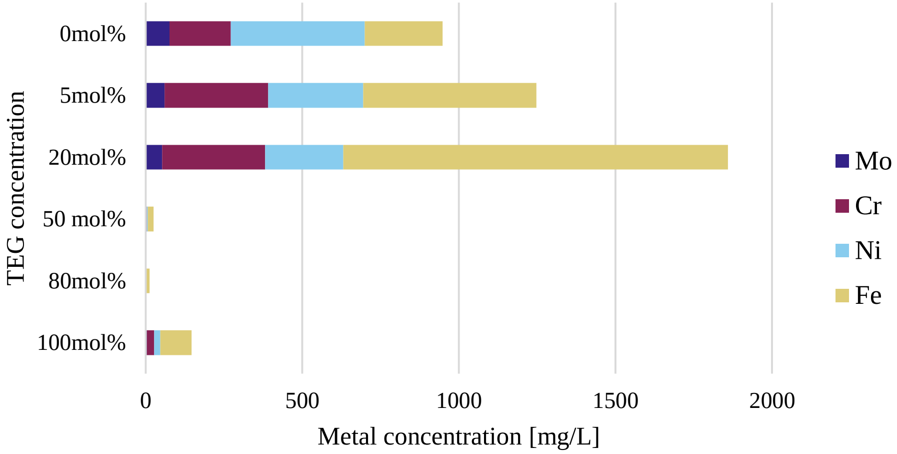

Figure 5.2.2: Metal concentrations in thermally degraded solutions (5 weeks, 135 °C) of loaded MEA (5 Molal, α=0.5) in changing TEG/water ratios.

c. A comparison of solutions with various loaded amines in water and solutions of the same loaded amines in 50mol% TEG in water is shown in Figure 5.2.3. In these solutions, exchanging water for TEG resulted in higher thermal degradation rates for the different amines included in the study. Form the metal concentrations found in these solutions, it is clear that the choice of amine strongly influences corrosion. The results for the amines in water compared with their corresponding solution with TEG and water shows that the presence of TEG has a strong effect on the corrosivity of the amine solutions. Similar to the trend seen for loaded MEA, the various loaded amines show significantly lowered metal content with TEG present. As an exception, the solutions with DMMEA are less affected by TEG, though why this is, is not clear. It is feasible that the concentration at which TEG results in the protective property that is seen for the other amines is higher for DMMEA.

d. The metal concentration in solutions of loaded MEA in some organic solvents is presented in Figure 5.2.4. In this experiment, thermal degradation experiments were conducted with MEA in a selection of organic solvents. The three glycols, MEG, DEG and TEG, were tested with loaded MEA without any water present. Loading MEA in pure NFM, however, resulted in phase separation. To avoid this, solutions of loaded MEA in mixtures of NFM and water (20:80 mol ratio) were studied. The three glycols all had a low metal content, while the NFM water mixture had a noticeably higher concentration of metals. This is probably due to the high water content of this solution.

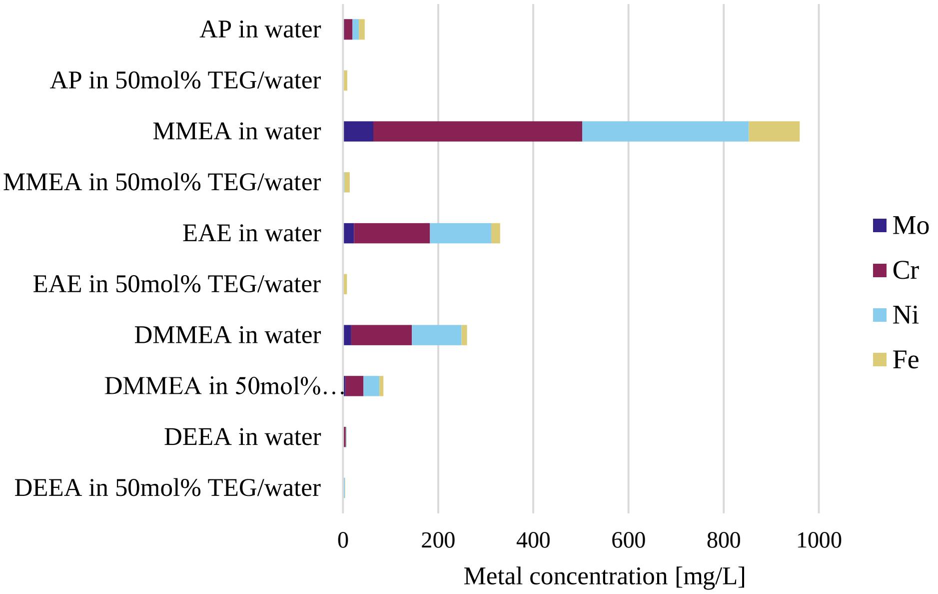

Figure 5.2.3: Comparison of metal concentrations in thermally degraded solutions (5-12 weeks, 135 °C) of loaded primary (5 Molal, α=0.5), secondary (5 Molal, α=0.5) and tertiary amines (5 Molal, α=0.3) in water and TEG/water mixtures thermally degraded for 5 weeks.

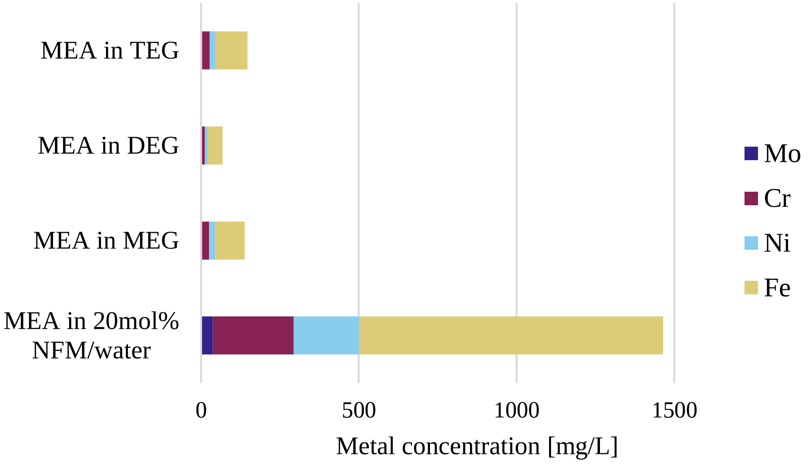

Figure 5.2.4: Metal concentrations in thermally degraded solutions (5 weeks, 135 °C) of loaded MEA (5 Molal, α=0.5) in a selection of organic solvents.

In these experiments, the water content was reduced by increasing the amine concentration and by introducing organic solvents as replacements for the water as diluents. Overall, the results from these corrosion tests are somewhat inconclusive. Experiments with increasing MEA concentrations showed that the amine concentration has an effect on the corrosion, though there is no clear trend. High concentrations of organic diluents gave very low metal concentrations for all solutions included in this study compared to their corresponding aqueous solutions. The choice of amine also affected the corrosion. It is still unclear what is causing these trends. More work should be done to better understand the effects observed.

References

(1) Eide-Haugmo, I. Environmental Impacts and Aspects of Absorbents Used for CO_2 Capture, 2011.

(2) Kittel, J.; Idem, R.; Gelowitz, D.; Tontiwachwuthikul, P.; Parrain, G.; Bonneau, A. Corrosion in MEA Units for CO_2 Capture: Pilot Plant Studies. *Energy Procedia* **2009**, 1 (1), 791–797. https://doi.org/10.1016/J.EGYPRO.2009.01.105.

(3) Fischer, K. B. Corrosion of Stainless and Carbon Steel in Aqueous Amine for CO_2 Capture, University of Texas at Austin, 2019.

(4) Kittel, J.; Gonzalez, S. Corrosion in CO_2 Post-Combustion Capture with Alkanolamines – a Review. *Oil Gas Sci. Technol.* **2014**, 69 (5), 915–929. https://doi.org/10.2516/OGST/2013161.

(5) Nielsen, R. B.; Lewis, K. R.; McCullough, J. G.; Hansen, D. a. Controlling Corrosion in Amine Treating Plants. *Proc. Laurence Reid Gas Cond. Conf.* **1995**.

(6) Cousins, A.; Ilyushechkin, A.; Pearson, P.; Cottrell, A.; Huang, S.; Feron, P. H. M. Corrosion Coupon Evaluation under Pilot-Scale CO_2 Capture Conditions at an Australian Coal-Fi Red Power Station. *Greenh. Gases Sci. Technol.* **2013**, 3 (3), 169–184. https://doi.org/10.1002/GHG.1341.

(7) DuPart, M. S.; Bacon, T. R.; Edwards, D. J. Understanding Corrosion in Alkanolamine Gas Treating Plants. *Hydrocarb. Process.* **1993**, 72 (5), 89–94.

(8) Campbell, K. L. S.; Zhao, Y.; Hall, J. J.; Williams, D. R. The Effect of CO_2-Loaded Amine Solvents on the Corrosion of a Carbon Steel Stripper. *Int. J.*

Greenh. Gas Control **2016**, 47, 376–385. https://doi.org/10.1016/J.IJGGC.2016.02.011.

(9) Sadeek, S. A.; Williams, D. R.; Sedransk Campbell, K. L. Using Sodium Thiosulphate for Carbon Steel Corrosion Protection against Monoethanolamine and 2-Amino-2-Methyl-1-Propanol. *Int. J. Greenh. Gas Control* **2018**, 78, 125–134. https://doi.org/10.1016/J.IJGGC.2018.08.004.

(10) Fytianos, G.; Ucar, S.; Grimstvedt, A.; Hyldbakk, A.; Svendsen, H. F.; Knuutila, H. K. Corrosion and Degradation in MEA Based Post-Combustion CO_2 Capture. *Int. J. Greenh. Gas Control* **2016**, 46, 48–56. https://doi.org/10.1016/J.IJGGC.2015.12.028.

(11) Kohl, A. L.; Nielsen, R. B. Alkanolamines for Hydrogen Sulfide and Carbon Dioxide Removal. In *Gas Purification*; 1997; pp 40–186. https://doi.org/10.1016/b978-088415220-0/50002-1.

(12) Davoudi, M.; Safadoust, A. R.; Akbar Mansoori, S. A.; Mottaghi, H. R. The Impurities Effect on Thermal Degradation and Corrosivity of Amine Solution in South Pars Gas Sweetening Plants. *J. Nat. Gas Sci. Eng.* **2014**, 19, 116–124. https://doi.org/10.1016/J.JNGSE.2014.05.001.

(13) Fytianos, G.; Grimstvedt, A.; Knuutila, H.; Svendsen, H. F. Effect of MEA's Degradation Products on Corrosion at CO_2 Capture Plants. In *Energy Procedia*; Elsevier Ltd, 2014; Vol. 63, pp 1869–1875. https://doi.org/10.1016/j.egypro.2014.11.195.

(14) Davoudi, M.; Heidari, Y.; Safadoost, A.; Samieirad, S. Chemical Injection Policy for Internal Corrosion Prevention of South Pars Sea-Pipeline: A Case Study. *J. Nat. Gas Sci. Eng.* **2014**, 21, 592–599. https://doi.org/10.1016/J.JNGSE.2014.09.017.

(15) Moser, P.; Schmidt, S.; Uerlings, R.; Sieder, G.; Titz, J. T.; Hahn, A.; Stoffregen, T. Material Testing for Future Commercial Post-Combustion Capture Plants - Results of the Testing Programme Conducted at the Niederaussem Pilot Plant. *Energy Procedia* **2011**, 4, 1317–1322. https://doi.org/10.1016/J.EGYPRO.2011.01.189.

(16) Fytianos, G.; Ucar, S.; Grimstvedt, A.; Svendsen, H. F.; Knuutila, H. Corrosion Evaluation of MEA Solutions by SEM-EDS, ICP-MS and XRD. In *Energy Procedia*; 2016; Vol. 86, pp 197–204. https://doi.org/10.1016/j.egypro.2016.01.020.

Chapter 6

The Impact of the Solvent on the Oxidative Stability of Amines

In this chapter, studies on the oxidative degradation of amine solvent systems with reduced water content are presented. An overview of some challenges met while studying the oxidative degradation of water-lean solvents will be presented in the first section. The second section contains a conference publication on the impact of amine concentration on the oxidative degradation of MEA. This has been published in Proceedings of the 16th Greenhouse Gas Control Technologies Conference in October 2022.

6.1 Challenges when Studying Water-Lean Solvent Systems

Few studies on the effect of the solvents on the oxidative stability of the amines are available in the literature. This includes the effect of organic cosolvents, but also the effect of the water itself. To contribute to an improved understanding in this regard, oxidative degradation experiments with water-lean amine solutions were conducted. There were, however, challenges along the way. This subchapter will go through some learnings from these.

Open batch-reactors were initially used for the oxidative degradation study of the water-lean solvents. Open batch-reactors have previously been used for oxidative degradation studies of aqueous amines.[1] In these setups, gas is sparged into a continuously heated and stirred solution in a jacketed glass reactor. The gas leaves the systems through a cooler connected to the reactor, and condensed liquids are returned to the reactors.

The initial experiments conducted included solutions of an amine (MEA or MMEA) in various ratios of water and organic diluents (TEG or NMP). An example of one of these experiments will be presented. The general for all of these experiments was volatility problems and inconsistent results.

Solutions of 5 Molal MEA in 0mol%, 50mol%, and 80mol% TEG in water were prepared gravimetrically. Iron sulfate (0.5 mmol/L) was added, and all solutions were loaded to 0.5 mol CO_2 per mol MEA. The solutions (200 mL) were heated to 60 °C in the glass reactors and the coolers were 5 °C. The gas sparged into the solutions consisted of 98% O_2 and 2% CO_2, and the gas flow was 60 mL/min. All experiments were conducted with two parallels. They lasted for three weeks and samples were taken regularly. The results presented here will be from amine titration following the procedure described in Chapter 3.

During the experiments, crystalline structures formed in the reactors with 80mol% TEG. This occurred in the connections between the reactor and the cooler and is depicted in Figure 6.1.1. An NMR analysis of the crystals was conducted, but as the crystals could not be isolated, identification was not achieved. In addition, liquid gathered in the coil at the top of the coolers, indicating volatility issues.

Figure 6.1.1: Crystalline structures formed in the connection between the reactor and cooler during the experiments with 5 Molal MEA in 80wt% TEG.

The results from these experiments are presented in Figure 6.1.2. Error bars in the plot represent deviation between the two parallels. Initially, two parallels of each solution with different ratios of TEG and water were run. The loss in alkalinity in the 0mol% and 50mol% TEG solutions during the experiment was quite similar, while it was higher for the 80mol% solution. Due to the similarities in the results, in addition to the high standard deviation between the parallels of the 50mol% solution, the

50mol% solution was then rerun. Surprisingly, the results were quite different from the original run and had once again higher deviations than the other solutions.

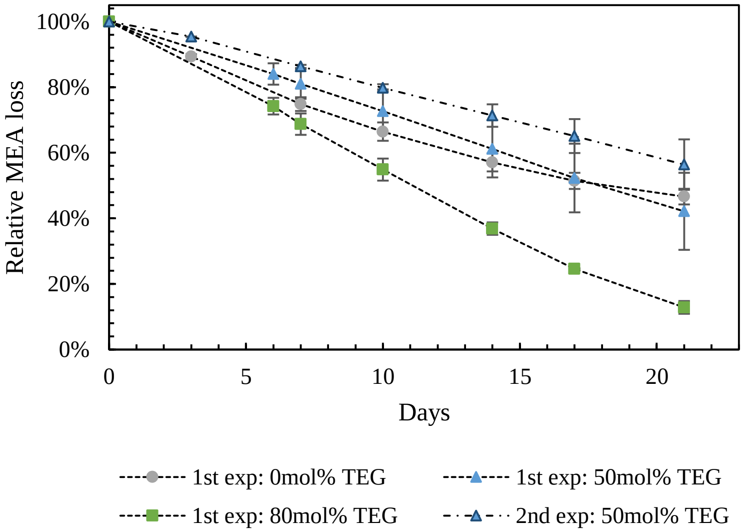

Figure 6.1.2: Results from an oxidative degradation experiment with MEA (5 M, α=0.5, 60 °C) in various ratios of TEG in water, conducted in an open set-up.

It was hard to draw any conclusions from these results, but it opens for reflection over challenges arising from the change in solvent composition on the experimental setup, procedure, and analysis. First, as observed in these experiments, the volatility of the solvents becomes an issue, even with the coolers in place. Volatility is considered a problem for water-lean solvent systems in general, where solvent losses is an expected drawback.[2] As seen from the liquid collecting in the coolers, it is also a problem in these experiments. How it is affecting the results, however, is unclear.

A way of handling this is by changing the setup to more closed-off systems. In the continued work, a semi-open system as described in Chapter 3, was employed. In this semi-open setup, the volatility of the solvent will be decreased due to the gas being recirculated. A drawback is that the potential accumulation of components in the gas phase could affect the degradation. This is not necessarily a problem, as long as the intent is to study trends and effects of the solvent systems and not to mirror what would happen at a full-scale plant.

Another factor to be aware of is the stability of the cosolvent itself. It is possible that organic solvents chosen as cosolvents also have a sensitivity towards oxidizing species and elevated temperatures. TEG is an example of this, as will be seen in the following chapters. If the cosolvent can degrade, degradation products could influence the overall degradation and operability of the system. This is not necessarily a problem for studying the degradation of the mixed solvent, it will just make it more complex. Moreover, it would require some knowledge about the degradation of the cosolvent in addition to the development of methods for monitoring the major components in the solvent systems.

A last consideration is the effect of the potentially increased viscosity of the systems. This would likely result in mass transfer limitations for the oxygen from the gas bubbles to the solvents.[3] This is especially important to be aware of when looking into the effect of changing the oxygen and temperature as both parameters are linked to the viscosity. In the semi-open batch reactors efforts were made to overcome this issue. This was done by introducing vigorous stirring, increased bubbling, and recycling of the gas to increase the number of bubbles without increasing the water/solvent loss in the system. To be certain of removing mass transfer limitations, a cyclic system, where the gas and liquid are contacted in packing, could be used.

References

(1) Buvik, V.; Vevelstad, S. J.; Brakstad, O. G.; Knuutila, H. K. Stability of Structurally Varied Aqueous Amines for CO_2 Capture. *Ind. Eng. Chem. Res* **2021**, 60, 5638. https://doi.org/10.1021/acs.iecr.1c00502.

(2) Heldebrant, D. J.; Koech, P. K.; Glezakou, V.-A.; Rousseau, R.; Malhotra, D.; Cantu, D. C. Water-Lean Solvents for Post-Combustion CO_2 Capture: Fundamentals, Uncertainties, Opportunities, and Outlook. *Chem. Rev.* **2017**, 117 (14), 9594. https://doi.org/10.1021/acs.chemrev.6b00768.

(3) Braakhuis, L.; Knuutila, H. K. Predicting Solvent Degradation in Absorption-Based CO_2 Capture from Industrial Flue Gases. *Chem. Eng. Sci.* **2023**, 279, 118940. https://doi.org/10.1016/j.ces.2023.118940.

6.2 An Experimental Assessment on the Impact of Amine Concentration on the Oxidative Degradation of Amines

Conference publication:

Høisæter, Karen K., Nordberg, Andrea E., Buvik, Vanja, Vevelstad, Solrun J., Grimstvedt, Andreas & Knuutila, Hanna K. An Experimental Assessment on the Impact of Amine Concentration on the Oxidative Degradation of Amines. Proceedings of the 16th Greenhouse Gas Control Technologies Conference (GHGT-16) 23-24 Oct 2022.

An Experimental Assessment on the Impact of Amine Concentration on the Oxidative Degradation of Amines

Karen K. Høisæter[a], Andrea E. Nordberg[a], Vanja Buvik[a], Solrun J. Vevelstad[b], Andreas Grimstvedt[b], Hanna K. Knuutila[a]*

[a] Department of Chemical Engineering, NTNU, NO-7491 Trondheim, Norway

[b] SINTEF Industry, P.O.Box 4760 Torgarden, NO-7465, Norway

* Corresponding author: hanna.knuutila@ntnu.no

Abstract

An important aspect when developing new solvent systems for CO_2 capture is to understand how the change in solvent composition influence the degradation. In this work, experimental data from the oxidative degradation of MEA with increasing amine concentration was studied. By varying the concentration of the CO_2, MEA, and water, we investigated the impact of the solvent composition on the oxidative degradation. To this end, two series of experiments were conducted. In the first series, the absolute amount of CO_2 was kept constant while the MEA/water ratio was varied. Both the MEA loss and degradation product formation decreased suggesting that the stability of MEA increases with increased amine concentrations. In the second series, the amine concentrations were varied while the loading is kept constant, i.e. the concentration of CO_2 increased with the increasing amine concentration. From these experiments, trends seen from the measured MEA loss and degradation product formation did not correspond. The MEA loss showed no clear trend. Degradation product formation, however, decreased with increasing MEA concentration, indicating that there are different mechanisms taking place in the different solvent compositions.

Keywords

Oxidative; Degradation; Amine; MEA; PCCC; LCMS

1 Introduction

Post combustion CO_2 capture is an essential measure in reducing the greenhouse effect. Chemical absorption utilizing amines is a mature technology within this field.[1,2] In this process, CO_2 is separated from the flue gas through selective absorption with an amine solvent. The chemical reaction taking place results in the formation of carbamates, bicarbonates, and carbonates. The CO_2 is released, and the solvent regenerated, with increasing temperatures in a desorber.[3] This process step is very energy intensive, and the extra cost this entails is one of the main obstacles for this process.[4]

Another challenge for this technology is the issue of solvent degradation. Flue gas usually contains multiple components that, together with increased temperatures, influence the lifetime of the solvent amines.[5] The compounds formed during the solvent degradation cause issues for the capture plant performance, such as corrosion, fouling, increased viscosity, and possible emissions of hazardous compounds.[6–8] Additionally, treatment of degraded solvent is costly and non-eco-friendly.

Oxidative degradation of the amines occurs when oxygen is brought into contact with the solvent, through the flue gas in the form of O_2, SO_X, or NO_X. The primary oxidation reactions form oxidized fragments of the amine in the form of small organic acids and NH_3.[9] The acids are mainly formic, acetic, and oxalic acid. The acids formed are largely held responsible for corrosion and fouling in the pilot plants. From here, most secondary degradation products are formed through reactions between the primary degradation products and the solvent amine.

To minimize the problems accompanying both the energy intensity of the process and the solvent degradation, searching for improved solvent systems with favorable kinetics is important. In recent years, utilizing water-lean solvents has been proposed in literature as an option to reduce the energy needed for solvent regeneration.[10] The common denominator for water-lean solvents is a reduction in the water content. The idea behind this is to reduce the energy required in the energy intensive solvent regeneration step by removing water. There is little data available on how the change in solvent composition influences the stability of the amines.[11] Understanding the chemistry behind this process will be very helpful in the endeavor to develop new, or improve existing, solvent systems.[4,12]

This work will study experimental data from the oxidative degradation of amines with increasing concentrations. By varying the concentration of the CO_2, amines, and water, we looked into the impact of the solvent composition on oxidative degradation. Monoethanolamine (MEA) was chosen in this study as it degrades more readily than many other amines. Moreover, the degradation products of MEA are also mostly known, and analytical methods are available. Other, more stable primary and secondary amines are expected to degrade through similar mechanisms. Therefore, studying MEA allows for a faster gathering of data. The tendencies which are found for MEA can then be extrapolated to other amine systems.

2 Experimental

2.1 Chemicals

The chemicals used to prepare the solutions in this study were monoethanolamine (MEA, CAS: 141-43-5, purity ≥ 99.0%) and ferrous sulfate heptahydrate ($FeSO_4 \cdot 7H_2O$, CAS: 7782-63-0, purity ≥ 99.0%). Both were purchased from Sigma-Aldrich Norway. Oxygen (O_2, N5.0) and carbon dioxide (CO_2, N5.0) were purchased from AGA. The deionized (DI) water was obtained from the local water purifying system at NTNU. All solutions were prepared gravimetrically.

2.2 Oxidative degradation experiments

In this study, the effect of the concentration of MEA and CO_2 on the oxidative stability of MEA was studied. This was done through two series of experiments. In the first series of experiments, solutions with aqueous MEA in varying concentrations and a constant absolute CO_2 concentration (2 mol CO_2/kg unloaded solution) were prepared. The prepared solutions contained 30wt%, 50wt% and 70wt% MEA. In the second series, aqueous MEA solutions with changing amine concentration and constant loadings ($\alpha = 0.4$) were prepared. All solutions contained 0.5 mM iron sulfate ($FeSO_4 \cdot H_2O$).

The solutions were oxidatively degraded in a custom-made open-batch setup simulating absorber conditions. The solvent was heated up in glass reactors placed in heating mantles with integrated magnetic stirrers. The liquid temperature was maintained at 75 °C, while the Graham condensers were cooled to 5 °C. A continuous flow of O_2, CO_2 and N_2 was sparged into the constantly stirred solution through gas distribution tubes of porosity grade 1. The oxygen percentage was 6% of the total gas flow, and the CO_2 content was adjusted to maintain the wanted loading. For each experiment, the glass reactors were filled up with 1 L of the prepared solvent. Each experiment ran for one week, and sampling was done regularly through a sampling point in the glass reactors.

2.3 Analytical methods

Total alkalinity measurements were used to estimate the amine concentration. This was done by titration with sulfuric acid (H_2SO_4, 0.1 M) as described by Ma’mun et al.[13] The CO_2 concentration was monitored with *Total Inorganic Carbon* (TIC) analysis. For this, a Shimazu TOC-L_{CPH} in TIC mode was used. From these measurements, the loading could be monitored, and a more accurate amine concentration was found by correcting for water lost to evaporation and excluding CO_2 present in the solutions.

Liquid Chromatography-Mass Spectroscopy (LC-MS) was used to analyze the concentration of MEA and degradation products. All samples were analyzed on a UHPLC Agilent 1290 Infinity System equipped with an Agilent 6490 Triple Quadrupole detector. The analyte separation used an Ascentis Express Phenyl-Hexyl, 2.7 m HPLC Column and a Discovery HS F5 HPLC Column, both from Sigma-Aldrich. An isotope-labelled standard was used for quantification. The components that were analyzed are presented in Table A1 in the Appendix.

3 Results

This study investigated the effect of the concentration of MEA and CO_2 in loaded aqueous MEA. This was done through two sets of experiments. In the first set, the MEA concentration was varied, and the absolute amount of CO_2 was kept constant. In the second set, the MEA concentration was varied, and the loading was kept constant. The oxidative degradation of MEA was quantified by LC-MS analysis measuring the concentration of MEA remaining in the solution and the degradation products formed. Not all the experiments had a duplicate, but for the ones that did, the average value is represented in the graph. Standard deviation is also given for the series in question. The experiments without a duplicate will be clearly marked in the figures.

Figure 1 shows the results from the oxidative degradation experiments with increasing concentrations of MEA. All solutions were loaded to 2 mol CO_2 per kg unloaded solution. This concentration corresponds with the amount needed to load the 30wt% solution to 0.4 mol CO_2 per mol MEA. After 7 days, it appeared that the increase in MEA concentration resulted in a decrease in the degradation rate of MEA. At higher MEA concentrations, the viscosity of the solution increases. It could therefore be tempting to assume that this increase causes less oxygen to be available for the oxidation reaction. However, Buvik et al.[14] have performed oxygen solubility measurements comparing MEA in varying concentrations and found that the MEA concentration does not affect the oxygen solubility. It is, therefore, likely that there is another parameter or effect that influences the stability of MEA. It should be noted that due to the short time span of the experiment, the trend observed is somewhat uncertain.

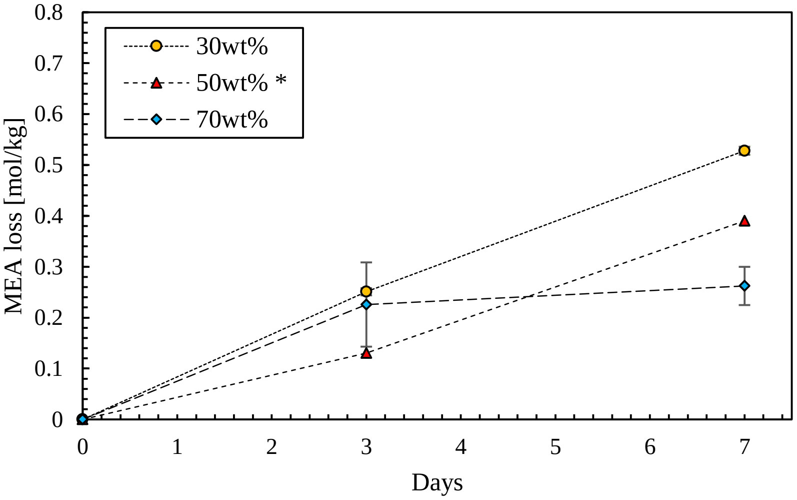

*Figure 1: MEA loss from oxidative degradation experiments with increasing MEA concentration and constant CO_2 concentrations (2 mol CO_2/kg unloaded solution). The error bars represent the standard deviations between the duplicate experiments. *No duplicate*

The results from the oxidative degradation experiments of solutions with increasing MEA concentrations and constant loading is presented in Figure 2. These results do not show any clear trends with the increasing MEA and CO_2 concentrations. Increased CO_2 concentrations have been found to result in what is known as the "salting out" effect.[14] This effect describes a solvent's reduced ability to dissolve oxygen caused by the presence of ionic species in the solution.[15] With this in mind, one would expect the oxygen solubility, and therefore also the degradation rates, to go down with the increasing CO_2 concentration. This is not what is observed. The lack of a clear effect could be because the CO_2 concentration does not influence the degradation rates – maybe due to the constant mol ratio between MEA and CO_2 – or there might be more than one effect taking place.

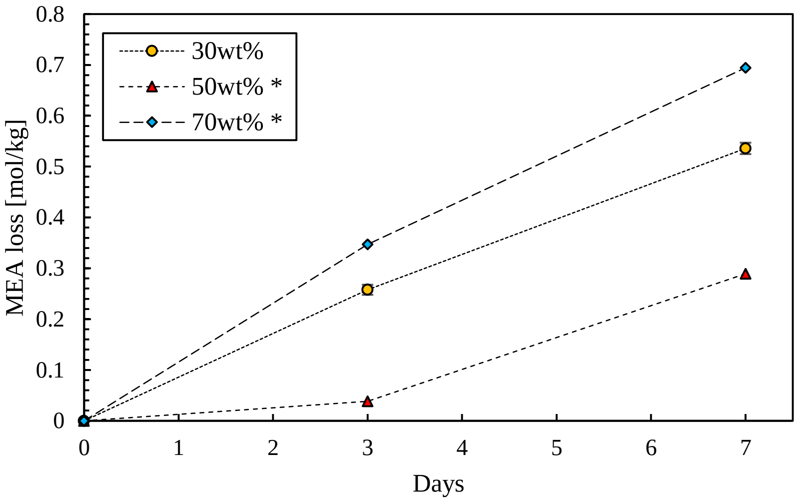

*Figure 2: MEA loss from oxidative degradation experiments of loaded aqueous MEA (α = 0.4) with increasing MEA concentrations. The error bars represent the standard deviations between the duplicate experiments. *No duplicate*

Trends were hard to decern from MEA loss alone due to the short time span of the experiments. Examining the degradation products formed in the two experiment series can help make it clearer. All common degradation products of MEA were analyzed, see Table A1 in the Appendix. Degradation products with concentrations higher than 1.5 mmol/kg were defined as the main degradation products in these experiments. These were ammonia, *N*-(2-hydroxyethyl)-glycine (HeGly), *N*-(2-hydroxyethyl)-formamide (HEF), *N*-(2-hydroxyethyl)-imidazole (HEI), (*N*-(2-hydroxyethyl)-2-(hydroxyethyl)-amino)acetamide (HEHEAA), and formic acid. Figure 3 shows the main oxidative degradation products, apart from ammonia, formed in the experiment with constant CO_2 concentration. Comparing the degradation products formed in these experiments to their corresponding degradation rates, presented in Figure 1, seems to be in accordance. At lower MEA concentrations, higher concentrations of the main degradation products are formed. These then decrease with increasing MEA concentration. This is also the case for the ammonia formation, which decreases from around 70 mmol/kg to below 10 mmol/kg with the increase in MEA from 30wt% to 70wt%. An interesting point to notice here is the behavior of HeGly and HEHEAA. HeGly has a concentration peak at 50wt% MEA, while HEHEAA is the only component that increases steadily with increasing MEA concentration.

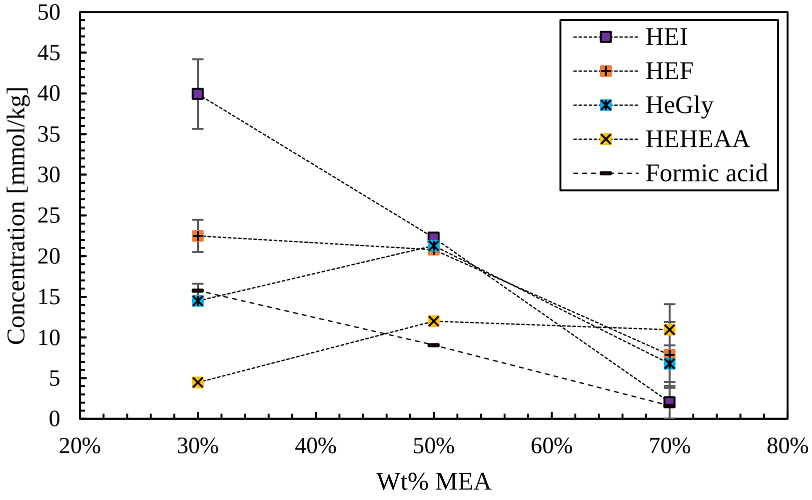

Figure 3: Selection of oxidative degradation products formed after 7 days for aqueous loaded MEA solutions (2 mol CO_2/kg unloaded solution).

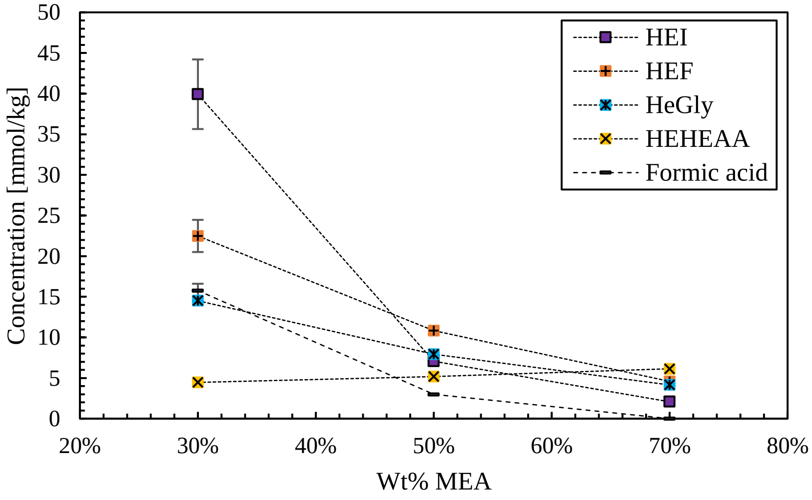

Figure 4: Selection of oxidative degradation products formed after 7 days for aqueous loaded MEA solutions ($\alpha = 0.4$).

Figure 4 shows the main oxidative degradation products formed in the experiments with constant loading. When comparing these with the degradation trends, presented in Figure 2, something unexpected can be observed. Even though the MEA loss was highest for the 70wt% MEA solution, the main oxidative degradation products are only formed in low concentrations here. There is also little ammonia present at high MEA concentrations, measuring at 73 mmol/kg, 140 mmol/kg, and 7 mmol/kg for 30wt%, 50wt%, and 70wt%, respectively. Of the other known oxidative degradation products that were analyzed, only MEA-urea was found in marginally greater amounts in the 70wt% MEA than in the 30wt% or 50wt% solutions.

Looking only at the degradation products formed, one would expect that the stability of MEA decreases with increased MEA and CO_2 concentration. Since this is not the case for the MEA loss, something else must be happening. Figure 5 highlights this by comparing the MEA loss with the total amount of nitrogen detected in the degradation products in the 30wt% and 70wt% MEA solutions. A possible explanation is that higher concentrations of ammonia is formed in the 70wt% MEA than what is measured, but that this leaves the open system due to a possible lower solubility. Alternatively, the high MEA concentration might give rise to the formation of unknown degradation products which are not looked for in the analysis. The actual reason for this discrepancy is unfortunately not known. Overall, these results show that there are most probably some unknown mechanisms taking place at higher amine concentrations. Further studies should be conducted to enable a better understanding of these effects.

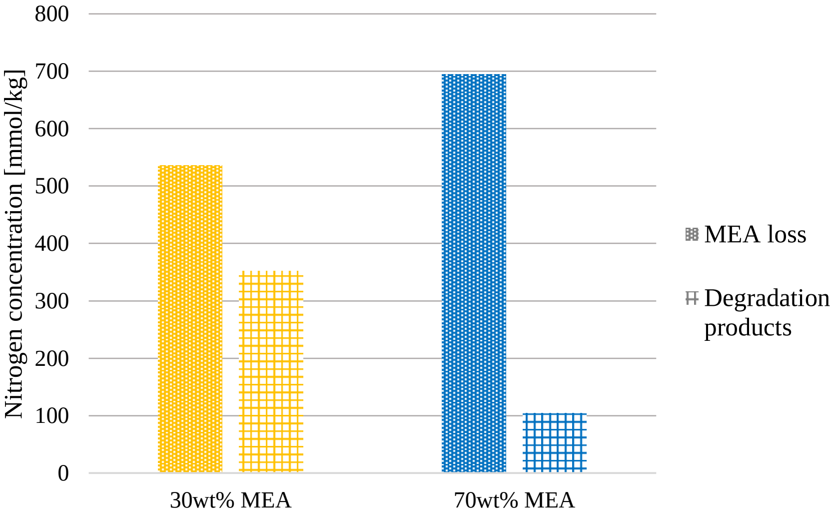

Figure 5: Comparison of MEA loss and nitrogen present in degradation products detected in oxidatively degraded solutions of loaded aqueous MEA (2 mol CO_2/kg unloaded solution) on day 7.

4 Conclusion

Today, high cost is associated with many of the existing chemical absorption systems for CO_2 capture. One of the main problems is solvent degradation. Finding better, more stable solvents is therefore important on the road towards making this technology interesting for the industry to implement. In this endeavor, understanding the effect of the different parameters of the solvent system is important.

In this study, oxidative degradation experiments were conducted to investigate the effect of solvent composition on the amine stability. The concentration of MEA and CO_2 was varied to determine their influence. Increased MEA concentrations with a constant CO_2 concentration seemed to result in a decrease in MEA loss, as well as a decrease in oxidative degradation product formation. It is not clear which property of the solvent gave this effect.

Increased MEA concentrations with constant loading gave divided results. On one hand, there was no clear trend seen from the MEA loss. On the other hand, the formation of known oxidative degradation products clearly decreased. The reason for the discrepancy between these findings is unknown. All experiments conducted had a short time span. Extending the experimental time can be a good way of reducing uncertainty and gaining better insights into these systems.

Acknowledgements

The LAUNCH project (Project No. 299662) is co-funded by the ERA-NET Accelerating CCS Technologies initiative, which supports the delivery of safe and cost-effective carbon capture, utilization, and storage. The governments of each participating country have contributed funding through the ACT2 initiative.

Appendix A

Table A1: Analysed degradation products with their corresponding abbreviations and CAS numbers.

Compound	*Abbreviation*	*CAS number*
Acetic acid	-	64-19-7
Ammonia	-	7664-41-7
Bicine	-	150-25-4
***N,N'*-Bis(2-hydroxyethyl)oxamide**	BHEOX	1871-89-2

Butyric acid	-	107-92-6
3-Hydoxybutyric acid	3-OH Butyric Acid	300-85-6
Diethanolamine	DEA	109-89-7
Diethylamine	-	109-89-7
Dimethylamine	-	124-40-3
Dipropylamine	-	142-84-7
Ethylamine	-	75-04-7
Ethylmethylamine	-	624-78-2
Formic acid	-	71-47-6
Glycine	-	56-40-6
Glycolic acid	-	79-14-1
Glyoxylic acid	-	298-12-4
_N_-(2-Hydroxyethyl)-acetamide	HEA	142−26-7
_N_-(2-Hydroxyethyl)-2-imidazolidione	HEIA	3699-54-5
2-(2-Hydroxyethyl-amino)ethanol	HEEDA	111-41-1
_N_-(2-Hydroxyethyl)-formamide	HEF	693−06-1
_N_-(2-Hydroxyethyl)-glycine	HeGly	5835−28-9
(_N_-(2-Hydroxyethyl)-2-(hydroxyethyl)-amino)acetamide	HEHEAA	144236-39-5
_N_-(2-Hydroxyethyl)-imidazole	HEI	1615−14-1
4-(2-Hydroxyethyl)-2-piperazinone	HEPO	23936-04-1
1-(2-Hydroxyethyl)-2-piperazinone	1HEPO	59702-23-7
2-Hydroxy-_N_-(2-hydroxyethyl)-acetamide	HHEA	3586-25-2
Isobutyric acid	-	79-31-2
Lactic acid	-	50-21-5
Monoethanolamine	MEA	141-43-5

***N,N’*-Bis(2-hydroxyethyl)-urea**	MEA-urea	15438-70-7
Methylamine	-	74-89-5
2-(Methyl)-aminoethanol	MMEA	109-83-1
3-Methylpyridine	3-Mpy	108-99-6
Morpholine	-	110-91-8
2-Oxazolidinone	OZD	497−25-6
Piperazine	PZ	110-85-0
Propionic acid	-	79-09-4
3-Hydroxypropionic acid	3-OH Propionic acid	503-66-2
Propylamine	-	107-10-8

References

(1) Bui, M.; Adjiman, C. S.; Bardow, A.; Anthony, E. J.; Boston, A.; Brown, S.; Fennell, P. S.; Fuss, S.; Galindo, A.; Hackett, L. A.; Hallett, J. P.; Herzog, H. J.; Jackson, G.; Kemper, J.; Krevor, S.; Maitland, G. C.; Matuszewski, M.; Metcalfe, I. S.; Petit, C.; Puxty, G.; Reimer, J.; Reiner, D. M.; Rubin, E. S.; Scott, S. A.; Shah, N.; Smit, B.; Trusler, J. P. M.; Webley, P.; Wilcox, J.; Mac Dowell, N. Carbon Capture and Storage (CCS): The Way Forward. *Energy Environ. Sci*. **2018**, 11 (5), 1062–1176. https://doi.org/10.1039/c7ee02342a.

(2) Rochelle, G. T. Amine Scrubbing for CO_2 Capture. Science. 2009, pp 1652–1654. https://doi.org/10.1126/science.1176731.

(3) Notz, R. J.; Tönnies, I.; McCann, N.; Scheffknecht, G.; Hasse, H. CO_2 Capture for Fossil Fuel-Fired Power Plants. *Chem. Eng. Technol.* **2011**, 34 (2), 163–172. https://doi.org/10.1002/CEAT.201000491.

(4) Aaron, D.; Tsouris, C. Separation of CO_2 from Flue Gas: A Review. *Sep. Sci. Technol.* **2005**, 40, 321–348. https://doi.org/10.1081/SS-200042244.

(5) Sexton, A. J.; Rochelle, G. T. Catalysts and Inhibitors for MEA Oxidation. In *Energy Procedia*; 2009; Vol. 1, pp 1179–1185. https://doi.org/10.1016/j.egypro.2009.01.155.

(6) Mazari, S. A.; Si Ali, B.; Jan, B. M.; Saeed, I. M.; Nizamuddin, S. An Overview of Solvent Management and Emissions of Amine-Based CO_2 Capture Technology. *Int. J. Greenh. Gas Control* **2015**, 34, 129–140. https://doi.org/10.1016/j.ijggc.2014.12.017.

(7) Martin, S.; Lepaumier, H.; Picq, D.; Kittel, J.; de Bruin, T.; Faraj, A.; Carrette, P.-L. L. New Amines for CO_2 Capture. IV. Degradation, Corrosion, and Quantitative Structure Property Relationship Model. *Ind. Eng. Chem. Res.* **2012**, 51 (18), 6283–6289. https://doi.org/10.1021/ie2029877.

(8) Kennard, M. L.; Melserv, A. Mechanisms and Kinetics of Diethanolamine Degradation. *Ind. Eng. Chem. Fundam* **1985**, 24, 129–140.

(9) Da Silva, E. F.; Lepaumier, H.; Grimstvedt, A.; Vevelstad, S. J.; Einbu, A.; Vernstad, K.; Svendsen, H. F.; Zahlsen, K. Understanding 2-Ethanolamine Degradation in Postcombustion CO_2 Capture. *Ind. Eng. Chem. Res*. **2012**, 51, 13329–13338. https://doi.org/10.1021/ie300718a.

(10) Heldebrant, D. J.; Koech, P. K.; Rousseau, R.; Glezakou, V. A.; Cantu, D.; Malhotra, D.; Zheng, F.; Whyatt, G.; Freeman, C. J.; Bearden, M. D. Are Water-Lean Solvent Systems Viable for Post-Combustion CO_2 Capture? In *Energy Procedia*; Elsevier Ltd, 2017; Vol. 114, pp 756–763. https://doi.org/10.1016/j.egypro.2017.03.1218.

(11) Wanderley, R. R.; Pinto, D. D. D.; Knuutila, H. K. From Hybrid Solvents to Water-Lean Solvents – A Critical and Historical Review. *Sep. Purif. Technol.* **2021**, 260, 1383–5866. https://doi.org/10.1016/j.seppur.2020.118193.

(12) Da Silva, E. F.; Svendsen, H. F. Computational Chemistry Study of Reactions, Equilibrium and Kinetics of Chemical CO_2 Absorption. *Int. J. Greenh. Gas Control* **2007**, 1 (2), 151–157. https://doi.org/10.1016/S1750-5836(07)00022-9.

(13) Ma'mun, S.; Jakobsen, J. P.; Svendsen, H. F.; Juliussen, O. Experimental and Modeling Study of the Solubility of Carbon Dioxide in Aqueous 30 Mass% 2-((2-Aminoethyl)Amino)Ethanol Solution. *Ind. Eng. Chem. Res.* **2006**, 44, 8, 2505–2512. https://doi.org/10.1021/ie0505209.

(14) Buvik, V.; Bernhardsen, I. M.; Figueiredo, R. V.; Vevelstad, S. J.; Goetheer, E.; van Os, P.; Knuutila, H. K. Measurement and Prediction of Oxygen Solubility in Post-Combustion CO_2 Capture Solvents. *Int. J. Greenh. Gas Control* **2021**, 104, 103205. https://doi.org/10.1016/J.IJGGC.2020.103205.

(15) Battino, R.; Clever, H. L. The Solubility of Gases in Liquids. *Chem. Rev.* **1966**, 66 (4), 395. https://doi.org/10.1021/cr60242a003.

Chapter 7

Analytical Tools for Monitoring Glycol Degradation

The following chapter contains a manuscript on analytical tools for monitoring glycol degradation. Methods for quantification of glycols by GC-FID and quantitative ^{13}C NMR, and for quantification of small organic acids by HPLC-UV and HSS analysis are described. Oxidatively and thermally degraded TEG samples are studied, and some observations on color changes and sample stability are discussed.

Manuscript:

Høisæter, Karen K.; Buvik, Vanja; Vevelstad, Solrun; & Knuutila, Hanna K. Analytical Tools for Monitoring Glycol Degradation. *To be submitted*.

Analytical Tools for Monitoring Glycol Degradation

Karen K. Høisæter[a], Vanja Buvik[a], Solrun J. Vevelstad[b], Hanna K. Knuutila[a]*

[a] Department of Chemical Engineering, NTNU, NO-7491 Trondheim, Norway

[b] SINTEF Industry, P.O.Box 4760 Torgarden, NO-7465, Norway

* Corresponding author: hanna.knuutila@ntnu.no

Abstract

This paper focuses on investigating possible methods for monitoring glycol degradation with solvent analysis. Oxidatively and thermally degraded triethylene glycol (TEG) samples were studied. Methods for quantifying TEG, and for quantifying some degradation products (small glycols and acids), were developed. Two independent methods were chosen for each component group to validate the analytical methods. The glycols were successfully quantified with gas chromatography coupled with flame ionization detection (GC-FID) and with quantitative carbon-13 nuclear magnetic resonance (^{13}C NMR) spectroscopy. The acidic degradation compounds were successfully quantified with high-performance liquid chromatography coupled with ultraviolet detection (HPLC-UV) and heat-stable salt (HSS) analysis. The analytical techniques were used to study thermally degraded TEG. The thermal stability of TEG decreased with addition of impurities, especially formic acid. Some color changes were observed, but it was not linked with amount of TEG degraded. Finally, it was found that TEG samples have limited stability, even if stored cold.

Keywords

Gas dehydration, oxidative degradation, thermal degradation, GC, NMR, HPLC, HSS

1 Introduction

Raw natural gas must be processed to remove impurities to achieve a pipeline-quality gas. An important step in this regard is removal of water. A mature technology used to achieve this is dehydration with glycols.[1] Glycols are hygroscopic, non-corrosive, non-toxic, their regeneration is easy, and they absorb little of the hydrocarbons from the gas.[2] Triethylene glycol (TEG) is the most common glycol used for gas dehydration due to its low cost and relatively low vapor pressure.

In the gas dehydration process, the wet gas enters an absorption column and flows counter current to TEG, which will absorb the water content in the gas. The dried gas leaves the column at the top, while the rich TEG is pumped to separate units where water, as well as other contaminants, are removed. The regenerated TEG is then pumped back and reused in the absorption column. During this process, TEG can undergo degradation reactions caused by the presence of oxygen and high temperatures.[2] This can cause operational issues, such as foaming, corrosion, and performance loss.[1] To avoid these issues, the process is often designed so, that temperatures above the cracking temperature of the glycol are avoided (204 °C)[3].

The degradation of a solvent can be monitored by quantifying the solvent or by measuring the buildup of degradation compounds in the solution. Though the possibility of glycol degradation is a well-known issue, there is, however, not much published on the chemistry happening during the degradation of TEG. This makes the task of monitoring this solvent a challenge. Industrially, dehydration capacity is often used as an indicator of degradation.

In degradation studies of TEG, no analytical methods for quantifying the glycol are published. The degradation of TEG has been described by Forster[4], who proposes formation of smaller fragments formed both through oxidative and thermal degradation. Examples of these are ethylene glycol (MEG) and diethylene glycol (DEG). No analytical technique for the quantification of these is given in the literature on glycol degradation, but there are method descriptions in other fields.[5–8]

The glycols are known to form small organic acids as they oxidatively degrade. In the literature, formation of formic, acetic, glycolic, glyoxylic, and oxalic acid during the oxidative degradation of MEG has been reported.[9–12] These acids have been quantified using ion chromatography (IC)[9,11] or ion chromatography exclusion (ICE)[9]. Measuring the pH of the degraded solutions has also been proposed as a possibility to quantify the acidic components in the solution.[13] This option, however, has been found to not correlate well with actual acid concentration.[9]

Discoloration is often used as an indicator of degradation. Experiments done by AlHarooni et al.[14] indicate that increased degradation results in increased darkening of MEG. Glycols are initially clear, but as the solvents turn browner in color with use, reduced dehydration capacity is observed.[15] TEG with prolonged operation time often looks black and has an increased viscosity. Forster[4] reports finding contaminants in their spent TEG, originating from the natural gas being treated.

In this paper, analyses of glycols (TEG, DEG, and MEG) and organic acids (formic, glycolic, oxalic, glyoxylic, and acetic acid) are presented. Each of the two compound groups are analyzed with two independent methods. The glycols are quantified with gas chromatography coupled with flame ionization detection (GC-FID) and quantitative ^{13}C nuclear magnetic resonance spectroscopy (carbon-13 NMR). The acids are quantified with high-performance liquid chromatography coupled with ultraviolet detection (HPLC-UV) and heat stable salts (HSS) analysis. The analytical methods are first tested on samples from an oxidative degradation experiment of pure TEG. Then, thermal degradation experiments have been conducted, and the results from these are presented. Lastly, color changes and sample stability are shortly discussed.

2 Materials and Methods

2.1 Chemicals

The chemicals used in this work are listed in Table 1. All solutions were prepared gravimetrically. Deionized (DI) water was acquired from the water purifying system at NTNU, and MilliPore water from an ICW-3000 Millipore purification system. All chemicals were purchased from Sigma-Aldrich Norway AS/Merck Life Sciences. Oxygen (O_2, N5.0) was purchased from AGA.

Table 1: Overview of chemicals used in this work.

Chemical name (Abbreviation)	Structure	CAS-number	% Purity
Triethylene glycol (TEG)	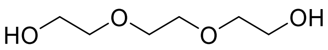	112-27-6	> 99
Diethylene glycol (DEG)	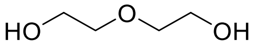	111-46-6	> 99
Ethylene glycol (MEG)	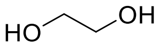	107-21-1	> 99

Acetic acid	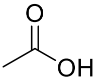	64-19-7	> 99.8
Formic acid	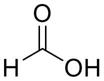	64-18-6	> 98
Glycolic acid	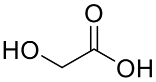	79-14-1	99
Glyoxylic acid	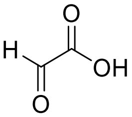	298-12-4	50wt% in water
Oxalic acid	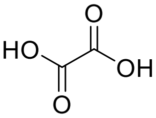	144-62-7	> 99
Methanol (MeOH)	—OH	67-56-1	Hypergrade for LC-MS
Acetonitrile (AcN)	$H_3C-C\equiv N$	75-05-8	Anhydrous 99.8%
Tris(trimethylsilyl)-phosphine (TMSP)	$P(SiMe_3)_3$	15573-38-3	95%

2.2 Analytical Methods

2.2.1 Gas Chromatography Coupled with Flame Ionization Detection (GC-FID)

One of the techniques used in this study to quantify the three glycols, TEG, DEG, and MEG, was GC-FID. An Agilent 7890A equipped with a DB-WAX Ultra Inert fused silica column (length 30 m, inner diameter 0.25mm, film thickness 0.25 µm) was used, and the injection volume was 10 µL with a 1:20 split ratio. The following temperature gradient was used to elute the three glycols: hold at 100 °C for 1 min, increase to 250 °C in increments of 10 °C/min and hold at 250 °C for 4 min. The carrier gas was helium, and methanol was used to dilute samples to contain <1000 ppm glycol. The limit of detection (LOD) and limit of quantification (LOQ) was defined as three times signal-to-noise (3·S/N) and 10·S/N. For all three compounds, linear calibration curves were obtained with R^2 of >0.999. Retention times, LOD, LOQ, and the linear calibration range for MEG, DEG and TEG are given in Table 2. The high LOD, LOQ, and start concentration of the calibration range for TEG were caused by column bleed.

Table 2: Retention time, LOD, LOQ, and linear calibration range for MEG, DEG and TEG analyzed with GC-FID.

Chemical	Retention time [s]	LOD [ppm]	LOQ [ppm]	Linear calibration range [ppm]
MEG	5.5	1.5	4.5	5-1000
DEG	8.9	2.0	5.1	5-1000
TEG	12.2	34	47	50-1000

Before the quantification of laboratory degraded samples, validation tests were performed with mixtures of known amounts of MEG, DEG, and TEG in methanol. Mixed samples with MEG, DEG, and TEG were also spiked with compounds that were expected to be present in degraded glycol solutions, such as water, formic acid, acetic acid, glycolic acid, glyoxylic acid, and oxalic acid. None of these "contaminants" influenced the quantification of the glycols. Acetic acid shows up as a peak in the FID spectrum but elutes much earlier than the three glycols. To continuously validate the results from the real samples, mixed standards with known concentrations were run periodically between real samples. The accuracy of the method was 3%, and the precision was 1%.

2.2.2 Quantitative ^{13}C Nuclear Magnetic Resonance (NMR) Spectroscopy

The quantification of the glycols, TEG, DEG, and MEG, was performed on a Bruker 600 MHz Avance III HD equipped with a 5 mm cryogenic CP-TCI z-gradient probe at 26.8 °C. The spectra were processed using the software Bruker TopSpin 4.0.7.

To quantify the carbon in the samples, an internal reference standard was used. The reference standard, AcN (10 µL), was added to the solution with a Hamilton syringe model 802 as described by Perinu et al.[16] Deuterated water (D_2O) and TMSP was used as the lock solvent and the zero calibration. The sample for analysis was added into an NMR tube, and a coaxial insert with the D_2O and TMSP (2wt%) was placed inside.

The acquisition and processing parameters were adjusted to allow the integrals of the areas to relate to the true quantity of the carbons. First, the recycle delay time must be more than five times higher than the highest T_1. The spin-lattice relaxation time (T_1) of the glycols and the internal reference standard was measured by the inversion-recovery method[17] and the recycle delay time was set to 120 s. The sequence used to obtain the spectra was inverse-gated decoupling acquisition to minimize the effect of the nuclear Overhauser effect (NOE). The pulse width was 9.58 μs (90° pulse angle) and the number of scans was 256.

Validation tests were performed with mixtures of TEG, DEG, and MEG, with known concentrations. The three glycols were also spiked with components expected to be in the degraded solutions, such as formic and acetic acid. None of these influenced the quantification of the glycols. The accuracy was 2% for TEG and 5% for DEG and MEG. The precision was 1% for TEG and 0.5% for DEG and MEG.

2.2.3 High-Performance Liquid Chromatography coupled with Ultraviolet Detection (HPLC UV)

Quantification of the organic acids, formic, acetic, glycolic, glyoxylic, and oxalic acid, was performed with HPLC-UV. The method was performed on a PL1170-6830 (Agilent Hi-Plex H) column. Aqueous sulfuric acid (H_2SO_4, 0.05 mol/L, CAS: 7664-93-9) was used as an isocratic eluent with a flow of 0.5 mL/min. The column temperature was 40 °C and the injection volume was 10 μL. The method lasted for 20 minutes to allow all acids and potential contaminants that could be stuck in the column to eluate. Real samples were diluted in MilliPore water to approximately 50 000 ppm and filtered through 0.2 μm syringe filters before analysis. One calibration curve was used for the lower concentrations and one for the higher concentrations. The LOD and LOQ were defined as $3 \cdot S/N$ and $10 \cdot S/N$. See Table 3 for retention time, LOD, LOQ, the lower calibration range, and the higher calibration range for the five acids. In all cases, R^2 was >0.999. The peaks were baseline separated in a standard solution of all acids.

During the setting up of the method, both HPLC with refractive index (RI) and UV detection were tested. UV was found to be a good choice for the small organic acids as all of the acids are UV-active species. Calibration with each acid gave a linear calibration curve. The higher calibration range of formic acid was used as it was established early that in the oxidative degradation of TEG, this was the main acidic degradation compound and always present in higher abundance than the other acids.

2.2.4 Heat Stable Salt (HSS) Analysis

The analysis was performed following a method described by Reynolds et al.[18] Approximately 2 g of the sample was added to 40 mL activated Dowex 50W-X8 ion

Table 3: Retention time, LOD, LOQ, lower calibration range, and higher calibration range for oxalic acid, glyoxylic acid, glycolic acid, formic acid, and acetic acid analyzed with HPLC-UV.

Chemical	Retention time [s]	LOD [ppm]	LOQ [ppm]	Lower calibration range [ppm]	Higher calibration range [ppm]
Oxalic acid	9.50	0.67	0.84	2.5-50	50-400
Glyoxylic acid	10.84	1.9	3.7	10-50	50-400
Glycolic acid	13.45	2.0	4.5	10-50	50-400
Formic acid	15.09	12	13	50-1000	1000-8000
Acetic acid	16.45	5.3	8.3	10-50	50-400

exchange resin (CAS: 69011-20-7) and 40 mL DI water. The solution was then covered and heated to 70 °C with stirring for 1 hour, before letting it cool and allowing the resin to settle. The supernatant was then transferred to a new container through a frit. The resin was then rinsed multiple times until the pH of the supernatant reached that of DI water. The rinsing consisted of adding 40 mL DI water, stirring for 1 minute and leaving the resin to settle before filtering. All combined supernatants were titrated with sodium hydroxide (NaOH, CAS: 1310-73-2). For samples where TEG had degraded >50%, the titrant concentration was 0.5 M, while for the rest, the titrant concentration was 0.05 M.

This is originally a method for quantifying heat-stable salts formed during the degradation of amines.[18] It was, however, found to be transferable to the acidic degradation components formed during the degradation of TEG. Validation tests performed on artificial samples with glycols and acids in known concentrations gave overall coinciding results. The lowest accuracy was found to be ±8% corresponding to ±0.18 mol/kg.

2.3 Experimental Procedure

2.3.1 Oxidatively Degradation Experiments

The oxidatively degraded samples for analyses were produced using an oxidative degradation setup. The oxidative degradation experiments presented in this work are part of a larger experimental set, focusing on the impact of oxygen and temperature on TEG degradation. The oxidative degradation experiments with pure TEG were conducted in a custom-made oxidative degradation setup. This consisted of two parallel semi-open batch reactors. TEG (1.2 L) was added to the reactors (1.5 L), which were placed within electrical heating mantles (from ITA), and heated to 100 °C. The mantles had built-in magnetic stirring. A Graham condenser cooled by a water bath (5 °C) and a sparger (grade 1) were connected to each reactor. The gas going to the spargers entered the system through mass flow controllers at 200 mL/min. The composition of the gas was 24vol% oxygen and 76vol% nitrogen. The gas was recycled through a pump (400 L/h), and a small fraction was bled out through a 2,4-dinitrophenylhydrazine (DNPH, 800 mg) cartridge and an acid wash (1M H_2SO_4, aq.). The experiment was ended after 12 days.[19]

2.3.2 Thermal Degradation Experiments

The thermal degradation experiments were performed in 10 cm long SS316 cylinders with an outer diameter of 1.3 cm, and thickness of 0.1 cm, equipped with Swagelok® end caps. The cylinders are filled with 8 mL of solution. The solutions included in this study were (1) pure TEG, (2) 30mol% water in TEG, and (3) 2mol% formic acid and 28mol% water in TEG. For each experiment, 10 cylinders were prepared so that during each sampling, two cylinders could be removed from the heating cabinet. This would result in five data points, each representing two parallels. After closing the cylinder, they were placed in an oven at 220 °C. The cylinders were weighed before and after the experiment to detect possible leakages, but no leakages were detected.

2.3.3 Durability Tests

Fresh samples of TEG were introduced to glass vials (4 mL). The samples were not degassed, but the vials were blanketed with nitrogen before they were closed. The vials were put in a fridge (5 °C) and in a box in a fume cabinet (20-24 °C). Samples from each of the two locations were analyzed periodically. Once opened, sample vials were discarded.

3 Results and Discussion

This work aims to investigate possible methods for monitoring glycol degradation with solvent analysis. There are two possible approaches when doing this. The concentration of TEG in the solutions can be analyzed, thus, the decrease as the solvent degrades can be observed. Alternatively, or additionally, the degradation products formed and accumulated over time in the solvent can be monitored. In the following section, both possibilities will be explored.

In the following sections, different degraded samples of TEG will be discussed. In Section 3.1, oxidatively degraded TEG samples will be studied. As mentioned earlier, the oxidatively degraded samples were produced in a larger oxidative degradation study published elsewhere, focusing on the effect of temperature and oxygen concentration.[19] In that article, additional degradation compounds were identified and some of these were also quantified. The experiment which had most degradation in that study (100 °C and 24% oxygen) was chosen as a test system for the analytical methods in this work. To validate the analytical tools, independent analytical methods were used to quantify degradation compounds and TEG concentration in the laboratory degraded samples. The glycols, TEG, DEG, and MEG were quantified using GC-FID and quantitative ^{13}C NMR. Acidic degradation compounds were quantified using HPLC-UV and HSS analysis. In Section 3.2, results from thermally degraded samples of TEG will be presented. Lastly, some observations on color changes and sample stability will be presented. Numerical data from the graphs and example spectra from the analyses will be given in Supporting Information.

3.1 Oxidatively Degraded TEG

The oxidatively degraded samples were analyzed with GC-FID and NMR to quantify the glycols, TEG, DEG, and MEG. In the GC-FID spectra, the peaks of the tree glycols are well separated with retention times of 5.5 (MEG), 8.9 (DEG), and 12.2 (TEG) minutes. As the TEG degraded, however, unknown degradation compounds formed with peaks which did not have proper baseline separation from the peaks of MEG and TEG, complicating their quantification. DEG was not affected.

In the NMR spectra, both TEG (75.3, 73.1 and 63.98 ppm) and MEG (66.2 ppm) had one peak well separated from the others. DEG (75.2 and 64.05 ppm), on the other hand, did not, as both peaks are close to those of TEG. This did not cause a problem for the accuracy of the DEG in mixed standards of the glycols but can potentially be a challenge for the quantification of DEG in more degraded samples. Furthermore, like for the GC-FID method, the new components forming as TEG degraded had peaks partially overlapping those of the glycols. This affects the accuracy of this method as well. Quantification was performed using the integral of the least affected peaks.

The result from the quantification of TEG in the oxidatively degraded samples is presented in Figure 1. The two analytical techniques show the same degradation trends for TEG, with only small variations. Even for the most degraded sample, at day 12, the two analytical methods agree very well.

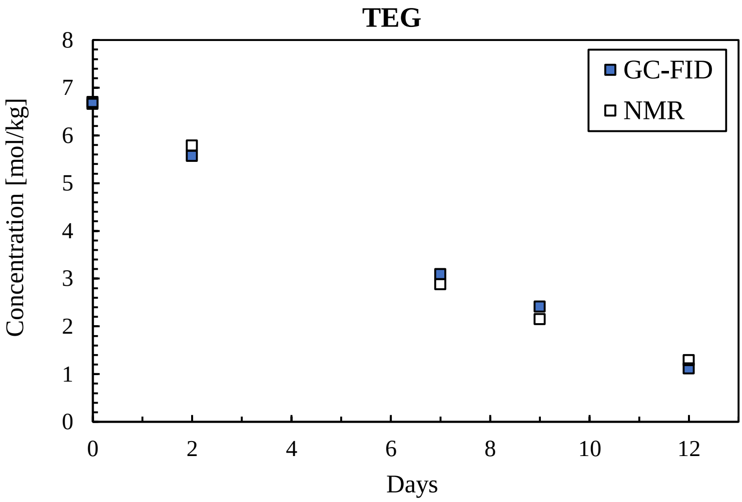

Figure 1: Quantification of oxidatively degraded TEG (100 °C, 24% O$_2$*) with GC-FID and NMR.*

The results from the quantification of MEG and DEG are presented in Figure 2 and Figure 3. The two analytical methods give results that coincide for the quantification of DEG. For the sample from day 12, there is a higher discrepancy between the two. The reason for this is not understood. For the quantification of MEG, both techniques give results showing a steady increase in MEG with time. The values quantified with NMR, however, are steadily lower than those from the GC-FID analysis. Experiments with longer recycle delay times (150 s) were conducted to ensure that the relaxation time for the carbon had not been affected by unknown components in the solutions. This was not the case. It might be caused by the increased overlapping of the MEG peak in the NMR spectra as the solvent becomes more and more degraded. It could also be due to ionic interactions of the smaller glycols with the acidic components in the solution. A plot showing the linear relationship of the quantification of the glycols by the two methods is presented in Figure S1 in Supporting Information.

Generally, for both these quantitative techniques, the standard addition method could have been an option for acquiring more reliable results when peaks were no longer baseline separated in the most degraded samples. This was found to be problematic for the degraded glycol samples, though. In a previous study[19], it was found that mixing formic acid and TEG resulted in the formation of triethylene glycol formate (CAS: 1240369-67-8), identified by qualitative NMR. As formic acid, as well as other organic acids, are found in the degraded solutions, this would affect the quantitative results of a standard addition.

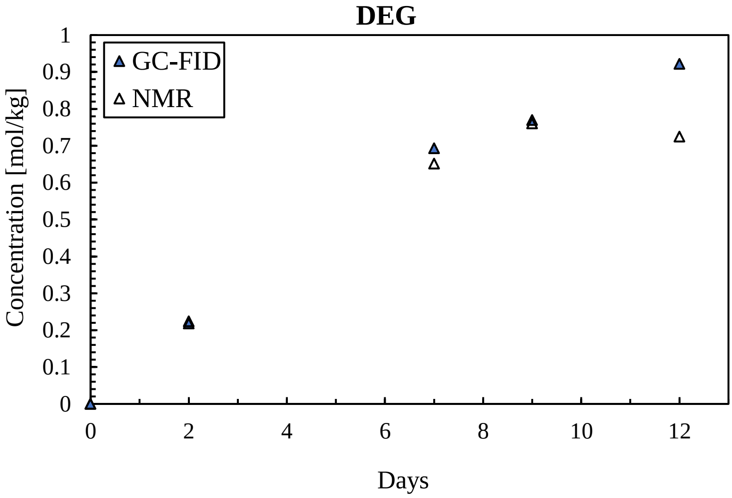

Figure 2: Quantification of DEG formed through oxidative degradation of TEG (100 °C, 24% O_2) with GC-FID and NMR.

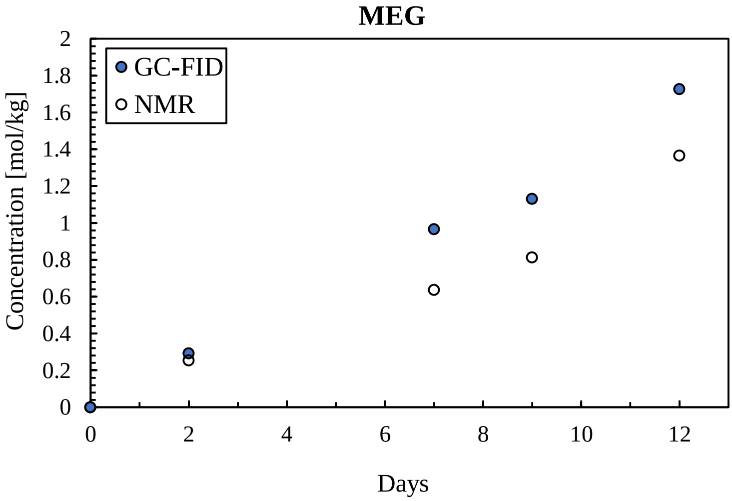

Figure 3: Quantification of MEG formed through oxidative degradation of TEG (100 °C, 24% O_2) with GC-FID and NMR.

The two independent analytical methods tested here show somewhat varying results for the quantification of the three glycols, TEG, DEG, and MEG. They showed coinciding results for the quantification of TEG and DEG. For MEG, larger differences are observed. It is important to remember, that in this work is performed on highly degraded samples. The day 12 sample, shown in Figure 3, contains only 20mol% of the original TEG. This level of degradation was selected to detect as many degradation compounds as possible in the original study. In an industrial process, the TEG would be far less degraded. Therefore, the quantification of MEG would be less problematic.

Overall, the quantitative ^{13}C NMR experiment is time-consuming and expensive and is therefore not well suited for quick monitoring of TEG. It is, however, a valuable technique for acquiring insights into the composition of the degraded solvent. This can be information on which chemical groups are present in a degraded solution depending on their chemical shift region, but also characterization of unknown degradation compounds. GC-FID, on the other hand, is a quick and easy method and more suitable for at-line monitoring and industrial application. GC-FID has a high LOQ for TEG due to the column bleed. For very low concentrations of TEG, quantitative ^{13}C NMR would therefore be a better choice. This would, however, most likely not be an issue for industrial samples.

The concentration of the small organic acids formed during the degradation of TEG were quantified with HPLC-UV and HSS analysis. The HPLC-UV method was set up to quantify the small organic acids, formic, acetic, glycolic, glyoxylic, and oxalic acid. The structure of these acids is presented in Figure 4. While the HPLC-UV technique quantifies specific acids, the HSS analysis is a nonspecific method. It gives the total amount of cationic groups in the sample, which corresponds to the total ion concentration due to charge neutrality. It should be noted that this entails that for example oxalic acid will count double. The comparison of the two methods will be done based on the sum of the acids quantified. Figure 5 presents the sum of the acids in the oxidatively degraded TEG samples, analyzed with HPLC-UV and HSS analysis. Overall, the same trend can be seen for both analytical methods. The results from the HSS analysis, however, are increasingly higher than the sum of the acids quantified with HPLC. The cause of this is likely that some acids are formed during the oxidative degradation of TEG that are not quantified with the HPLC method. To verify this, more oxidative degradation compounds should be identified.

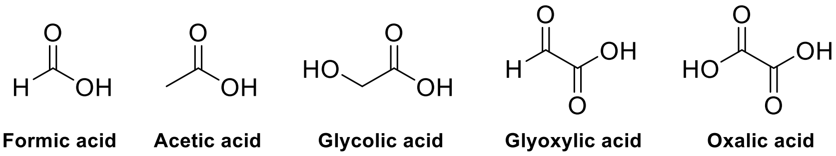

Figure 4: Structure of small organic acids, formic, acetic, glycolic, glyoxylic, and oxalic acid.

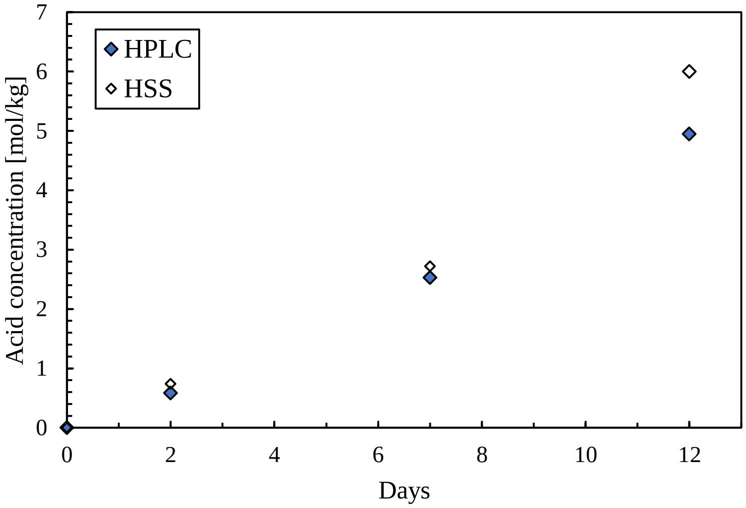

Figure 5: Quantification of the acids formed through oxidative degradation of TEG (100 °C, 24% O_2) with HPLC-UV and HSS analysis.

Of the two analytical techniques, HPLC-UV is the most expensive. Though the HSS analysis is an unspecific analytical technique, it gives a good indication of the status of the solvent. HSS offers an advantage over pH measurements, as it will determine the actual acid concentration of the sample, while pH has been proven in the literature to not correlate with degradation.[9] If more advanced techniques are unavailable, this technique is inexpensive and relatively easy to set up. At the same time, it is a time-consuming analysis and is difficult to automate. This makes it less suited for quick liquid analysis to monitor the solvent status on-line or at-line.

3.2 Thermally Degraded TEG

The thermal stability of TEG was studied through thermal degradation experiments with various solutions of TEG. The solutions included in this study were (1) pure TEG, (2) 30mol% water in TEG, and (3) 2mol% formic acid and 28mol% water in TEG. The experiment with added water was included, as water would naturally be present in the dehydration process. The experiment with the added formic acid was conducted as formic acid is one of the major identified degradation compounds for TEG. The quantitative results for the glycols presented in this section stem from GC-FID analysis. Results from some samples analyzed with quantitative ^{13}C NMR is presented in the Supporting Information.

The loss of TEG in the three solutions is presented in Figure 6. The error bars represent the deviation between the two parallels of each experiment. At 220 °C, the thermal degradation is not rapid. After 9 weeks only about 12% loss of TEG is measured. It should, however, be noted that as the solutions were transferred from the cylinders to storage containers that the solutions were bubbling. This could indicate that gaseous degradation products had formed. These would not be included in the liquid analysis presented above. The gaseous compounds formed could not be identified or quantified in these experiments but studying these should be included in future work. The additives do not seem to have any clear effect on the thermal stability of TEG. It might, however, be difficult to determine due to the low thermal degradation rates compared to the experimental uncertainty.

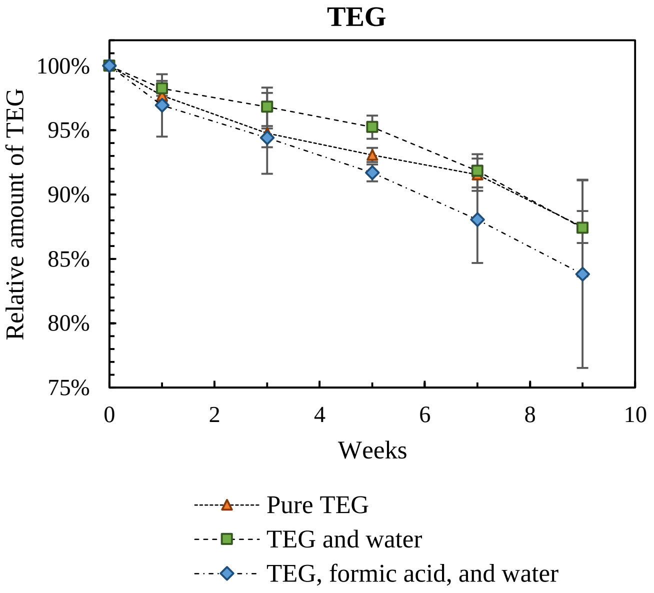

Figure 6: Results from thermal degradation experiments (220 °C) for (1) pure TEG, (2) 30mol% water in TEG, and (3) 2mol% formic acid and 28mol% water in TEG.

The formation of DEG and MEG in the three experiments is presented in Figure 7 and Figure 8. The samples following the x-axis in the graph were found to be below LOQ. DEG is formed in all three solutions and in slightly higher quantities for the two solutions containing water. MEG, however, is only formed in solutions containing water, and most in the solution containing water and formic acid. The thermal degradation of TEG seems to be affected by the presence of impurities, especially formic acid.

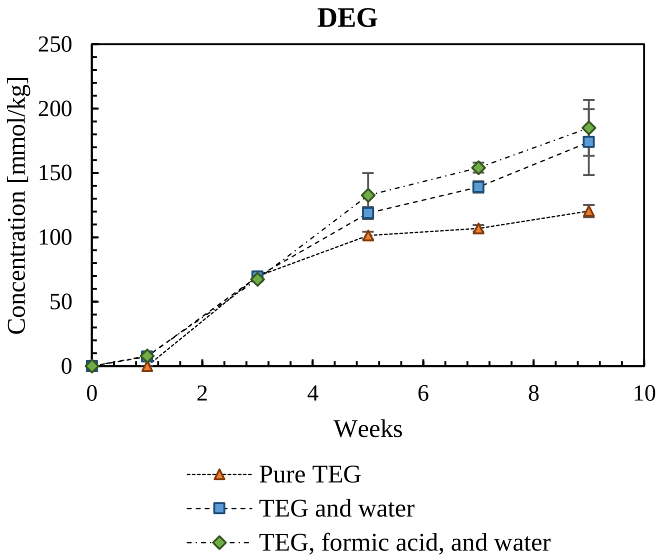

Figure 7: Formation of DEG in thermal degradation experiments of TEG (220 °C).

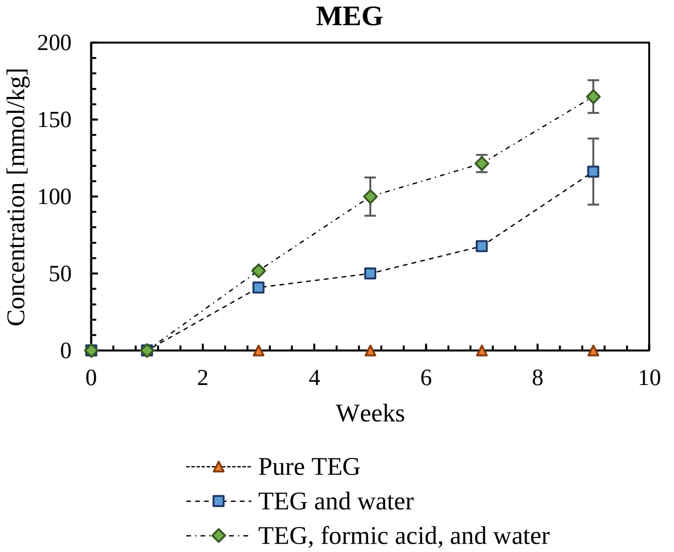

Figure 8: Formation of MEG in thermal degradation experiments of TEG (220 °C).

Little is known about the thermal degradation mechanisms of TEG. Forster[4] proposed a radical splitting of the TEG, resulting in smaller fragments such as MEG and DEG. A general overview of this radical fragmentation is shown in Scheme 1. In general, water is not expected to have a solvent effect on radical reactions.[20] It can, however, help with the proton transfer necessary for the radical hydrogenation (RH) step by forming OH$^{\cdot}$ radicals.[21] This might be what is giving the enhanced formation of MEG and DEG in the solutions with water present. Whether formic acid has a similar effect with its readily available proton, or if another mechanism is taking place, is unclear. Additionally, the formation of the radical fragments could potentially result in the formation of larger polymeric components. Further work should include the identification of more thermal degradation components.

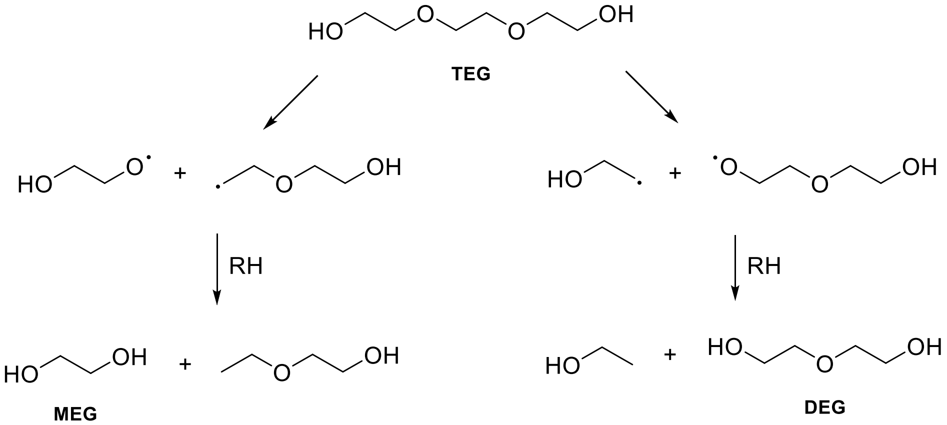

Scheme 1: Overview of the possible radical fragmentation of TEG occurring during thermal degradation.

None of the small organic acids could be detected by HPLC during the thermal degradation experiments. In the solutions initially containing formic acid, the acid was depleted in one week. Karl-Fischer titration was used to investigate water formation in the solution without any initial water. Only small quantities (201 mmol/kg, 0.4wt%) were found. This could stem from still unknown thermal degradation mechanisms of TEG, or it could potentially be present due to the hygroscopic nature of TEG. No other thermal degradation compounds have been identified.

3.3 Color

Degradation has been reported to cause color change in degraded glycol solutions. For the degradation of MEG, increased degradation, i.e., the concentration of degradation products, has been found to give an increasingly deep color to the solution.[14] In this study, the oxidatively degraded TEG samples were without any color even though 80mol% of the TEG had degraded. The thermally degraded TEG samples, on the other hand, had a yellow tint even with their low degradation. In our other article, oxidatively degraded TEG samples at high temperatures (150 °C, 6% O_2) also acquired a yellow tint. In this case, the degradation was high, and no metals were introduced to the system.[19] It is difficult to conclude what is causing the color change in the degraded TEG. From what is seen in these experiments, it does not seem to be caused by high degradation of TEG alone. As color change was observed in the thermal degradation experiments where little degradation was achieved, it could point to that the color is caused by the presence of specific degradation components formed at high temperatures, and potentially also the presence of metals. Overall, one should be careful with using color as an indicator of the solvent's "health".

3.4 Recommendations for Sample Storage

It has been suspected that neither fresh TEG nor degraded TEG samples are stable over prolonged periods. To investigate the extent of this, durability tests were conducted with fresh TEG. The amount of DEG, MEG, formic, acetic, and glyoxylic acid formed in these solutions after 4 months is presented in Table 4. Glyoxylic and oxalic acid were not detected in any of the solutions. As can be observed from these results, it only took 4 months for the samples at room temperature to get substantial degradation product formation. Decreasing the temperature was effective as it reduced the amount of degradation products formed. Formation of DEG and formic acid were, however, still occurring to some extent.

Table 4: Formation of DEG, MEG, formic, acetic, and glycolic acid in samples of TEG in closed vials stored in a fridge and at room temperature.

Component	Fridge [mmol/kg]	Room temperature [mmol/kg]
DEG	36.5*	66.7*
MEG	< LOD	57.9
Formic acid	9.67	57.5
Acetic acid	< LOQ	2.51
Glycolic acid	< LOQ	1.53

* 11 mmol/kg of DEG was found in the fresh TEG solution.

As seen from these results, some regard should be taken when storing TEG samples. At the very least, samples should be stored at cold temperatures. Potentially, blanketing the samples with nitrogen will reduce the possibility for additional oxidation of the sample. The best option is of course to perform any analysis of the samples within a reasonable timeframe of sampling to avoid these problems altogether.

4 Conclusions

This work has focused on investigating possible methods for monitoring glycol degradation with solvent analysis. Four analytical methods were successfully employed. Oxidatively and thermally degraded triethylene glycol (TEG) samples were studied.

Initially, methods for quantifying the solvent glycol and some of the degradation compounds were set up. Two component groups in focus were the glycols, TEG, diethylene glycol (DEG), and ethylene glycol (MEG), and the small organic acids, formic, acetic, glycolic, glyoxylic, and oxalic acid. Two independent methods were chosen for each component group to validate the analytical methods.

TEG, DEG, and MEG in the oxidatively degraded TEG samples were quantified with gas chromatography coupled with flame ionization detection (GC-FID) and with quantitative carbon-13 nuclear magnetic resonance (^{13}C NMR) spectroscopy. For TEG and DEG, both methods gave coinciding results. For the quantification of MEG, the values found with NMR were lower than the ones found with GC-FID for the more degraded samples. This could be due to the peak overlapping in the NMR spectra of the degraded samples. This is not expected to be a problem when applied to industrial sample, as these are not expected to reach this level of degradation.

The acidic degradation compounds in the oxidatively degraded samples were quantified with high-performance liquid chromatography coupled with ultraviolet detection (HPLC-UV) and heat-stable salt (HSS) analysis. Both methods show the same overall trend, but the values registered by the HSS analysis were higher than the HPLC-UV results, indicating the presence of some unidentified ionic degradation compounds in the degraded TEG.

Thermal degradation of TEG was studied through three sets of solutions: pure TEG, 30mol% water in TEG, and 2mol% formic acid and 28mol% water in TEG. The effect of the impurities on the rate of TEG loss was difficult to discern, but the formation of MEG and DEG were increased by the presence of water and additionally by the presence of formic acid. This could be caused by the impurities' ability to aid in the proposed radical mechanism during MEG and DEG formation. No other degradation compounds were detected. Further work should include identification of more thermal degradation compounds.

There does not seem to be a clear correlation between the level of degradation of TEG and the color of the solvent. Solvents with very little degradation acquired a yellow tint, while very degraded samples remained colorless. High temperature and the presence of metals might be underlying factors, but more work needs to be conducted to get a better understanding of these observations. TEG can degrade if stored over a long period. Formic acid and DEG were found to have formed in fresh TEG samples stored in the fridge for 4 months. Care should be taken to avoid invalid analytical results for stored samples.

Acknowledgement

The authors would like to acknowledge Max Lukas Teschner for preparing dilutions and performing some of the analyses of degraded TEG.

This publication has been produced with support from the Knowledge-building Project for Industry (KPN), MORE: Monitoring of glycol quality to Reduce operational risks (Project Manager: Marion Seiersten, Institute for Energy Technology (IFE)). The authors acknowledge the following partners for their contributions: Aker BP, Equinor, IFE, Kanfa, Neptune Energy, Slb, Shell, and the Research Council of Norway (320257).

The LAUNCH project (Project No. 299662) is co-funded by the ERA-NET Accelerating CCS Technologies initiative, which supports the delivery of safe and cost-effective carbon capture, utilization, and storage. The governments of each participating country have contributed funding through the ACT2 initiative.

References

(1) John M. Campbell and Company. *Gas Conditioning and Processing*; 2004.

(2) Mokhatab, S.; Poe, W. A.; Mak, J. Y. Natural Gas Dehydration. In *Handbook of Natural Gas Transmission and Processing*; **2015**; pp 223–263. https://doi.org/10.1016/b978-0-12-801499-8.00007-9.

(3) Piemonte, V.; Maschietti, M.; Gironi, F. A Triethylene Glycol-Water System: A Study of the TEG Regeneration Processes in Natural Gas Dehydration Plants. *Energy Sources, Part A Recover. Util. Environ. Eff.* **2012**, 34 (5), 456–464. https://doi.org/10.1080/15567031003627930.

(4) Forster, R. Extending Glycol Life in Natural Gas Dehydration Systems. In International Gas Research Conference; San Diego, 1998; pp 113–125.

(5) Giesen, Y.; Friedrich, C.; Breuer, D.; Fauss, J.; Hebisch, R.; Brock, T. H.; Hartwig, A. Glycols - Method for the Determination of Diethylene Glycol, Ethylene Glycol and Propylene Glycol in Workplace Air Using Gas Chromatography. *MAK-Collection Occup. Heal. Saf.* **2018**, 1584–1599. https://doi.org/10.1002/3527600418.AM10721E1918.

(6) Fu, Y.; Hao, Z.; Parker, B.; Knapp, M. A Greener Way to Screen Toothpaste for Diethylene Glycol. *Am. J. Anal. Chem.* **2011**, 02 (08), 938–943. https://doi.org/10.4236/ajac.2011.28109.

(7) Caldeira, L. R.; Madureira, F. D.; Maia, T. D. F.; Muller, C. V.; Fernandes, C. Simultaneous Quantification of Ethylene Glycol and Diethylene Glycol in Beer by Gas Chromatography Coupled to Mass Spectrometry. *Food Chem.* **2021**, 346 (August 2020), 128871. https://doi.org/10.1016/j.foodchem.2020.128871.

(8) Wurita, A.; Suzuki, O.; Hasegawa, K.; Gonmori, K.; Minakata, K.; Yamagishi, I.; Nozawa, H.; Watanabe, K. Sensitive Determination of Ethylene Glycol, Propylene Glycol and Diethylene Glycol in Human Whole Blood by Isotope Dilution Gas Chromatography-Mass Spectrometry, and the Presence of Appreciable Amounts of the Glycols in Blood of Healthy Subjects. *Forensic Toxicol.* **2013**, 31 (2), 272–280. https://doi.org/10.1007/s11419-013-0188-3.

(9) Rossiter, W. J.; Brown, P. W.; Godette, M. The Determination of Acidic Degradation Products in Aqueous Ethylene Glycol and Propylene Glycol Solutions Using Ion Chromatography. *Sol. Energy Mater.* **1983**, 9 (3), 267–279. https://doi.org/10.1016/0165-1633(83)90049-7.

(10) Brown, P. W.; Galuk, K. G.; Rossiter, W. J. Characterization of Potential Thermal Degradation Products from the Reactions of Aqueous Ethylene Glycol and Propylene Glycol Solutions with Copper Metal. *Sol. Energy Mater.* **1987**, 16 (4), 309–313. https://doi.org/10.1016/0165-1633(87)90079-7.

(11) Madera, M.; Höflinger, W.; Kadnar, R. Ion Chromatographic Identification and Quantification of Glycol Degradation Products. *J. Chromatogr. A* **2003**, 997 (1), 279–284. https://doi.org/10.1016/S0021-9673(03)00060-8.

(12) Psarrou, M. N.; Jøsang, L. O.; Sandengen, K.; Østvold, T. Carbon Dioxide Solubility and Monoethylene Glycol (MEG) Degradation at MEG

Reclaiming/Regeneration Conditions. *J. Chem. Eng. Data* **2011**, 56 (12), 4720–4724. https://doi.org/10.1021/je200709h.

(13) Brown, P. W.; Rossiter, W. J.; Galuk, K. G. A Mass Spectrometric Investigation of the Thermal Oxidative Reactivity of Ethylene Glycol. *Sol. Energy Mater.* **1986**, 13 (3), 197–202. https://doi.org/10.1016/0165-1633(86)90018-3.

(14) AlHarooni, K.; Pack, D.; Iglauer, S.; Gubner, R.; Ghodkay, V.; Barifcani, A. Analytical Techniques for Analyzing Thermally Degraded Monoethylene Glycol with Methyl Diethanolamine and Film Formation Corrosion Inhibitor. *Energy and Fuels* **2016**, 30 (12), 10937–10949. https://doi.org/10.1021/acs.energyfuels.6b02116.

(15) Alef, K.; Smith, C.; Iglauer, S.; Gubner, R.; Barifcani, A. MEG on Hydrate Inhibition Performance over Multiple Regeneration Cycles. *Fuel* **2018**, 222, 638–647. https://doi.org/10.1016/j.fuel.2018.02.190.

(16) Perinu, C.; Bernhardsen, I. M.; Pinto, D. D. D.; Knuutila, H. K.; Jens, K. J. NMR Speciation of Aqueous MAPA, Tertiary Amines, and Their Blends in the Presence of CO2: Influence of PKa and Reaction Mechanisms. *Ind. Eng. Chem. Res.* **2018**, 57 (5), 1337–1349. https://doi.org/10.1021/acs.iecr.7b03795.

(17) Shoulders, B. *High-Resolution NMR Techniques in Organic Chemistry. Tetrahedron Organic Chemistry Series Volume 19.* Pergamon: Oxford. 1999. https://doi.org/10.1021/ja004717y.

(18) Reynolds, A. J.; Verheyen, T. V.; Adeloju, S. B.; Chaffee, A. L.; Meuleman, E. Evaluation of Methods for Monitoring MEA Degradation during Pilot Scale Post-Combustion Capture of CO_2. *Int. J. Greenh. Gas Control* **2015**, 39, 407–419. https://doi.org/10.1016/j.ijggc.2015.06.001.

(19) Høisæter, K. K.; Buvik, V.; Gonzalez, S. V.; Vevelstad, S. J.; Knuutila, H. K. Oxidative Degradation of Triethylene Glycol. *To be Published.*

(20) Yorimitsu, H.; Nakamura, T.; Shinokubo, H.; Oshima, K.; Omoto, K.; Fujimoto, H. Powerful Solvent Effect of Water in Radical Reaction: Triethylborane-Induced Atom-Transfer Radical Cyclization in Water. *J. Am. Chem. Soc.* **2000**, 122, 45, 11041-11047. https://doi.org/10.1021/ja0014281.

(21) Id, J. M.; Wang, F.; Mostafavi, M. Ultrafast Chemistry of Water Radical Cation, $H_2O^{\bullet+}$, in Aqueous Solutions. *Molecules **2018**, 23 (2), 244.* https://doi.org/10.3390/molecules23020244.

Supporting information

Analytical tools for monitoring glycol degradation

Karen K. Høisæter[a], Vanja Buvik[a], Solrun J. Vevelstad[b], Hanna K. Knuutila[a]*

[a] Department of Chemical Engineering, NTNU, NO-7491 Trondheim, Norway

[b] SINTEF Industry, P.O.Box 4760 Torgarden, NO-7465, Norway

* E-mail address: Hanna.knuutila@ntnu.no

A. Numerical data

Table S1: Quantification of TEG, DEG, and MEG in oxidatively degraded samples (100 °C, 24vol% O_2) by GC-FID and (quantitative ^{13}C) NMR.

	TEG		**DEG**		**MEG**	
Day	**GC-FID**	**NMR**	**GC-FID**	**NMR**	**GC-FID**	**NMR**
0	6.66	6.70	< LOD	< LOD	< LOD	< LOD
2	5.57	5.79	0.22	0.22	0.29	0.25
7	3.09	2.88	0.69	0.65	0.97	0.64
9	2.41	2.15	0.77	0.76	1.13	0.81
12	1.12	1.29	0.92	0.72	1.73	1.37

Table S2: Sum of small organic acids quantified by HPLC-UV and ionic components quantified by HSS in oxidatively degraded samples (100 °C, 24vol% O_2).

Day	**HPLC-UV**	**HSS**
0	0	0
2	0.59	0.74
7	2.53	2.72
12	4.95	6.00

Table S3: GC-FID quantification of TEG in thermally degraded TEG solutions (120 °C).

Week	**Pure TEG [mmol/kg]**		**TEG and water [mmol/kg]**		**TEG, formic acid, and water [mmol/kg]**	
	P1	**P2**	**P1**	**P2**	**P1**	**P2**
0	6652	6652	6326	6326	6319	6319
1	6477	6520	6190	6242	6024	6241
3	6156	6452	6058	6192	6005	5940
5	6166	6218	5985	6065	5830	5771
7	6149	6031	5753	5868	5420	5721
9	5761	5878	5361	5697	5629	4976

Table S4: GC-FID quantification of DEG in thermally degraded TEG solutions (120 °C).

Week	**Pure TEG [mmol/kg]**		**TEG and water [mmol/kg]**		**TEG, formic acid, and water [mmol/kg]**	
	P1	**P2**	**P1**	**P2**	**P1**	**P2**
0	0	0	0	0	0	0
1	0	0	6.39	8.62	6.71	8.88
3	68.7	71.0	69.7	69.4	67.3	67.4
5	97.3	106	116	122	145	120
7	109	105	142	136	151	157
9	117	124	192	156	170	200

Table S5: GC-FID quantification of MEG in thermally degraded TEG solutions (120 °C).

Week	**Pure TEG [mmol/kg]**		**TEG and water [mmol/kg]**		**TEG, formic acid, and water [mmol/kg]**	
	P1	**P2**	**P1**	**P2**	**P1**	**P2**
0	0	0	0	0	0	0
1	0	0	0	0	0	0
3	0	0	41.0	40.8	52.9	50.9
5	0	0	50.6	49.5	109	91
7	0	0	67.2	68.2	125	118
9	0	0	131	101	157	172

Table S6: Comparison of the quantification of TEG in thermally degraded TEG samples (220 °C) with GC-FID and (quantitative ^{13}C) NMR.

Week	**CG-FID [mol/kg]**	**NMR [mol/kg]**
1	6.50	6.49
5	6.19	6.24
9	5.82	5.83

B. Additional graphs

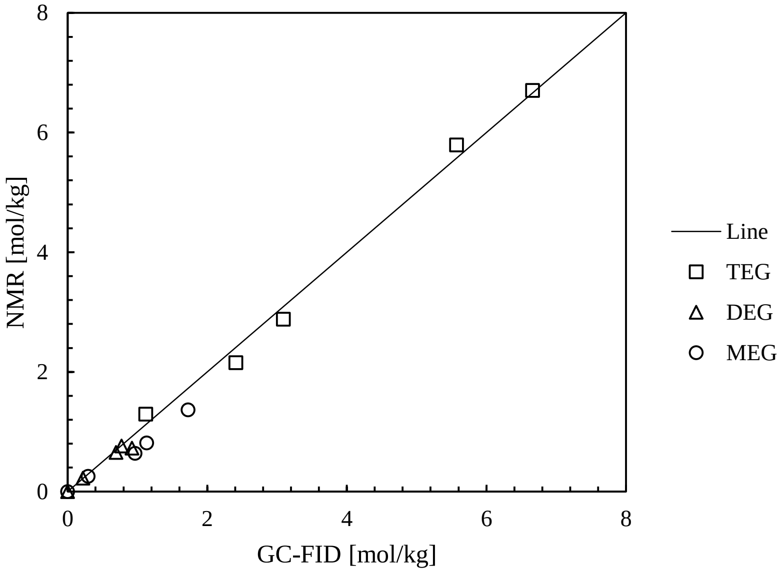

Figure S1: Linear relationship of the quantification of TEG, DEG, and MEG with GC-FID and NMR.

A. Spectra

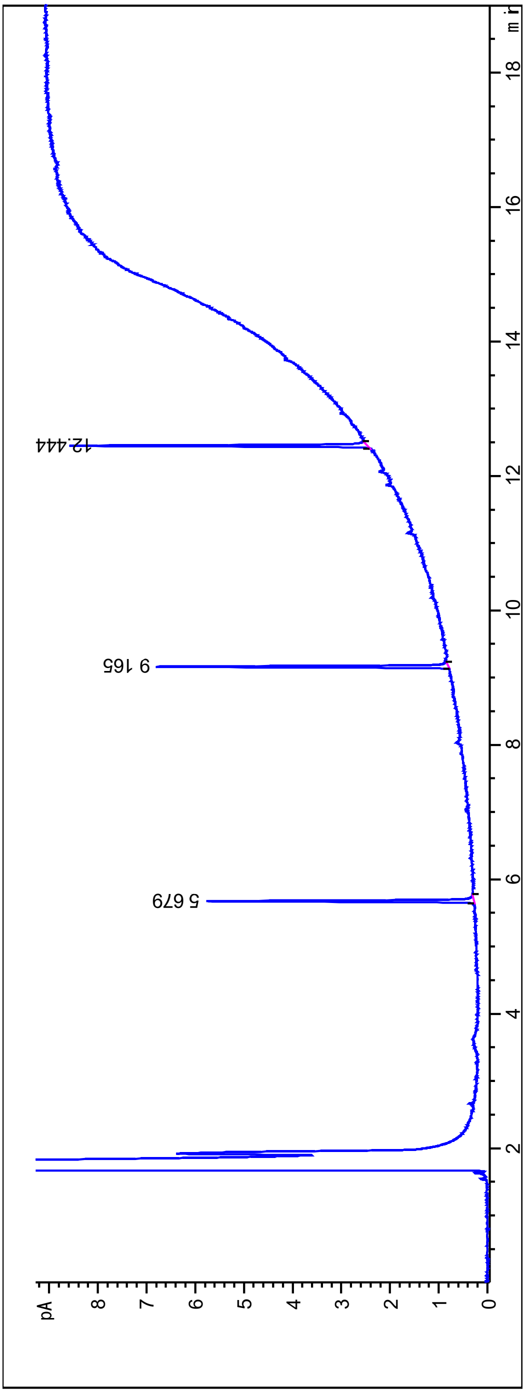

Figure S1: GC-FID spectrum of mixed sample of TEG (75 ppm), DEG (75 ppm) and MEG (75 ppm).

Figure S2: GC-FID spectrum of oxidatively degraded TEG (100 °C, 24vol% O₂, day 12).

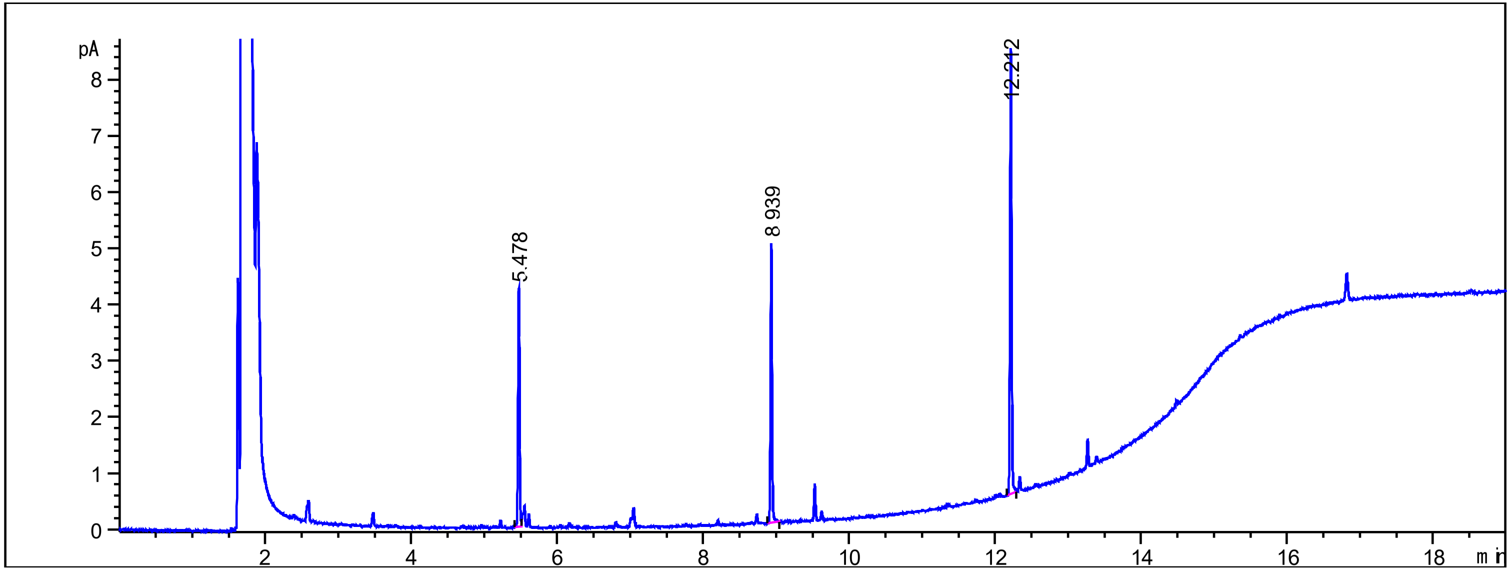

Figure S3: ^{13}C NMR spectrum of pure TEG.

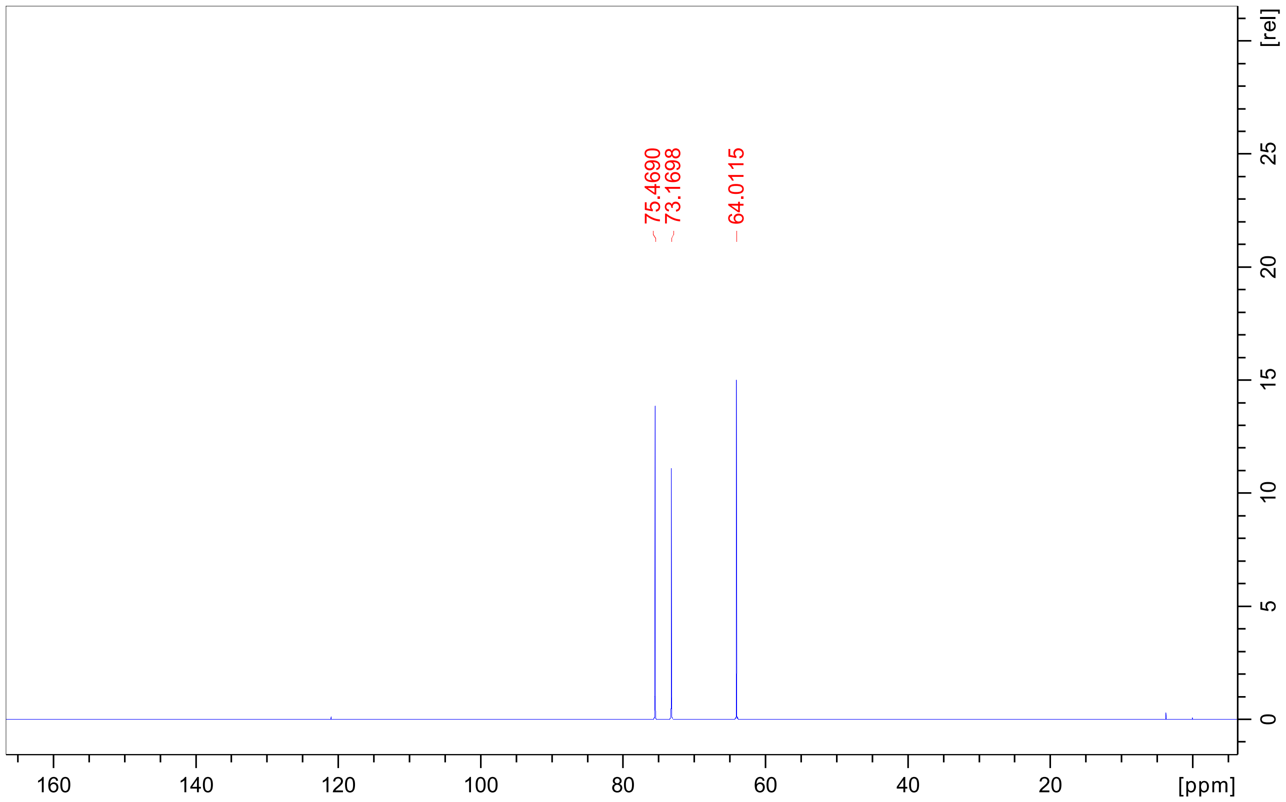

Figure S4: ^{13}C NMR spectrum of mixed sample of TEG (200 g/kg), DEG (25 g/kg) and MEG (20 75 g/kg).

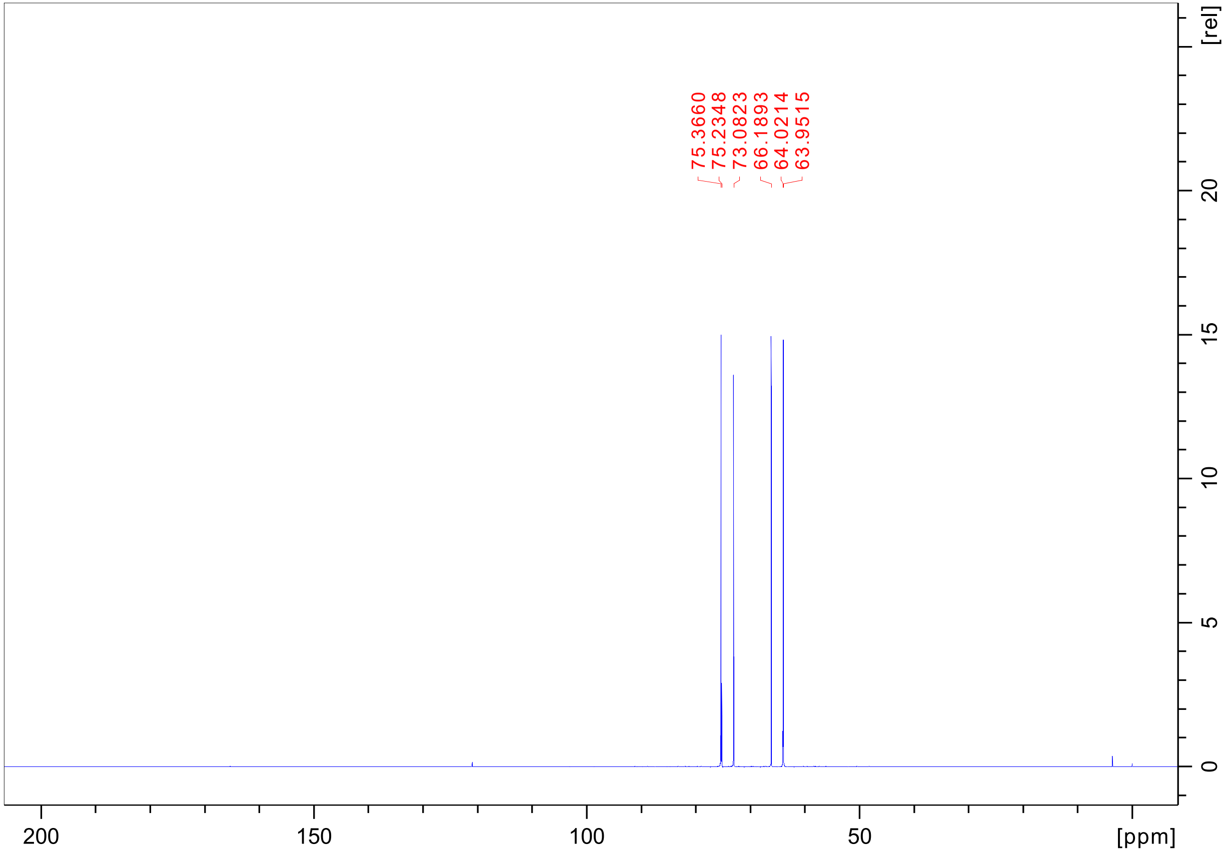

Figure S5: ^{13}C NMR spectrum of oxidatively degraded TEG (100 °C, 24vol% O_2, day 12).

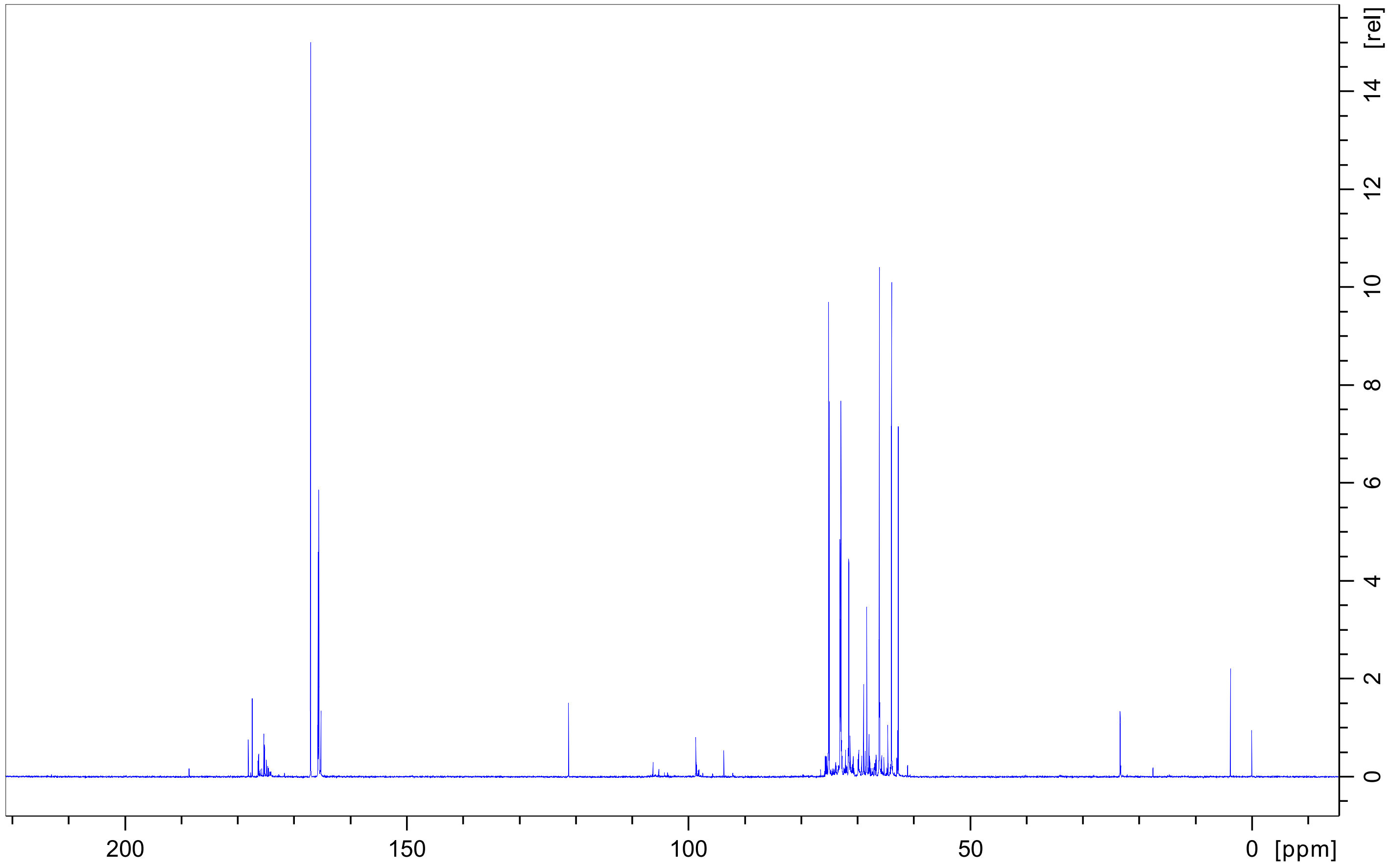

Figure S6: HPLC-UV spectrum of mixed sample of formic acid (4000 ppm), acetic acid (200 ppm), glycolic acid (200 ppm), glyoxylic acid (200 ppm), and oxalic acid (200 ppm).

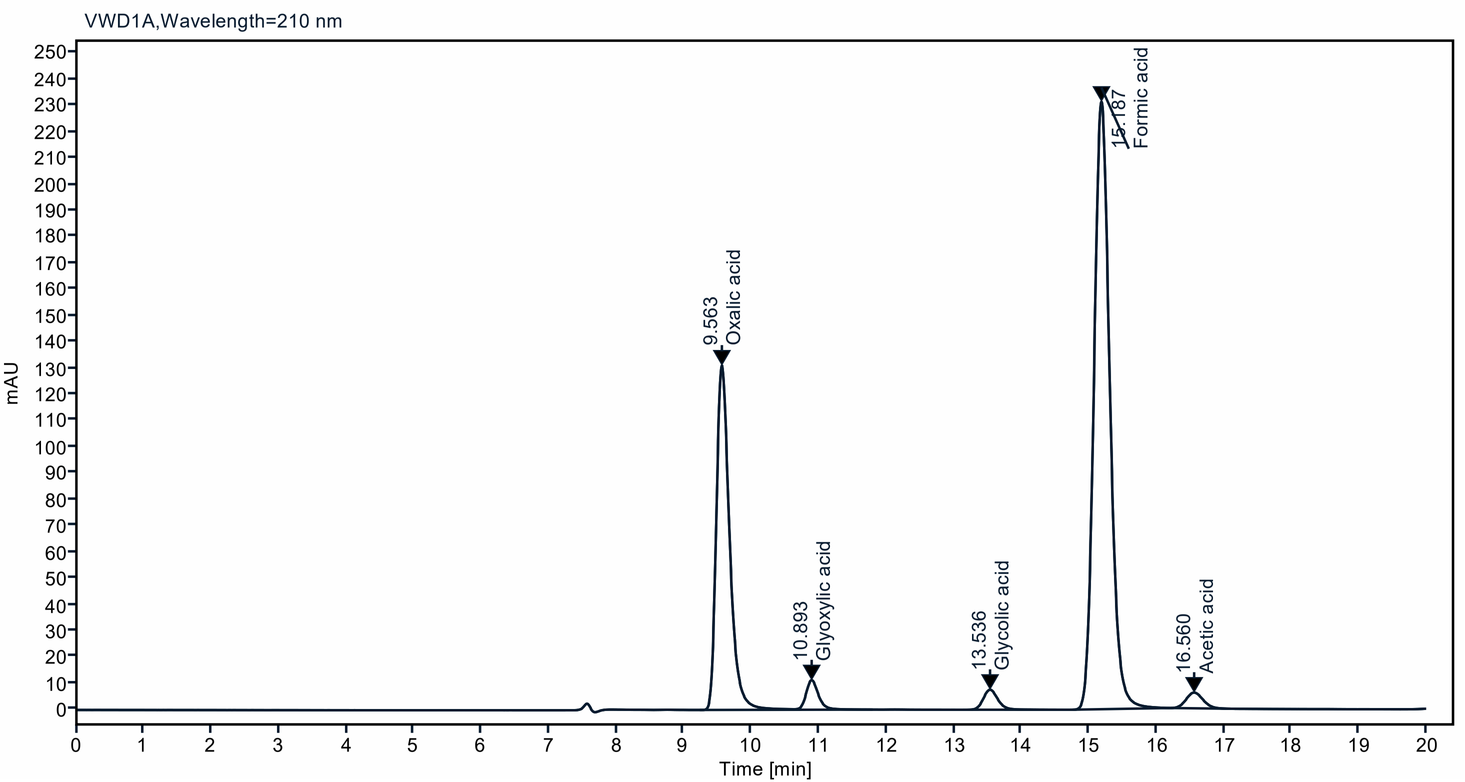

Figure S7: HPLC-UV spectrum of oxidatively degraded TEG (100 °C, 24vol% O_2, day 12).

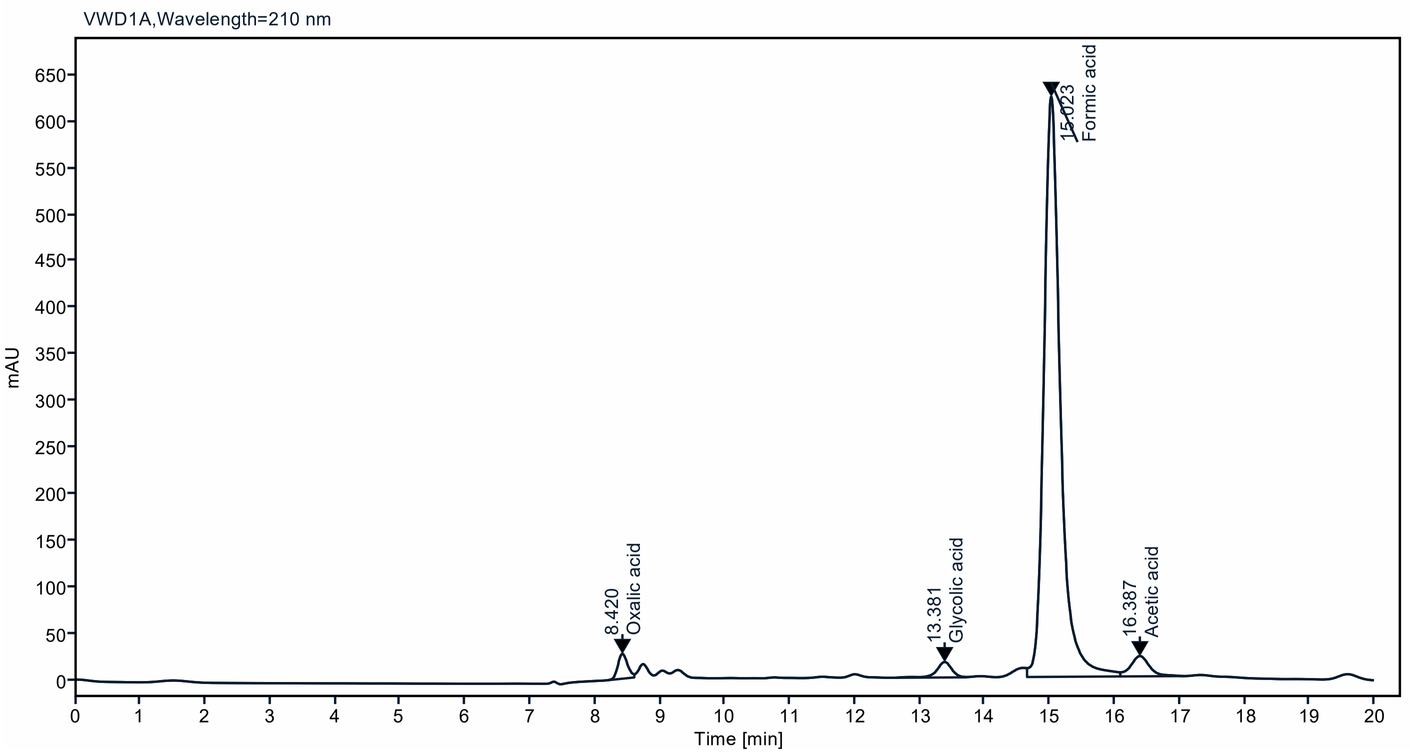

Chapter 8

Oxidative Degradation of Triethylene Glycol

This chapter contains a manuscript on the oxidative degradation of triethylene glycol. The effect of temperature and oxygen on the stability of TEG was studied. Oxidative degradation products were identified and quantified. In addition, mechanisms for the formation of these are proposed.

Manuscript:

Høisæter, Karen K.; Buvik, Vanja; Gonzalez, Susana V.; Vevelstad, Solrun; & Knuutila, Hanna K. Oxidative Degradation of Triethylene Glycol. *Under revision*.

Oxidative Degradation of Triethylene Glycol

Karen K. Høisæter[a], Vanja Buvik[a], Susana V. Gonzalez[b], Solrun J. Vevelstad[c], Hanna K. Knuutila[a]*

[a] Department of Chemical Engineering, NTNU, NO-7491 Trondheim, Norway

[b] Department of Chemistry, NTNU, NO-7491 Trondheim, Norway

[c] SINTEF Industry, P.O.Box 4760 Torgarden, NO-7465, Norway

* Corresponding author: hanna.knuutila@ntnu.no

Abstract

Triethylene glycol (TEG) is unstable in the presence of oxygen and at high temperatures, though the degradation mechanisms occurring are not properly understood. In attempting to close some of the knowledge gaps, laboratory-scale degradation experiments have been conducted to assess the effect of temperature and oxygen on the stability of TEG. Oxidative degradation experiments with TEG and ethylene glycol (MEG) were conducted.

The oxidative degradation mechanism seems to change with temperature and oxygen concentration. Multiple oxidative degradation compounds of TEG were detected and quantified. These included MEG, diethylene glycol (DEG), formic acid, acetic acid, glycolic acid, formaldehyde, acetaldehyde, and water. Formic acid, MEG, and DEG are the dominant identified degradation products both at high temperatures and at high oxygen concentrations. In addition, the formation of CO_2 and larger, polymeric glycols was confirmed. The carbon and mass balance indicate unidentified degradation products in both the liquid and the gas phase.

Keywords

Gas dehydration, oxidative degradation, glycols

1 Introduction

When extracting natural gas from reservoirs, it typically consists of a complex mixture of components, including water.[1,2] The presence of water during processing and transportation can cause problems. The most severe one is the potential clogging of the pipelines caused by the formation of crystalline structures called hydrates.[3,4] These are cages of water surrounding smaller molecules, such as methane. Corrosion can also occur, as water condenses on the equipment.[5,6] Additionally, the presence of water in the natural gas increases the volume of the gas, while decreasing the heating value.[7] To reach quality specifications for transportation and sale, water must therefore be removed from the natural gas.

The most used technique to achieve this is glycol dehydration.[5,8,9] During this process, the wet natural gas is brought into contact with a glycol solvent and the water is absorbed. The water can afterwards be released from the glycol by applying heat, regenerating the glycol for reuse. Ethylene glycol (MEG), diethylene glycol (DEG), triethylene glycol (TEG) and tetraethylene glycol (TREG) are commonly available glycols for dehydration. For this application, they have high absorption efficiency, can be easily regenerated, are in themselves non-corrosive, have a minimal capacity to absorb hydrocarbons and have a low cost.[7] Of the beforementioned glycols, TEG is the most common glycol used in the industry.[10] This is because it gives lower solvent losses and has a higher thermal degradation temperature than the others, meaning that a higher purity of the lean glycol is possible to achieve.

When glycols are exposed to oxygen or high temperatures it can lead to oxidative or thermal degradation of the glycol. The degradation products formed can cause operational issues, such as foaming, corrosion, and loss of performance.[7,11] Glycol degradation is an acknowledged problem, but little has been published on the degradation reactions taking place or on the compounds formed. Of the glycols mentioned above, most literature is available on the degradation of MEG. Of the remaining, the published literature is scarce.

In this work, we endeavor to identify the degradation patterns of TEG. To do this, oxidation experiments have been conducted at lab-scale. In the oxidative degradation experiments, the effects of oxygen and temperature were studied by varying these parameters in solutions of pure TEG. As a comparison, and to gain a better understanding of the chemical reactions taking place during the degradation of TEG, oxidative degradation of MEG was also studied. In addition to studying the effect of oxygen and temperature on the stability of TEG, this study aimed at identifying and quantifying degradation products.

1.1 Oxidative Degradation

Oxidative degradation, often called thermal oxidative degradation, is the degradation mechanisms occurring when the glycol decomposes in the presence of an oxidizing agent, such as oxygen. In general, the literature on the oxidative degradation of TEG is lacking. There is, however, some literature available on the oxidative degradation of other glycols than TEG. This can be of relevance for the degradation of TEG, as the likeness in the structure of the glycols can make the chemical reactions occurring for other glycols transferable to the TEG system.

Mokhatab et al.[7] describe that as TEG oxidatively degrades, corrosive acids are formed. This is supported by Forster,[12] who further proposed that the oxidative degradation of TEG occurs through oxidation reactions of the ether groups to form peroxide radicals. These then degrade into smaller compounds, like smaller glycols (e.g., MEG), ethers, esters, organic acids, and aldehydes. These are presented as possible products of the degradation, but no data on their formation is provided. Their formation, however, is supported by literature on comparable reactions of ether and alcohol oxidation.[13]

In a study performed by Lloyd et al.[14], the oxidative degradation of DEG is studied. They report that formic acid, formaldehyde, diethylene glycol formate, water, MEG, and 1,3-dioxolane is formed during autoxidation of DEG. In addition to these, peroxides were suspected to have formed. No CO_2 was detected in the gas phase during these experiments.

The literature on MEG degradation describes mainly the formation of organic acids, formic acid, acetic acid, glycolic acid, oxalic acid, and glyoxylic acid.[15–18] These are expected to form through the oxidation of the alcohol groups. There is a focus on these in the literature, as they have been found to be a simple but good indicator to determine the state of the glycol.[19] Brown et al.[20] reports the formation of CO_2 during the oxidative degradation of aqueous MEG solutions and Psarrou et al.[18] propose the formation of water during the oxidation, but no data is provided for the latter.

Oxidative degradation of TREG has been reported to result in radical reactions forming hydroperoxides of the ethers in a study by Glastrup et al.[21] and Glastrup[22]. Hydroperoxides of the glycol ethers were reported to form through radical reactions. In addition, the oxidation of TREG was found to result in bond breakage and formation of a shortened glycol molecule and formic acid. The formed formic acid was reported to react with TREG to form monoTREG formate followed by diTREG formate.

2 Materials and Methods

2.1 Chemicals

All solutions were prepared gravimetrically. The chemicals used in the experiments and analyses are listed in Table 1. Oxygen (O_2, N5.0) was purchased from AGA. The deionized water was obtained from the local water purifying system at NTNU.

Table 1: Details on chemicals used in this study.

Chemical name	Abbrev.	Structure	CAS-number	Purity
Triethylene glycol [a]	TEG	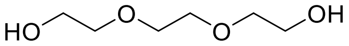	112-27-6	> 99%
Diethylene glycol [a]	DEG	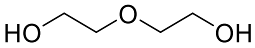	111-46-6	> 99%
Ethylene glycol [a]	MEG	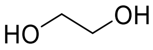	107-21-1	> 99%
Acetic acid [a]	-	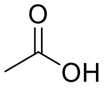	64-19-7	> 99.8%
Formic acid [a]	-	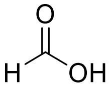	64-18-6	> 98%
Glycolic acid [a]	-	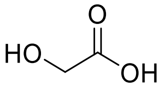	79-14-1	99%
Glyoxylic acid [a]	-	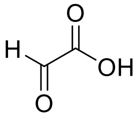	298-12-4	50wt% in water
Oxalic acid [a]	-	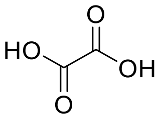	144-62-7	> 99%
Glycolaldehyde dimer [a]	-	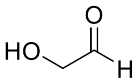	141-46-8	-

Glyoxal [a]	-	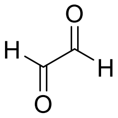	131543-46-9	40wt% in water
Formaldehyde	-	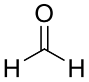	50-00-0	- [b]
Acetaldehyde	-	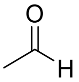	75-07-0	- [b]
Sulphuric acid [a]	H_2SO_4		7664-93-9	95-98%
Ethanolamine [a]	MEA	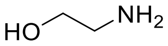	141-43-5	99%

[a] Purchased from Sigma-Aldrich Norway AS/Merck Life Sciences.

[b] Analysed by an external laboratory. Purity is not available.

2.2 Experimental Procedure

To study the oxidative degradation mechanisms of TEG, experiments were performed in a custom-made semi-open batch setup, as shown in Figure 1. The glass reactors (1.5 L) were filled with 1.2 L of glycol and placed in electrical heating mantles from ITA with magnetic stirring. Condensers cooled to 5 °C by a water bath were connected to the reactors. The gas, a blend of nitrogen and oxygen, entered the system through mass flow controllers at 200 mL/min and was introduced into the solutions through glass spargers (grade 1). The gas was recycled with a pump. Using the pump allowed the large circulation of gas and enhanced contact between the solutions and oxygen, while the small addition of oxygen and nitrogen blends ensure relatively constant oxygen concentration in the circulating gas. A small fraction of the gas was bled out of the system through a 2,4-dinitrophenylhydrazine (DNPH, 800 mg) cartridge and an acid wash (1M H_2SO_4). A similar approach to studying oxidative degradation has been employed previously in several works.[23]

The degradation experiment of TEG was conducted in the oxidative degradation set-up in two sets. In the first set, pure TEG was degraded at 75, 100, 125, and 150°C, with 6vol% oxygen in the gas flow. In the second set, pure TEG was degraded at 100°C, with oxygen concentrations of 1vol%, 6vol%, 12vol%, and 24vol%. Lastly, an additional experiment with TEG was conducted at 100 °C, with 24vol% oxygen. During this experiment, the DNPH cartridge and the acid wash were removed and replaced by three base washes (30wt% MEA, *aq.*), to capture and identify acidic components in the bleed gas. Lastly, the oxidative stability of MEG was studied in the degradation set-up. Two experiments were conducted with 24vol% O_2, one at 100 °C and one at 150 °C. All experiments were conducted with two parallel runs, and all the results are presented as averages of two experiments.

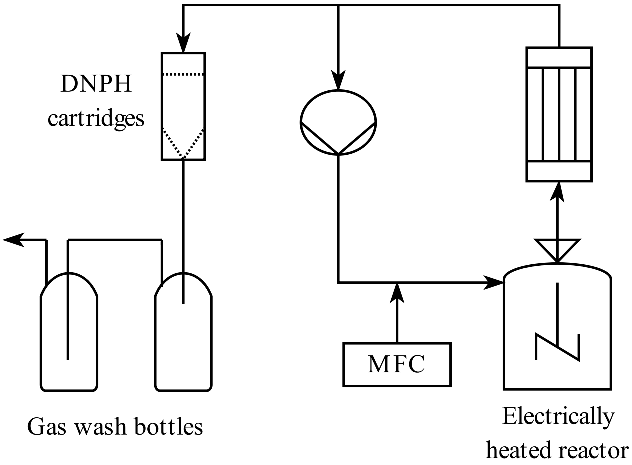

Figure 1: Schematic of degradation set-up used for the oxidative degradation experiments. The two parallels were run simultaneously on two identical set-ups.

2.3 Analytical Methods

Quantification of ethylene glycol (MEG), diethylene glycol (DEG), and triethylene glycol (TEG) was done using *Gas-Chromatography* coupled with a *Flame Ionization Detector* (GC-FID). This was done on an Agilent 7890A equipped with a DB-WAX Ultra Inert fused silica column (length 30 m, inner diameter 0.25mm, film thickness 0.25 µm). The samples were diluted with methanol to contain <1000 ppm glycol. The accuracy of the method was 3%, and the precision was 1%. The analytical method is described in detail elsewhere.[24]

Small organic acids were analyzed using *High-Performance Liquid Chromatography* coupled with an *Ultraviolet detector* (HPLC-UV). The method was performed on a PL1170-6830 (Agilent HiPlex H) column. Real samples were diluted in MilliPore water to approximately 50000 ppm of the sample and filtered through 0.2 µm syringe filters before analysis. The accuracy for the quantification of formic acid and acetic acid was 2%, glycolic acid was 4%, glyoxylic acid was 8%, and for oxalic acid it was

10%. The precision for all acids was 2%. The analytical method is described in detail elsewhere.[24]

Aldehydes captured in the DNPH cartridges and acid washes, as well as acids and nitrogen-containing components in the base washes, were analyzed by SINTEF Industries using *High Performance Liquid-Chromatography* (HPLC) coupled with a *Mass Spectrometer* (MS). All analyses were performed on an Agilent Technologies 1290 Infinity with an Agilent Technologies 6495 Triple Quad MS. For the analysis of formaldehyde and acetaldehyde an Ascentis® Express C8, 2.7 Micron HPLC column (53843-U) was used. The ionization technique was electrospray ionization (ESI). LOQ for both analytes were 10 ng/mL, and the uncertainty of the method was ± 3%. Before analysis, the samples were diluted and derivatized with DNPH. Formic, glycolic, and acetic acid were analyzed using a Waters Acquity UPLC HSS T3 column (100Å, 1.8µm, 2.1 x 150 mm) and ESI. LOQ was 100 ng/mL, 10 ng/mL, and 50 ng/mL for formic, glycolic, and acetic acid, respectively. The uncertainty of the method was ± 3% for formic and acetic acid and ± 5% for glycolic acid. Sample preparation consisted of dilution and derivatization with 3-nitrophenylhydrazine. The concentration of MEA in the base washes was analyzed on an Ascentis® Express Phenyl-Hexyl, 2.7 µm HPLC column and ESI. LOQ was 1 ng/mL, and the uncertainty was ± 3%. Lastly, the various amine-containing species were analyzed on a Discovery® HS F5 HPLC column and with EI. Samples were diluted before analysis, and the uncertainties were ± 5%. Compounds and their LOQ are presented in Table A1 in Supporting Information.

The water concentration in the end samples was measured by *Karl Fischer titration*. This was performed by SINTEF Industry on a Mettler Toledo V20 with a volumetric titration method. The solvent used was Methanol dry (Hydranal®) and the titrant was Composite 5 (Hydranal®). Each sample was analyzed two times and the presented value is the average of these results. For the degraded TEG samples, the highest relative standard deviation was 4%.

Amine titration with sulfuric acid (H_2SO_4, 0.2 N) as described by Ma'mun et al.[25] was used to analyze the concentration of MEA in the base washes. This procedure has an uncertainty of $\leq$ 2%.

Total Organic Carbon (TOC) analyses were performed on a Shimadzu TOC-LCPH analyzer equipped with an auto sample injector (ASI). The total amount of organic carbon in the end samples was determined by total carbon (TC) mode, subtracting the total inorganic carbon (TIC). The CO_2 content in the base washes was also determined by TIC analysis. The instrument was calibrated with a TC calibration standard

(1000 mg/L) acquired from Sigma-Aldrich for the TOC analysis and sodium bicarbonate ($NaHCO_3$, CAS: 144-55-8) for the TIC analysis. Samples were diluted 1:10000 with MilliPore water. The calibration range was 0-500 ppm. This was done over three calibration curves, 0-25 ppm, 25-150 ppm, and 150-500 ppm, which all had $R^2>0.9995$. The uncertainty was $\leq 2\%$.

The *Nuclear Magnetic Resonance* (NMR) experiments were performed at 26.8 °C on a Bruker 600 MHz Avance III HD equipped with a 5 mm cryogenic CP-TCI z-gradient probe. The lock solvent was deuterated water (D_2O), and the internal reference standard was tri(trimethylsilyl)phosphine (TMSP). These were added to coaxial inserts placed inside the NMR tubes. The coaxial insert was filled with D_2O and TMSP (2wt%), while the outer NMR tube was filled with the solution to be analyzed. For shift assignments, ^1H, ^{13}C, COSY (correlation spectroscopy), HSQC (heteronuclear single-quantum correlation spectroscopy), and HMBC (heteronuclear multiple-bond correlation spectroscopy) NMR spectra were obtained. The spectra were analyzed in the software Bruker TopSpin 4.0.7.

Two analytical setups were used for the MS scans of the most degraded samples, on a GC-MS system and one on an Ultra-Performance Liquid Chromatography (UPLC)-MS system. The samples from the experiment were diluted with methanol to 700 ppm. When running coelutions with standards, the solutions were diluted so the degraded samples had concentrations of 250 ppm and the standards had concentrations of 70 ppm. The GC analysis of the samples was performed with an Agilent 7890A gas chromatograph with an injector ALS 7683B autosampler coupled to an Agilent 5975 single quadrupole mass spectrometer. Chromatographic separation was performed on a DB Wax-UI GC Column (30 m x 0.25 mm inner diameter x 0.25 µm film thickness), keeping the carrier gas flow (helium) at 1 mL/min, and the transfer line and the injection port temperatures at 250 °C. One short and one extended temperature method were performed. The short method's temperature program was as follows: starting at 100 °C for 1 min, followed by a temperature increase at a rate of 10 °C/min to 250 °C and held for 4 min. The overall analysis time for one sample with the selected temperature program was 20 min. The extended method's temperature program was as follows: starting at 100 °C for 1 min, followed by a temperature increase at a rate of 10 °C/min to 250 °C and held for 1 min, then temperature increase by 1°C/min to 260 °C, and held for 5 min. The overall analysis time for one sample with the extended temperature program was 35 min. The injection volume was 1 µL in splitless mode and the solvent delay was set to 5 min. The mass detector was operated in full scan mode (from 30 m/z to

550 m/z) using electron impact ionization (EI) set at 70 eV. The source temperature was set to 230 °C and the quadrupole to 150 °C.

The LC analysis was performed using an ACQUITY UPLC I Class® system connected to a Synapt G2-S Mass spectrometry detector (Waters Corporation, Milford, USA) with positive electrospray ionization sources (ESI+). 200 ng/mL of leucine enkephalin was used as a Lockmass at a flow rate of 10 µL/min to allow correction of exact mass measurements. An Acquity UPLC HSS T3 (2.1 mm × 100 mm, 1.7 µm) chromatographic column was used for reverse-phase separation. Instrumental blanks were run before and after every sample to check for carryover or cross-contamination. A mix of water:methanol (95:5) with 2 mM ammonium acetate (A) and methanol with 2 mM ammonium acetate (B) was used as mobile phase. The injection volume was 1 µL and the flow rate was 0.3 mL/min. The chromatographic gradient used was: initial conditions 100% A; 0.00-1.00 min, 100-80% A; 1.00–6.00 min, 80-55% A; 6.00–13 min, 55-20% A; 13.00–14.00 min, 20-5% A; 14.00–17.00 min, 5% A; 17.00–18.00 min, 5-100% A; 18.00–22.00 min, 100% A. The column temperature was maintained at 35 °C. The capillary voltage was set at + 2.50 kV (ESI+), the desolvation flow was fixed at 800 L/h with a desolvation temperature set at 350°C and the cone voltage set at 20 V. Source Temperature was set to 120 °C. The full scan spectra were acquired within a range of 50 to 1500 m/z. The UPLC-QTOF-MS data was acquired using Masslynx V4.1 and processed with Progenesis QI V2.3 (Waters, Milford, USA).

3 Results and discussion

The focus of this work was to identify degradation patterns in TEG and assess the effect of different parameters on degradation. This has been done through two sets of oxidative degradation experiments with pure TEG: one with varying temperatures of the liquid and one with varying oxygen concentration in the gas flow. The results from these will be presented in Sections 3.1 and 3.2, respectively. Following this, the mass balance will be evaluated in Section 3.3 and the identification of additional degradation products by mass spectrometry (MS) will be presented in Section 3.4. Lastly, the results from the oxidative degradation of MEG will be presented in Section 3.5. All degradation data given will be presented as figures. The error bars included in the plots represent the standard deviation between the two parallels. Data for these, and associated analyses, are given in Section B in Supporting Information.

3.1 Effect of temperature

In the first set of oxidative experiments, the focus was on studying the effect of temperature on the oxidative degradation mechanisms of TEG. This was done through the degradation of pure TEG at four different temperatures. The temperatures were: 75 °C, 100 °C, 125 °C, and 150 °C. In all four cases, the oxygen content in the gas was 6%. Each experiment was supposed to last for 14 days, but the experiments at 125 °C and 150 °C were ended after 11 and 17 days, respectively, due to problems with temperature control. In both cases, there was a temperature drop in the solutions, possibly due to a change in the solvent composition. For the experiment at 150 °C, the temperature in both reactors dropped to 120-121 °C on day 7. Turning the effect of the heating mantle up on the two parallels over the next two days resulted in boiling/vapor formation in both solutions, while the temperature did not exceed 130-135 °C. Over these two days, the color of both solutions changed from light yellow to red/orange. On day 9, the temperature was back up to 146-147 °C and the boiling had stopped. The experiment at 125 °C had a similar temperature drop during day 9 when the temperature dropped to 120-121 °C. For this experiment, however, the heater effect was kept constant, and the experiment ended on day 11.

During the oxidative degradation experiments, the concentration of TEG was monitored with GC-FID. The results from the experiments at different temperatures are presented in Figure 2. The oxidative degradation rate increases with increased temperature. This is in line with what has been suggested in the literature.[12]

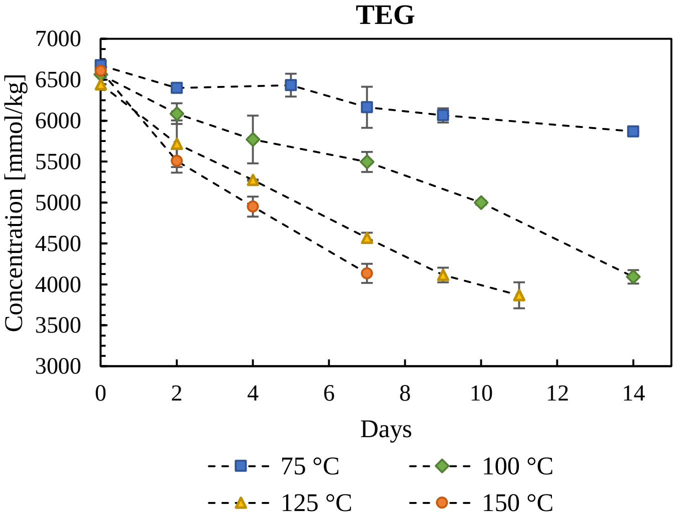

Figure 2: Effect of temperature on the oxidative degradation of TEG (6% O_2) at various temperatures.

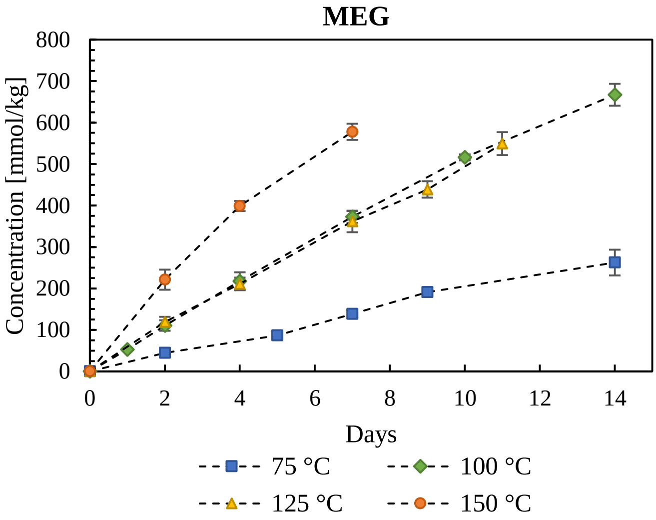

Figure 3: Effect of temperature on the formation of MEG during oxidative degradation of TEG (6% O_2).

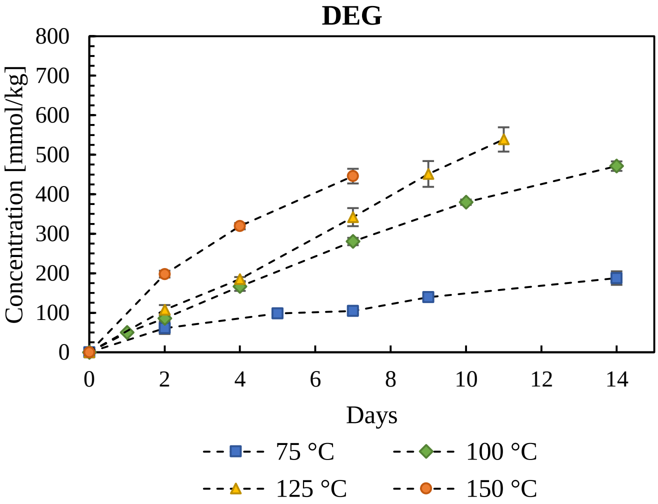

Figure 4: Effect of temperature on the formation of DEG during oxidative degradation of TEG (6% O_2).

The formation of monoethylene glycol (MEG) and diethylene glycol (DEG) was also monitored throughout the experiments with GC-FID. The results are presented in Figure 3 and Figure 4, respectively. Small amounts of DEG were found in the start solution of TEG, though these were below LOQ. The increase in temperature results in an increase in the formation rate of both MEG and DEG. There is, however, little distinction between the amounts of MEG formed at 100 °C and 125 °C. The reason for this is unknown. In general, MEG was found in larger quantities than DEG, though throughout the experiment at 125 °C they are found at almost identical concentrations. Higher concentrations of MEG can either point to DEG having a shorter lifetime as an intermediate or that the mechanism forming MEG is favored.

The formation of MEG and DEG can be expected to stem from the oxidation of the ether groups of TEG.[13] Depending on which side of the ether groups the radical propagation occurs, either MEG or DEG can be formed. Scheme 1 shows a proposed oxidation pathway for the formation of DEG. In this case, the oxygen radical breaks the ether bond on the side closest to the alcohol group. After the termination of the radical by radical hydrogenation (RH), the result is DEG and glycolaldehyde (CAS: 141-46-8). If the oxygen radical breaks the ether bond on the other side following the same reaction path, MEG would be formed, see Scheme 2 a). The resulting aldehyde would in this case be 2-(2-hydroxyethoxy)acetaldehyde (CAS: 17976-70-4). Once DEG is formed, it is also possible that MEG forms from the oxidation of DEG. A proposed oxidation path for this is shown in Scheme 2 b). In this case, glycol aldehyde would be formed. Both aldehydes can potentially be further oxidized to form their corresponding carboxylic acids.

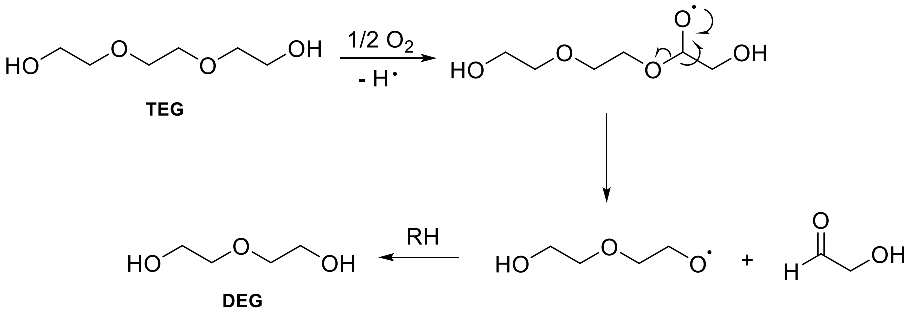

Scheme 1: Proposed oxidation path for the formation of DEG from TEG.

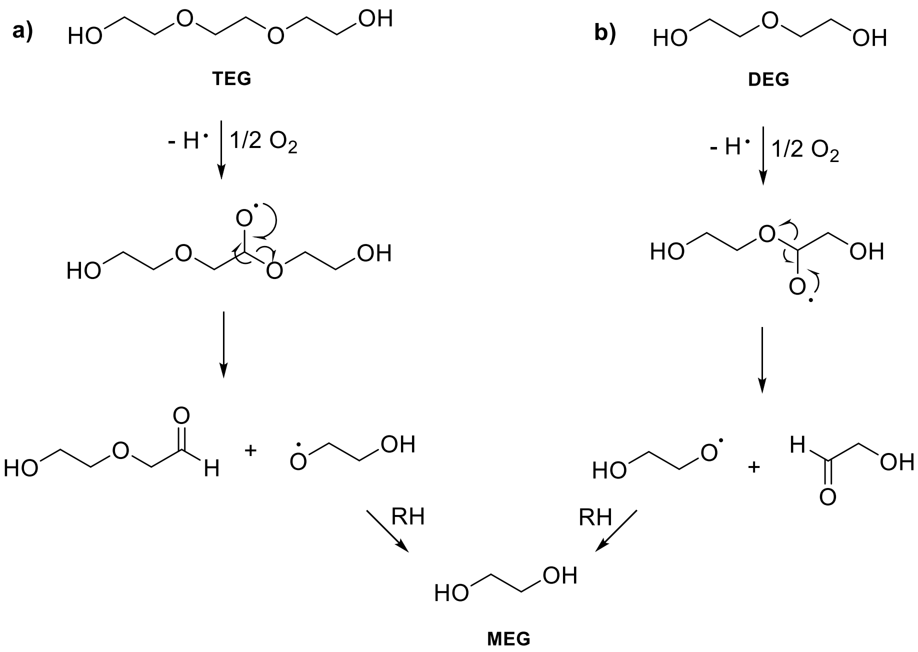

Scheme 2: Proposed oxidation path for the formation of MEG from TEG (a) or DEG (b).

Formic, glycolic, acetic, and glyoxylic acids were analyzed with HPLC and found to have formed in all these experiments. Figure 5 shows the formation of formic acid. The formic acid buildup increases with increasing temperature. At higher temperatures, however, the effect of this increase seems to lessen. A possible explanation can be the increased volatility of the acid at higher temperatures. To investigate this, the acid washes of the end solutions were analyzed, and formic acid was detected. It was, however, not found in significant amounts compared to the concentrations in the reactors. Ruling this out, a likely possibility can therefore be that the oxygen concentration becomes the limiting factor at a certain temperature above 100 °C. The concentrations of the organic acids found in the acid washes are presented in Table B5 in the Supporting Information.

Glycolic and acetic acid, presented in Figure 6 and Figure 7, were formed in lower concentrations than formic acid. In both cases, the formation does not seem to be temperature dependent. Above 100 °C, the formation of glycolic acid goes down. This can be because it further oxidized more quickly at higher temperatures, thus becoming a less stable intermediate. It can also be that at temperatures above 100 °C, reactions between glycolic acid and other compounds in the solution become more favorable. These were not detected in the acid washes. Oxalic acid was only formed in a concentration above the LOQ at the end of the experiments, while glyoxylic acid was not detected at all.

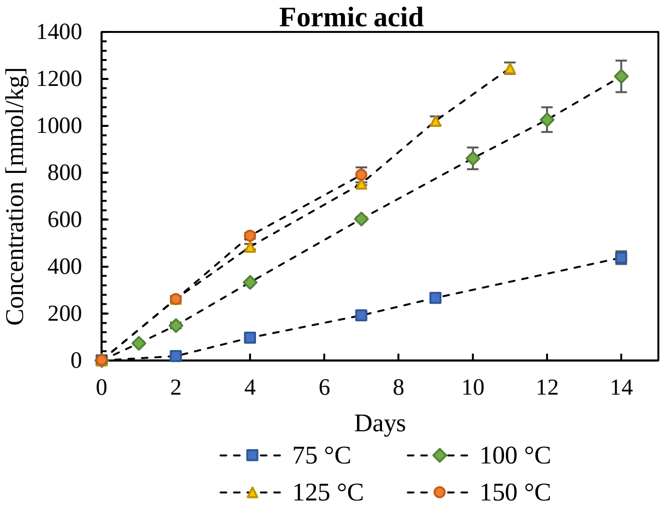

Figure 5: Effect of temperature on the formation of formic acid during oxidative degradation of TEG (6% O_2).

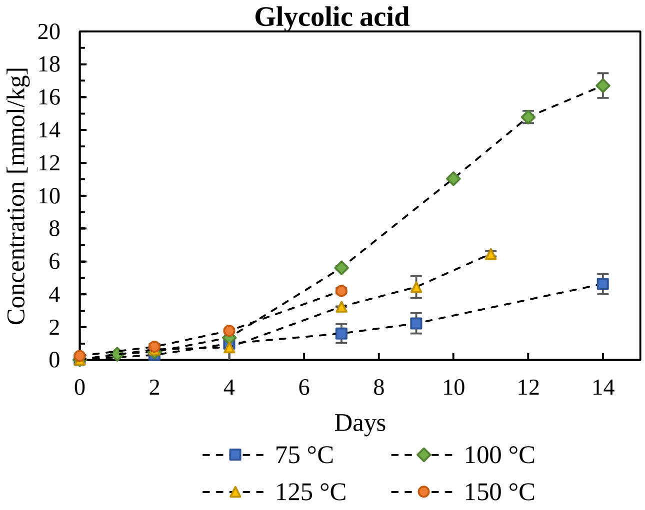

Figure 6: Effect of temperature on the formation of glycolic during oxidative degradation of TEG (6% O_2).

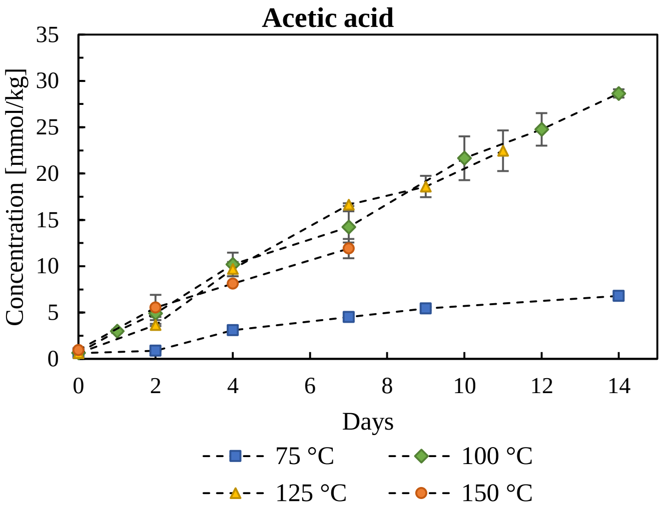

Figure 7: Effect of temperature on the formation of acetic during oxidative degradation of TEG (6% O_2).

The detected acids are known oxidative degradation products of MEG. It is therefore conceivable that they are formed as secondary degradation products of MEG in the degraded solutions. A proposed oxidation path of the acids starting from MEG is presented in Scheme 3. This pathway follows a general oxidation route where alcohols are oxidized to aldehydes, and aldehydes are oxidized to carboxylic acids.[13] Each step would consume 0.5 mol O_2 and could potentially produce one mole of water. The last step of this pathway is the decarboxylation of oxalic acid, forming formic acid and CO_2. Theoretical studies of the decarboxylation from oxalic acid to formic acid and CO_2 have been performed in other works.[26] Similar pathways have been proposed for oxidation reactions of MEG on palladium and platinum[27,28]. If glycolaldehyde forms in the routes to MEG and DEG, as presented in Scheme 1 and Scheme 2, the oxidation of this will also contribute to the acid formation.

The reaction path presented in Scheme 3 covers all the acids detected in the experiments except acetic acid. However, the formation of acetic acid can be accounted for as an expected oxidation product from the oxidation of acetaldehyde, as presented in Scheme 4. The formation of acetaldehyde will be covered later in this section. The presence of glyoxal and glycolaldehyde was also tested with HPLC-UV and -RI, but these were not detected in any of the samples.

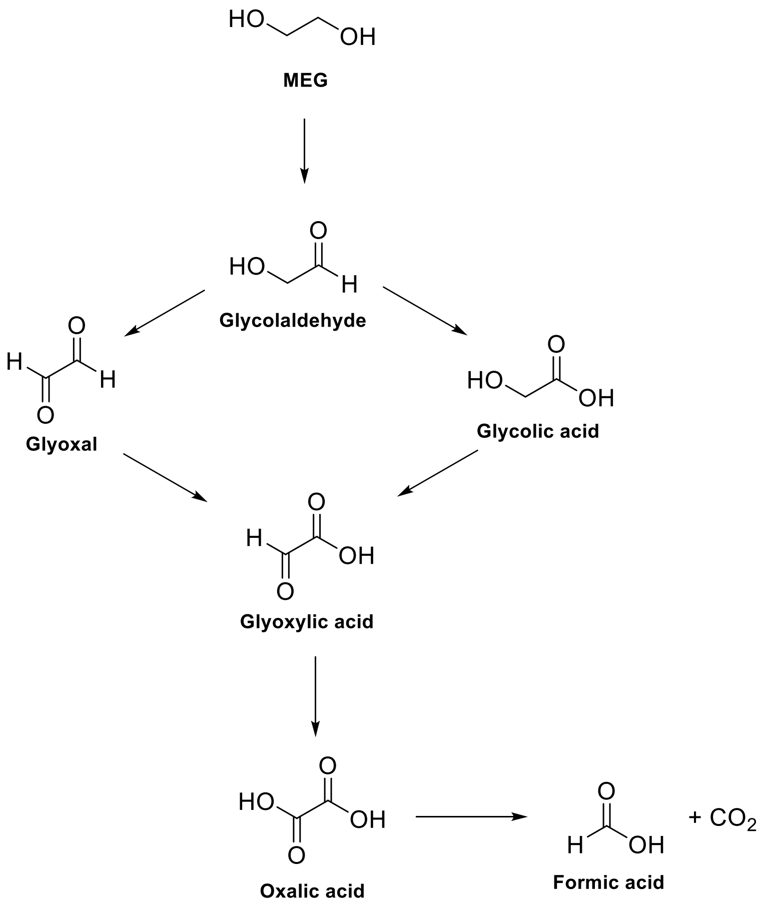

Scheme 3: Proposed oxidation path from MEG to form the different organic acids.

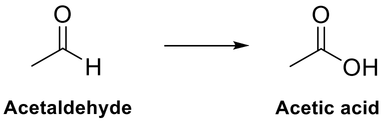

Scheme 4: Oxidation of acetaldehyde to acetic acid.

To investigate the possible formation of water during the oxidative degradation of TEG, the water concentration in the start and end solutions was measured by Karl-Fischer titration. Since the degradation rig is semi-closed and the gas is dry, the water that was found was expected to have formed through the degradation of compounds in the solution. Figure 8 shows the amount of water formed in the different experiments. As the experiments had different durations, the values are normalized to show formation per day the experiment ran. It can be observed that with the increase in temperature, and thus the increase in TEG degradation, increasing amounts of water were formed.

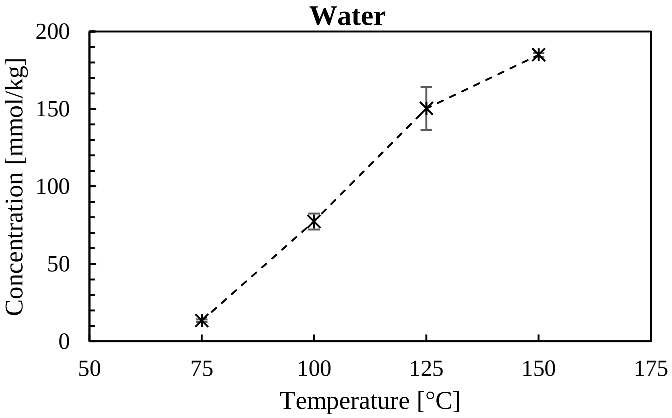

Figure 8: Formation of water per day during the oxidative degradation of TEG (6% O_2) at various temperatures.

In reactions including alcohols and carboxylic acids, water is typically formed through dehydration reactions like etherification and esterification. Etherification is a typically acid-catalyzed dehydration reaction between two alcohol groups, forming an ether. Scheme 5 a) shows a general etherification reaction. Depending on which glycols are reacting in this dehydration, bigger glycol compounds could be formed. Esterification is also typically acid-catalyzed and occurs as an alcohol attacks the carbon in a carboxyl group. A simplified reaction is shown in Scheme 5 b). Also, in this case, the resulting ester depends on which glycol and which acid is reacting.

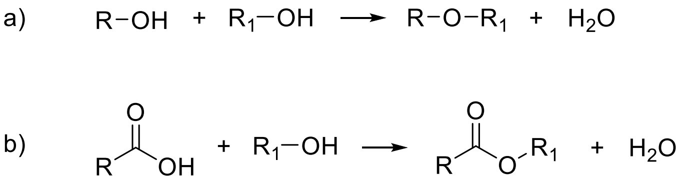

Scheme 5: a) General etherification reaction resulting in the formation of water and b) general esterification reaction resulting in the formation of water.

A DNPH cartridge and an acid wash were added to the bleed gas outlet of the oxidation rig. With these connected, volatile, organic compounds such as small aldehydes could be captured and detected if these formed during the degradation experiments. The compounds that were analyzed are formaldehyde and acetaldehyde. The total amount of each compound captured in the DNPH cartridge and acid wash in each experiment, normalized per day, is shown in Figure 9. At the two lower temperatures, the concentrations of formaldehyde are quite low, while in the higher temperature ranges, more is being captured. This can be both because more of the compounds are formed at the higher temperatures, but also because the evaporation is higher. The formation of acetaldehyde seems to increase with the increasing temperature but falls again at 150 °C. The cause of this is unknown. If it is an intermediate, it might be that the relative rate of formation and disappearance reaction changes with the temperature. It should be noted that it is uncertain whether all the volatile compounds formed were captured, so the actual amount formed might be higher than what is presented in the graph.

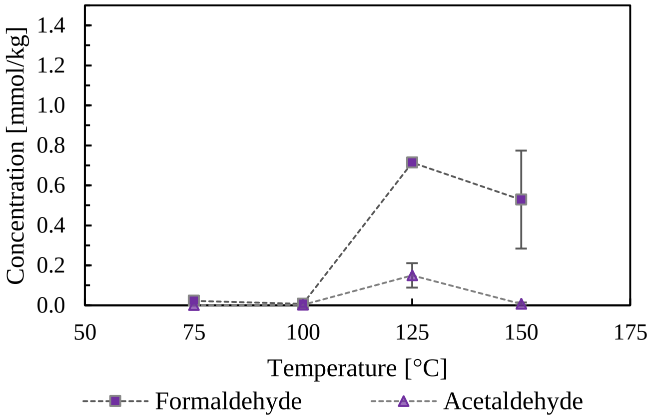

Figure 9: Total amount of captured formaldehyde and acetaldehyde in the DNPH cartridge and acid wash (1M H_2SO_4) per day during the oxidative degradation of TEG (6% O_2) at various temperatures. The values are corrected to correspond to per mass of the end solution in the reactor.

The formation of the aldehydes can occur along the formation of MEG and DEG, as described in Scheme 1 and Scheme 2. The formation of acetaldehyde could also be taking place through a rearrangement reaction from MEG. This rearrangement involves a hydrogen migration. The mechanism for this rearrangement reported to be the most favorable by Smith[29] is presented in Scheme 6 a). The formation of formaldehyde could potentially happen through a rearrangement of the oxidized MEG, following a radical propagation (RP) and an addition of a hydroperoxyl radical. In addition to formaldehyde, formic acid would be formed through this reaction. This proposed oxidation rearrangement is presented in Scheme 6 b). Forster[12] reported the formation of ethanol and methanol during the degradation of TEG. These are not analyzed in this work due to a lack of suitable analytical methods. However, if these are formed, acetaldehyde and formaldehyde can also form through the oxidation of these.

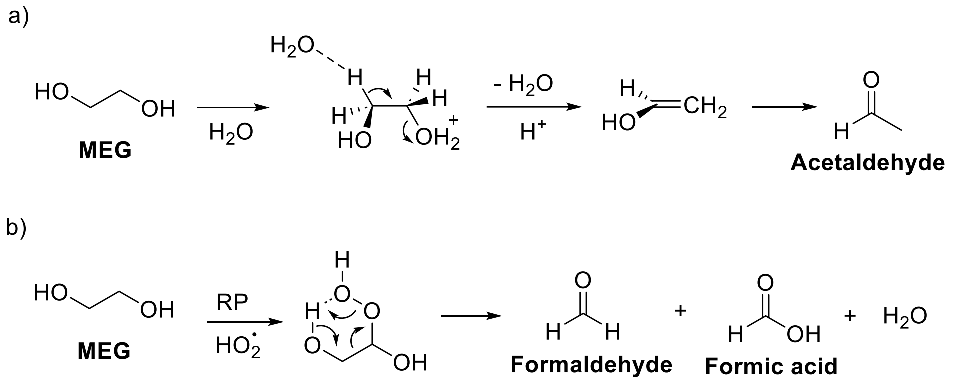

Scheme 6: a) Rearrangement mechanism from MEG to acetaldehyde[29] and b) proposed oxidation rearrangement from MEG to formaldehyde and formic acid.

3.2 Effect of oxygen concentration

In the second set of experiments, the effect of varying the oxygen concentration on the oxidative degradation of TEG was investigated. This was done through four oxidative degradation experiments of pure TEG at 100 °C, with 1%, 6%, 12%, and 24% oxygen in the gas flow. As in the previous set, the TEG degradation was monitored using GC-FID. The resulting loss of TEG in these experiments is shown in Figure 10. The degradation rate increases substantially with oxygen concentration.

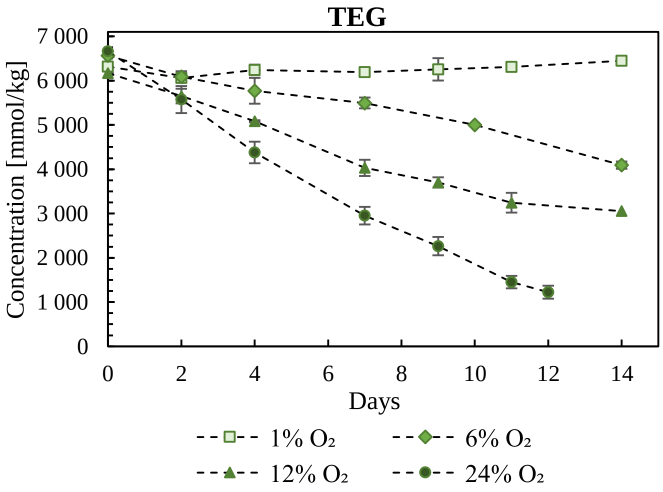

Figure 10: Effect of oxygen on the loss of TEG (100 °C) with various oxygen concentrations.

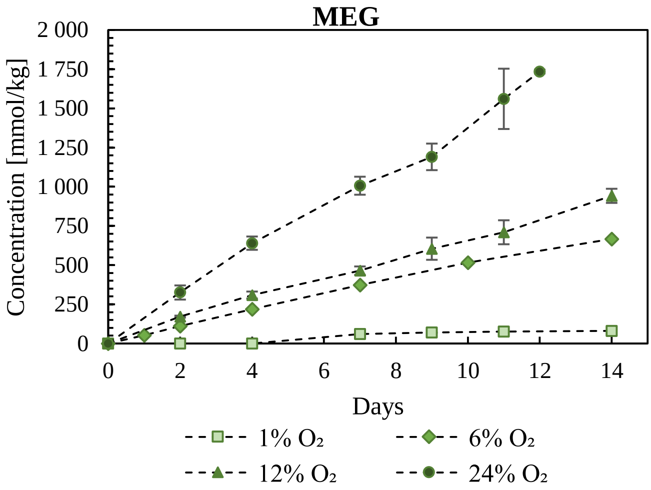

Figure 11: Formation of MEG during oxidative degradation of TEG (100 °C) with various oxygen concentrations in the gas flow.

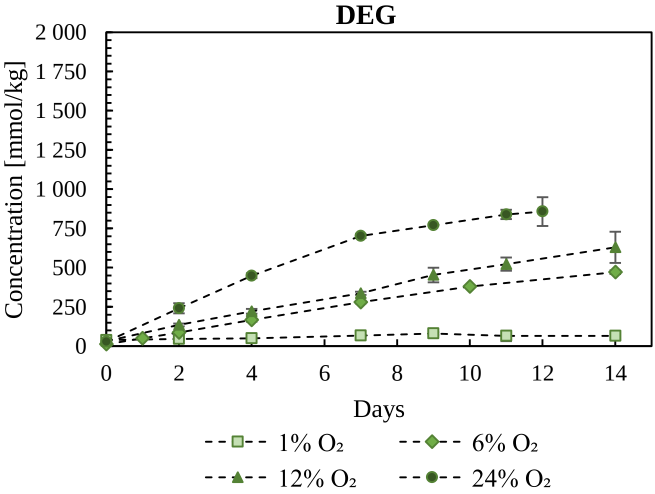

Figure 12: Formation of DEG during oxidative degradation of TEG (100 °C) with various oxygen concentrations in the gas flow.

The results from the analysis of MEG and DEG are shown in Figure 11 and Figure 12, respectively. The formation rates increase with the increase in oxygen available in the system, and in all experiments, MEG was formed in larger quantities than DEG. At the three lower oxygen concentrations, the formation of MEG and DEG follows a similar trend. At 24% oxygen, however, the formation of DEG seems to somewhat stagnate, while the MEG formation still has a steep increase. This can indicate that DEG is an intermediate that reaches an equilibrium at a certain stage.

The concentration of formic, glycolic, and acetic acid formed in these experiments are presented in Figure 13, Figure 14, and Figure 15, respectively. The formation of all three acids increases with the increase in oxygen concentration. For the experiment with 1% O_2, only formic acid is found above LOQ. The formation of formic acid with 24% in the gas flow is quite substantial, as it even surpasses the concentration of TEG in the system. Temperature and oxygen concentration do not seem to influence any favoritism of the acids. Although almost all acids were in higher concentration in this set of experiments, the formation of the acids is in the same order in the experiments with varying temperatures. In both cases, formic acid is the predominant acidic compound formed, followed by acetic acid and then glycolic acid. Glyoxylic and oxalic acid were only detected at the end of the experiment with 24% oxygen.

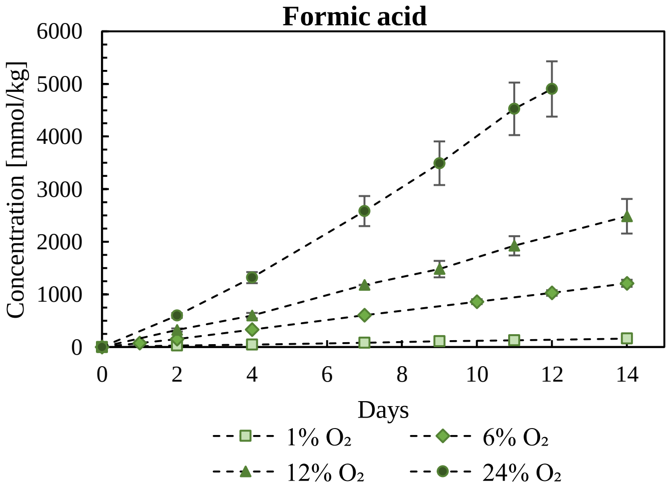

Figure 13: Formation of formic acid during oxidative degradation of TEG (100 °C) with various oxygen concentrations in the gas flow.

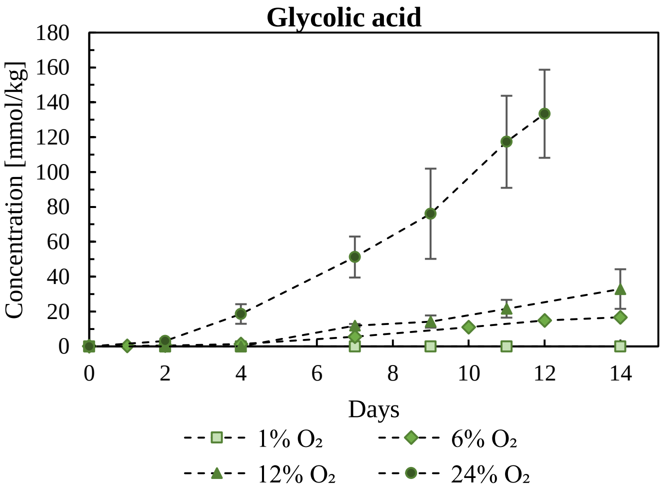

Figure 14: Formation of glycolic acid during oxidative degradation of TEG (100 °C) with various oxygen concentrations in the gas flow.

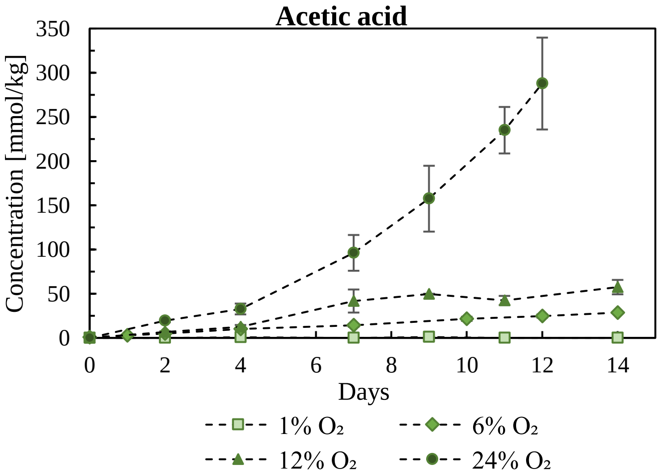

Figure 15: Formation of glycolic acid during oxidative degradation of TEG (100 °C) with various oxygen concentrations in the gas flow.

The formation of water was also measured for the solutions with increasing oxygen concentration. The resulting water concentrations are presented in Figure 16. The values are normalized to show formation per day the experiment ran. With an increase in oxygen concentration in the gas flow, the formation of water increases linearly. The water formation in the experiment at 150 °C and 6% oxygen was 0.51 mol water formed per mol TEG degraded, while it was 0.88 in the experiment at 100 °C and

24% oxygen. Hence, increasing either oxygen concentration or temperature increased the degradation rate, but this difference in water formation indicates that the degradation mechanisms are not the same.

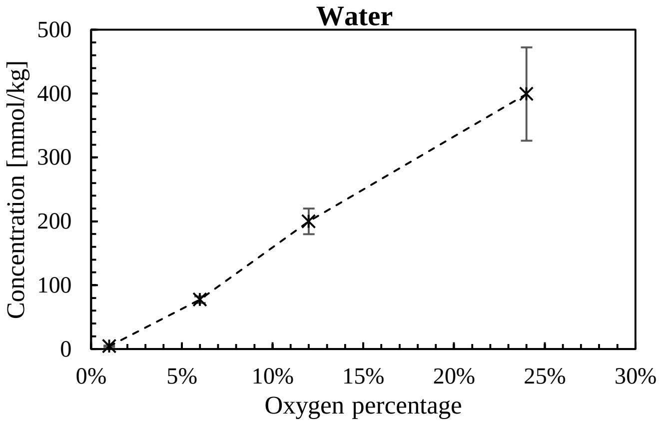

Figure 16: Formation of water per day during oxidative degradation of TEG (100 °C) with various oxygen concentrations in the gas flow.

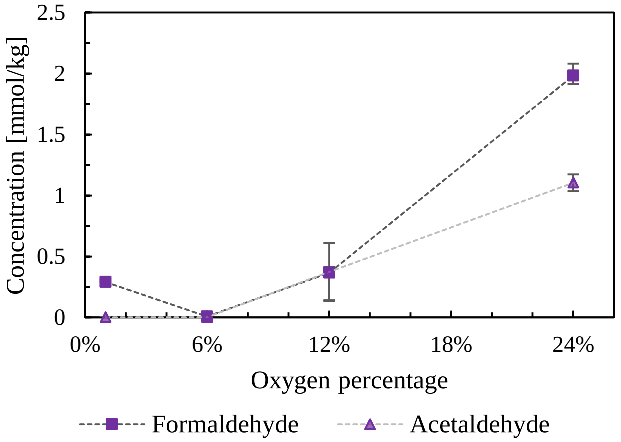

Figure 17: Total amount of captured formaldehyde and acetaldehyde in the DNPH cartridge and acid wash (1M H_2SO_4) per day during the oxidative degradation of TEG (100 °C) with various oxygen concentrations in the gas flow. The values are corrected to correspond to per mass of the end solution in the reactor.

Volatile, organic compounds were also captured in the experiments with higher oxygen concentrations. Figure 17 presents the total amount captured in the DNPH cartridge and the acid wash (1M H_2SO_4) normalized per day. With an increase in oxygen concentration, an increase in the formation of both compounds can be seen. The formaldehyde found at 1% oxygen is unexpected. At this oxygen concentration, there was very little degradation of TEG. It is unclear what is the reason for this, but the formaldehyde was found in both parallel experiments.

3.3 Mass and carbon balance

By summarizing the masses of the quantified degradation products and comparing this to the total mass of the end solutions, an estimate of the unidentified degradation compounds in the solution can be made. An overview of the composition of the end solution of the two experiments with the highest degradation in the two sets of experiments is presented in Figure 18. “High temperature” is the solution from day 7 of the experiment at 150 °C and 6% oxygen, while “High O_2 concentration” is the solution from day 12 of the experiment at 100 °C and 24% oxygen. The term marked “Unknown” accounts for the mass in each end-solution not covered by the quantified degradation products. It is important to note that as oxygen is added to the solutions, some of the detected mass might stem from oxygen that was not in the solution originally. Likewise, volatile degradation compounds have left the system, reducing the mass. Nevertheless, 20% and 27% of the mass in the end-solutions are not accounted for by the quantified degradation compounds.

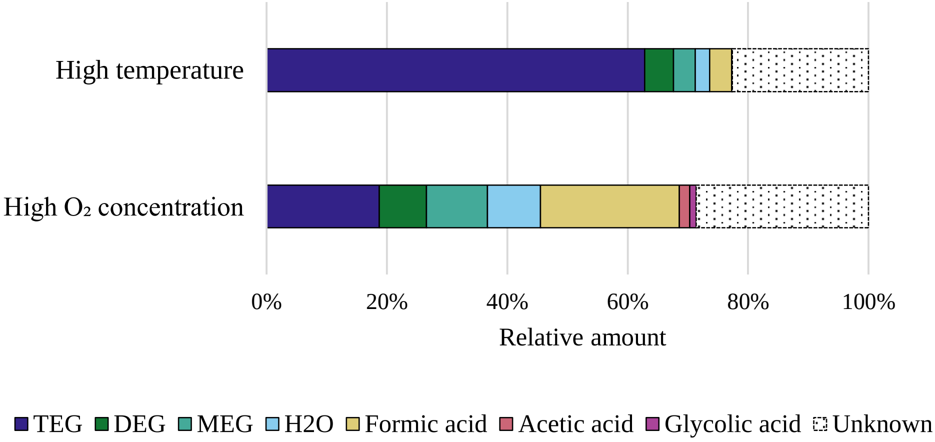

Figure 18: Overview of the different components’ contribution to the total mass of the end solutions in high temperature (150 °C, 6% O_2, day 7) and high O_2 concentration (100 °C, 24% O_2, day 12) experiments.

An interesting side note when comparing the composition of these two degraded solutions is their color. After the experiment with the highest oxygen concentration, the solution was still transparent and colorless like pure TEG. During the experiment at the highest temperature, however, the solution got a yellow tinge. This indicates that the component or components giving color to the solution have probably not been identified and are predominantly formed at high temperatures.

To further investigate the possibility of volatile degradation compounds no longer in the system, the total amount of carbon at the beginning of the experiments was compared to the amount of carbon detected in the solutions with TOC analysis. Figure 19 shows the overview of the carbon in the solutions with the highest loss of TEG in the two sets. The part named “Unknown” is the total sum of organic carbon detected in the solutions with the carbon accounted for by the quantified degradation compounds subtracted. The remaining part, named “Lost”, corresponds to the difference in carbon found in the end sample compared to the start sample of pure TEG. Glyoxylic acid, formaldehyde, and acetaldehyde are not included, as they do not contribute significantly to the end sum.

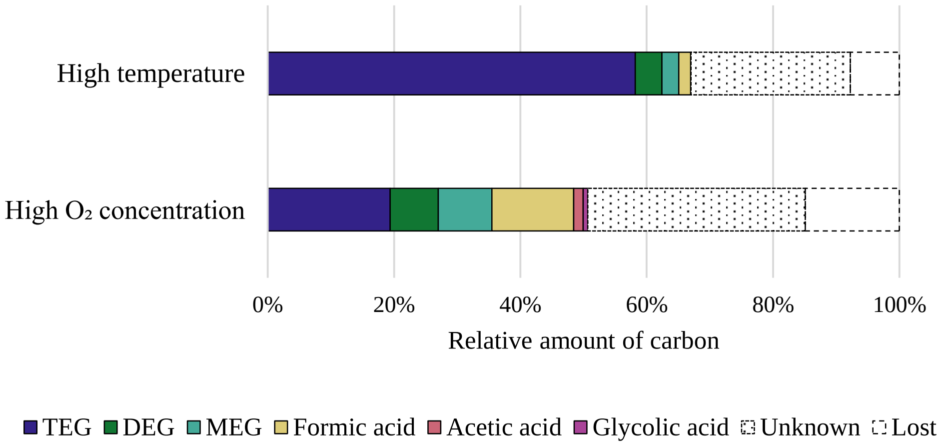

Figure 19: Overview of the different components' contribution to the carbon balance in high temperature (150 °C, 6% O_2, day 7) and high O_2 concentration (100 °C, 24% O_2, day 12) experiments.

As becomes clear from this overview, some carbon-containing compounds have left the system and have not been trapped or analyzed in the cartridges or the acid washes. A probable candidate as a volatile, carbon-containing degradation product is CO_2. As shown in the oxidation path in Scheme 3, CO_2 can potentially form through the decarboxylation of oxalic acid. It might also be formed through the decarboxylation of bigger compounds containing carboxylic acids. The mechanism of a general decarboxylation reaction is shown in Scheme 7.[13] To investigate the possible formation of CO_2 during the degradation of TEG, a new experiment with pure TEG was conducted with the purpose of capturing CO_2. Instead of the DNPH cartridge and acid wash, three base washes (30wt% MEA, aq.) were added to the outlet of each reactor. MEA is a well-known solvent commonly used for capturing CO_2 industrially. The reaction occurs between two moles of MEA with one mol of CO_2 resulting in the formation of MEA-carbamate and protonated MEA.[30,31] The reaction is presented in Scheme C1 in Supporting Information.

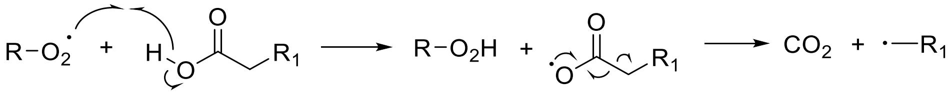

Scheme 7: General decarboxylation mechanism.[13]

The CO_2 captured in the base washes was analyzed with TIC and the total alkalinity with titration. These results can be found in Section C in the Supporting Information. The end solutions of the base washes were then analyzed with LC-MS for quantification of the organic acids and possible compounds formed through the reaction of MEA and the different acids.[32] In the latter category, the main compounds detected were (2-hydroxyethyl)-formamide (HEF, CAS: 693-06-1) and *N*-(2-hydroxyethyl)-acetamide (HEA, CAS: 142-26-7) shown in Figure C2 in the Supporting Information. These compounds are expected to stem from the reaction between MEA and formic acid and acetic acid, respectively. The resulting carbon balance for the last experiment is presented in Figure 24. In the carbon sum, each HEF molecule detected was assumed to stem from formic acid leaving the degradation setup. Oxidative degradation of MEA itself has been shown to form both HEF and HEA, but this is not expected to contribute significantly here due to the low

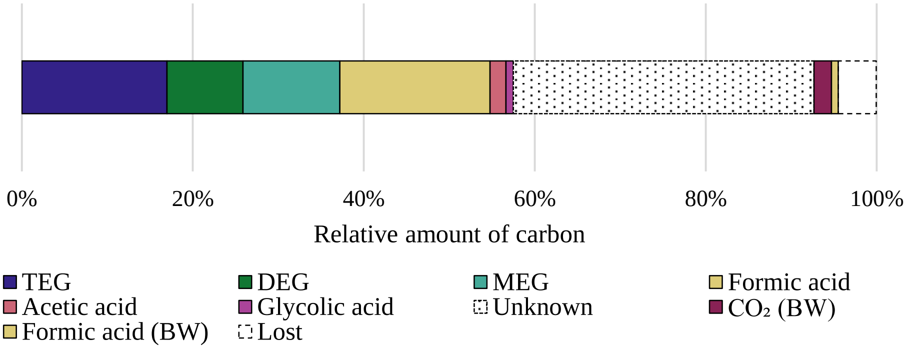

Figure 22: Overview of the different components' contribution to the carbon balance in the oxidative degradation experiment of TEG (100 °C, 24% O_2, day 14). BW indicates components detected in the base washes.

temperature in the base washes.[33] The base washes were also analyzed with GC-FID to determine whether any glycol had left the system. None were detected. With regards to the CO_2, though it was captured and quantified, it is plausible that some have escaped due to mass transfer limitations. Attempting to identify more of the unknown components in the solution.

3.4 Identification of New Degradation Compounds

In attempting to identify some of the unknown compounds in the liquid phase of the degraded TEG, a GC-MS analysis and a UPLC-MS analysis were conducted. Scans of the solution from day 12 of the experiment at 100 °C and 24% oxygen were conducted. The signal identification was confirmed by using standards and the full scan EI mass spectra of the identified compounds were in agreement with available MS Library spectra (NIST MS library). Additionally, some standards were acquired based on theoretically possible degradation compounds. All compounds positively identified with GC-MS are presented in Table 2, and all compounds tested with standards are presented in Section E in Supporting Information. All identified compounds were identified by retention time (RT) matching with known standards. However, a potential positive identification of 12-Crown-4 was debunked. This was because, even though the retention times and mass matched with a compound in the degraded solution, their fragmentation patterns did not match.

Processing the UPLC-MS data, Progenesis DFS studio software was used to create a library with mol files of possible molecules of interest. The peaks that were tested were based on this library, as well as the online Chemspider library. In addition, the tentative identifications were limited to those with ppm error below 5 ppm, and with the highest isotopic similarity and fragmentation score. From the results, one peak was tentatively identified, presented in Table 2. A standard was not available for the confirmation of this compound. Additional data for the UPLC-MS analysis can be found in Table D3 in Supporting Information.

The route for the formation of tetraethylene glycol and pentaethylene glycol is likely through etherifications of various glycols. In the reaction mixture, TEG, DEG, and MEG are known to be present. From these, tetraethylene glycol can either form through the etherification of a TEG and a MEG or from two DEG molecules. Likewise, pentaethylene glycol can form either through the etherification of tetraethylene glycol and MEG or from TEG and DEG. These reactions result in the formation of a water molecule, as presented in Scheme 5. The formation of the bigger glycols opens the possibility for bigger polymerization compounds being formed over longer timespans. Diethylene glycol monoethyl ether is likely formed through the dehydration reaction of TEG. This reaction is acid catalyzed and like the etherification reaction it results in the formation of a water molecule. The formation of diethylene glycol monoethyl ether presents an additional possibility for the formation of acetaldehyde. Starting with diethylene glycol monoethyl ether and following an oxidation path as presented in Scheme 1, acetaldehyde and DEG would be formed.

Table 2: Compounds positively and tentatively identified with MS scans.

Name	**CAS-number**	**Structure**
Positively identified compounds on GC-MS		
Diethylene glycol monoethyl ether	111-90-0	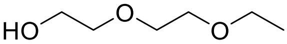
Tetraethylene glycol	112-60-7	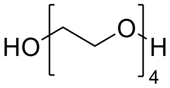
Pentaethylene glycol	4792-15-8	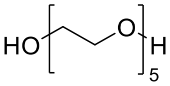
Tentatively identified compounds on LC-MS		
Triethylene glycol formate	1240369-67-8	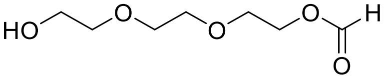

The formation of triethylene glycol formate could be the result of a dehydration reaction with TEG and formic acid. Some tests were conducted to strengthen this possibility. By mixing the TEG and formic acid at room temperature and analyzing with NMR, triethylene glycol formate was found to have formed. Details of this test can be found in Section F in the Supporting Information. The possible formation of triethylene glycol formate also opens to the formation of other mono- or even dialdehydes of the glycols. Following a similar reaction path with other acids, various ethers could potentially form. These possibilities should be further investigated, as there are still prominent peaks in the spectrums that are unidentified. Further work should include the identification of these. In addition, quantification of all new degradation compounds should be attempted to close the mass and carbon balance.

3.5 Oxidative degradation of MEG

To look closer at the stability of MEG, two oxidative degradation experiments with MEG were conducted. This is interesting firstly because MEG is a hydrate inhibitor, which is also in need of regeneration similar to TEG. Secondly, as MEG is a degradation compound of TEG, knowing how it reacts under similar conditions could give further insights into the degradation paths of TEG. The first experiment was conducted with pure MEG at 100 °C and 24% oxygen in the gas flow. This was to enable comparison with TEG degradation under the same conditions. The second experiment was conducted with pure MEG at 150 °C and 24% oxygen in the gas flow. This was done in an attempt to significantly enhance the degradation of MEG and produce detectable amounts of its degradation products. During this experiment, one of the reactors had a leakage. The results from the last experiment will therefore stem from only one parallel.

The resulting MEG degradation was monitored by GC-FID. In both experiments, MEG degradation was difficult to discern. This was due to insignificant changes in MEG concentration. No formation of DEG or TEG was detected in the two experiments. However, during the high-temperature experiment, an unidentified peak was detected in the GC-FID chromatogram (RT = 5.55 min). Due to the very similar retention time, this peak possibly stems from something with a similar structure to MEG.

The formation of the small organic acid was also limited. For the experiment with the lowest temperature, no acids were above LOD. For the experiment at the highest temperature, formic acid was detected, but at concentrations below LOQ. Water formation was detected in the end samples of both experiments. The concentration was low in both cases, with 5.6 mmol/kg for the experiment with the lowest temperature and 10.5 mmol/kg for the experiment with high temperature. Both values were normalized per day the experiments ran.

The formation of acetaldehyde in the two experiments was low. The concentration normalized per day was below 0.008 mmol/kg. The proposed formation of acetaldehyde from MEG, see Scheme 7, is acid catalyzed. Due to the low acid concentration in these solutions, the low formation of acetaldehyde is not unexpected. The formation of formaldehyde normalized per day was 0.6 mmol/kg for the experiment with the lowest temperature and 2.3 mmol/kg in the experiment with high temperature. This can indicate that the formaldehyde formation is temperature dependent.

In total, compared to TEG, MEG seems to be very stable under the experimental conditions. Even with high temperatures and high oxygen concentration combined, the degradation rate of MEG stays low. Looking back to the acid formation during the TEG degradation, it was proposed that the formation could stem from the oxidation of MEG formed as a degradation product of TEG, see Scheme 3. As MEG seems to be stable under the given conditions, however, the possibility that the acids are formed through the oxidation of the aldehydes formed during the formation of MEG and DEG is strengthened, see Scheme 1 and Scheme 2. This is of course not conclusive, as it is still possible that factors within the degraded TEG system influence the stability of MEG.

4 Conclusions

The oxidative degradation of triethylene glycol (TEG) increases with temperature (above 70 °C) and with oxygen concentrations. However, the reaction mechanisms favored with each variable seem to be different. The degradation products of TEG detected and quantified were mono- and diethylene glycols (MEG and DEG), formic, acetic, and glycolic acid, formaldehyde and acetaldehyde, water, and CO_2. In the experiment with increasing oxygen concentration, the formation of all degradation products increased with the increase in oxygen. The formation of MEG, DEG, water, formaldehyde, and acetaldehyde increased with the increase in temperature. The concentration of acids increased when the temperature was raised from 75 to 100 °C, but the rise diminished with a further increase in temperature. On the other hand, the formation of acids increased with an increase in oxygen concentration at 100 °C.

A separate oxidative degradation experiment with base washes was conducted to capture formed CO_2. In addition to formic and acetic acid, CO_2 was captured and quantified. A mass and carbon balance for the solutions were studied, and it was found that a considerable part is not accounted for by the degradation products quantified so far. Also, some carbon-containing compounds are leaving the system with the gas flow and are not accounted for by compounds identified in the base washes. Oxidative degradation experiments with MEG showed that MEG is considerably more stable than TEG under the given conditions. This could indicate that the degradation products formed do not form with MEG as an intermediate.

An MS scan of the solutions allowed for the positive identification of the tetraethylene glycol, pentaethylene glycol, and diethylene glycol monoethyl ether. Furthermore, there are indications from the carbon- and mass balance of here to unidentified degradation compounds. The identified longer chained glycols open the possibility of polymerization of glycols. Further work is needed to identify the unknown compounds in the degraded TEG solution. One should also investigate what effect the degradation products, especially the longer chained glycols, has on the dehydration efficiency of TEG.

Acknowledgement

The authors would like to acknowledge Max Lukas Teschner for preparing dilutions and performing some of the analysis on degraded TEG. In addition, the authors would like to acknowledge Kai Vernstad and Merete Wiig from SINTEF Industry for performing analyses.

This publication has been produced with support from the Knowledge-building Project for Industry (KPN), MORE: Monitoring of glycol quality to Reduce operational risks (Project Manager: Marion Seiersten, Institute for Energy Technology (IFE)). The authors acknowledge the following partners for their contributions: Aker BP, Equinor, IFE, Kanfa, Slb, Neptune Energy, Shell, and the Research Council of Norway (320257).

The LAUNCH project (Project No. 299662) is co-funded by the ERA-NET Accelerating CCS Technologies initiative, which supports the delivery of safe and cost-effective carbon capture, utilization, and storage. The governments of each participating country have contributed funding through the ACT2 initiative.

References:

(1) Wang, X.; Economides, M. Advanced Natural Gas Engineering; 2013. https://doi.org/10.1016/C2013-0-15532-8.

(2) Kong, Z. Y.; Mahmoud, A.; Liu, S.; Sunarso, J. Revamping Existing Glycol Technologies in Natural Gas Dehydration to Improve the Purity and Absorption Efficiency: Available Methods and Recent Developments. *J Nat Gas Sci Eng*. **2018**, 56, 486-503. https://doi.org/10.1016/j.jngse.2018.06.008.

(3) Englezos, P. REVIEWS Clathrate Hydrates. *Ind. Eng. Chem. Res.* **1993**, 32, 1251–1274.

(4) Bai, Y.; Bai, Q. Hydrates. In *Subsea Engineering Handbook*; Gulf Professional Publishing, 2019; pp 409–434. https://doi.org/10.1016/B978-0-12-812622-6.00015-4.

(5) Chebbi, R.; Qasim, M.; Abdel Jabbar, N.; Jabbar, N. A. Optimization of Triethylene Glycol Dehydration of Natural Gas. *Energy Reports* **2019**, 5, 723–732. https://doi.org/10.1016/J.EGYR.2019.06.014.

(6) Karimi, A.; Abedinzadegan Abdi, M. Selective Dehydration of High-Pressure Natural Gas Using Supersonic Nozzles. *Chem. Eng. Process.* **2009**, 48, 560–568. https://doi.org/10.1016/j.cep.2008.09.002.

(7) Mokhatab, S.; Poe, W. A.; Mak, J. Y. Natural Gas Dehydration. In *Handbook of Natural Gas Transmission and Processing*; 2015; pp 223–263. https://doi.org/10.1016/b978-0-12-801499-8.00007-9.

(8) Stewart, M. Gas Sweetening. In *Surface Production Operations*; 2014. https://doi.org/10.1016/B978-0-12-382207-9.00009-3.

(9) Kohl, A. L.; Nielsen, R. Absorption of Water Vapor by Dehydrating Solutions. In *Gas purification*; 1997; pp 946–988.

(10) Bahadori, A.; Vuthaluru, H. B.; Mokhatab, S. Analyzing Solubility of Acid Gas and Light Alkanes in Triethylene Glycol. *J. Nat. Gas Chem*. **2008**, 17 (1), 51–58. https://doi.org/https://doi.org/10.1016/supporting003-9953(08)60025-0.

(11) John M. Campbell and Company. Gas Conditioning and Processing; 2004.

(12) Forster, R. Extending Glycol Life in Natural Gas Dehydration Systems. In *International Gas Research Conference*; San Diego, 1998; pp 113–125.

(13) Denisov, E. T. The Oxidation of Alcohols, Ketones, Ethers, Esters and Acids in Solution. *Compr. Chem. Kinet.* **1980**, 16 (C), 125–203. https://doi.org/10.1016/S0069-8040(08)70038-4.

(14) Lloyd, W. G.; Taylor, Jr., F.; Taylor, F. C. Corrosion by and Deterioration of Glycol and Glycol-Amine Solutions. *Ind. Eng. Chem.* **1954**, 46 (11), 51–53. https://doi.org/10.1021/ie50539a456.

(15) Rossiter, W. J.; Brown, P. W.; Godette, M. The Determination of Acidic Degradation Products in Aqueous Ethylene Glycol and Propylene Glycol Solutions Using Ion Chromatography. *Sol. Energy Mater.* **1983**, 9 (3), 267–279. https://doi.org/10.1016/0165-1633(83)90049-7.

(16) Brown, P. W.; Galuk, K. G.; Rossiter, W. J. Characterization of Potential Thermal Degradation Products from the Reactions of Aqueous Ethylene Glycol and Propylene Glycol Solutions with Copper Metal. *Sol. Energy Mater.* **1987**, 16 (4), 309–313. https://doi.org/10.1016/0165-1633(87)90079-7.

(17) Madera, M.; Höflinger, W.; Kadnar, R. Ion Chromatographic Identification and Quantification of Glycol Degradation Products. *J. Chromatogr. A* **2003**, 997 (1), 279–284. https://doi.org/10.1016/S0021-9673(03)00060-8.

(18) Psarrou, M. N.; Jøsang, L. O.; Sandengen, K.; Østvold, T. Carbon Dioxide Solubility and Monoethylene Glycol (MEG) Degradation at MEG Reclaiming/Regeneration Conditions. *J. Chem. Eng. Data* **2011**, 56 (12), 4720–4724. https://doi.org/10.1021/je200709h.

(19) AlHarooni, K.; Pack, D.; Iglauer, S.; Gubner, R.; Ghodkay, V.; Barifcani, A. Analytical Techniques for Analyzing Thermally Degraded Monoethylene Glycol with Methyl Diethanolamine and Film Formation Corrosion Inhibitor. *Energy and Fuels* **2016**, 30 (12), 10937–10949. https://doi.org/10.1021/acs.energyfuels.6b02116.

(20) Brown, P. W.; Rossiter, W. J.; Galuk, K. G. A Mass Spectrometric Investigation of the Thermal Oxidative Reactivity of Ethylene Glycol. *Sol. Energy Mater.* **1986**, 13 (3), 197–202. https://doi.org/10.1016/0165-1633(86)90018-3.

(21) Glastrup, J.; Padfield, T. The Thermal Degradation of Tetraethylene Glycol, a Model Molecule for Polyethylene Glycol. *ICOM Comm. Conserv. 10th Trienn. Meet. Washington, DC, 22-27 August 1993 Prepr*. **1993**, 251–256.

(22) Glastrup, J. Degradation of Polyethylene Glycol. A Study of the Reaction Mechanism in a Model Molecule: Tetraethylene Glycol. *Polym. Degrad. Stab.* **1996**, 52 (3), 217–222.

(23) Buvik, V.; Vevelstad, S. J.; Brakstad, O. G.; Knuutila, H. K. Stability of Structurally Varied Aqueous Amines for CO 2 Capture. *Ind. Eng. Chem. Res.* **2021**, 60, 5638. https://doi.org/10.1021/acs.iecr.1c00502.

(24) Høisæter, K. K.; Buvik, V.; Vevelstad, S. J.; Knuutila, H. K. Analytical Tools for Monitoring Glycol Degradation. *To be Published*.

(25) Ma'mun, S.; Jakobsen, J. P.; Svendsen, H. F.; Juliussen, O. Experimental and Modeling Study of the Solubility of Carbon Dioxide in Aqueous 30 Mass% 2-((2-Aminoethyl)Amino)Ethanol Solution. *Ind. Eng. Chem. Res.* **2006**, 44, 8, 2505–2512. https://doi.org/10.1021/ie0505209.

(26) Kidd, R. W.; Huang, T. T. S.; Yankwich, P. E. Intramolecular ^{13}C Kinetic Isotope Effects in the Decarboxylation of Oxalic Acid in Dioxane Solution. *J. Chem. Phys.* **1976**, 65 (2), 801–807. https://doi.org/10.1063/1.433097.

(27) Bambagioni, V.; Bevilacqua, M.; Bianchini, C.; Filippi, J.; Marchionni, A.; Vizza, F.; Wang, L. Q.; Shen, P. K. Ethylene Glycol Electrooxidation on Smooth and Nanostructured Pd Electrodes in Alkaline Media. *Fuel Cells* **2010**, 10 (4), 582–590. https://doi.org/10.1002/fuce.200900120.

(28) Wieland, B.; Lancaster, J. P.; Hoaglund, C. S.; Holota, P.; Tornquist, W. J. Electrochemical and Infrared Spectroscopic Quantitative Determination of the Platinum-Catalyzed Ethylene Glycol Oxidation Mechanism at CO Adsorption Potentials. *Langmuir* **1996**, 12 (10), 2594–2601. https://doi.org/10.1021/la9506943.

(29) Smith, W. B. Ethylene Glycol to Acetaldehyde-Dehydration or a Concerted Mechanism. *Tetrahedron* **2002**, 58 (11), 2091–2094. https://doi.org/10.1016/S0040-4020(02)00103-5.

(30) Gouedard, C.; Picq, D.; Launay, F.; Carrette, P. L. Amine Degradation in CO_2 Capture. I. A Review. *Int. J. Greenh. Gas Control* **2012**, 10, 244–270. https://doi.org/10.1016/j.ijggc.2012.06.015.

(31) Feron, P. H. M. M. Introduction. In *Absorption-Based Post-combustion Capture of Carbon Dioxide*; Elsevier Inc., 2016; pp 3–12. https://doi.org/10.1016/b978-0-08-100514-9.00001-9.

(32) Lepaumier, H.; Da Silva, E. F.; Einbu, A.; Grimstvedt, A.; Knudsen, J. N.; Zahlsen, K.; Svendsen, H. F. Comparison of MEA Degradation in Pilot-Scale with Lab-Scale Experiments. In *Energy Procedia*; Elsevier Ltd, 2011; Vol. 4, pp 1652–1659. https://doi.org/10.1016/j.egypro.2011.02.037.

(33) Vevelstad, S. J.; Johansen, M. T.; Knuutila, H.; Svendsen, H. F. Extensive Dataset for Oxidative Degradation of Ethanolamine at 55–75 °C and Oxygen Concentrations from 6 to 98%. *Int. J. Greenh. Gas Control* **2016**, 50, 158–178. https://doi.org/10.1016/J.IJGGC.2016.04.013.

Supporting information

Oxidative Degradation of Triethylene Glycol

Karen K. Høisæter[a], Vanja Buvik[a], Susana V. Gonzalez[b], Solrun J. Vevelstad[c], Hanna K. Knuutila[a]*

[a] Department of Chemical Engineering, NTNU, NO-7491 Trondheim, Norway

[b] Department of Chemistry, NTNU, NO-7491 Trondheim, Norway

[c] SINTEF Industry, P.O.Box 4760 Torgarden, NO-7465, Norway

* E-mail address: Hanna.knuutila@ntnu.no

A. Additional experimental data

Table A1: Compounds analyzed with LC-MS by SINTEF Industry with the corresponding LOQ.

Compound	**CAS**	**LOQ [ng/mL]**
***N*,*N'*-bis(2-hydroxyethyl)-ethanediamide**	5835-28-9	0.1
1H-imidazole-1-ethanol	1615-14-1	1.0
***N*-(2-hydroxyethyl)-formamide**	693-06-1	0.1
4-(2-hydroxyethyl)-2-piperazinone	23936-04-1	0.1
***N*-(2-hydroxyethyl)-acetamide**	142-26-7	0.1
***N*,*N'*-bis(2-hydroxyethyl)-oxamide**	1871-89-2	10
1-(2-hydroxyethyl)-2-imidazolidinone	3699-54-5	0.1
2-oxazolidinone	497-25-6	1.0
***N*,*N'*-bis(2-hydroxyethyl)-urea**	15438-70-7	0.1
2-hydroxy-*N*-(2-hydroxyethyl)-acetamide	3586-25-2	0.1
1-(2-hydroxyethyl)-2-piperazinone	59702-23-7	0.1
(*N*-(2-Hydroxyethyl)-2-(hydroxyethyl)-amino)acetamide	144236-39-5	0.1
Diethanolamine	111-42-2	1.0
2-(Methyl)-aminoethanol	109-83-1	0.1
2-(2-Hydroxyethyl-amino)ethanol	111-41-1	1.0

B. Numerical data

Table B1: GC-FID results of quantification of TEG, MEG, and DEG in samples from oxidative degradation experiment of pure TEG (6% O_2).

		TEG		MEG		DEG	
Temperature [°C]	**Day**	**R1 [mmol/kg]**	**R2 [mmol/kg]**	**R1 [mmol/kg]**	**R2 [mmol/kg]**	**R1 [mmol/kg]**	**R2 [mmol/kg]**
75	*0*	6676	6676	<LOQ	<LOQ	<LOQ	<LOQ
	2	6416	6386	45.4	44.6	71.9	50.7
	5	6532	6335	93.8	79.9	100.0	95.7
	7	5986	6340	145	132	110	99.4
	9	6003	6125	194	189	136	142
	14	5870	5866	284	241	200	176
100	*0*	6564	6564	<LOQ	<LOQ	<LOQ	<LOQ
	2	5997	6175	80.2	91.4	102	120
	4	5564	5976	159	175	203	233
	7	5582	5409	287	274	383	363
	10	4981	5014	385	375	521	511
	14	4033	4150	480	463	686	648
125	*0*	6445	6445	<LOQ	<LOQ	<LOQ	<LOQ
	2	5516	5919	98.7	116	111	128
	4	5279	5268	189	182	222	200
	7	4524	4613	358	326	380	343
	9	4051	4178	474	428	453	425
	11	3754	3979	560	517	569	530
150	*0*	6610	6610	<LOQ	<LOQ	<LOQ	<LOQ
	2	5611	5407	192	204	204	238
	4	5036	4863	314	325	390	407
	7	4217	4052	433	459	564	591

Table B2: GC-FID results of quantification of TEG, MEG, and DEG in samples from oxidative degradation experiment of pure TEG (100 °C).

Temperature [°C]	Day	TEG R1 [mmol/kg]	TEG R2 [mmol/kg]	MEG R1 [mmol/kg]	MEG R2 [mmol/kg]	DEG R1 [mmol/kg]	DEG R2 [mmol/kg]
1 %	*0*	6317	6317	<LOQ	<LOQ	<LOQ	<LOQ
	2	6122	5992	<LOQ	<LOQ	43.9	46.5
	5	6157	6325	<LOQ	<LOQ	48.9	50.2
	7	6128	6251	60.0	60.1	70.0	64.6
	9	6075	6433	70.2	68.9	85.9	74.1
	11	6248	6369	84.1	67.4	87.8	41.3
	14	6414	6480	67.4	94.0	79.9	48.4
12 %	*0*	6168	6168	<LOQ	<LOQ	<LOQ	<LOQ
	2	5767	5534	167	176	128	141
	4	5098	5068	294	325	211	233
	7	4159	3900	446	484	330	344
	9	3783	3618	555	655	420	486
	11	3401	3086	656	764	493	552
	14	3309	2797	910	974	700	559
24 %	*0*	6661	6661	<LOQ	<LOQ	<LOQ	<LOQ
	2	5356	5788	293	357	218	264
	4	4550	4205	610	670	437	460
	7	3091	2810	966	1047	693	711
	9	2410	2117	1131	1250	770	769
	11	1550	1351	1409	1459	918	817
	12	1327	1120	1726	1743	922	792

Table B3: Results from HPLC-UC quantification of formic, glycolic, acetic, glyoxylic, and oxalic acid in samples from oxidative degradation experiment of pure TEG (6% O_2).

Temperature [°C]	Day	Formic acid		Glycolic acid		Acetic acid		Glyoxylic acid		Oxalic acid	
		R1 [mmol/kg]	R2 [mmol/kg]	R1 [mmol/kg]	R2 [mmol/kg]	R1 [mmol/kg]	R2 [mmol/kg]	R1 [mmol/kg]	R2 [mmol/kg]	R1 [mmol/kg]	R2 [mmol/kg]
75	0	<LOQ	<LOQ	<LOQ	<LOQ	<LOQ	<LOQ	<LOQ	<LOQ	<LOQ	<LOQ
	2	20.5	17.8	0.314	0.313	0.850	0.912	<LOQ	<LOQ	<LOQ	<LOQ
	5	105	88.5	0.873	1.11	3.00	3.19	<LOQ	<LOQ	<LOQ	<LOQ
	7	203	182	1.20	2.01	7.20	7.81	<LOQ	<LOQ	<LOQ	<LOQ
	9	278	244	1.86	2.91	9.72	9.22	<LOQ	<LOQ	<LOQ	<LOQ
	14	457	419	4.21	5.07	6.75	6.84	<LOQ	<LOQ	<LOQ	<LOQ
100	0	<LOQ	<LOQ	<LOQ	<LOQ	<LOQ	<LOQ	<LOQ	<LOQ	<LOQ	<LOQ
	1	68.9	77.6	0.336	0.376	2.85	3.11	<LOQ	<LOQ	<LOQ	<LOQ
	2	141	158	0.496	0.488	4.64	5.19	<LOQ	<LOQ	<LOQ	<LOQ
	4	331	334	1.35	1.39	11.1	9.29	<LOQ	<LOQ	<LOQ	<LOQ
	7	609	598	5.69	5.54	13.1	15.4	<LOQ	<LOQ	0.173	0.282
	10	829	894	11.0	11.1	20.0	23.3	<LOQ	<LOQ	0.483	0.208
	12	1064	989	15.1	14.5	26.0	23.5	<LOQ	<LOQ	0.574	0.454
	14	1258	1163	17.2	16.2	28.3	29.0	<LOQ	<LOQ	0.897	0.759
125	0	<LOQ	<LOQ	<LOQ	<LOQ	<LOQ	<LOQ	<LOQ	<LOQ	<LOQ	<LOQ
	2	255	271	0.602	0.665	3.58	3.74	<LOQ	<LOQ	<LOQ	<LOQ
	4	476	493	1.52	1.25	9.14	10.2	<LOQ	<LOQ	0.182	0.179
	7	749	757	3.26	2.57	16.5	16.8	<LOQ	<LOQ	0.201	0.998
	9	1007	1034	4.91	3.98	19.4	17.8	<LOQ	<LOQ	0.473	0.458
	11	1228	1263	6.58	6.35	20.9	24.0	<LOQ	<LOQ	0.631	0.611
150	0	<LOQ	<LOQ	<LOQ	<LOQ	<LOQ	<LOQ	<LOQ	<LOQ	<LOQ	<LOQ
	2	252	269	0.93	0.704	6.51	4.58	<LOQ	<LOQ	<LOQ	<LOQ
	4	523	540	1.86	1.72	8.12	8.12	<LOQ	<LOQ	<LOQ	<LOQ
	7	768	813	4.32	4.10	12.6	11.2	<LOQ	<LOQ	0.265	0.420

Table B4: Results from HPLC-UV quantification of formic, glycolic, acetic, glyoxylic, and oxalic acid in samples from oxidative degradation experiment of pure TEG (100 °C).

Temperature [°C]	Day	Formic acid		Glycolic acid		Acetic acid		Glyoxylic acid		Oxalic acid	
		R1 [mmol/kg]	R2 [mmol/kg]	R1 [mmol/kg]	R2 [mmol/kg]	R1 [mmol/kg]	R2 [mmol/kg]	R1 [mmol/kg]	R2 [mmol/kg]	R1 [mmol/kg]	R2 [mmol/kg]
1 %	*0*	<LOQ	<LOQ	<LOQ	<LOQ	<LOQ	<LOQ	<LOQ	<LOQ	<LOQ	<LOQ
	2	22.2	31.8	<LOQ	<LOQ	<LOQ	<LOQ	<LOQ	<LOQ	<LOQ	<LOQ
	5	53.5	41.0	<LOQ	<LOQ	<LOQ	<LOQ	<LOQ	<LOQ	<LOQ	<LOQ
	7	90.5	71.2	<LOQ	<LOQ	<LOQ	<LOQ	<LOQ	<LOQ	<LOQ	<LOQ
	9	124	91.7	<LOQ	<LOQ	<LOQ	<LOQ	<LOQ	<LOQ	<LOQ	<LOQ
	11	144	108	<LOQ	<LOQ	<LOQ	<LOQ	<LOQ	<LOQ	<LOQ	<LOQ
	14	182	136	<LOQ	<LOQ	<LOQ	<LOQ	<LOQ	<LOQ	<LOQ	<LOQ
12 %	*0*	<LOQ	<LOQ	<LOQ	<LOQ	<LOQ	<LOQ	<LOQ	<LOQ	<LOQ	<LOQ
	2	302	344	<LOQ	<LOQ	6.14	7.30	<LOQ	<LOQ	<LOQ	<LOQ
	4	560	632	<LOQ	<LOQ	11.0	14.0	<LOQ	<LOQ	<LOQ	<LOQ
	7	1179	1179	12.6	11.3	51.0	32.5	<LOQ	<LOQ	<LOQ	<LOQ
	9	1370	1591	11.8	16.7	49.9	49.4	<LOQ	<LOQ	<LOQ	<LOQ
	11	1794	2053	18.0	25.2	38.7	46.1	<LOQ	<LOQ	1.07	1.36
	14	2252	2718	24.9	40.9	51.7	63.3	<LOQ	<LOQ	1.57	1.88
24 %	*0*	<LOQ	<LOQ	<LOQ	<LOQ	<LOQ	<LOQ	<LOQ	<LOQ	<LOQ	<LOQ
	2	568	631	2.22	3.98	18.4	20.9	3.69	3.59	<LOQ	<LOQ
	4	1244	1393	14.6	22.6	37.1	28.5	11.0	10.9	<LOQ	<LOQ
	7	2382	2785	42.9	59.6	82.0	111	23.8	26.0	<LOQ	<LOQ
	9	3200	3786	57.8	94.4	131	184	33.0	34.9	<LOQ	<LOQ
	11	4174	4879	98.7	136	216	254	42.1	44.8	<LOQ	<LOQ
	12	4532	5276	116	151	251	324	45.8	48.7	<LOQ	<LOQ

Table B5: Quantitative HPLC-UV results of formic and acetic acid in end samples of acid washes (1M H_2SO_4) from oxidative degradation experiment of pure TEG.

Experiment	***Formic acid [mmol/kg]***	***Acetic acid [mmol/kg]***
T = 75, [O_2] = 6%, day 14, R1	5.16	2.25
T = 75, [O_2] = 6%, day 14, R2	7.48	2.87
T = 100, [O_2] = 6%, day 14, R1	1.53	3.39
T = 100, [O_2] = 6%, day 14, R2	2.47	4.29
T = 125, [O_2] = 6%, day 11, R1	6.74	6.15
T = 125, [O_2] = 6%, day 11, R2	5.03	4.30
T = 150, [O_2] = 6%, day 9, R1	11.5	9.81
T = 150, [O_2] = 6%, day 9, R2	6.62	5.59
T = 100, [O_2] = 1%, day 14, R1	1.24	0.357
T = 100, [O_2] = 1%, day 14, R2	0.518	0.366
T = 100, [O_2] = 12%, day 14, R1	14.1	10.6
T = 100, [O_2] = 12%, day 14, R2	12.1	8.92
T = 100, [O_2] = 24%, day 12, R1	24.7	29.9
T = 100, [O_2] = 24%, day 12, R2	22.0	19.4

Table B6: Karl-Fischer titration results end samples from oxidative degradation experiment of pure TEG.

Experiment	***Water [mmol/kg]***
Undegraded TEG	0.0152
T = 75, [O_2] = 6%, day 14, R1	178
T = 75, [O_2] = 6%, day 14, R2	194
T = 100, [O_2] = 6%, day 14, R1	1134
T = 100, [O_2] = 6%, day 14, R2	1032
T = 125, [O_2] = 6%, day 11, R1	1791
T = 125, [O_2] = 6%, day 11, R2	1517
T = 150, [O_2] = 6%, day 7, R1	1300
T = 150, [O_2] = 6%, day 7, R2	1288
T = 100, [O_2] = 1%, day 14, R1	73.0
T = 100, [O_2] = 1%, day 14, R2	53.0
T = 100, [O_2] = 12%, day 14, R1	2601
T = 100, [O_2] = 12%, day 14, R2	2998
T = 100, [O_2] = 24%, day 12, R1	4171
T = 100, [O_2] = 24%, day 12, R2	5411

Table B7: LC-MS quantification of formaldehyde and acetaldehyde in end samples of acid washed and DNPH cartridges from oxidative degradation experiment of pure TEG.

Experiment	***Formaldehyde [mmol/kg]***	***Acetaldehyde [mmol/kg]***
T = 75, [O$_2$] = 6%, day 14, R1	0.0640	0.00100
T = 75, [O$_2$] = 6%, day 14, R2	0.546	0.00119
T = 100, [O$_2$] = 6%, day 14, R1	0.0831	0.0445
T = 100, [O$_2$] = 6%, day 14, R2	0.116	0.0154
T = 125, [O$_2$] = 6%, day 11, R1	7.92	2.12
T = 125, [O$_2$] = 6%, day 11, R2	7.78	1.17
T = 150, [O$_2$] = 6%, day 7, R1	3.20	0.0195
T = 150, [O$_2$] = 6%, day 7, R2	6.32	0.109
T = 100, [O$_2$] = 1%, day 14, R1	3.87	0.000497
T = 100, [O$_2$] = 1%, day 14, R2	4.23	0.000650
T = 100, [O$_2$] = 12%, day 14, R1	4.66	2.93
T = 100, [O$_2$] = 12%, day 14, R2	5.59	7.55
T = 100, [O$_2$] = 24%, day 12, R1	22.9	12.7
T = 100, [O$_2$] = 24%, day 12, R2	24.6	13.8

Table B8: Degradation compounds quantified in the oxidative degradation experiment of pure TEG (100 °C, 24% O$_2$) connecnted to three base washes (BW, 30wt% MEA, aq.). The amount given for the base washes is the sum of the component found in all three.

Compound	**R1 [mmol/kg]**	**R2 [mmol/kg]**
TEG	1149	829
MEG	1952	2001
DEG	846	711
Fromic acid	5617	6678
Glycolic acid	130	169
Acetic acid	308	348
Glyoxylic acid	48.2	65.0
Oxalic acid	5.93	8.12
HEF (BW)	618	707
HEA (BW)	36.5	31.2
Formic acid (BW)	89.5	79.2
Acetic acid (BW)	8.23	7.51

Table B9: Results from TIC analysis and total alkalinity analysis of the base washes (BW, 30wt% MEA, aq.). In each reactor, three BW were connected in series. BW1 is the first, BW2 is the second, and BW3 is the last.

Sample	**CO_2 [mmol/kg]**	**Total alkalinity [mmol/kg]**
30wt% MEA	0.00591	5.65
R1, BW1, Day 2	0.0962	5.83
R1, BW2, Day 2	0.00483	5.62
R1, BW3, Day 2	0.00659	5.56
R2, BW1, Day 2	0.123	5.78
R2, BW2, Day 2	0.00448	5.58
R2, BW3, Day 2	0.00560	5.48
R1, BW1, Day 4	0.280	6.16
R1, BW2, Day 4	0.00359	5.71
R1, BW3, Day 4	0.00192	5.50
R2, BW1, Day 4	0.322	5.81
R2, BW2, Day 4	0.0142	5.66
R2, BW3, Day 4	0.00302	5.45
R1, BW1, Day 7	0.901	5.21
R1, BW2, Day 7	0.0153	5.58
R1, BW3, Day 7	0.0105	5.15
R2, BW1, Day 7	1.06	5.57
R2, BW2, Day 7	0.0191	5.59
R2, BW3, Day 7	0.00460	5.65
R1, BW1, Day 9	1.64	4.29
R1, BW2, Day 9	0.0393	5.53
R1, BW3, Day 9	0.00646	5.54
R2, BW1, Day 9	1.85	4.14
R2, BW2, Day 9	0.115	5.47
R2, BW3, Day 9	0.0108	5.43
R1, BW1, Day 11	1.12	2.98
R1, BW2, Day 11	1.96	4.98
R1, BW3, Day 11	0.0235	5.44
R2, BW1, Day 11	1.28	2.99
R2, BW2, Day 11	2.66	4.81
R2, BW3, Day 11	0.109	5.38
R1, BW1, Day 14	0.505	1.95
R1, BW2, Day 14	2.69	4.74
R1, BW3, Day 14	2.15	4.95
R2, BW1, Day 14	0.670	2.05
R2, BW2, Day 14	2.62	4.70
R2, BW3, Day 14	2.84	3.44

Table B10: Results from the most prominent compounds in the end solutions of the base washes (BW, 30wt% MEA, aq.) quantified with LC-MS analysis.

Sample	**Formic acid [mmol/kg]**	**Acetic acid [mmol/kg]**	**HEF [mmol/kg]**	**HEA [mmol/kg]**
R1, BW1, Day 14	257.5	17.92	1677	31.14
R1, BW2, Day 14	10.31	3.918	163.7	42.58
R1, BW3, Day 14	0.8318	2.848	12.04	35.68
R2, BW1, Day 14	221.7	16.81	1867	22.96
R2, BW2, Day 14	15.23	3.042	239.2	38.44
R2, BW3, Day 14	0.8250	2.674	13.75	32.27

C. Results from 30wt% MEA base washes

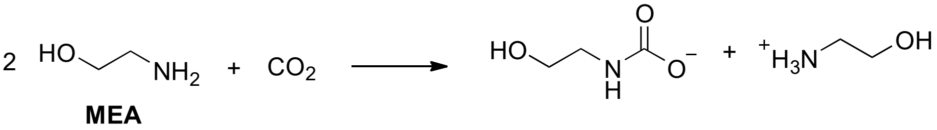

Scheme C1: Chemical absorption of CO_2 with MEA forming MEA-carbamate and protonated MEA.

The first base washes in the series (1st) do not reach 0.5 mol CO_2 per mol MEA, which would indicate a fully loaded solution, but instead stabilize at 0.4 and then decrease. During this decrease in loading, both the CO_2 and amine concentrations are decreasing. This hints at other reactions taking place in this base wash. The progression of the loading of the amine can be seen in Figure C1 and shows that CO_2 indeed is formed as a degradation product during oxidative degradation of TEG. Therefore, the end sample of the 1st base washes was investigated by NMR. The most abundant compound in the NMR spectrum was found to be (2-hydroxyethyl)-formamide (HEF, CAS: 693-06-1), see the following paragraph for shift assignment. In addition, multiple peaks from other compounds could be discerned but not identified due to lower peak intensities.

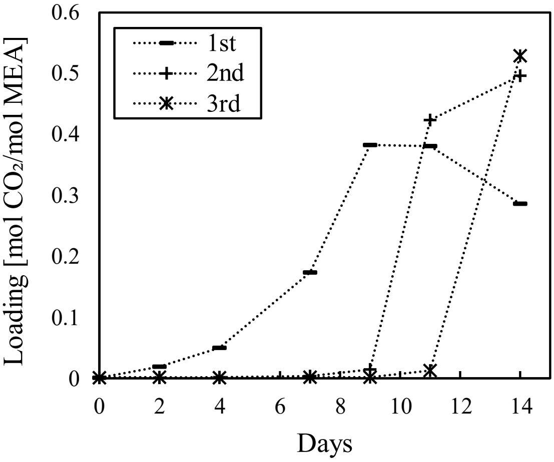

Figure C1: Loading [mol CO_2/mol MEA] in the three base wash solutions at the outlet of the oxidative degradation rig during oxidative degradation of TEG (100 °C, 24% O_2).

With regards to the carbon lost from the system, unidentified compounds in the base washes were detected by NMR but not identified and quantified. Also, the base washes connected closest to the reactors (1st) quickly gained a deep red color and became quite viscous. As both HEF, protonated MEA, and MEA-carbamate are colorless, other unidentified compounds are expected to cause this change.

HEF **HEA**

Figure C2: Structure of HEF and HEA.

Shift assignment of HEF

(2-Hydroxyethyl)-formamide (HEF) is expected to have formed through a reaction between MEA and formic acid in the base washes (30wt% MEA, aq.). An NMR analysis of the first base washes showed that the peaks with highest intensities derived from HEF. Shift assignment and spectra are presented below.

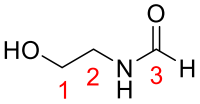

Data for ^{1}H NMR (600 MHz, D_2O) δ: 7.92 (s, 1H, H-3), 3.49-3.45 (m, 2H, H-1), 3.20-3.16 (m, 2H, H-2). Data for ^{13}C NMR (150 MHz, D_2O) δ: 166.6 (C-3), 62.6 (C-1), 43.1 (C-2).

^{1}H:

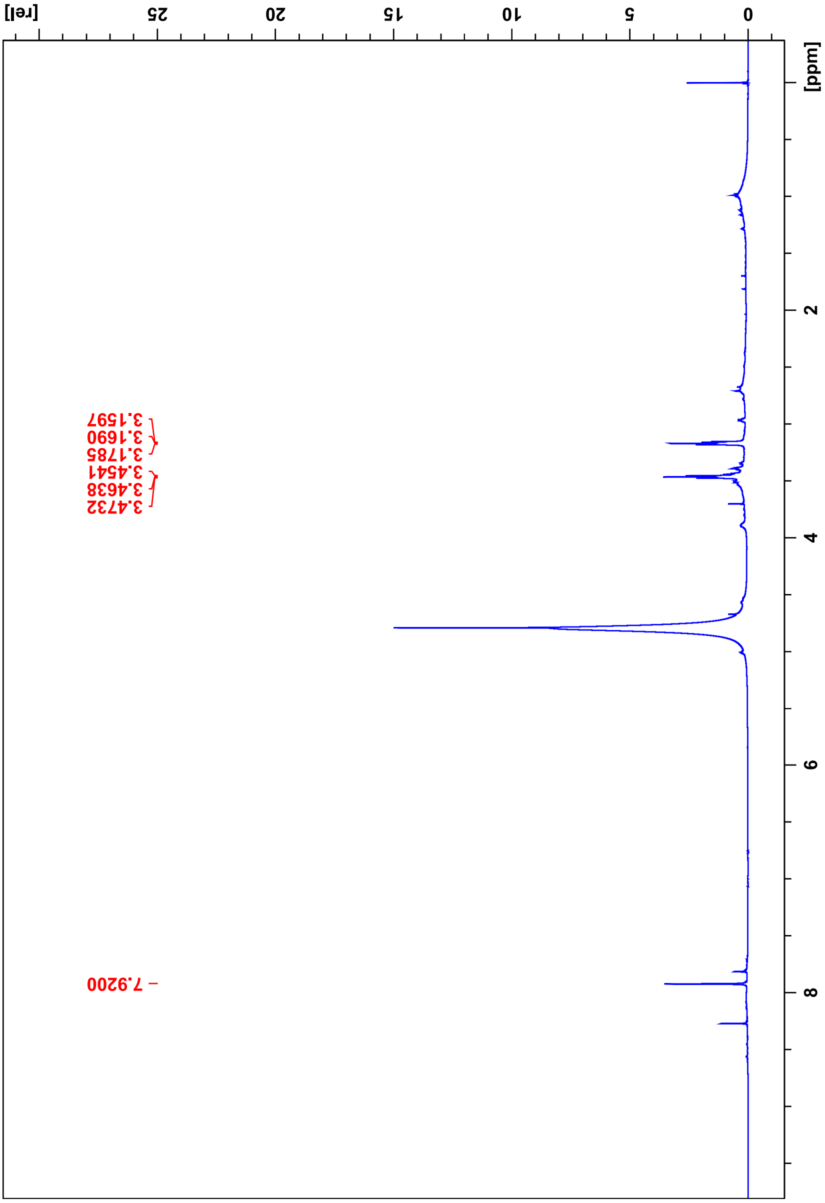
[rel]
25
20
15
10
5
0
[ppm]
2
4
6
8
7.9200
3.1597
3.1690
3.1785
3.4541
3.4638
3.4732

^{13}C:

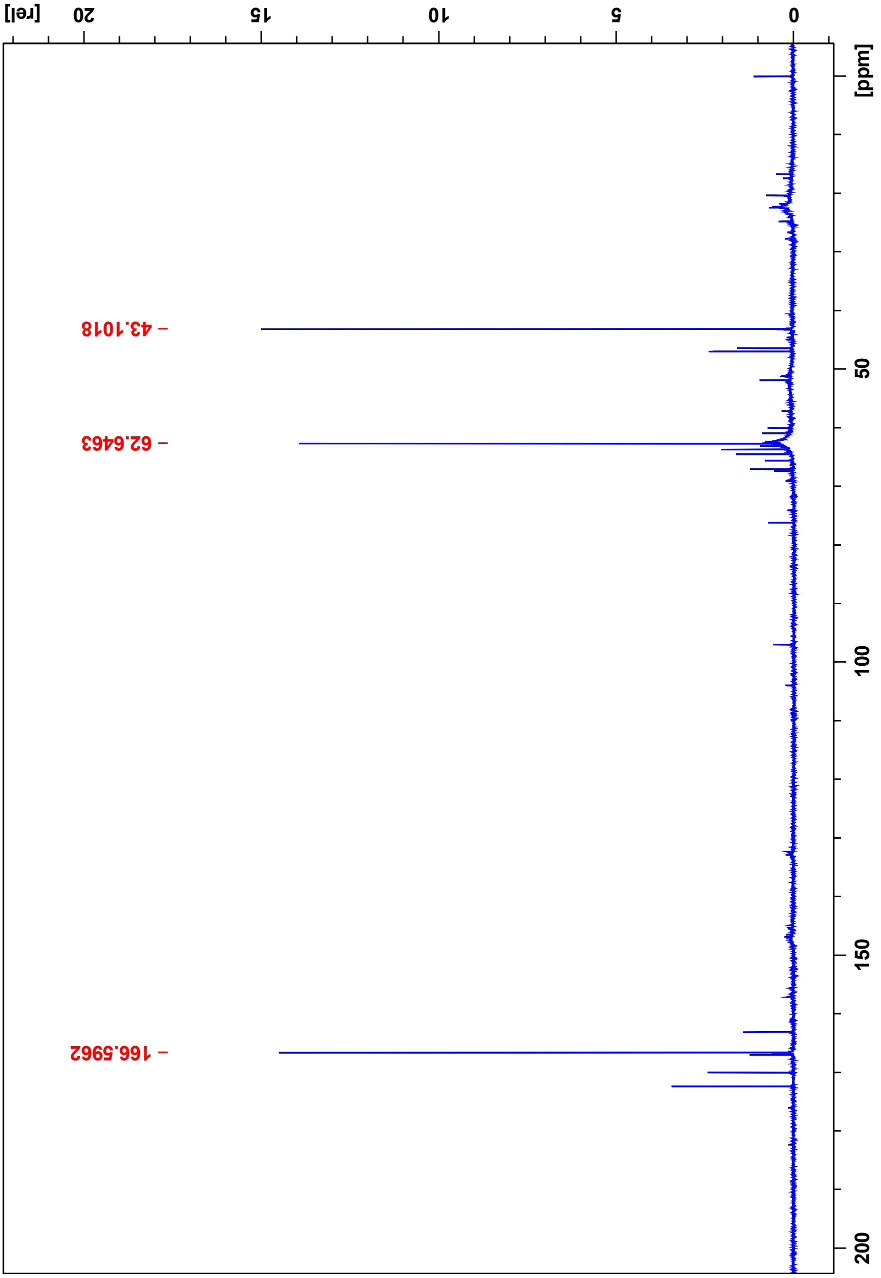

COSY:

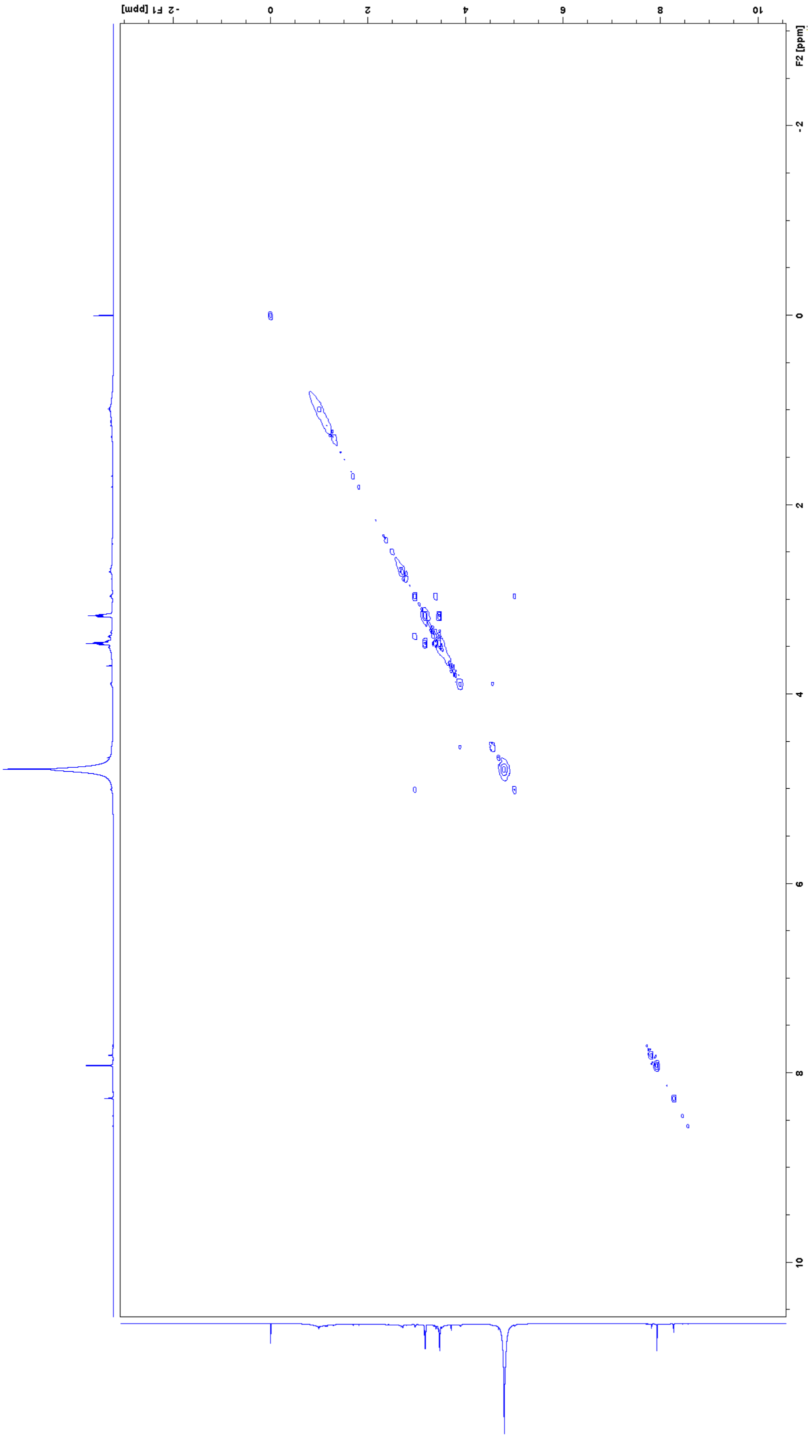

HSQC:

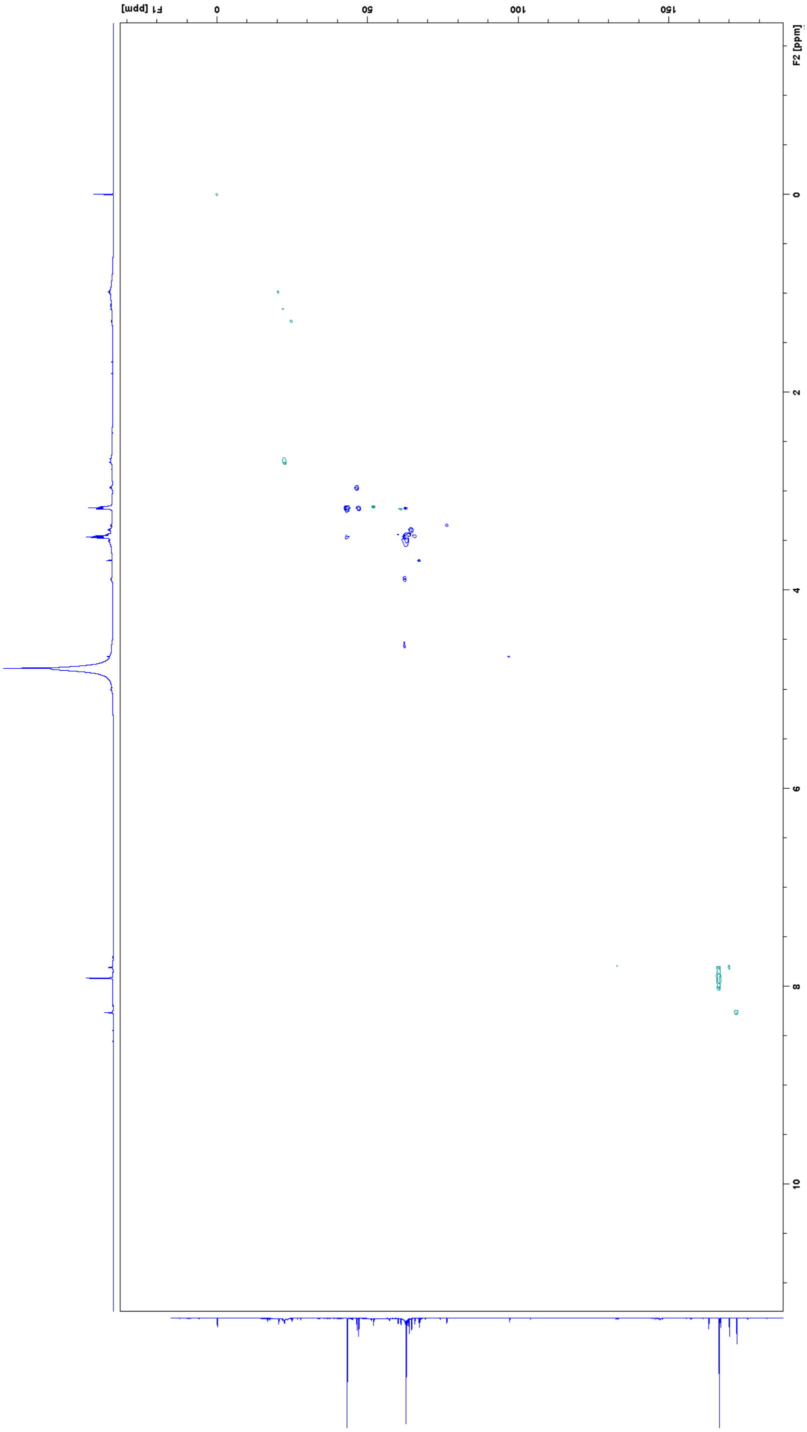

HMBC:

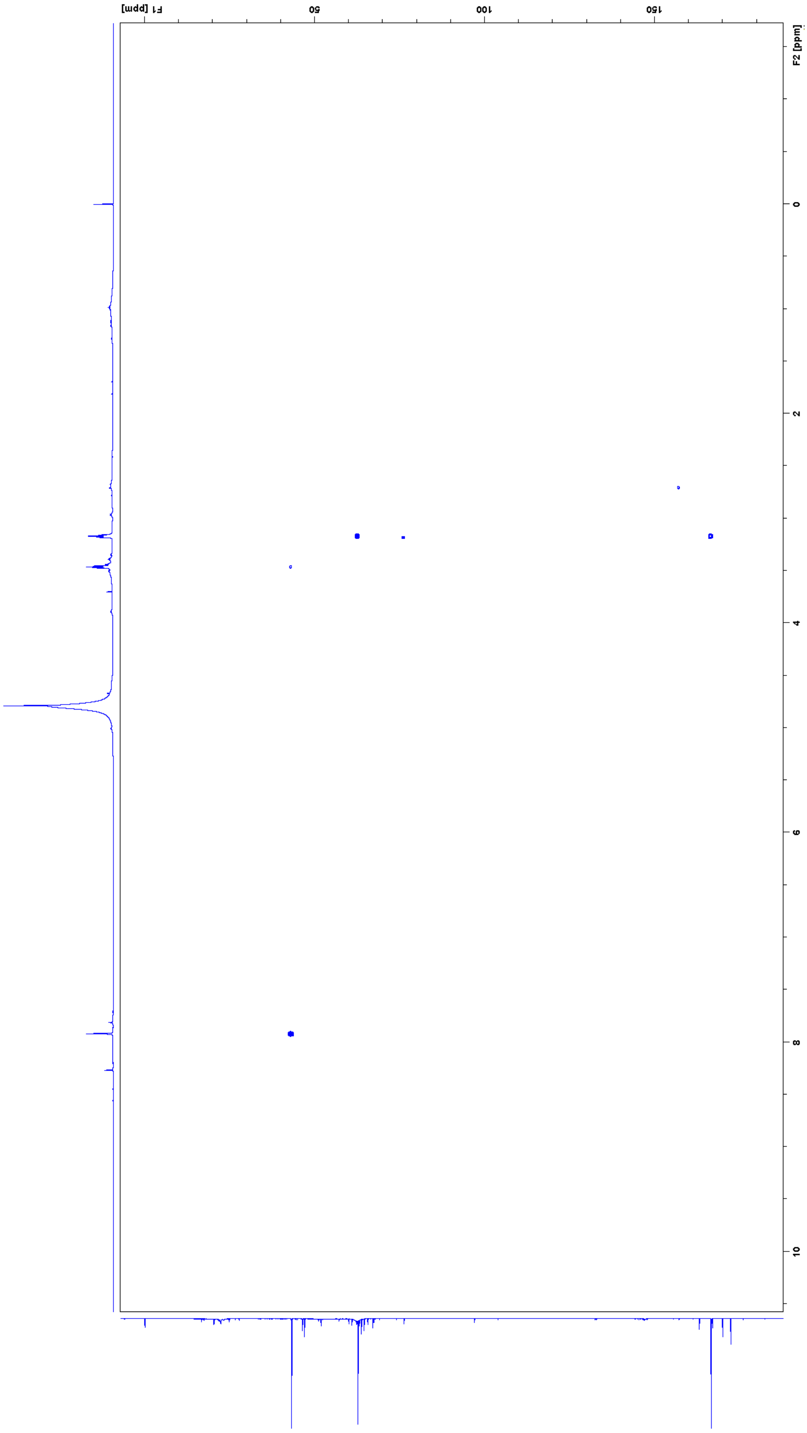

D. MS Data

Table D1: Compounds identified with standard addition in GC-MS.

Name	RT [min]	Spiked test	CAS	Structure
Diethylene glycol monoethyl ether	6.33	Yes	111-90-0	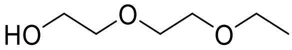
Monoethylene glycol	3.34	No	107-21-1	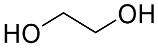
Diethylene glycol	9.66	Yes	111-46-6	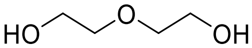
Triethylene glycol	9.97	Yes	112-27-6	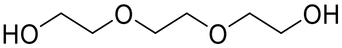
Tetraethylene glycol	16.61	Yes	112-60-7	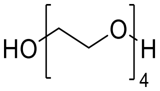
Pentaethylene glycol	21.74	Yes	4792-15-8	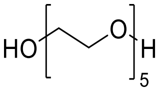

Table D2: Compounds not found when tested with standard addition in GC-MS.

Name	RT [min]	CAS	Structure
2-Methoxy-1,3-dioxolane	9.31 (Diluted in diethyl ether)	19693-75-5	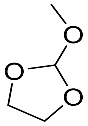
1,1-Diethoxyethane (acetaldehyde diethyl acetal)	9.32	105-57-7	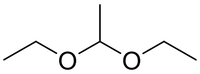

12-Crown-4	9.66	294-93-9	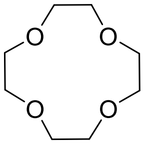
Tri(ethylene glycol) monoethyl ether	10.51	112-50-5	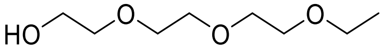
15-Crown-5	13.58	33100-27-5	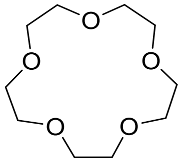
2-Hydroxymethyl-12-crown-4	16.17	75507-26-5	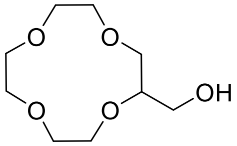
18-Crown-6	17.25	17455-13-9	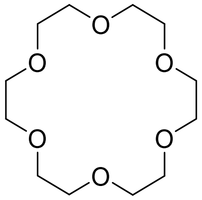
Hexaethylene glycol	31.22	2615-15-8	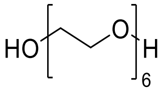
2-Hydroxymethyl-15-crown-5	Higher than 35 min	75507-25-4	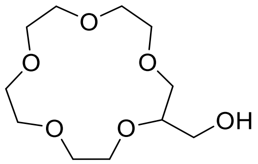
2-Hydroxymethyl-18-crown-6	Higher than 35 min	70069-04-4	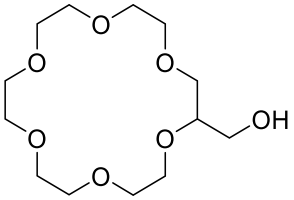
2-Ethoxyethan-1-ol	Not detected under the GC-MS method conditions	110-80-5	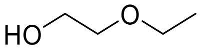

Table D3: *Tentatively identified degradation compound in LC-MS scan.*

Tentative identification	RT [min]	Natural mass [Da]	m/z	Adducts	Formula	Fragmentation score	Mass error [ppm]	Isotope similarity	CAS	Structure
Triethylene glycol formate	4.03	178.0846	179.0918	[M+H-H_2O], [M+H]	C7H14O5	42.8	2.49	99.56	1240369-67-8	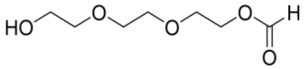

E. Triethylene glycol formate experiment

A mixture of 70wt% formic acid in triethylene glycol (TEG) was prepared at room temperature. An NMR analysis of the mixture showed that triethylene glycol formate had formed. Shift assignment and spectra are presented below.

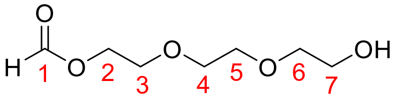

Data for triethylene glycol formate. ^{1}H NMR (600 MHz, D_2O) δ: 8.55 (s, H-8), 8.50 (s, H-1), 4.70-4.63 (m, H-2), 4.23 (m, H-3), 4.17 (s (br), H-4/H-5), 4.16 (m, H-6), 4.11 (m, H-7). Data for ^{13}C NMR (150 MHz, D_2O) δ: 166.7 (C-1), 74.8 (C-7), 72.9 (C-4/C-5), 72.7 (C-6), 71.6 (C-3), 66.5 (C-2).

^{1}H:

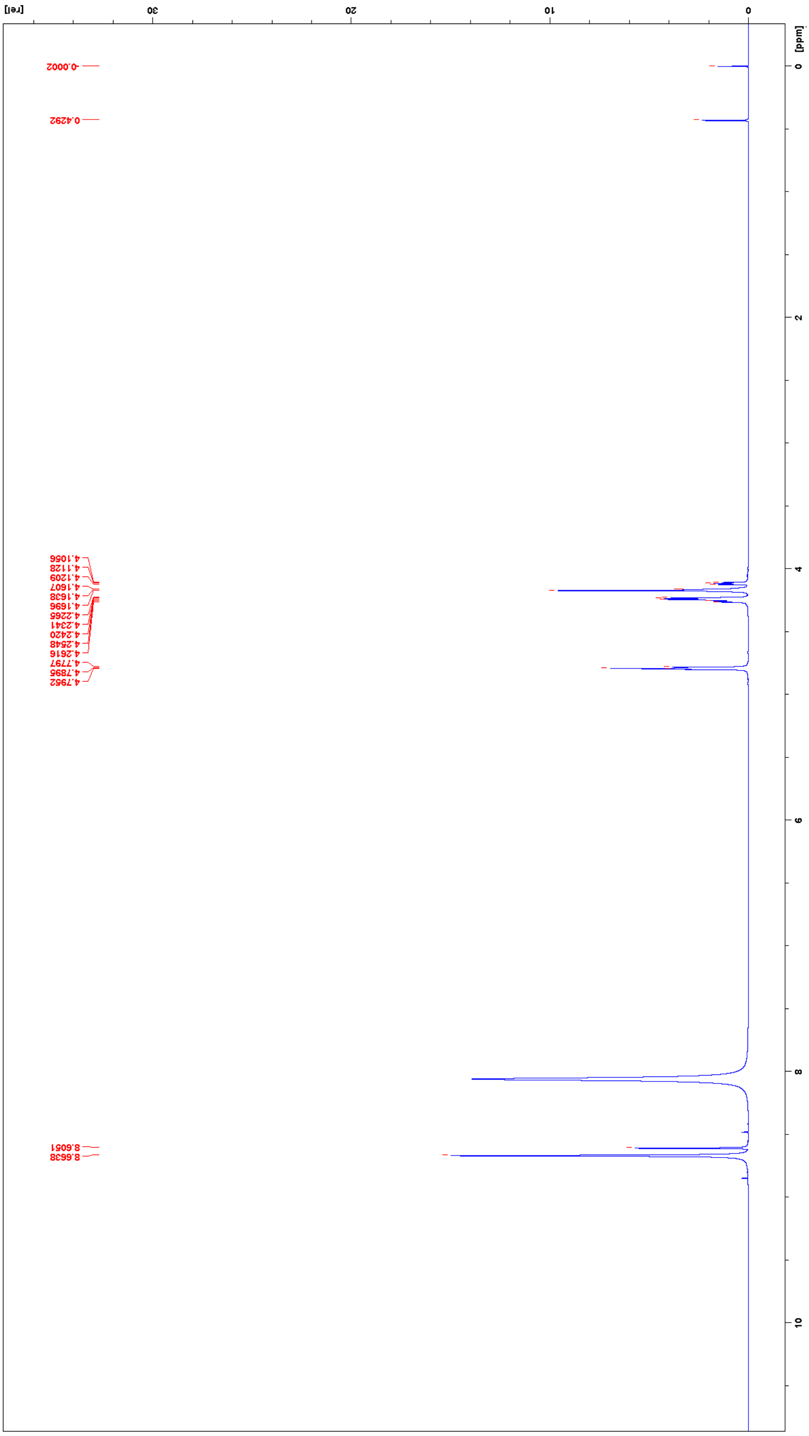

[rel]
30
20
10
0
[ppm]
0
2
4
6
8
10
-0.0002
0.4292
4.1056
4.1128
4.1209
4.1607
4.1638
4.1696
4.2265
4.2341
4.2420
4.2548
4.2616
4.7797
4.7896
4.7962
8.6051
8.6638

^{13}C:

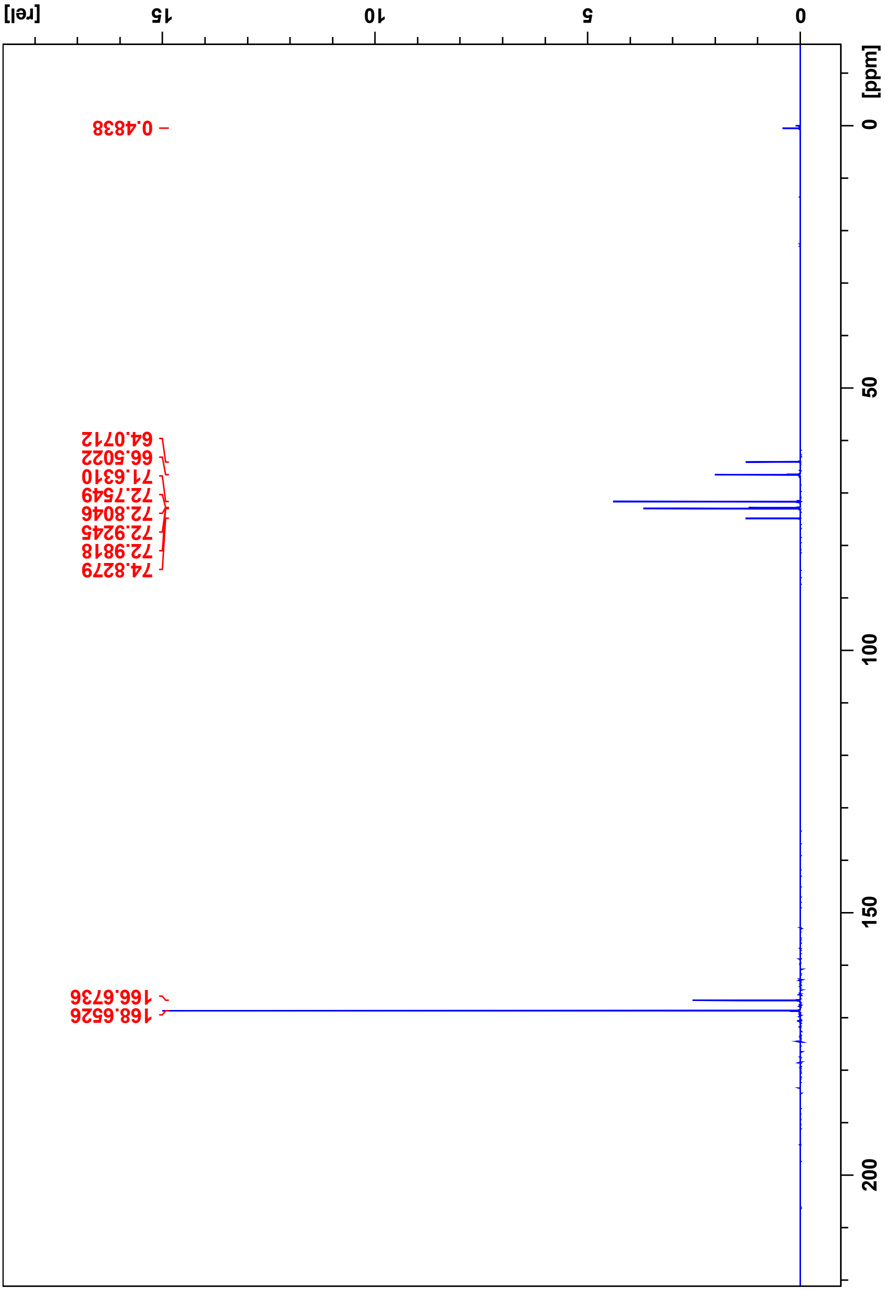

[rel]
15
10
5
0
[ppm]
0
50
100
150
200
0.4838
64.0712
66.5022
71.6310
72.7549
72.8046
72.9245
72.9818
74.8279
166.6736
168.6526

COSY:

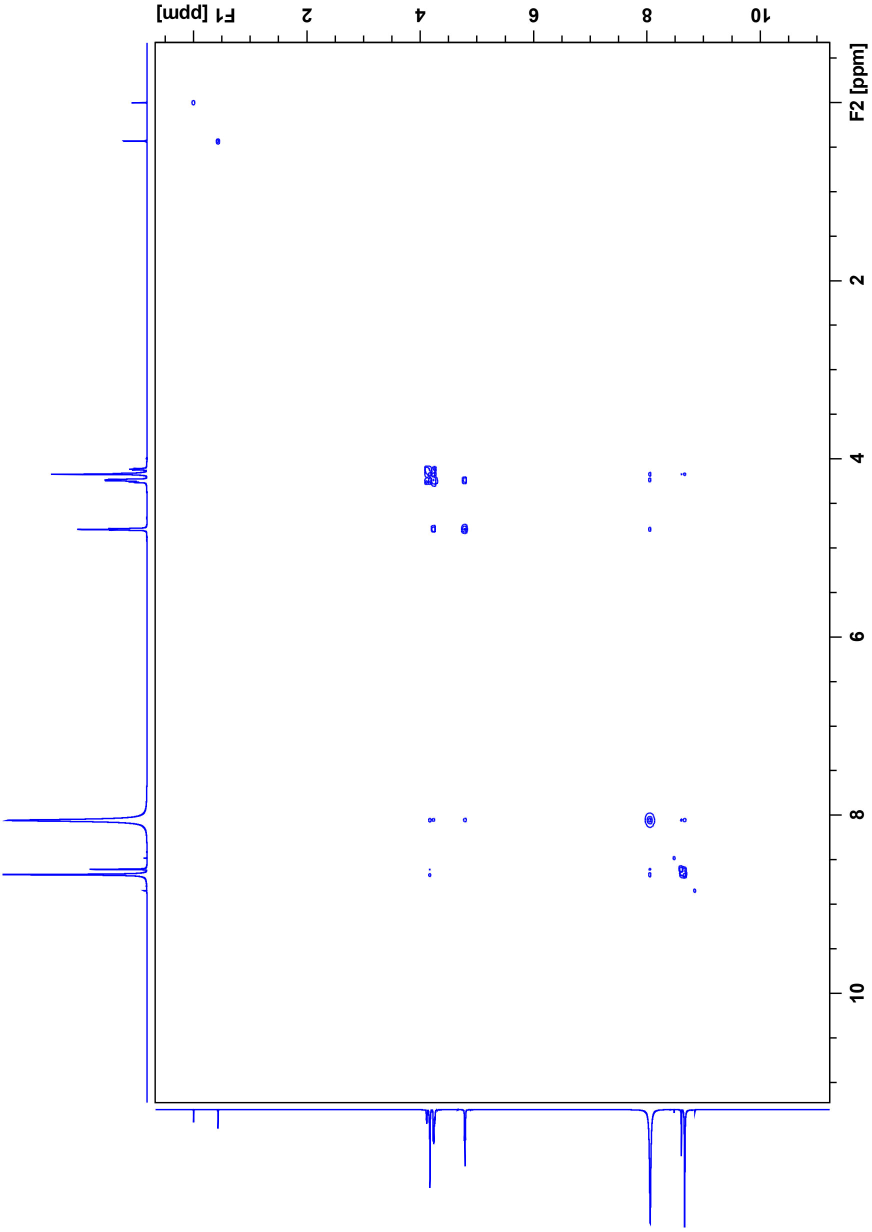

HSQC:

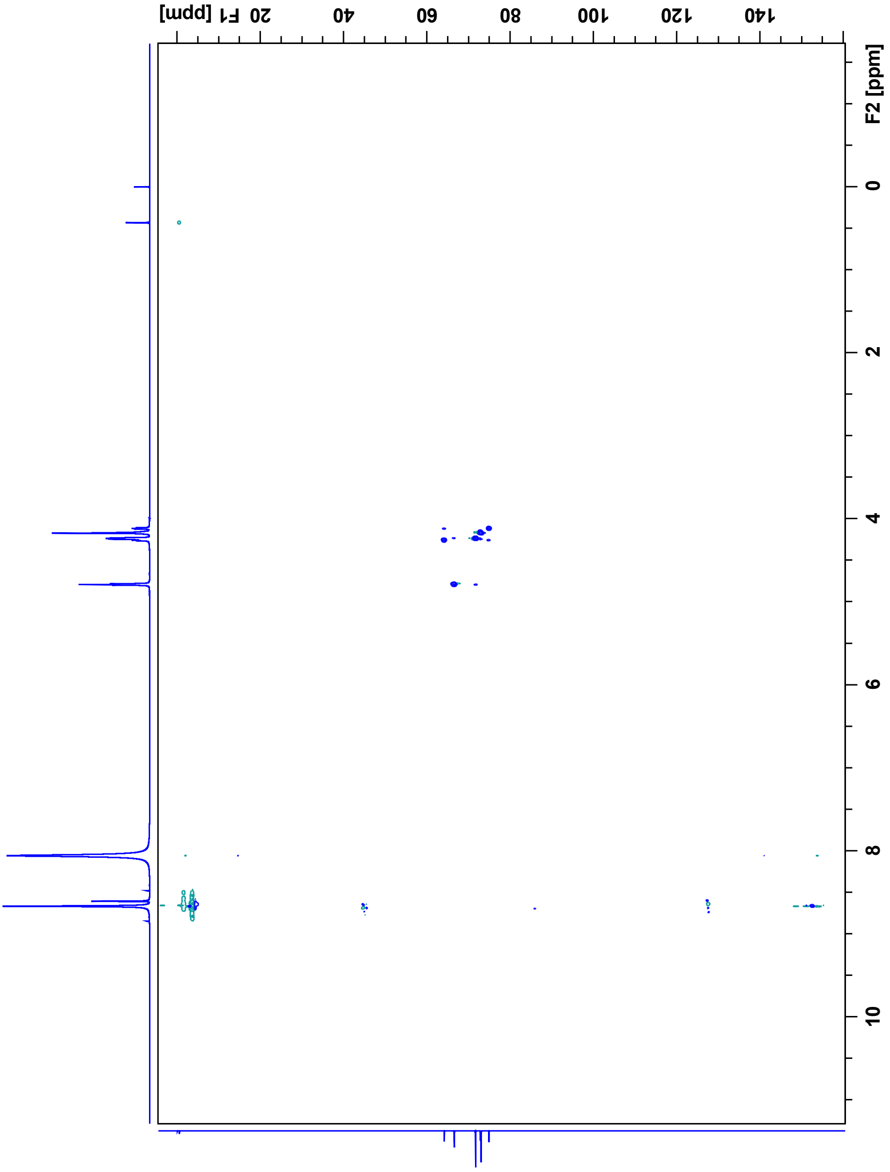

HMBC:

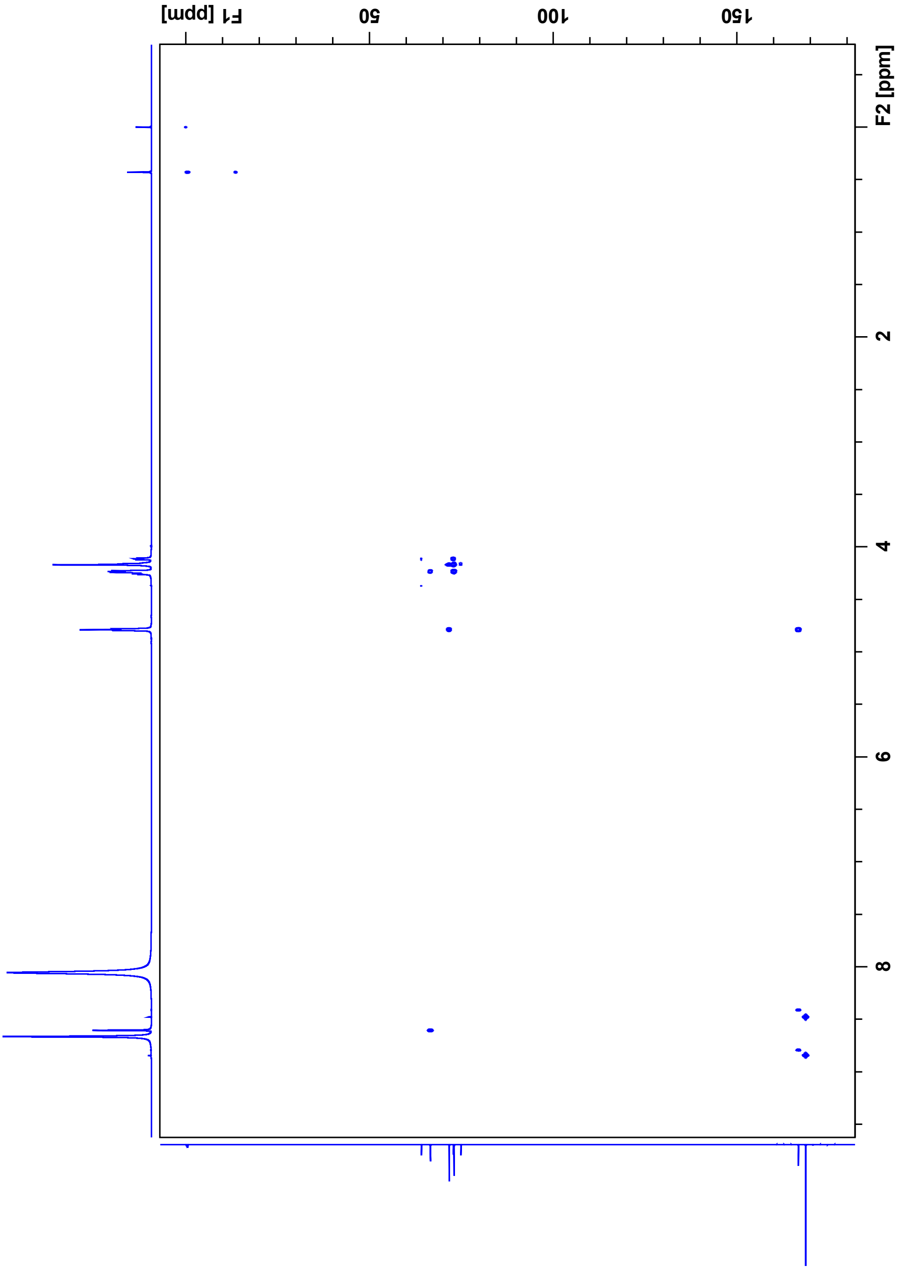

Chapter 9

Conclusions and Recommendations for Future Work

This chapter contains a summary of the findings of this thesis and recommendations for future work based on these.

9.1 Conclusions

The main objective of this work was to increase the understanding of the chemical processes occurring as solvents used in gas purification degrade. The solvent systems studied were amine-based solvents used for CO_2 capture and glycol-based solvents used for gas dehydration. The work included a literature study, oxidative and thermal degradation experiments of amines and glycols, in addition to analytical method development.

From the gathered pilot plant data presented in the review article on degradation and emissions in post-combustion CO_2 capture pilot plants, some interesting conclusions could be drawn. Pretreatment of the flue gas seems to be a good measure to increase the solvents stability. When interested in the health of the solvent, not any one component could be recommended for monitoring. If any, monitoring ammonia in the gas-phase in combination with the HSS concentration in the liquid phase can be proposed as a good option, if these are known degradation components of the solvent. For proprietary solvents, there is not enough data available to draw any conclusions. When degradation, as well as emission, data is published, there is a general lack in the reporting of analytical methods used. As an overall tendency, there seems to be no universal agreement on routines for monitoring, sampling, and reporting methodology used.

Water-lean solvents are proposed as an alternative to aqueous amine solutions. Even though many systems have been developed or proposed, very little has been done to understand how this change in the solvent composition will affect the stability of the amine. In the first degradation study, the effect of the solvent on the thermal stability of amines was investigated. Initially, the effect of just the water, amine and CO_2 concentration was considered. It was found that the amine and water concentration does not affect the thermal stability of MEA, but that the CO_2 concentration does. Next, in thermal degradation experiments where the water was replaced with TEG, increased degradation rates were observed. This was the case for primary amine, MEA and AP, and secondary amines, MMEA and EAE. Due to the high thermal stability of tertiary amines, no conclusions could be drawn from the experiments with DMMEA, DEEA, and DMPA. Testing the stability of MEA in other organic diluents, DEG, MEG, THFA, NFM/water, and NMP, all resulted in increased degradation of MEA. Parameters possibly affecting the amine stability, such as acid-base behavior, polarity, and relative permittivities, were investigated, but none were singled out as the cause. For all solutions tested with MEA, the typical thermal degradation products were formed. Overall, it seems to be necessary to study each water-lean solvent system separately to rule out amine stability issues.

When studying the oxidative stability of water-lean solvents, volatility and viscosity issues caused by the change in solvent composition was found to occur. These were lessened by using a semi-open setup, but further improvements could be beneficial. Oxidative degradation experiments of aqueous MEA were conducted, with changing amine and CO_2 concentration. Increasing the MEA concentration while keeping the CO_2 concentration constant resulted in decreased MEA loss and increased degradation product formation. Increasing both the MEA and CO_2 concentration did not result in any clear trend for the degradation of MEA, but formation of degradation components increased. It is not clear what caused these discrepancies.

Very little is published on the stability of glycols, and especially triethylene glycol (TEG). Oxidative and thermal degradation experiments with TEG were conducted and degradation components were mapped. To do this, analytical methods had to be developed for the degradation components of TEG. The focus was on finding two independent methods for the quantification of TEG and the smaller glycols diethylene glycol (DEG) and ethylene glycol (MEG), and two independent methods for quantifying the small organic acids, formic, acetic, glycolic, glyoxylic, and oxalic acid. Gas-chromatography coupled with flame ionization detection (GC-FID) and quantitative ^{13}C NMR were successfully used to quantify the three glycols. High-performance liquid-chromatography coupled with ultraviolet detection (HPLC-UV) and heat-stable salt (HSS) analysis were successfully used to quantify the acids.

With analytical tools in place, thermal and oxidative degradation of TEG were conducted. Thermal degradation experiments were performed with pure TEG and with two solutions with added impurities of water and formic acid. It was not possible to clearly discern any effect of the impurities on the loss of TEG. The formation of MEG and DEG, however, increased by the addition of water and even more by addition of formic acid. Gas bubbles were observed in the degraded solutions, but no other degradation components were identified in the thermally degraded solutions.

Oxidative degradation experiments with pure TEG were conducted to study the effect of temperature and oxygen on the solvent stability. An increase in both resulted in increased degradation rates of TEG. The degradation products identified and quantified were DEG, MEG, formic, acetic, glycolic, glyoxylic, and oxalic acid, formaldehyde and acetaldehyde, water, and CO_2. The formation of all these degradation products increased with increased oxygen concentrations in the gas. The formation of MEG, DEG, water, formaldehyde, and acetaldehyde increased with the increase in temperature. The formation of the acids increased with the increase in temperature at the lower temperatures but stagnated at the higher temperatures. Identification of additional degradation compounds, tetraethylene glycol, pentaethylene glycol, and diethylene glycol monoethyl ether was achieved by a GC-MS analysis. Oxidative degradation experiments with MEG showed that the stability of MEG is considerably higher than TEG under the given conditions.

9.2 Suggestions for Future Work

When changing the composition of the amine solvent systems, issues such as increased volatility and mass transfer limitation of oxygen can arise. Efforts should be made to reduce these when studying these systems. Semi-open batch setups with increased gas bubbling or cyclic setups using packings to increase contact between gas and liquid can be good options. The semi-open batch setups are the easier to set up of the two, but as the liquid is stagnant, it is not certain that mass transfer limitations of the oxygen will not be a problem. The gas and the liquid have a lot more contact in the cyclic system using packing material, so there will not be any mass transfer limitations in this system. The cyclic system is, however, more complex to set up, so the necessity should be considered. There are also some points to keep in mind if introducing water-lean solvents to a cyclic system. First, one must do a careful selection of pumps and tubing for the setup. Due to the increased viscosity of these systems, more robust pumps and piping might be required. Furthermore, some of the organic diluents proposed as cosolvents for water-lean solvent are quite harsh on the equipment.[1] So, the setup must be built with materials that can withstand them.

Cosolvents in a water-lean amine system can potentially be sensitive to oxygen or elevated temperatures. Analytical methods to keep an eye on these, or their degradation components, can be useful to understand the chemistry of the system. In some cases, it might be enough to be able to keep track of the cosolvent itself. If the degradation components are to be analyzed, some knowledge of the degradation of the cosolvent would be required.

During the thermal degradation experiments with TEG, little degradation was observed. This made it difficult to identify degradation components. To be able to identify more of the thermal degradation products of TEG, working with more degraded solutions would be advantageous. This could be achieved either by letting the experiment run for a longer period or by increasing the temperature. Some caution should be taken if these experiments are conducted in closed systems and more degradation is to be achieved. During the degradation experiment with low degradation, gas bubbles were observed in the solutions at the end of the experiment. This could imply that gaseous degradation components are being formed. If this is the case, closed systems should be avoided. An experimental setup with the possibility of gas analysis would be advantageous, to allow identification and quantification of these gaseous degradation components.

Though many oxidative degradation products of TEG were identified and quantified, there was still a considerable amount of unknown carbon in the solutions. These could be interesting to identify, especially as the confirmed formation of some larger glycols, e.g. tetraethylene glycol and pentaethylene glycol, indicate that larger polymeric components could be formed. The effect of these, and the other degradation components, on the dehydration efficiency of TEG should be investigated.

The analytical techniques used to analyze the degraded glycol solutions are off-line techniques. For on-line monitoring, there are as for yet no options. An interesting possibility in this regard is FTIR. This technique has been proposed for online monitoring in the industry. In addition, it has been used for studying acid formation of MEG during catalytic oxidation and for quantifying components in systems containing TEG.[2–4] Development of FTIR as an on-line technique could be beneficial for quicker evaluation of changes in the system during the dehydration process.

9.3 References

(1) Wanderley, R. R. Water-Lean Solvents for Biogas Upgrading, NTNU, 2020.

(2) Shoukat, U.; Baumeister, E.; Knuutila, H. K. ATR-FTIR Model Development and Verification for Qualitative and Quantitative Analysis in MDEA–H_2O–MEG/TEG–CO_2 Blends. *Energies* **2019**, 12 (17). https://doi.org/10.3390/EN12173285.

(3) Wang, L.; Meng, H.; Shen, P. K.; Bianchini, C.; Vizza, F.; Wei, Z. In Situ FTIR Spectroelectrochemical Study on the Mechanism of Ethylene Glycol Electrocatalytic Oxidation at a Pd Electrode. *Phys. Chem. Chem. Phys.* **2011**, 13 (7), 2667. https://doi.org/10.1039/c0cp01913e.

(4) Lin, J.-L.; Ren, J.; Tian, N.; Zhou, Z.-Y.; Sun, S.-G. In Situ FTIR Spectroscopic Studies of Ethylene Glycol Electrooxidation on Pd Electrode in Alkaline Solution: The Effects of Concentration. *J. Electroanal. Chem.* **2012**, 688, 165-171. https://doi.org/10.1016/j.jelechem.2012.08.027.

ISBN 978-82-326-7286-8 (printed ver.)
ISBN 978-82-326-7285-1 (electronic ver.)
ISSN 1503-8181 (printed ver.)
ISSN 2703-8084 (online ver.)

NTNU
Norwegian University of
Science and Technology